Development and characterisation of a responsive polyvalent bacteriophage therapeutic

Alves, Diana

Award date:
2015

Awarding institution:
University of Bath

Development and characterisation of a responsive polyvalent bacteriophage therapeutic

Ph.D. Thesis

Diana Ribeiro Alves

Thesis for the degree of Doctor of Philosophy

DEPARTMENT OF CHEMISTRY

UNIVERSITY OF BATH

July 2015

COPYRIGHT

Diana Ribeiro Alves

Acknowledgments

I am very delighted to finally be able to write and put together this PhD thesis that certainly has been a long and exciting journey, where I had the chance to meet several bright minds that somehow contributed to and supported me through this work.

My journey into the phage therapeutics world started when Dr David Harper and his infinite and passionate knowledge about bacteriophage, kindly gave me the opportunity for a placement at Ampliphi Biosciences. It greatly opened my curiosity and interest in bacteriophages and how they can become such a valuable asset for society, but also gave me essential tools and basis to have excellence allied to my work. Here many people gave me their valuable contribution, guidance and amazing friendship, especially Dr Helena Parracho, but not least Dr Catherine Easom, Dr Katy Blake, Dr Hannah Patrick and Dr Alison Gaudion. Also, a very special thanks to my friend Dr Malcolm McConville, apart the distance, he kept me always on my feet on every moment, showing me always the light at the end of the tunnel and giving the best advice, and finally to all his time spent revising this thesis.

The second half of this thesis took place at the University of Bath and I would like to thank my supervisor Dr Toby Jenkins for his care and support all way through, allowing me to build up my independence as a scientist with always an enthusiastic attitude towards my work and life. Also, I am extremely grateful to my group and in particular would like to extend this to Dr Thet, Maisem, Hollie, Jess and Oscar for our fruitful discussions and friendship. A special thank also to Dr Michael Beeton for all the scientific discussion and such a fruitful collaboration, where in only one year we were able to plan the experiments, execute them, discuss them and have the work published. A special thank also goes to my funding body EPSRC.

Also, I have to thank deeply my supervisor Professor Mark Enright who I consider to be an incredible bright researcher, always giving me very valuable advice towards my research, but also his eager attitude and his friendship always since the beginning.

I am also very grateful and most of all happy to have found the most amazing friends, that always made me laugh with whom I have the most amazing time that obviously contributed for the accomplish of this thesis, especially to my friend Maria Cravo. But this is also extended to Khadija, Patricia, Borja, Nuno, Stive, Sian, Bertrand and to my two best friends Marta and Carolina.

A very special acknowledgment goes to Manuel Nuño, an unexpected friend and later on the most amazing housemate, who brings me beauty and simplicity. We were able to share all the downs of a final year of a PhD, supporting greatly each other, but most importantly we've been sharing a very exceptional and enduring good moment.

Finally, I would like to thank my super family that have always given me all the support throughout these four years, giving me their wise advice and all the courage to keep doing my work: to my mother Fatima, my father António and my little brother João.

Abstract

Bacteriophages (phages) are obligate intracellular parasites of bacteria that usually kill the bacterial host. Bacteriophage therapy is a recently revived approach for treating bacterial infection that relies on the traits of the phage lytic cycle. A lot of attention has been given to phage therapy with new research being published weekly and international conferences organised every year, bringing together the academic and industrial phage communities. However, despite this huge effort and considerable scientific interest there is still a great lack of understanding on how to use phage effectively and overcome the many obstacles in the near future. One of the main triggers for such interest was the increasing evidence of antibiotic resistance among human bacterial pathogens, which were once efficiently eliminated by drugs but are now causing alarmingly high levels of morbidity and mortality.

Also, bacteria when causing a disease are able to produce highly protective biofilm communities. Biofilms are major causes of impairment of wound healing and two of the most common and aggressive wound pathogens are *Staphylococcus aureus* (Gram-positive) and *Pseudomonas aeruginosa* (Gram-negative), both displaying a large repertoire of virulence factors and reduced susceptibility to antibiotics.

This work reports and explores the use of phages to target both *S. aureus* and *P. aeruginosa* pathogen biofilm producers. Firstly, isolation of promising phage candidates was performed and cocktails were established. Two phages (DRA88 and phage K) formed the cocktail to target *S. aureus* and six phages (DL52, DL54, DL60, DL62, DL64 and DL68) formed a cocktail to target *P. aeruginosa*. A thorough characterisation of each of the selected phages was performed, including their range of host infectivity and their genome sequences were analysed. The phage's ability to infect and kill planktonic cultures was successfully studied and afterwards such ability was assayed

on biofilms using an *in vitro* static biofilm system (microtitre-plate), followed by an *in vitro* dynamic biofilm system (The Modified Robbins Device). Both cocktails were shown to be effective in reducing and dispersing biofilms formed by the clinical strains showing them to be promising not only to combat topical bacterial infections (related to biofilm production), but also to control biofilms produced on the surfaces of medical devices, such as catheters. Finally, the phage cocktail's ability to treat systemic infections caused by the two pathogens was assessed in an *in vivo G. mellonella* infection model. In the case of the *P. aeruginosa* infection, although the phages were not able to fully treat the larvae, the cocktail allowed a delay of larval death, caused by the infection. For the *S. aureus* infection, the cocktail did not show the same trend, but most likely the high bacterial cell numbers involved in the experiment interfered with a successful study on the phage cocktail.

The phage mixture may form the basis of an effective treatment for infections caused by *S. aureus* and *P. aeruginosa* biofilms.

Dissemination of the research work

Posters and oral presentations

26th – 28th January 2015 - 1st International Caparica Conference in Antibiotic Resistance (Lisbon, Portugal)

- **INVITED SPEAKER,** presentation title "The potential use of bacteriophages for the treatment of *Staphylococcus aureus* and *Pseudomonas aeruginosa* biofilm infections"

5th – 7th November 2014 - Antibiotic alternatives for the new millennium (London, UK)

- **INVITED SPEAKER**, presentation title "Utilisation of bacteriophages for the treatment of bacterial biofilms"

16th - 18th September 2014 – Phages 2014 (Oxford, UK)

- Presentation titled "Prospecting for and utilisation of bacteriophages for the treatment of bacterial biofilms"

17th - 23th August 2014 - BioNano 2014 summer school (Hirschegg, Austria)

- Presentation titled "Prospecting for and utilisation of bacteriophages for the treatment of bacterial biofilms"

14th – 18th August 2014 – Viruses of Microbes III (Zurich, Switzerland)

- Poster presentation titled "An *in vitro* model to evaluate the effect of a polyvalent bacteriophage combination on a *Staphylococcus aureus* biofilm under continuous flow conditions"

23rd January 2014 - Exploiting bacteriophages for bioscience, biotechnology and medicine (London, UK)

- Presentation titled "Isolation of bacteriophage cocktail effective on the eradication of *Staphylococcus aureus* biofilms"

10th – 12th September 2014 - Phages2013: Bacteriophage in Medicine, Food and Biotechnology (Oxford, UK)

- Poster presentation titled “Development and characterization of a responsive polyvalent bacteriophage therapeutic”

17th - 24th August 2013 - BioNano 2013 summer school (Hirschegg, Austria)

- Presentation titled “Model systems to study biofilm formation”

14th - 16th January 2013 - NTU workshop on Materials for Smart Wound Dressings (Singapore)

- Poster presentation titled “Development and characterization of a responsive polyvalent bacteriophage therapeutic”

Awards

June 2013 – Image of research short selected to be exhibited in the Fringe Arts Bath Festival, Bath. Event: Images of Research Competition, University of Bath

http://www.bath.ac.uk/research/images-of-research

Publications

Alves, D.R., Beeton, M.L., Enright, M.C. and Jenkins, A.T.A. (2015) Assessing phage therapy against Pseudomonas aeruginosa using a *Galleria mellonella* infection model. J Antimic Chem. 46 (2), pp.196-200 (IF = 4.26)

Bean, J.E., **Alves, D.R.**, Laabei, M., Pérez Esteban, P., Thet, N.T., Enright, M.C. and Jenkins, A.T.A. (2014) Triggered Release of Bacteriophage K from agarose/hyaluronan hydrogel matrixes by *Staphylococcus aureus* virulence factors. Chem Mater. 26 (24), pp. 7201-7208 (IF = 8.54)

Alves, D.R., Gaudion, A., Bean, J., Pérez Esteban, P., Arnot, T.C., Harper, D.R., Kot, W., Hansen, L.H., Enright, M.C. and Jenkins, A.T.A. (2014) Combined use of bacteriophage K and a novel bacteriophage to reduce *Staphylococcus aureus* biofilm. Applied and Environmental Microbiology. 80 (21), pp. 6694-6703 (IF = 3.95)

Esteban, P.P., **Alves, D.R.**, Enright, M.C., Gaudion, A., Jenkins, A.T., Young, A.E., Arnot, T.C. (2014). Enhancement of the antimicrobial properties of bacteriophage-k via stabilisation using oil-in-water nano-emulsions. Biotechnol Prog. 30 (4), pp. 932-944 (IF = 1.88)

Submitted

Alves, D.R., Pérez Esteban, Kot, W., Bean, J., P., Arnot, T.C., Hansen, L.H., Enright, M.C. and Jenkins, A.T.A. (2015) A novel bacteriophage cocktail reduces and disperses Pseudomonas aeruginosa biofilms under static and flow conditions. Microbial Biotecnology.

Table of contents

List of tables

List of figures

Acronyms and abbreviations

Abbreviation	Full Name
ATCC	American Type Culture Collection
CA-MRSA	Community-acquired MRSA
CF	Cystic Fibrosis
Cfu	Colony Forming Units
CI	Confidence Interval
CLSM	Confocal Laser Scanning Microscopy
CsCl	Cesium Chloride
CV	Crystal Violet
DLS	Dynamic Light Scattering
EPS	Extracellular Polymeric Substance
ETA	Exotoxin A
FAS	Ferrous Ammonium Sulphate
G. mellonella	*Galleria mellonella*
GISA	Glycopeptide intermediate *S. aureus*
HA-MRSA	Hospital-acquired MRSA
HGT	Horizontal Gene Transfer
ICTV	International Committee for Taxonomy of Viruses
IgG	Immunoglobulin G
LB	Luria-Bertani
LPS	Lipopolysaccharide
MDR	Multi Drug Resistance
MDT	Multi Drug Tolerance
MIC	Minimum Inhibitory Concentration
MLST	Multi-locus Sequence Typing
MOI	Multiplicity of Infection
MRD	The Modified Robbins Device
MRSA	Methicillin resistant *Staphylococcus aureus*
MSCRAMMS	Microbial Surface Components Recognizing Adhesive Matrix
MSSA	Methicillin sensitive *Staphylococcus aureus*
OD_{590}	Optical Density at 590 nm
ORF	Open Reading Frame
P. aeruginosa	*Pseudomonas aeruginosa*
PBS	Phosphate Buffered Solution
PCR	Polymerase Chain Reaction
PEG	Polyethylene Glycol

pfu	Plaque Forming Units
VL	Panton Valentine Leukocidin
RFLP	Restriction Fragment Length Polymorphism
S. aureus	*Staphylococcus aureus*
S. epidermidis	*Staphylococcus epidermidis*
SCCmec	Staphylococcal cassette chromosome *mec*
TBE	Tris/Borate/EDTA
TEM	Transmission Electron Microscopy
TSA	Tryptic Soy Agar
TSB	Tryptic Soy Broth
TSS	Toxic Shock Syndrome
TSST-1	Toxic Shock Syndrome Toxin-1
UV	Ultraviolet
VISA	Vancomycin Intermediate *Staphylococcus aureus*
YPD	Yeast Extract-Peptone-Dextrose

Chapter One:

LITERATURE REVIEW

1.1. The clinical problem and the challenge

The discovery of antibiotics in the last century was one of the most important developments in medicine and a milestone in the history of modern human society. Before the introduction of antibiotics infectious diseases were a major cause of mortality due to the systemic infection and sepsis resulting from wound infections, pneumonia, childbirth and even, in modern-day terms, comparatively minor infections such as gonorrhoea. In the absence of antibiotics performing organ transplants, routine surgery and cancer chemotherapy would be impossible.

Antibiotics have been poorly regulated, leading to inappropriate use, for example to treat viral infections, as growth promoters in animals and the widespread use of broad-spectrum antibiotics. In many countries antibiotics are widely available over the counter. This behaviour, going on around the world for several decades, has led to the emergence of bacteria that have evolved resistance to multiple antibiotics and currently some infections once easily curable are now difficult or impossible to treat (1). Figure 1.1 illustrates the development process for new antimicrobials which has become increasingly contracted (2) and every time a drug comes to market bacteria rapidly develop resistance to it (Figure 1.2). One notable exception to this is the newly formulated gram-positive antibiotic, teixobactin that inhibits cell wall synthesis yet in the initial report at least did not lead to the development of resistant mutants, which is some cause for optimism (3). This current situation alongside the massive costs associated with antibiotic discovery and clinical trials make investment in developing new antibiotic drugs by pharmaceutical companies less appealing (i.e. low return on investment) (4), instead they are redirecting their efforts towards the development of drugs targeting chronic diseases (with the potential for prolonged profits). For example, in 2004 only 1.6 % of drugs in clinical development by the major pharmaceutical companies were antibiotics (5). This lack of new agents aggravates the problem of emerging resistance which results in higher patient mortality and larger health care

costs (6). Infections caused by a pathogen resistant to the drug of treatment generally have a higher risk of poor clinical outcome (possibly death) and are also linked to a greater consumption of healthcare resources, when compared to infections caused by antibiotic-sensitive organisms. In the US it was estimated that annual healthcare costs of infections related to antibiotic resistance range from $21 billion to $34 billion and more than 8 million additional hospital days (7). Comparatively, in the EU it was estimated that costs reach €1.5 billion annually for hospital care (8). Inappropriate antibiotic prescribing often starts in the young, with infants and children being prescribed improperly with antibiotics for self-limiting infections, viral upper respiratory tract infections and prophylactic use (9). Bergus and colleagues in a study conducted in Iowa, United States, concluded that of all the antibiotic prescriptions for children, 53 % were given to children under four years old and 70 % of infants received at least one antibiotic during their first 200 days of life (10, 11).

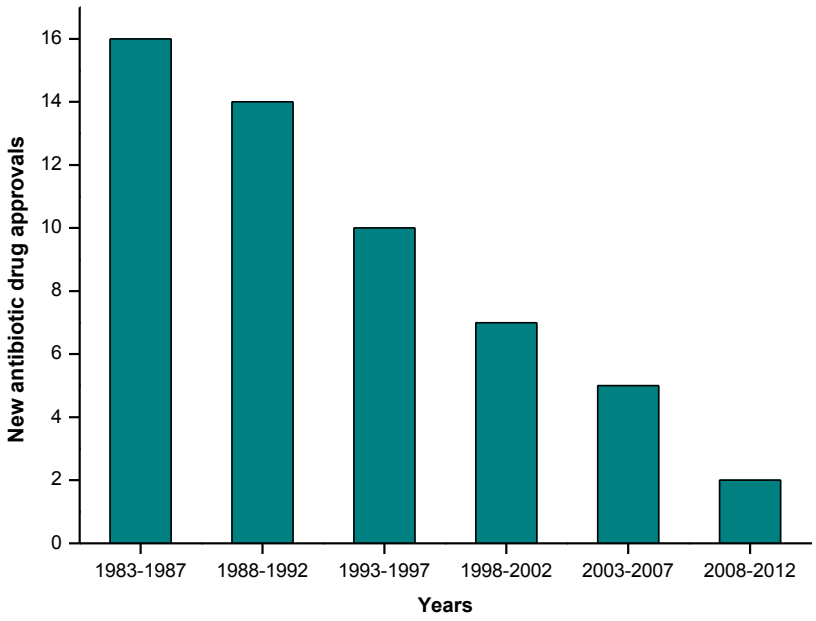

Figure 1.1: Number of new systemic antibiotics approved by the US FDA per five-year period (adapted from 6).

The misuse and overuse of antibiotics has not only been a problem seen in human clinical settings, but also a frequent scenario in agriculture, aquaculture and animal farming. Alarmingly, they are mainly used as a disease preventive measure and are used as a normal component, for instance, of the normal feed of the animals, often given in sub-therapeutic concentrations (12). This situation has also lead to selection and propagation of antibiotic resistant strains in such environments, turning them into reservoirs that contribute to transmission and introduction of new superbugs. These antibiotic resistance "networks" go on to cause diseases in humans, where foodborne transmission is the more likely route of transmission (13).

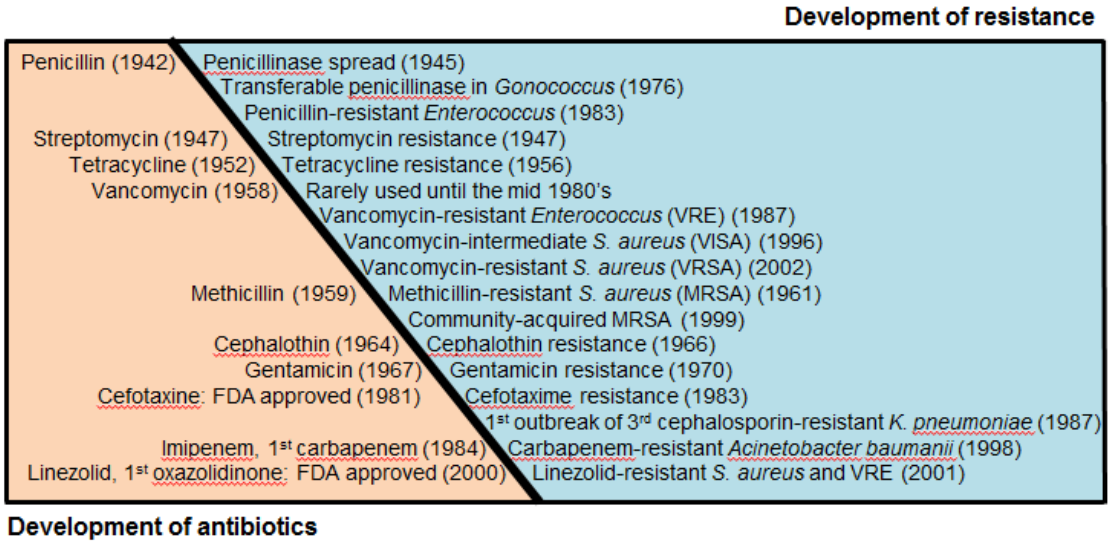

Figure 1.2: History of antimicrobial agent development and the subsequent appearance of resistance by bacteria (adapted from 14).

In recent years, awareness regarding bacterial antibiotic resistance has been increasing and several measures have come out worldwide to tackle and control the problem. In 1998, the first of a series of 'World Health Assembly (WHA) resolutions on antimicrobial resistance (AMR)' (15) were established, followed by the '2001 WHO Global Strategy for Containment of AMR' (16), the '2011 EU AMR Strategic Action Plan' (17) and the '2012 EU Council Conclusions' (18). In 2003 the European Union banned the use of antibiotics for animal growth promotion (19) and in 2012 the FDA

stopped the arbitrary use of antibiotics on animals, so that they are only permitted when prescribed by a veterinarian (20). The British government also issued 'The Five Year Antimicrobial Resistance Strategy 2013 to 2018' where the main issues to address are (21):

- A better prevention, management and surveillance of infections both in people and farming;
- Improving education and training of both medical and nursery staff, but also of patients;
- A better data collection on resistance profiles for an earlier and more efficient treatment of infections;
- Providing funding for research, exploring alternative ways for development of new antibiotics, a rapid diagnosis and other therapeutic alternatives.

Antibiotic resistance needs to be accepted as a huge, complex and multifactorial global problem that requires a substantial change of behaviour. The key feature of these strategies and the upcoming ones is the synchronisation of efforts from all sectors, all working together towards a common direction; these include not only the human health side, but also the animal and agriculture one, industry and Governments, doctors, vets, farmers, patients and obligatory, scientists.

Research plays an important role in overcoming the antibiotic resistance problem; hence efforts are ongoing to discover and develop new ways of treating antibiotic resistant bacteria and to reduce their clinical impact on our lives.

1.2. Wound infections

The skin is our body's largest defence from invading harmful microorganisms that can colonise and damage the underlying tissues, but it plays a multitude of other roles,

including thermoregulation and body fluid homeostasis. However, the skin being the most exposed organ can be vulnerable to environmental threats and when a breach of the skin occurs following a burn or a wound for example, normal skin colonising bacteria can enter the deeper tissues, where a moist, warm and nutritive environment allows bacteria to proliferate causing localised inflammation, sometimes followed by wider dissemination. In Figure 1.3 the anatomy of the skin is outlined.

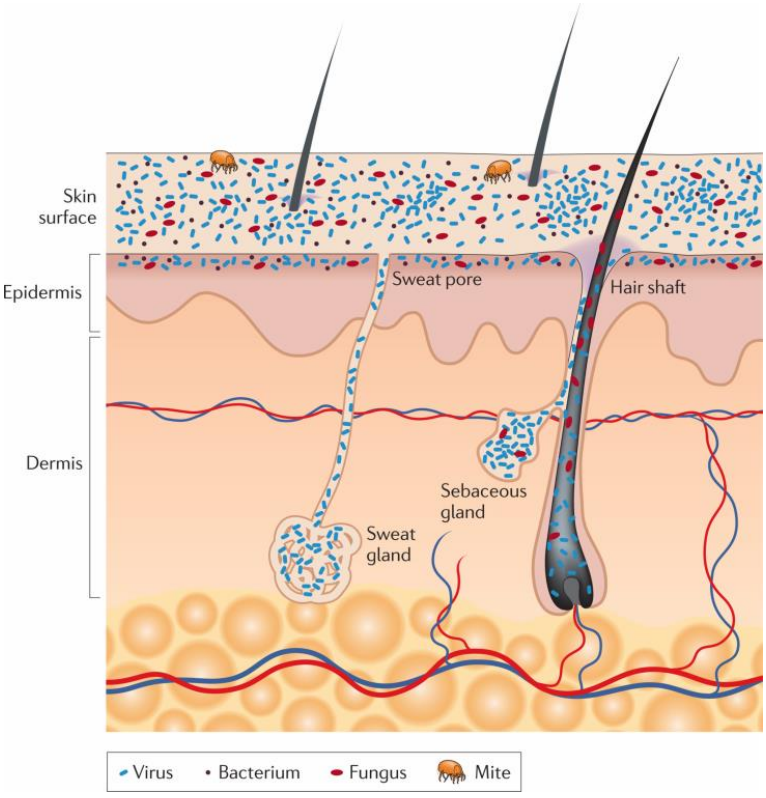

Figure 1.3: Skin anatomy with commensal flora viewed in cross-section. Reprinted from reference (22) and used with permission.

1.2.1. Wounds: acute and chronic

An acute wound is usually caused by an external factor that damages and breaches the skin. Examples of such wounds are surgical wounds, bites, burns, cuts and lacerations. The normal healing process of acute wounds shows four phases: coagulation, inflammation, formation of granulation tissue and scarring.

A chronic wound is described as a wound where the normal healing process observed for an acute wound does not take place. Usually the occurrence of a chronic wound happens with a small traumatic injury. However, due to patient pre-disposition, such as diabetes, it will develop to chronicity instead (23). The most common chronic wounds are diabetic foot ulcers, pressure ulcers, venous leg ulcers and ischemic ulcers (24). These always involve an unusually highly prolonged inflammatory phase, which predisposes for persistent infections and consequently the formation of persistent biofilm communities (24).

The advent of an infection on an acute wound will delay the normal healing process and for a chronic wound might result in non-healing for months (25).

1.2.2. Microbiology of wounds

In the moist surface of a wound, subcutaneous tissues are exposed and provide a nutrient-rich environment, mainly in the form of long-chain fatty acids (26), which often shows signs of low blood supply (ischaemia), inadequate oxygen supply (hypoxia), necrosis and most likely a disrupted normal immune response. Hence, the wound environment becomes ideal for bacteria to colonise, proliferate and establish an infection. The main source of bacterial wound contamination is the patient's normal body flora, whether living endogenously (essentially the gut, mouth and genitourinary tract) or from the skin as well as from the surrounding environment. Generally, a wound infection, whether acute or chronic, will be shown to have a mixture of several bacterial populations, where anaerobic and aerobic bacteria are present, but also fungi and viruses (27). However, standard culturing methods overlook many of these bacteria, especially the anaerobes, that can be revealed when molecular techniques are applied (28). The microbiome of the wound is also dependent on the wound type itself (site, depth) and the geographical area of the patient. For example, in a study in

an Indian hospital it was found that *P. aeruginosa* was the most common isolate from burn wounds (59 %), followed by *S. aureus* (17.9 %), *Acinetobacter* spp (7.2 %), *Klebsiella* spp (3.9 %), *Enterobacter* spp (3.9 %) and *Proteus* pp (3.3 %) (29). In another study in Turkey it was found that *Acinetobacter baumannii* was the isolate most frequently found in burn patients (23.6 %), followed by coagulase-negative *Staphylococci* (13.6 %), *P. aeruginosa* (12 %), *S. aureus* (11.2 %), and *Escherichia coli* (10 %) (30). The fate of a wound infection is determined by several factors, such as the location, size and depth of the wound, the load, virulence profile and interaction of the pathogens growing and colonising the wound, the levels of blood getting to the wound and, of course, the health condition of the patient. For example, Djahmi and colleagues (31) reported that patients suffering from diabetic foot ulcers had a worse outcome when colonised with PVL-positive *S. aureus* isolates (PVL is a potent cytotoxin).

Despite the multifactorial factors influencing the microbiology and development of a wound infection it is possible to generally identify the main causative organisms. Hence, *Staphylococcus aureus* (*S. aureus*) and *Pseudomonas aeruginosa* (*P. aeruginosa*) are the most common pathogens isolated from acute and chronic wounds (32, 33). The latter is usually the first pathogen to begin an infection on a chronic wound (34). Often, then associated with other less represented bacteria, such as *Enterococcus* spp, *S. epidermidis* and *Klebsiella pneumoniae*.

These pathogens, in order to colonise and invade the host tissues, display an array of enzymes and toxins harmful to the host cells and connective matrix and have multiple mechanisms involved in subverting host immune system responses.

1.2.3. Nosocomial infections

Generally, for patients suffering from a moderate to severe burn wound there is, at some point, a need to visit the hospital, where contamination from the hospital environment is of great concern. In this setting, bacterial pathogens may be transferred to the wounded patient through contact with contaminated surfaces, water, air and via health care worker's hands. *S. aureus and P. aeruginosa* are two of the pathogens most often isolated in hospital settings (35, 36), resulting in prolonged hospitalisation, increased morbidity (such as sepsis, bacteraemia) and large economic losses (37). Therefore, an effective infection control policy is needed in order to eradicate or reduce pathogenic bacteria, particularly antibiotic resistant ones, and prevent cross-infection (38).

1.2.4. Wound infections and biofilm formation

Wound infections can often develop into a biofilm and more often than not this is observed for chronic wound infection. It has been documented that more than 60 % of chronic wounds contain a biofilm, whereas only a small percentage (6 %) are of concern in acute wounds (39). The presence of a biofilm will delay the process of wound healing and scarring and in consequence adversely affect the patients' health (Figure 1.4). Biofilms are much less susceptible to the action of the immune system, for example chemotaxis is inhibited and polymorphonucleocytes (PMNs) are prevented from engulfing the bacterial cells trapped in the biofilm, causing a massive release of cytokines that contribute to the chronicity of the infection (necrotic tissue and inflammation) (40). Hence, it is very important to recognise the presence of a biofilm in order to deliver the best treatment approach.

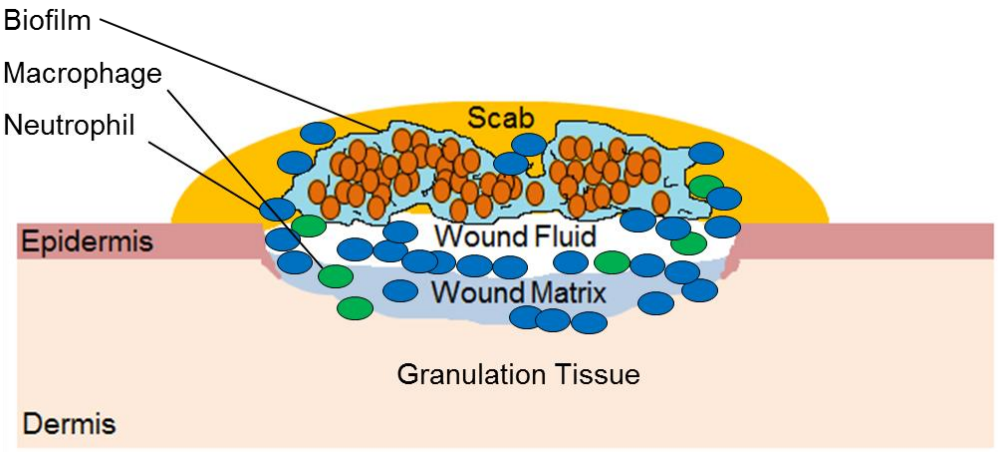

Figure 1.4: Representation of a biofilm established on a skin wound.

1.3. *Staphylococcus aureus*

Bacteria belonging to the genus *Staphylococcus* are gram-positive cocci that typically grow in clusters (from the Greek *staphylé*, meaning "a bunch of grapes"). Typical Staphylococci are 0.5 – 1.5 μm in diameter, non-motile, facultative anaerobic and are able to grow at high salt concentrations and at temperatures ranging from 18°C to 40°C. A number of species in the genus are human pathogens, including *S. aureus*, *S. epidermidis*, *S. haemolyticus*, *S. lugdunensis* and *S. saprophyticus*.

A distinguish feature of *Staphylococcus aureus* (Figure 1.5) is the fact that is the only species of the genus producing coagulase, an enzyme that catalyses the conversion of fibrinogen into fibrin, which is a distinguishing feature of this species. *S. aureus* is a ubiquitous organism and a common coloniser of humans, usually found in the anterior nares, but also in the skin, oropharynx, gastrointestinal tract and urogenital tract. Approximately 20 % of the population have the anterior nares colonised permanently by *S. aureus*, and around 60 % carry the bacterium periodically (41). Because the pathogen colonises our skin and nares and additionally adheres to dry surfaces, it is easily spread between individuals, either through direct or indirect contact (i.e. from

contaminated surfaces). *S. aureus* is known to cause a varied spectrum of diseases affecting tissues such as the skin (impetigo, wound infections), the respiratory tract (pneumonia, empyema), bone (osteomyelitis), the central nervous system (meningitis) and the vascular compartment (endocarditis, thrombophlebitis) (Lowy, 1998). In addition, the pathogen is one of the main causes of infection from medical devices such as catheters and surgical implants (42).

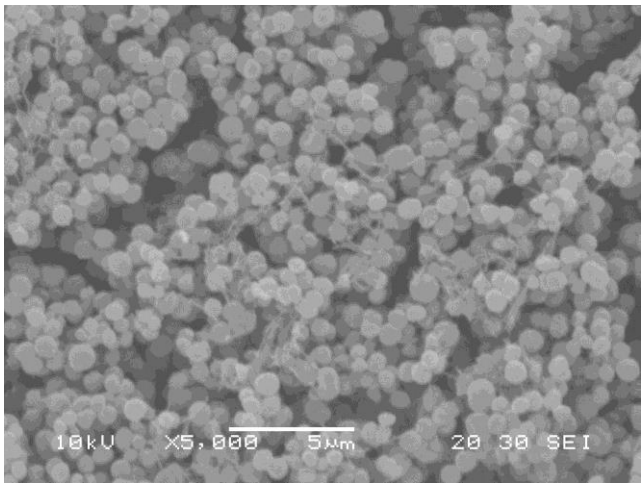

Figure 1.5: Scanning electron microscopy (SEM) of *Staphylococcus aureus* bacteria (courtesy of Dr Naing Thet).

1.3.1. Virulence Factors

S. aureus is known to be a dangerous pathogen able to counteract and avoid the human defences, causing serious disease. This is driven by a number of intrinsic aspects acting together that comprise structural components, toxins and enzymes (Figure 1.6).

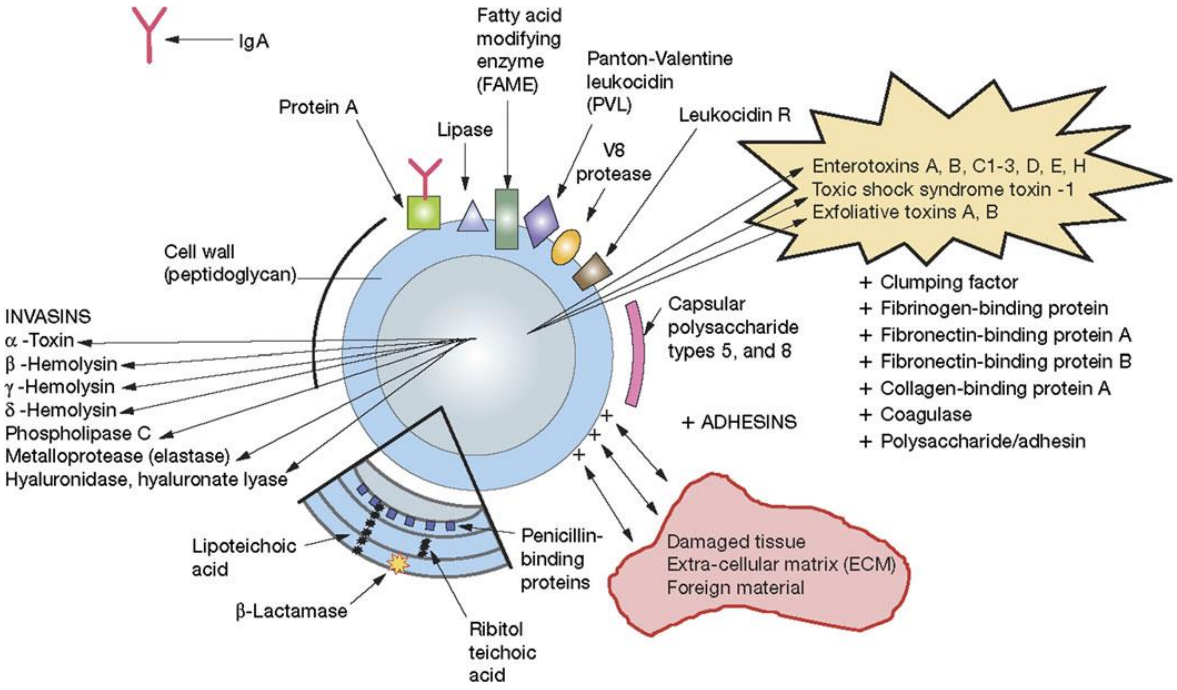

Figure 1.6: *Staphylococcus aureus* virulence factors. Reprinted from reference (43) and used with permission.

1.3.1.1. Structural Components

To initiate an infection, *S. aureus* adheres to host tissues and prosthetic devices driven by a range of surface proteins known as microbial surface components recognising adhesive matrix molecules (MSCRAMMS) (44). The majority of *S. aureus* strains express a polysaccharide capsule (45) which protects the bacterium from phagocytosis. There are 11 capsular serotypes described to date, but serotypes 5 and 8 are the most predominant and most clinically relevant (46). The capsule can be covered by a slime-layer, consisting of proteins and monosaccharides that facilitate the adherence of the bacterium to host tissue and other surfaces. The cell wall is composed of two major components: peptidoglycan and teichoic acids. Peptidoglycan displays endotoxin-like activity which stimulates the immune system and the teichoic acids facilitate the bacterium adhesion to mucosal surfaces. Anchored in the cell wall is Protein A, which plays an important role in the pathogenesis of *S. aureus*. It has high

affinity for the Fc region of Imunoglobulin G (IgG) (47), which results in IgG molecules coating the cell wall. However, the IgG molecules are in an incorrect orientation to be recognised by the neutrophil Fc receptors thus effective phagocyte recruitment is prevented (48). Experiments regarding animal infection models and protein A-deficient mutants of *S. aureus* demonstrate a reduction in virulence (49). *S. aureus* is able to resist the human bactericidal protein lysozyme by altering the structure of its cell wall muramic acid and lysis of the bacterial cell does not occur (50).

1.3.1.2. Toxins

S. aureus produces a large number of toxins that play an essential role in virulence: five cytolytic toxins, two exfoliative toxins, several enterotoxins and toxic shock syndrome toxin-1 (TSST-1) have been recognised. Cytolytic toxins – α, β, δ, γ and Panton Valentine leukocidin (PVL) - facilitate the lysis of host cells, such as erythrocytes, leukocytes, fibroblasts, macrophages and platelets, by forming β-barrel pores in the cytoplasmic membrane. This disruption causes the swelling of the cell due to an osmotic imbalance - efflux of K^+ and influx of Na^+ and Ca^{2+}, among other molecules. The PVL protein has specific toxicity to leukocytes and it is strongly associated with increased virulence in necrotising diseases (51). The *pvl* gene, carried in a lysogenic phage, is found in 2 % of randomly selected *S. aureus* strains (52), with higher occurrence identified in community-acquired MRSA (CA-MRSA) (53) lineages. The exfoliative toxins (ETs), ETA and ETB, are serine proteases that cleave an important molecule in the cell-cell adhesion (54). These toxins are responsible for the staphylococcal scalded skin syndrome (SSSS) (for review see 55, 56), a serious dermatitis affecting mostly young children (57). Staphylococcal enterotoxins are a family of heat-stable toxins, resistant to gastric enzymes that can cause food poisoning (58).

Enterotoxins along with TSST-1 act as superantigens causing T-cell activation leading to massive pro-inflammatory cytokine release (see below).

1.3.1.2.1. Toxic shock syndrome toxin-1 (TSST-1)

The superantigen toxin TSST-1 is able to bind to the exterior region of the MHC class II protein in the surface of antigen-presenting cells (APC) and link it to the receptor of a T-helper cell. The non-specific activation of T-cells - up to 30 % can be activated (59) - leads to a massive and uncontrolled proliferation of cytokines causing a cytotoxic effect to host cells. The toxin is also able to penetrate mucosal barriers (e.g. burn wound sites) and enter the bloodstream contributing to toxic shock syndrome (TSS), which can culminate in death caused by hypovolemic shock, leading to multi-organ failure (60). A proposed model of cascade signalling and invasion of TSST-1 on the vaginal surface is illustrated in Figure 1.7 and a parallel can be made to what happens on the surface of a burn wound. Antibodies against TSST-1 toxin have been shown to increase with age and 95 % of individuals show protection at the age of 30, so children are presumably at greater risk as a result of lower antibody protection (61).

1.3.1.3. Enzymes

S. aureus are “armed” with a pool of enzymes that, once more, enable the bacteria to spread and manipulate the human body defences. All *S. aureus* are producers of coagulase. Coagulase appears under two forms: bound and free. Both forms result in the same outcome – conversion of fibrinogen to insoluble fibrin – however one is able to react directly (bound form) and the other goes through a reaction cascade (free form). Fibrin covers the bacterial surface and phagocytosis is prevented. The enzyme catalase acts to convert hydrogen peroxide to water and oxygen. Hydrogen peroxide is

a toxic molecule resulting from bacterial metabolism and is a commonly accumulated molecule inside phagocytic cells. Another enzyme that aids bacterial invasion of host tissue is hyaluronidase. Hyaluronidase breaks down the hyaluronic acids, a major element of the matrix in the connective tissue (63). Staphylokinase interacts with and inactivates the bactericidal α-defensins (64) produced by neutrophils (65). Such enzyme interacts with plasminogen which results in a complex capable of dissolving fibrin, hence, enabling the bacteria to penetrate the human tissue (66).

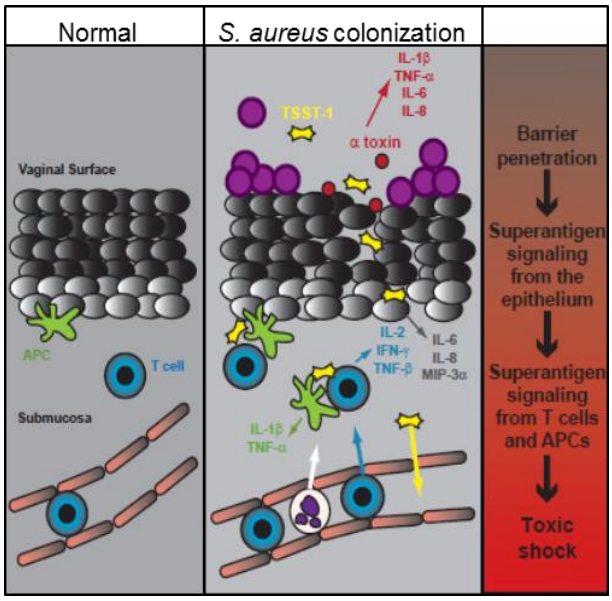

Figure 1.7: Proposed model for the cascade signalling caused by TSST-1 on the vaginal surface. *S. aureus* (purple) colonising a body surface secretes cytolysins, such as α-toxin (red), causing mucosal barrier disruption. Then, TSST-1 (yellow) can penetrate more easily the mucosa to reach the lower levels of the epithelium, where the superantigen toxin stimulates production of cytokines (such as, IL-8), that in turn recruit adaptive immune cells to the submucosa. TSST-1 interacts with T-cells (blue) and APCs (green) to stimulate a cytokine cascades that leads to TSS. Adapted and reprinted from reference (62) and used with permission.

1.4. *Pseudomonas aeruginosa*

Bacteria belonging to the genus *Pseudomonas* are gram-negative non-fermentative motile rods, typically measure 0.5 – 1 by 1.5 – 5 μm and are arranged in doublets that resemble a single cell (from the Greek "*pseudes*" and "monas", meaning false unit) (Figure 1.9). The bacteria can tolerate a wide range of temperatures (from 4^{o}C to 42^{o}C) and despite being considered as obligate aerobes this is not entirely true, as these bacteria can also grow anaerobically by using nitrate or arginine as the final electron acceptor. Colonies from this genus can appear mucoid and/or pigmented as many strains produce a thick and viscous polysaccharide capsid and produce diffusible pigments, such as pyocyanin (blue), pyorubin (red-brown) and pyoverdin (yellow-green). More than 200 species compose the genus; however *Pseudomonas aeruginosa* is the major human pathogen considered the most important.

P. aeruginosa are bacteria with minimal growth requirements that are highly versatile, triggering different metabolic pathways depending on the available energy source, this allows them to be ubiquitous in nature (67) and, if given the opportunity, are able to become serious and even fatal disease causing agents. *P. aeruginosa*, contrasting to what was described above for *S. aureus*, usually is not part of the normal commensal flora in humans. Hence, disease scenarios occur mainly in hospital settings, where the environmental bacterium closely related to water environments can cause infections via, for example aerosols aspiration of contaminated tap water or direct contact with contaminated humid surfaces (68), that readily colonises the human skin (69), being particularly problematic for patients with a compromised immune system (70). From the wide range of infections caused by *P. aeruginosa*, one can mention the chronic pulmonary infections in cystic fibrosis patients, skin and soft tissue infections of severe burn wound victims that can lead to bacteraemia, but nevertheless pneumonia and infections associated to the urinary tract, the ear (external otitis) and the eye (corneal ulcers).

1.4.1. Virulence factors

Pseudomonas aeruginosa (Figure 1.8) is armed with several virulence factors, ranging from adhesins, toxins and enzymes to a type III secretion system that together allow the bacteria to propagate and counteract the host immune "guard", causing an infection.

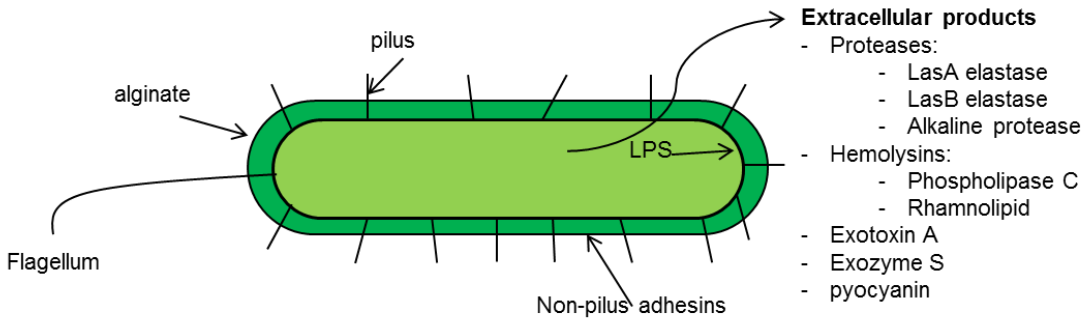

Figure 1.8: *Pseudomonas aeruginosa* virulence (adapted from 70).

1.4.1.1. Adhesins

P. aeruginosa is provided with four types of structures that assist them in host adherence: flagella, pili, lipopolysaccharide (LPS) and alginate. Both the flagella and the type IV pili are responsible for motility (72) and adherence to epithelial tissues (73–75). The LPS is responsible for the inflammatory effects that play an important role in virulence (76) and it slows down the entrance of antibiotics (77). It consists of a lipid A region that anchors the LPS to the outer membrane of the bacterium, the core oligosaccharide and a projected highly variable O-antigen side chain, that is composed of a series of saccharide units conferring serotype specificity. So far there are 20 recognised *P. aeruginosa* serotypes (78). The O-antigen seems to be crucial for the virulence phenotype of the LPS; several studies using mutants deficient in O-antigen showed a reduced virulence along with a reduced dissemination when compared to the

wild-type bacteria (79, 80). Another virulence factor that many strains produce is the exopolysaccharide alginate. Its accumulation produces a thick capsule around the bacterial surface, which gives protection from external threats; this includes reduced chemotaxis and consequently phagocytosis and inhibition of complement (81, 82). Alginate, together with two other exopolysaccharides, PsI and Pel, have a major role in *P. aeruginosa* biofilm formation stages and protection from antibiotic drugs (83), their regulation is complex posing an additional major problem for CF patients infected by the bacteria (discussed below).

1.4.1.2. Toxins and enzymes

Several toxins and enzymes produced by *P. aeruginosa* make them common, versatile and difficult pathogens to eradicate. Exotoxin A (ETA) contributes for its pathogenesis (84); the exotoxin once inside eukaryotic cells is able to disrupt protein synthesis, by causing the ADP ribosylation of the eukaryotic elongation factor 2 (85). This will result in tissue damaging, that is often observed in ocular and chronic pulmonary infections.

The pigments also act as virulence factors: pyocyanin interferes with several eukaryotic cell functions, including cell respiration (86) and apoptosis of neutrophils (87); pyoverdin is a siderophore which binds to iron and transports it through the bacterial membrane to be used in the bacterial metabolism (88); it also regulates production of other virulence factors, including ETA (89).

Two elastases, LasA (a serine protease) and LasB (a zinc metalloprotease) are produced by the *P. aeruginosa* that by acting together degrade elastin (90). Elastin is a major component of human connective tissue and these enzymes are responsible for their damage causing the typical ecthyma gangrenosum (lung parenchymal damage and haemorrhagic lesions) associated with disseminated *P. aeruginosa* lung infections. It also regulates the secretion of two other extracellular enzymes: exoenzymes S and

T (91). The type III secretion system is then responsible for introducing the enzymes into the eukaryotic cells, facilitating bacterial dissemination, tissue invasion and necrosis. Two homologous phospholipases C (PLC) are secreted - a non-haemolytic and a haemolytic one. Whereas the first seems not to be associated with pathogenicity, the haemolytic PLC is highly virulent being responsible for degrading lipids and lecithin, facilitating tissue destruction and death when it is administered into mice (92).

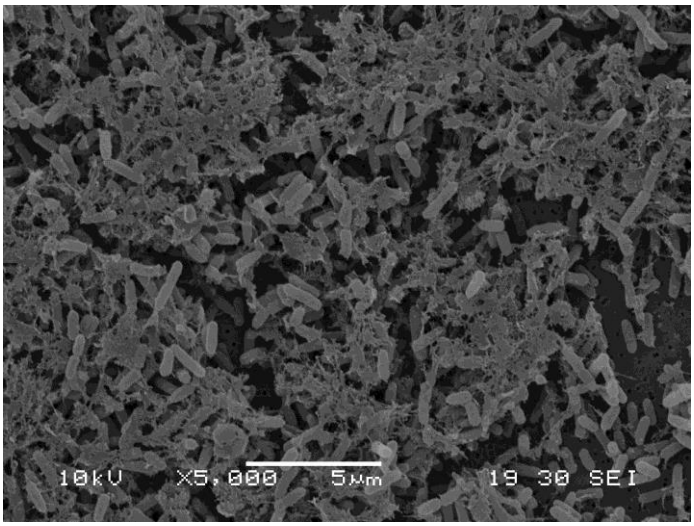

Figure 1.9: Scanning electron microscopy (SEM) of *Pseudomonas aeruginosa* bacteria (courtesy of Dr Naing Thet).

1.4.2. Cystic fibrosis

Cystic fibrosis (CF) is a genetic disorder associated with high mortality rates which is caused by mutations in the cystic fibrosis conductance regulator (CFTR) gene (93). It is the most common genetic disease amongst Caucasian populations (94). The defect in the regulator, a channel expressed primarily in the epithelial cells that pumps chloride to the extracellular space, disrupts electrolyte secretion, commonly leading to several complications, including pancreatic insufficiency, abnormal function of secretory glands and highly viscous bronchial secretions. Such a situation in the lungs impairs the

normal control of bacterial colonisation as the thick mucus in the airways is not efficiently cleared; resulting in ideal environments for the establishment of chronic infections mainly populated by *P. aeruginosa* biofilms (95).

.

1.5. Antibiotic resistance

Antibiotic resistance occurs through genetic mutations and/or acquisition through horizontal gene transfer (HGT) of resistant determinants (for review 92). The rate at which bacteria acquire resistance is determined by the bacterial mutation and recombination rates, the biological cost of resistance (97) and selective pressure, e.g. antibiotic use (98). Resistance genes can be found on transferable genetic elements, such as plasmids, integrons and transposons. These elements can spread very fast in bacterial populations crossing species barriers to accelerate the rate of resistance determinant acquisition (99).

The most common mechanisms for antibiotic resistance are: alteration of antibiotic targets, enzymatic modification and degradation of the antibiotic and drug efflux from the bacteria cell (100).

1.5.1. Methicillin-resistant *Staphylococcus aureus* (MRSA)

The first *S. aureus* isolate resistant to methicillin was identified one year after the introduction of methicillin (Figure 1.2). Methicillin is a narrow-spectrum beta-lactam antibiotic and resistance to it is caused by production of a modified penicillin-binding protein – PBP2a. PBPs are enzymatic proteins responsible for peptidoglycan synthesis that occur in the bacterial cell wall. The modified PBP shows lower affinity for binding the beta-lactam drugs (101), and bacterial growth is not affected. It is encoded by the *mecA* gene carried in the staphylococcal cassette chromosome mec (SCCmec), a

mobile genetic element integrated in the MRSA chromosome (102). The SCCmec element is composed of the *mec* gene complex – *mecA* and its regulator - and the *ccr* gene complex – *ccrA*, *ccrB* and *ccrC* site-specific recombinases. The recombinases are the ones responsible for the dissemination of the genetic element within *S. aureus* populations (103). Depending on how the *mec* gene complex and the *ccr* are combined they can be classified into different types; so far eight types of SCCmec have been reported , however VI – VII are rarely observed (104). Hospital-acquired MRSA strains are more related to SCCmec types I-III, whereas community-acquired MRSA are associated to SCCmec types IV and V. The acronym MRSA is currently used to refer any *S. aureus* strain resistant to antibiotics of the β-lactam group, such as oxacillin, penicillin and amoxicillin.

MRSA is currently one of the most prevalent pathogenic bacteria causing nosocomial and community infections, such as acute skin and soft-tissue infections, but also chronic wounds (105–107). According to a study in 2005 there were almost 19,000 deaths in United States caused by MRSA (108) and more than 65 % of all the community acquired *S. aureus* infections were methicillin-resistant (109). As a result, MRSA is recognised as a major public health threat.

Additionally, vancomycin intermediate *S. aureus* (VISA) and glycopeptide-intermediate *S. aureus* (GISA) isolates have started to emerge (110), in fact vancomycin resistant *S. aureus* (VRSA) isolates were also already reported (111) and the same is being observed for antibiotics such as linezolid (oxazolidinone) and daptomycin (lipopeptide) (112, 113). Therefore, even antibiotics such as vancomycin, the so called antibiotic of ‘last resort’ that used to be effective against MRSA are becoming increasingly ineffective in treating *S. aureus* infections.

1.5.2. Multidrug Resistant (MDR) *P. aeruginosa*

P. aeruginosa antibiotic resistant isolates have been significantly increasing for the past two decades (114) and we are therefore dealing with a bacterium that has been shown to display almost all known mutational mechanisms of bacterial resistance (115). The combination of all the mechanisms is translated into a bacterium showing a multidrug resistant phenotype (resistance to at least 3 antibiotics) and is a result of several situations. The low permeability of the cell wall makes the bacteria intrinsically resistant to many drugs, the expression of several efflux pumps and the acquisition of chromosomal mutations in the genes that code for the drug target are examples of some of the resistance mechanisms in *P. aeruginosa* (115). Its high rate of recombination and acquisition of new genes also contributes to such fast evolution causing a high gene diversification among isolates (116). Chromosomal mutations, accelerated certainly by the use of antibiotics, are related as well to the hypermutability character found in several *P. aeruginosa* isolates. Hypermutability is related to defects in the methyl-directed mismatch repair (MMR). Such a system is responsible for recognition and repair of any mutation inserted while DNA replication takes place; if this system fails as a consequence higher mutation rates are going to arise in the population. Hence, *P. aeruginosa* isolates have the chance to become resistant to a drug very quickly, sometimes this is even observed while the treatment is running (117). This is a major problem concerning CF patients, where it has been documented that rates of mutation are higher for strains isolated from this patients than rates observed in other settings (118). In fact, it was reported in a study in CF patients suffering from a chronic *P. aeruginosa* infection that 36 % of the isolates showed a hypermutability phenotype (118). For this reason, it was suggested that monotherapy for *P. aeruginosa* in CF patients should be restricted and only drug combinations should be administered in an attempt to avoid resistance emergence (119).

1.5.3. Alternatives to treat antibiotic resistant bacteria

The occurrence of antibiotic resistance in such globally prevalent pathogens, such as *S. aureus* and *P. aeruginosa*, has triggered an immense focus on research for alternatives that might complement or replace the conventional drug therapeutics. Several alternatives are now in the spotlight, including bacteriocins and bacteriophages. The latter is going to be further explored in the forthcoming sections.

Bacteriocins, a type of antimicrobial peptide (AMP), are small ribosomally synthesised peptides that are produced by practically all types of bacteria and are lethal to other bacteria as a mechanism of defence. The peptides insert into the membrane of the target bacteria, causing pores on the membrane and consequently lysis is the general mode of action (120). Being considered relatively safe, many bacteriocins are indeed already in use by the food industry. This includes nisin, a bacteriocin secreted by lactic acid bacteria, with potential to disrupt biofilms produced by MRSA isolates (121). It has GRAS (generally recognised as safe) status and has been long used as a food preservative. Resistance can be observed usually if alterations on the membrane take place (122).

Bacterial cell wall hydrolases (BCWH) are enzymes able to bind to target sites in the peptidoglycan and cleave specific bonds, hence degrading the peptidoglycan of the bacterial cell wall and consequently lysing the cell. There are several enzyme types being studied and assessed for clinical use, including lysozymes, produced by eukaryotic cells; autolysins, produced by the bacteria itself and virolysins, encoded by phages. The latter ones are commonly referred as endolysins and these enzymes are produced by phages at the end of their lytic life cycle. Several studies, both *in vitro* and *in vivo,* showed that endolysins are effective to eliminate bacterial infections (123), when applied exogenously. $CHAP_K$, the phage lysin generated from the *S. aureus* endolysin LysK showed lytic activity not only against bacterial cultures of *S. aureus*, but also showed to eliminate *S. aureus* colonising the nares of BALB/c mice (124).

However, due to the presence of an outer protective membrane on gram-negative bacteria, BCWH are not as effective against these bacteria.

In order to take advantage and restore the activity of some antibiotics, strategies are under research focus to overcome several of the resistance mechanisms observed. As examples: efflux pump inhibitors to neutralise antibiotics to be pumped out of the cell just after uptake by plasma membrane translocases (125); LPS inhibitors to disrupt the LPS protective barrier, usually inhibiting KDO 8-p synthase, an enzyme essential in the LPS pathway (126).

Each one of these approaches is always associated with some advantages and limitations and is not universally effective; therefore it will be important when facing a bacterial infection to tackle it with the best approach on a case by case basis. It may be that one single approach will never be the best option, but rather a synchronised combination of them.

1.6. Bacteriophages

Bacteriophages, or phages for short, are viruses that infect bacterial cells (from bacteria and the Greek *phagein*, meaning 'to eat'). Phages were first discovered independently by Frederick Twort in 1915 and Felix d'Hérelle in 1917 (127, 128). Yet, it was d'Hérelle that devotedly pursued the study of phage and their uses (128, 129). He was the author of the terms *bacteriophages* as well as *plaque* (130), the small clear areas seen in agar plates caused by bacterial killing by phage. He performed experimental treatments of patients with bacterial infections, like dysentery, and he demonstrated the usefulness of phage lysates in treating bacterial infection (130). After several promising studies (131–133), phage preparations were widely used in the treatment of infectious diseases over the world, including cholera, diphtheria, bubonic

plague and anthrax. Commercialisation of phages was the next step. This began in d'Hérelle's commercial laboratory, that later became the well-known company L'Oreal. The phage preparations were named, for instance, Bacté-intestini-phage and Bacté-staphy-phage, and were widely marketed (130). Other large companies joined the phage market, including Bacteriophage/Robert et Carriere in France, Antipol in Germany, Medico-Biological Laboratories in the United Kingdom and Eli Lilly & Co, Parke-Davies, Squibb & Sons and Swan-Myers in the United States. Unfortunately, at that time the nature of phages was still poorly understood and this gave rise to an erroneous targeting of treatment, where conditions like herpes, eczema and gallstones were claimed to be curable using phage lysates. Failure in establishing scientific proof of phages, mainly due to clinical trials lacking placebo controls, phage preparations with low viability and stability and/or containing high levels of endotoxins that would compromise phage effectiveness, led to a lack of confidence in the capacity of phages to eliminate infectious diseases. With the discovery of penicillin in 1928 by Alexander Fleming a new period began where treatment of infectious diseases relied almost exclusively on antibiotic drugs and phage therapy was largely forgotten in United States and Western Europe. Despite this, the former Soviet Union and Eastern Europe (134–136) kept the interest in the bacteria-killing-virus to the present day, studying and treating a wide spectrum of bacterial diseases.

Although therapeutic use of phages was left behind in the western countries, phage particles as models were intensively studied and contributed in a significant manner for the understanding of basic molecular mechanisms of genes and, consequently for the development of modern molecular biology (137). In 1952 using bacteriophages selectively tagged, Alfred Hershey and Martha Chase demonstrated one of the genetic breakthrough discoveries (Figure 1.10): the observation that DNA was the molecule carrying genetic information (138).

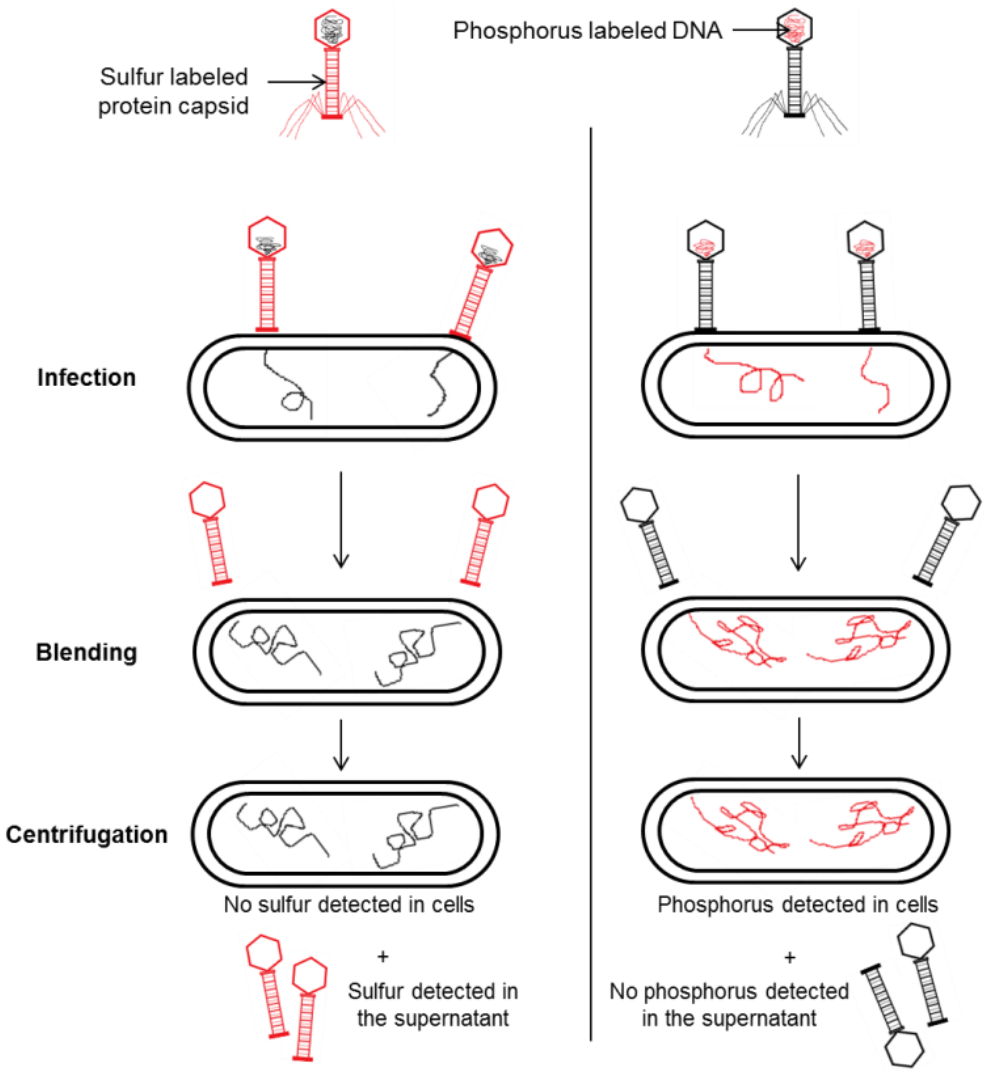

Figure 1.10: The Hershey-Chase experiment. Two parallel experiments are performed, where phages have their protein capsule labelled with radioactive sulfur or their DNA labelled with radioactive phosphorous. Phages are then allowed to infect the host bacteria and the mixtures are blended and centrifuge in order to obtain a phage supernatant (bacteria free) and a bacterial pellet. Radioactive phosphorus will be found in the bacterial pellet, where sulfur will be found in the supernatant, leading to the conclusion that the DNA holds the genetic information, being transmitting it to the next generation.

The dissemination of bacterial antibiotic resistance and the emergence of pan-resistant bacterial strains have led some to predict a return to the pre-antibiotic era. The efficacy of bacteriophages over antibiotics (discussed below) and a greater understanding of phage biology has led to a renaissance of interest in bacteriophage therapy.

1.6.1. Ecology and Classification

Phages are the most abundant and ubiquitous microorganisms on Earth, ten times more abundant in the environment than bacteria, with numbers estimated to be in the order of 10^{31} (139). Phages are ubiquitous, found in sites such as water, soil, humans and animals - skin, feces, gut (140) - and even in our food (141). One gram of fresh or processed meat contains about 10^{8} viable phages (142). In a general way, one might say that a phage can be found in any environment where bacteria or archaea are present.

Phages present an extensive diversity of shape, size, capsid symmetry and structure. Phages can have double-stranded (ds) or single-stranded (ss) DNA or RNA (Table 1.1). Phages are classified by the policies of the International Committee for Taxonomy of Viruses (ICTV) under a myriad of properties (143), but most important are the type of nucleic acid, morphology, physiochemical properties and genomic composition.

1.6.2. Polyvalent bacteriophages

Phages can be exquisitely specific in host range infecting only a small proportion of a species. However polyvalent phage exist that can multiply in most strains of a species and even other species within the same genus. Polyvalent phages are not difficult to find, in fact there is a whole diversity of phages infecting different bacteria described in the literature, particularly phages effective against Staphylococci, such as the twort-like phages (146), ϕ812 (147) or P27/HP (148), among others. These phages are the most promising therapeutically due to their extensive host range that sometimes extends into coagulase-negative staphylococcal species (147). A polyvalent phage or cocktail is valuable for situations when the bacterial pathogen causing the infection has not yet been identified and a prompt action has to be taken to deal with the infection. Also, some studies have demonstrated a lack of genetic diversity among antibiotic resistant

bacteria (149), meaning small differences between isolates and hopefully the same polyvalent phage is able to easily deal with bacterial infections caused by different isolates.

Table 1.1: Classification of phage families (adapted from 144). L, linear, C, circular.

Shape	Family	Nucleic acid	Characteristics	Member
	*Myoviridae*	dsDNA (L)	No envelope, contractile tail	T4
	*Siphoviridae*	dsDNA (L)	No envelope, non-contractile long tail	λ
	*Podoviridae*	dsDNA (L)	No envelope, non-contractile short tail	T7
	*Microviridae*	ssDNA (C)	Knoblike capsomers	ϕX174
	*Corticoviridae*	dsDNA (C)	No envelope, complex capsid	PM2
	*Tectiviridae*	dsDNA (L)	Inner lipidic vesicle, pseudo-tail	PRD1
	*Leviviridae*	ssRNA (L)	No envelope	MS2
	*Crystoviridae*	dsRNA (C)	Segmented, lipidic envelope	ϕ6
	*Inoviridae*	ssDNA (C)	No envelope, filaments or rods	Fd
	*Plasmaviridae*	dsDNA (C)	Lipidic envelope, no capsid	MVL2

It is estimated that over 96 % of phages worldwide belong to the *Caudovirales* order characterised by tailed helical particles, provided with adhesion structures (baseplate, spikes and fibres) and dsDNA genome, that can show a range size of 18 kb – 500 kb (145). The order is composed by three families: *Myoviridae* (contractile tail), *Siphoviridae* (long non-contractile tail) and *Podoviridae* (short non-contractile tail).

1.6.3. Phage life cycle

Like their counterpart viruses, phages are obligate parasites that require a specific host cell to reproduce which, in this case, are bacterial cells. This specificity is highly sophisticated. Adsorption of the phage to the host cell is mediated by the tail fibers, or

other equivalent structure on those phages lacking tail fibers, that recognise specific sites on the bacterial cell surface. The nature of the receptor sites is diverse: for instance, surface proteins, LPS, pili and lipoproteins. Note that phages evolve in order to target these bacterial receptors, which are required for normal bacterial function. Small differences in these receptors (e.g. between two strains of the same species) will prevent efficient adsorption occurring. Once the phage is irreversibly bound to the bacteria, injection of the genomic material into the cell takes place, commonly through formation of a hole in the bacterial cell wall. At this stage, two different scenarios can be established: lytic or lysogenic infection (Figure 1.11).

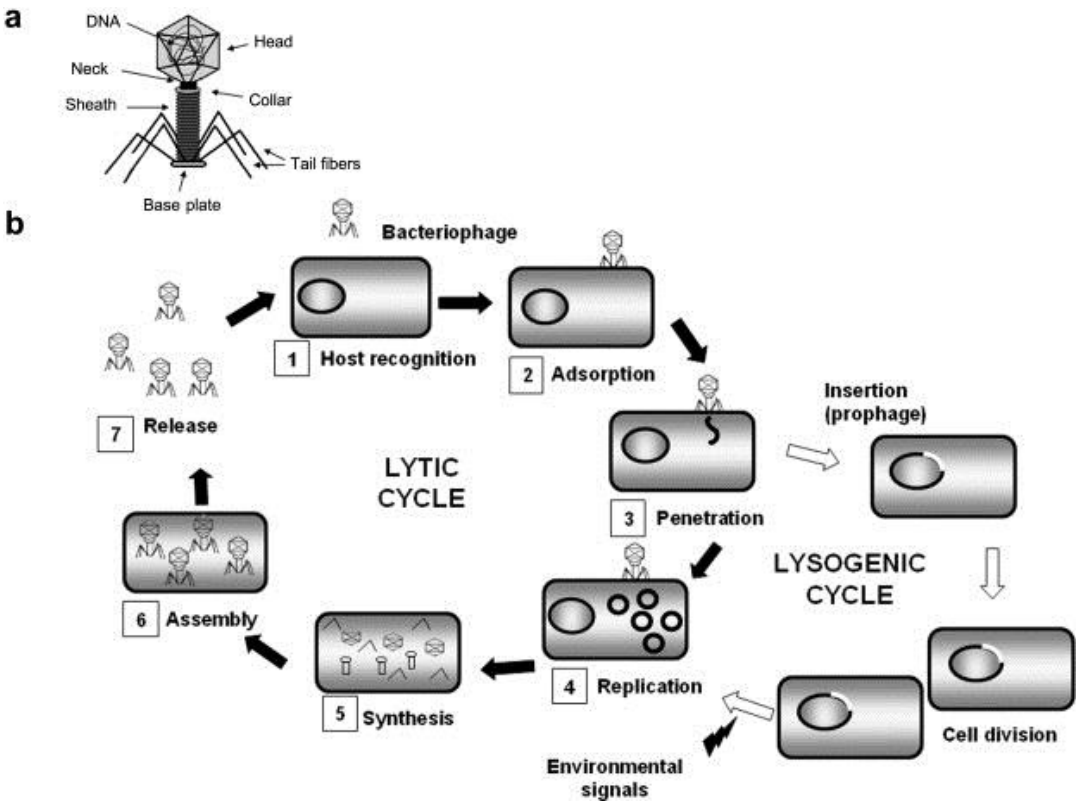

Figure 1.11: Structure of a typical tailed bacteriophage (a) and the stages of the lytic and lysogenic life cycle (b). Reprinted from reference (150) and used with permission.

1.6.3.1. Lytic infection

The viral genome now inside the bacterial cell is transcribed by the host RNA polymerases to produce mRNA, which is responsible for arresting all host cell synthetic machinery on behalf of phage reproduction (151) through a methodic and temporal regulated set of events: genome replication, gene expression and morphogenesis (assembly of the virion capsids and genome packaging). Once production of the virions is completed it is necessary to breakdown the bacterial cell wall in order to release the phage progeny (burst). Several lytic enzymes, including lysozymes, endopeptidases and amidases (152), are produced by the phage. Lysis of the bacterial cells, which can be accomplished within minutes or hours, is followed by release of hundreds of phage particles into the environment (153). These virulent phage particles are then able to infect other bacteria host and initiate new phage lytic cycles.

1.6.3.2. Lysogenic infection

Phages displaying a lysogenic infection integrate their genome into the chromosome of the host bacteria (prophage). As a result, the phage genome becomes dormant in a latent state, named lysogeny, and the genome is transmitted to each daughter cell always when a cell division occurs. A phage presenting this sort of growth is referred to as a temperate phage and cells carrying a prophage are called lysogenic. Nevertheless, the viral prophage can become activated (induction) and enter in a lytic growth by certain stimuli that impose a stress to the bacteria, such as DNA damage. Often, the prophage is excised incorrectly from the chromosome taking with it neighbouring bacterial genes. This situation is an important source of horizontal gene transfer (HGT) between bacteria, driving their evolution, and this has been widely exploited as a central technique in molecular biology. For therapeutic purposes, temperate phages are not desirable, not only because bacterial killing is not efficient

enough but there's an increased chance of HGT. This may lead to specific transfer of virulence factors (154).

A third life cycle is known, a chronic infection, where phages infect their host, replicate and are released into the environment without killing or disturbing the bacterial cell, which keeps growing and dividing. The phage M13 that infects *E. coli* is an example of such chronic infection.

1.6.4. Bacteriophage therapy

For a therapeutic approach, phages should be able to reduce bacterial numbers until eradication or to a point where the immune system is able to clear out the remaining infection-causing bacteria (155) and at the same time do not pose any health issue for the patient. Hence, there are some features that the selected phages as well as the phage preparation *per se* have to attain:

- Phages with obligate and effective lytic cycles that result in a rapid killing of the target host.
- The interaction of phage and bacteria should be understood, for instance, identification of the phage receptor(s).
- The phage preparation must meet all safety and regulatory requirements, equivalent to other medicines.
- The efficacy of the phage preparation should be tested in animal models, because efficacy *in vitro* is not always translated *in vivo*.
- The phage preparations should actually contain viable virus, therefore stability evaluations should be taken to identify preferably conditions for a longer shelf-life of the phages – storage conditions between individual phages exhibit great variability (156).

1.6.4.1. Bacteriophage therapy: advantages

Unlike antibiotics, phages are easily isolated from nature, often from human or environmental sources e.g. sewage samples, and have a relatively low cost of development (156). Most phages present a narrow host-range (infecting only a single strain and to some extent other strains within a bacterial species) as mentioned above. This specificity leads to a minimal risk of normal body flora disruption (148) when compared to antibiotics even those with a narrow-spectrum. Phages are natural constituents of the environment, being mainly composed of nucleic acids and proteins, and humans are constantly exposed to them, therefore they are not considered toxic or dangerous for human health (157–159). Phage treatment would only require few and low doses to be given to the patient, because of its self-replicating property – as long as the target cells are present the lytic cycle takes place. Observation of such a phenomenon might be limited to a certain degree in cases where bacterial densities are relatively high (160). Phage infection has a completely different mode of action to antibiotics and therefore antibiotic resistant bacteria present no special challenge to therapy (161, 162). Phages are versatile particles that can be used in liquids, impregnated into hydrogels or solids and are suitable for use by most delivery routes, such as oral and parenteral, but also local and by inhalation (for review 157). An additional phage advantage, showing so far promising results (164), is their ability to disrupt and eradicate bacterial biofilms; discussed later in this review.

1.6.4.2. Bacteriophage therapy: concerns

Some concerns have been expressed concerning phage therapy, however these may have been overstated. No therapeutic method is free of concerns regarding patient's safety but with certain safeguards phage therapy can be as safe, if not safer, than alternative anti-infectives.

Bacterial resistance to phages - for instance, mutation/loss of the phage receptor or acquisition of restriction-modification systems - is one cause for concern. Phages used in therapeutics are lytic and able to rapidly kill their biological target; this event besides the clearance of the pathogenic cell diminishes the chances for bacteria to evolve towards phage resistance. However, resistance emergence is still an issue and can be overcome, to some extent, by using combinations of phages (cocktails) displaying unrelated modes of infection (165). It is of note that antibiotics are chemical products not able to evolve, therefore when bacteria become resistant discovery of a new drug is required – this is costly from a patient point of view but also commercially expensive. On the other hand, phages are able to evolve and adapt in the same way their hosts are, and so, simply the isolation of new effective virus is required, which is considerably easier and cheaper.

Owing to the narrow-spectrum of phage infection the bacterial target has to be identified prior to phage isolation. This could result in a treatment delay which when dealing with infectious diseases can seriously compromise the patient's situation. One can outpace this by resorting, as mentioned, to broad-host spectrum phages, for instance, phage K is a polyvalent Staphylococcal phage (166) and/or a phage cocktail that together result in a broader range of activity.

DNA sequencing of phage genomes is a required step prior to their use in therapy in order to guarantee that the phages administered are not lysogenic (not carrying any functional lysogenic components) and do not harbor any virulence factor or toxin gene harmful for humans. Occurrence of virulence or toxins in phage particles is extensively described in the literature (167), as a result DNA sequencing is an imperative step.

Transduction is a common event linked to lysogenic phages and an undesirable trait regarding therapy. To counter such a possibility a PCR-based screen for transducing genes could be employed (168) or, again, DNA sequencing.

Although it is accepted that phages are not dangerous as human therapeutics, several studies show that they interact with antibodies, triggering strong immunogenic responses (169). Nonetheless, other drugs and treatments in use are as immunogenic and regulatory hurdles can be overcome by demonstrating safety in clinical trials. On the other hand, such interaction may result in an undesirable quick clearance of the virus particles before they achieve their purpose.

Phage preparations may contain bacterial debris containing endotoxins, compounds derived from the lysate preparation itself that if given to humans, might cause inflammatory responses. Hence, highly purified lysates should be produced, for instance, by ultracentrifugation/advanced filtration methods, for example monolith columns.

1.6.4.3. Bacteriophages - future applications

Bacterial resistance to antibiotics, such as is the case with MRSA, is an overwhelming situation seen every day and almost everywhere (170). Selection and spread of antibiotic resistance is a result, in part, of their uncontrolled and unjustifiable use for decades, among clinicians and also in agriculture and animal farming. Development of a drug is a slow process and in recent decades fewer and fewer antibiotics have come to light. Therefore, bacteriophages and the natural attributes that they possess have been seen as a reasonable alternative to antibiotics.

Treatment of bacterial diseases using phages is not restricted to humans, it is also an alternative for animals (171) and plants (172) and several studies have been carried out, showing different levels of efficacy. In addition, phages are currently in use in environmental decontamination and in food processing (173).

From a commercial point of view, phages have not been an attractive choice for big pharmaceutical companies. It is difficult to obtain clear intellectual property (IP) rights,

due to phages having been used in therapy during the past hundred years. Without adequate patent protection, there is a certain apprehension regarding the profitability of phage therapy, making funding expensive clinical trials hard to justify and achieve.

Other promising therapeutic approaches have also been studied, involving the use of lytic bacteriophage endolysins, as discussed previously (174), or genetically modified phages, that do not lyse the bacteria, but derail it by delivering DNA encoding antibacterials (175).

Recently it has been found that certain phages seem to show an antimetastatic activity and tumour inhibition (176, 177). It was shown (178) that this might be involved with the presence of a KGD (Lys-Gly-Asp) amino-acid motif present in a protein of the phage capsid. This motif in the phage is a homologue of the RGD motif, which blocks the activity of beta-3 integrin in cancer cells, involved in cancer cell motility and adhesion, promoting metastasis. Strikingly, this integrin is produced at higher levels in cancer cells and perhaps phages displaying these motifs can play an important role in the cancer therapeutics field.

Antibiotics and phages could be used together in therapy to enhance treatment efficiency and minimise the evolution of antibiotic and phage resistance. Bacteriophage therapy should not be seen as the only answer to (antibiotic resistant) bacterial infections, but as an additional one, complementing and working together with the many therapeutic alternatives that the scientific community is currently researching.

1.7. Bacterial biofilms

In nature, it is possible to find biofilm structures originated from fungi to protozoa and algae. Nonetheless, bacterial biofilms are the most widely described in the literature and may represent the most common form of bacterial life in nature (179). A bacterial

biofilm, first characterised almost 70 years ago (180), is described as an aggregation of bacterial multispecies embedded in a self-secreted extracellular polysaccharide matrix associated to a biotic or abiotic surface (181). Biofilms occur in most natural and artificial environments and play an important role in the pathogenesis of burn wound infections (182). A biofilm is a distinct way of living compared to the planktonic state, which provides several advantages to its 'residents'.

1.7.1. Biofilm formation

In a general way, formation of a biofilm occurs by a sequence of stages (Figure 1.12): bacterial attachment, formation of microcolonies, biofilm maturation and detachment. Firstly, planktonic cells adsorb to a surface, a transient event, where cell-surface and cell-cell interactions (e.g. through surface proteins) occur. For *P. aeruginosa* cells several factors are required for this initial binding to a surface, such as the flagella (183), the type IV pili (184), extracellular DNA (eDNA) (185) and the Psi polysaccharide (186). Irreversible association of the bacterial cells to the surface occurs by production of extracellular polymeric substance (EPS). Production of such a substance is a result of a metabolic shift from a planktonic to a biofilm state (181). Subsequently, there is a proliferation of the cells that is dependent upon nutrient availability (179) to constitute a three-dimensional mature biofilm. The biofilm structure, with their heterogeneous communities and presence of channels where water and nutrients circulate (187), is preserved and protected by the EPS matrix surrounding the microbial populations. Such heterogeneous communities are composed of cells experiencing different levels of growth states (active growth, stationary and quiescent) (179), where events of quorum-sensing (cell-cell communication) commonly take place playing important roles in the biofilm formation *per se* (188). Occasionally, sessile bacteria will detach from the biofilm matrix, for example as a consequence of disruption of cell-cell interactions for the production of the water and nutrient channels along the biofilm. This will not only

enable the biofilm to thicken and expand its structure, but also detached cells will be able to colonise other surfaces. Biofilm detachment plays an important role in infection expansion by spreading the cells to new infection sites (189). The mother-biofilm, despite all the disassembled “pieces” can return very quickly to its previous maturation state in no more than 24 hours (190).

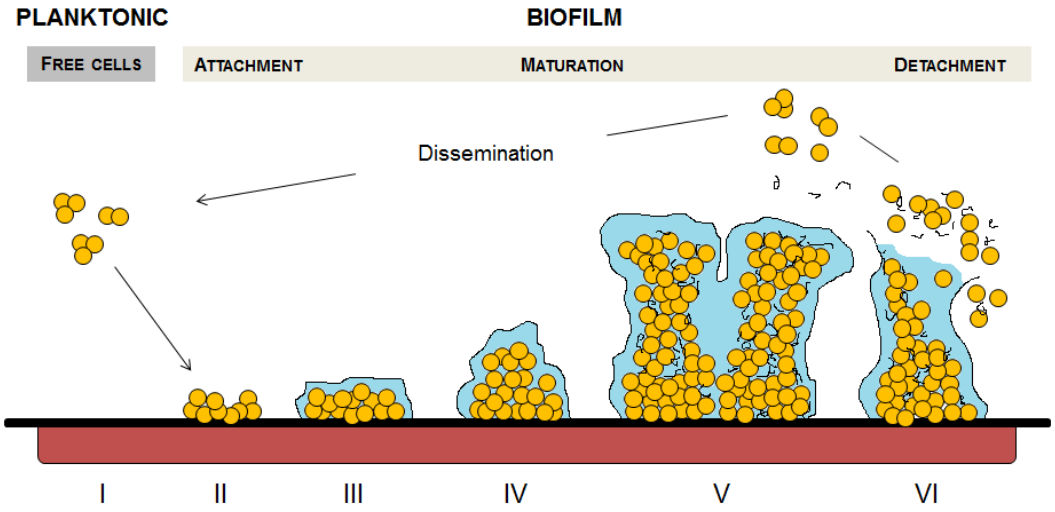

Figure 1.12: Representation of the biofilm formation stages. Free cells (I) adsorb to a surface to form microcolonies (II) that start producing an EPS matrix for protection and maturation of the biofilm (III,IV). Proliferation and maturation of the biofilm results in a three-dimensional mushroom structure (V) and occasionally sessile cells are going to detach from the structure to initiate other biofilms (VI).

In *S. aureus* the process of biofilm maturation and detachment is essentially controlled by a quorum sensing system encoded by the accessory gene regulator (*agr*) locus (Figure 1.13B). During growth an autoinducing peptide (AIP) is secreted by bacterial cells that upon accumulation (which happens if cells are growing on a biofilm) is recognised by a receptor on the cell surface and triggers a regulatory cascade ending with the control of toxin and adhesion factors production. In summary, the Agr system is composed by two operons with P2 and P3 promotors regulating them. The P2 operon, which contains agrBDCA genes, codes for an RNAII transcript where most of

the components are translated from, including the AIP molecule. On the other hand P3 operator codes for a RNAIII, which is responsible for the upregulation of some toxin factors, for instance δ-hemolysin, and downregulates the translation of adhesion factors, such as Protein A and fibronectin-binding protein. All the system gets upregulated when the secreted AIP is detected by the two-component system AgrA-AgrC on the cell membrane and both P2 and P3 operons are transcribed. Hence in a general way, biofilm colonisation is controlled by switching off the Agr system, whereas biofilm maturation and dispersal is performed when the Agr system is switched on and assisted by surfactant-like phenol-soluble modulins (PSMs) that degrade biofilm polymers (191, 192).

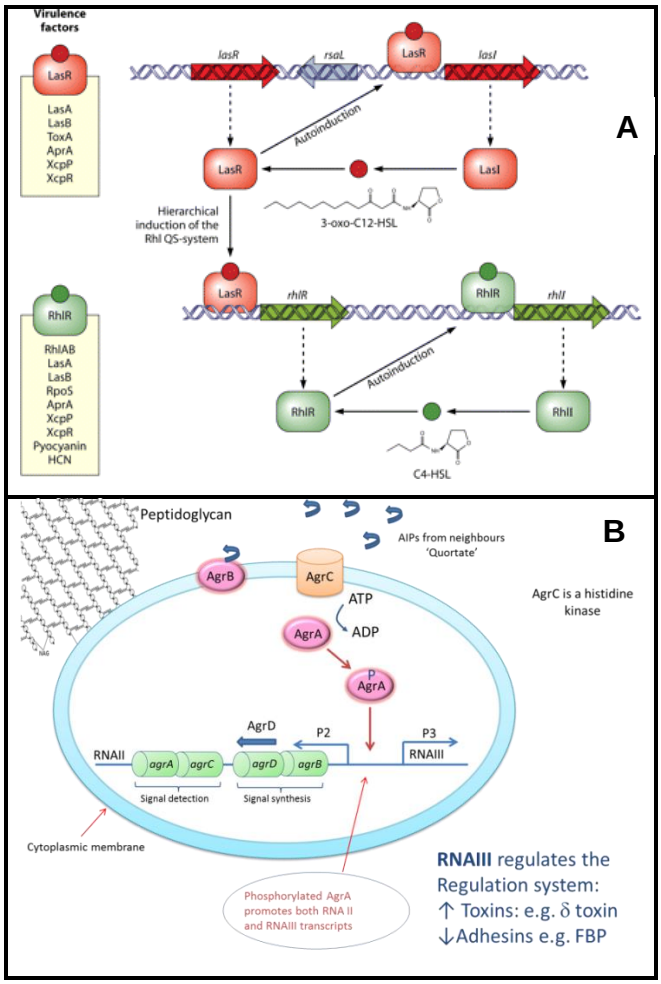

Figure 1.13: Quorum sensing pathways in (A) *P. aeruginosa*, reprinted from reference (193) and used with permission, and (B) *S. aureus* (courtesy of Dr Toby Jenkins).

P. aeruginosa biofilm formation is largely controlled by quorum sensing systems; however it is more complex and intricate than the one observed for *S. aureus* (Figure 1.13A). In a general way for biofilm formation two main quorum-sensing systems arranged into two distinct operons are present - Las and RhI. Both respond to a specific type of acylhomoserine lactone (AHL), a 3-oxo-C12-HSL (3OC12) and a N-butyryl-L-homoserine lactone (C4-HSL), respectively. The autoinducer molecule 3OC12 produced by LasI is recognised by LasR in the cell membrane. Such recognition will trigger the transcription of several genes, including rhIR gene coding for a second receptor protein. RhIR will recognise the second autoinducer - C4-HSL, produced by RhlI and several pathways are activated, including some genes belonging to the Las system. A third quorum sensing system based on quinolone signals (PQS) is also present in *P. aeruginosa* and all together play important roles in biofilm development and maturation (193–195). However factors such as medium composition and flow conditions also play a major role in biofilm development (196). Biofilm dispersal is also controlled by these systems, for instance the Rhl system controls the production of rhamonolipids (197), a surfactant molecule which other than acting as virulence factors also play important roles in disruption of cell-cell interactions (198), for maintenance of water channels, biofilm maturation and finally biofilm dispersion (199).

The matrix surrounding *S. aureus* bacterial cells is composed of several secreted polymers, including exopolysaccharide, teichoic acid, proteins and DNA from cells that eventually die (189). *P. aeruginosa* biofilm matrix is composed of at least three polysaccharides: alginate, Pel and Psl (200). They are an important factor for the stability of the biofilm and their concentration within the biofilm depends on the type of strain. For example, mucoid strains are great producers of alginate in comparison to non-mucoid strains (201). Generally, production of Pel and PsI play a key role in initial

colonisation and formation of biofilm, whereas alginate is crucial for the stability of the biofilm at later stages of its formation (201, 202).

1.7.2. Biofilm community advantages

Bacterial diseases, particularly those caused by *S. aureus*, are strictly linked to production of biofilm, being one of the first steps in infection initiation (203, 204). Once in a biofilm, bacterial cells are protected against antibiotics and the host immune system.

The EPS matrix blocks antibody penetration into biofilm matrix (205) and phagocytes are unable to interact with bacterial cells (206).

Bacterial tolerance to antibiotics within a biofilm is greatly enhanced compared to planktonic cells (207). In a biofilm, horizontal gene transfer is common due to increased cell-cell interactions; as a result resistance determinants are more easily spread (208). Moreover, resistance has been attributed to a lower ability of antimicrobial drugs to penetrate the EPS matrix, causing exposure of cells to sub-lethal antibiotic concentrations promoting resistance emergence. There is also a decrease in metabolic activity of the biofilm inner cells, due to reduced oxygen and nutrient concentrations (207), that makes antibiotics that are effective against dividing bacteria ineffective. The lower metabolic activity of some cells can also be related to the presence of ‘persister’ cells. Although not resistant to antimicrobials (209) they display tolerance to them and do not die. This ability of multidrug tolerance (MDT), while the causes are yet not very clear, is possibly due to a state where bacteria are deeply dormant. Antibiotics, in general effective against actively growing bacteria, reach their target in the cell and prevent its normal task, leading to a failure of the cell system (death). On the other hand, persister cells are not metabolizing, so even if the drug molecule reaches its target no function will be blocked because no function is taking place (210). Therefore,

persister cells are not eliminated and represent a possible source of repopulation of the biofilm, making the antibiotic therapy useless (211). In addition, bacteria in a biofilm are protected against other environmental stresses, such as UV light and acid exposure (212, 213), metal toxicity (214), dehydration and salinity (215).

Biofilm association therefore allows bacteria to colonise with fewer restrictions, persist and continue to establish infections and spread between hosts (32).

1.7.3. Interaction of phages and biofilms

Phages are natural constituents of biofilms, playing major roles in their architecture and also in their dispersal. Studies assessing phage efficacy on biofilm eradication are still at an early stage, but there are promising observations of the clear potential of phage therapy (216). However and according to a recent review (217) phages are no doubt a strategic device for biofilm removal: 1) their amplification allow them to get access to the deeper cells in the biofilm; 2) phages can carry or express depolymerising enzymes degrading the complex EPS matrix present in biofilm, an advantage regarding application of antimicrobial drugs; 3) if not coding for a depolymerase enzyme phages can induce their production from within the host genome; 4) persister cells can still be infected by phages, although no proliferation will occur once these cells are ‘awakened’ phage replication will take place and burst the cell.

Polysaccharide depolymerases degrade the EPS matrix that surrounds the bacteria ‘opening the way’ so that phages can interact with the bacterial receptors and the lytic cycle takes place; actually in a biofilm bacterial cells are static and in close proximity when compared to the planktonic state (e.g. liquid culture). Therefore, the interaction between phage and bacteria taking place is more stable and once phages are released from the infected host new lytic cycles can take place more quickly. Hence, phages are able to access to the deeper layers of the biofilm gradually. Illustrating this are Lu and

Collins (218) that engineered a bacterial depolymerase - dispersin B (DspB) – being expressed by a phage able to propagate on the cells (Figure 1.14). They observed a great disruption of *E. coli* biofilm over 24 hours. In the absence of depolymerase, phage access to the biofilm inner layers can also occur, probably slower, through the water-filled channels inherent to the biofilm architecture (219) or perhaps they are able to induce a depolymerase once inside the host. Kelly and colleagues (220) observed that *S. aureus* biofilms treated with phage K - a non-depolymerase producer (221) - showed a significant decrease in biofilm formation after 72 hours. In this experiment, the potential of phages to prevent biofilm formation was also observed. The same can be seen in experiments where only depolymerase molecules were used. In addition, the success of a phage to infect a biofilm is dependent on environmental factors, such as temperature, growth stage, media and phage concentration (222).

Biofilm-associated *S. aureus* infections are a major and concerning cause of morbidity and mortality. As a result the use of lytic phages, preferably accompanied by depolymerase activity, acts as an efficient and rapid treatment/prevention of such diseases that should be deeply understood both *in vitro* and *in vivo*.

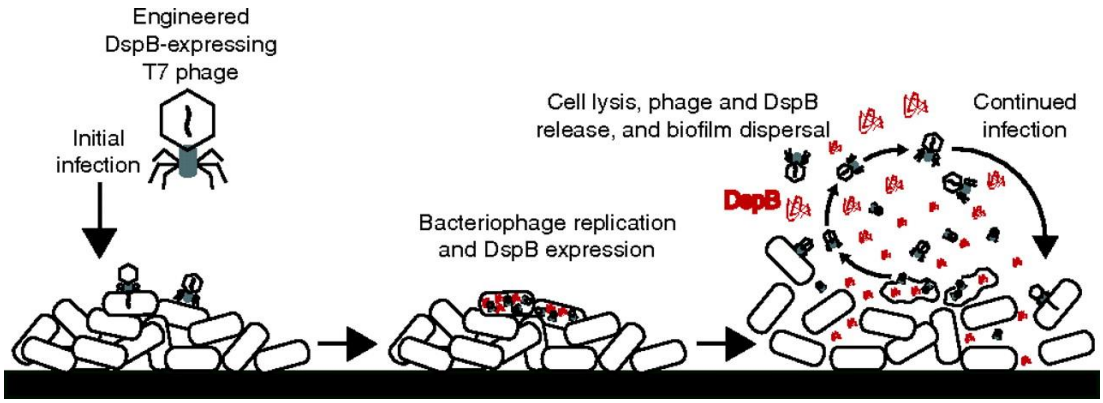

Figure 1.14: Engineered DpsB-expressing T7 infects an *E. coli* biofilm resulting in rapid multiplication of phage and expression of the DpsB enzyme. Reprinted from reference (218) and used with permission from PNAS.

1.8. Concluding remarks and project aims

The infectious diseases caused by *S. aureus* or *P. aeruginosa* and described in this chapter can be considered as major causes of public health concern, not only in their infectious effect but their ability to acquire resistance to causing increased mortality, morbidity and higher hospital costs. Hence, bacteriophages can be used as an alternate/adjunctive treatment for such bacterial pathogens.

The aim of this project was the development of two efficacious therapeutic bacteriophage cocktails targeting both *S. aureus* and *P. aeruginosa*. The work is divided into three main sections, where:

- Isolation from environmental samples and characterisation of bacteriophages was performed in order to establish cocktails potentially safe to be used.
- Assessment of the phage lytic activity and bacterial eradication on *in vitro* models, including on bacterial planktonic growth and in both static and dynamic biofilm models produced by clinical isolates.
- Assessment of the treatment efficacy of the phages cocktails on an *in vivo* infection model of *Galleria mellonella*.

Chapter Two:

MATERIALS, METHODS AND INSTRUMENTATION

THEORY

2.1. Preparation of bacterial cultures

2.1.1. Principles of bacterial growth

Bacterial cells reproduce by binary fission increasing their cell numbers in an environment. Bacterial growth is affected by several factors, including temperature, pH, salinity and oxygen. If those factors are optimal the bacterial growth is going to take a sequence of four stages (Figure 2.1). When setting up a culture there is an initial lag phase (A) where cells are preparing for reproduction (DNA replication and enzymes production, for instance), following that the cells start the division process and increase their numbers exponentially (B). During this phase each bacterium grows at a specific rate, that being dependent on external growth conditions as well as being intrinsic to each bacterial type. After this exponential phase the culture goes into a stationary phase (C) where growth rate equals death rate. Cells show a lower metabolic rate and more resistance to external stresses. Eventually, the cell numbers show a decline (D) as they are unable to grow further in a depleted environment.

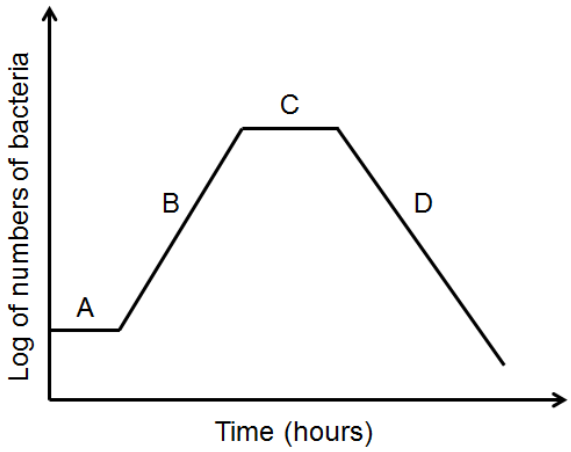

Figure 2.1: Growth curve of a bacterial culture. A – lag phase, B – log/exponential growth phase, C – stationary phase, D – death phase.

2.1.1.1. Estimation of bacterial cell numbers

Bacterial cell numbers in a culture can be estimated by several methods. The most common and direct is the standard plate count where serial dilutions of the original culture are performed and plated onto a nutrient agar plate. Each cell present will reproduce and form a visible colony that can be recorded and used to estimate the number of cells in the original culture, expressed as colony forming units/ml (cfu/ml):

$$cfu/ml = \frac{Number\ of\ colonies}{d \cdot V} \quad (2.1)$$

Where *d* stands for dilution factor and *V* for volume of inoculum. Another commonly used but indirect method is optical measurement. When bacterial cells are reproducing the turbidity of the culture increases resulting in more light scattered, that is recorded as an increase in optical density.

2.1.2. Bacterial strains

S. aureus strains (listed in Chapter III, Table 3.2) used in this study were from Professor Mark C. Enright's collection of >5,000 clinical isolates. They were selected to be genetically diverse (by multilocus sequence typing [MLST], see section 2.7) and also to contain members of the major MRSA and methicillin susceptible *S. aureus* (MSSA) clones present worldwide.

Examples of eight coagulase-negative staphylococci (listed in Chapter III, Table 3.3), *S. xylosus*, *S. sciuri* subsp. *sciuri*, *S. chromogenes*, *S. hyicus*, *S. arlettae*, *S. vitulinus*, *S. simulans*, and *S. epidermidis*, were also included in this study.

P. aeruginosa strains (listed in Chapter III, Table 3.1), including the common laboratory reference strain PAO1 and a diverse collection of clinical isolates from both chronic and acute conditions.

2.1.3. Growth conditions

Staphylococcus bacterial single colonies from tryptic soy agar (TSA) plates were grown at 37 °C with constant shaking (170 rpm) in tryptic soy broth (TSB). For *Pseudomonas aeruginosa* bacterial single colonies from Luria-Bertani agar (LA) plates were grown at 37 °C with constant shaking (170 rpm) in Luria-Bertani broth (LB). Aliquots of bacteria were stored at -80 °C in the respective broth containing 15 % (v/v) glycerol.

2.2. Bacteriophage methods

2.2.1. Growth conditions

TSA and TSB-soft agar containing 0.65 % bacteriological agar were used for bacteriophage propagation and plaque count assays of bacteriophages targeting Staphylococcal strains. In the case of bacteriophages targeting *Pseudomonas aeruginosa* strains TSB media was replaced by LB. Note that media was supplemented with 1 mM $CaCl_2$ and 1 mM $MgSO_4$ to improve phage adsorption (223).

2.2.2. Bacteriophage isolation

Bacteriophages for *S. aureus* were isolated from crude sewage (Thames Water PLC, Luton, United Kingdom) and for *P. aeruginosa* from flood water (Bath, UK) and crude sewage (Wessex Water, Somerset, UK).

Bacterial enrichments with bacterial isolates were performed to increase phage numbers as follows: 5 ml of actively growing bacterial cells (from overnight liquid culture in TSB or LB) and TSB or LB supplemented with 1 mM $MgSO_4$ and 1 mM $CaCl_2$. The enrichment was incubated overnight at 37°C. A 10 ml aliquot was taken from the overnight culture, and 1 M NaCl and 2 % chloroform were added. The culture was then centrifuged (30 min, 3,000 x g) to remove bacteria, and the supernatant was filter-sterilised (0.22 µm, pore size). This lysate (supernatant) was used to check the presence of lytic phages using the double layer method described below in section 2.2.4.1.

2.2.3. Single plaque purification

From each plate, isolated single plaques were picked using a pipette tip, a method called single plaque purification. Different plaque phenotypes, if present, from each plate were picked. Each plaque was re-suspended in 300 µl of SM buffer (5 M NaCl, 1 M $MgSO_4$, 1 M Tris–HCl [pH 7.5], gelatine solution distilled water). Dilutions were then prepared and plating performed to allow the purification and isolation of a single phage. Consecutive rounds of plaque purification were carried out, by repeated subculture on the respective host strain. The plaque purification process was repeated a minimum of three times for each plaque or until a purified plate of uniform plaques was obtained, reflected by single plaque morphology. Purified phages were stored in 50 % glycerol (v/v) in TSB at -80 ºC for long term use. Short term stock preparations were maintained at 4 °C.

2.2.4. Bacteriophage propagation

2.2.4.1. Double layer method

Phage lysates were propagated on their respective bacterial hosts (Figure 2.2) as described elsewhere (224). Briefly, 100 µl of phage lysate and 100 µl of host growing culture were mixed and left for 5 min at room temperature. Afterwards, 3 ml of soft agar was added and poured onto agar plates. The following day, after an overnight incubation at 37 °C, plates displaying confluent lysis were selected and 3 ml of SM buffer and 2 % (v/v) chloroform were added before incubation at 37 °C for 4 h. High-titre phage solution was removed from the plates, centrifuged (8,000 x g, 10 min) to remove cell debris, and then filter-sterilised (pore size, 0.22 µm) and stored at 4°C.

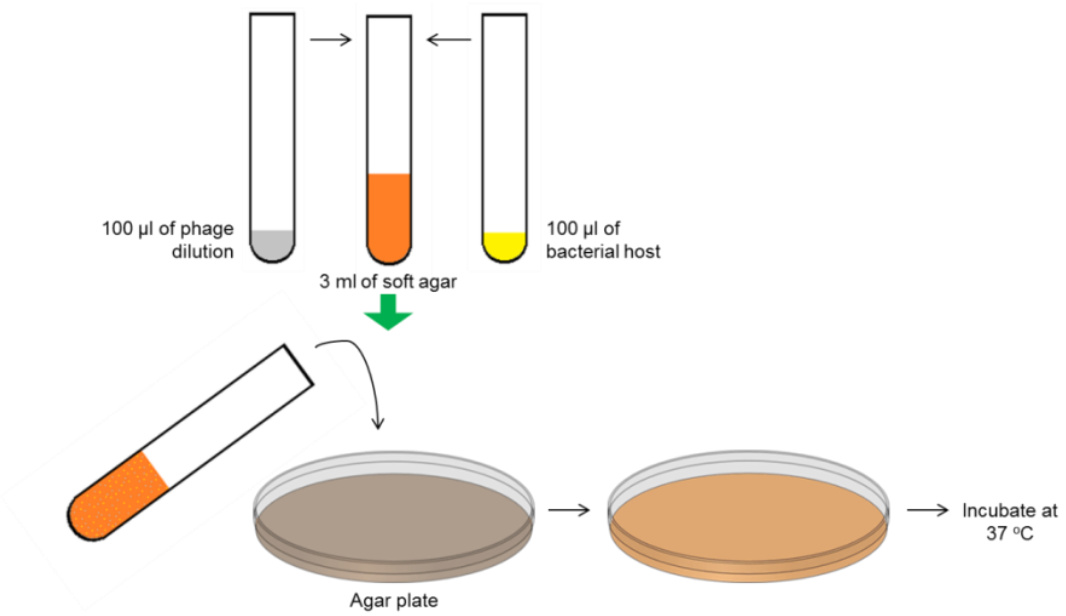

Figure 2.2: Representation of the double-layer method.

2.2.4.2. Liquid lysate method

For the liquid lysate method, 1 ml of an overnight bacterial culture was added to 100 ml of TSB. After incubation at 37 °C with shaking for 1 hour, phage lysate was added at a

multiplicity of infection (MOI) of approximately 0.1 and incubated for a further 5 hours. Following lysis the culture was centrifuged (4000 x g, 30 min) to remove bacterial debris, filter-sterilised (0.22 µm pore size) and stored at 4 °C.

2.2.5. Bacteriophage Titration

Bacteriophage titre was determined by the spot test (Figure 2.3). 3 ml of soft-agar was added to 100 µl of host growing culture and poured onto agar plates. Plates were left to dry for 20 min at 37 °C. Afterwards, 10-fold serial dilutions of the phage lysate were performed in SM buffer (5 M NaCl, 1 M $MgSO_4$, 1 M Tris–HCl [pH 7.5], 0.01 % w/v gelatine) and 10 µl of each dilution was spotted onto the bacterial lawn. This was performed twice. The plates were allowed to dry before incubating overnight. On the following day plaques were counted to determine phage titre, expressed as plaque forming units/ml (pfu/ml) by the following equation:

$$pfu/ml = \frac{Number of\ plaques}{d \cdot V} \quad (2.2)$$

where *d* stands for dilution factor and *V* for volume of inoculum.

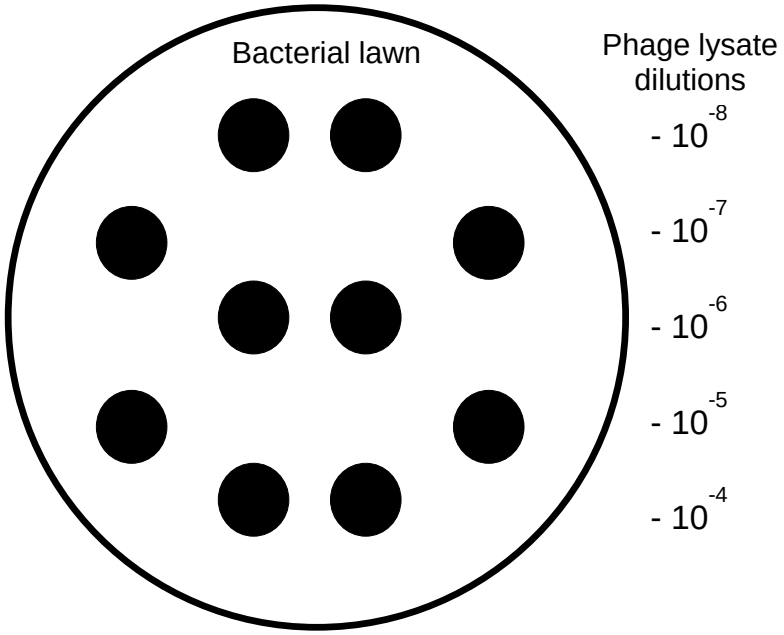

Figure 2.3: Representation of the spot test method for bacteriophage titration.

2.2.6. Sensitivity assays

2.2.6.1. Agar plates

To determine phage sensitivity of bacterial isolates, spot tests were performed. Briefly, 3 ml of TSB-soft agar was added to 100 µl of host growing culture and poured onto TSA. Plates were left to dry for 20 min at 37 °C. The different phage lysates were standardised to a titre of 10^9 pfu/ml, and 10 µl of each lysate was spotted onto the bacterial lawns. This assay was performed in triplicate. The plates were allowed to dry before incubation overnight at 37 °C. The following day, the sensitivity profiles of each of the bacterial strains were determined: if the bacterial lawn was lysed, slightly disrupted, or not disrupted, the bacterial isolate was described sensitive, intermediate, or resistant to the phage infection, respectively. To simplify the analysis of the recorded sensitivity results it was attributed a colour code, where green, yellow and red represented sensitive, intermediate and resistant, respectively (Figure 2.4).

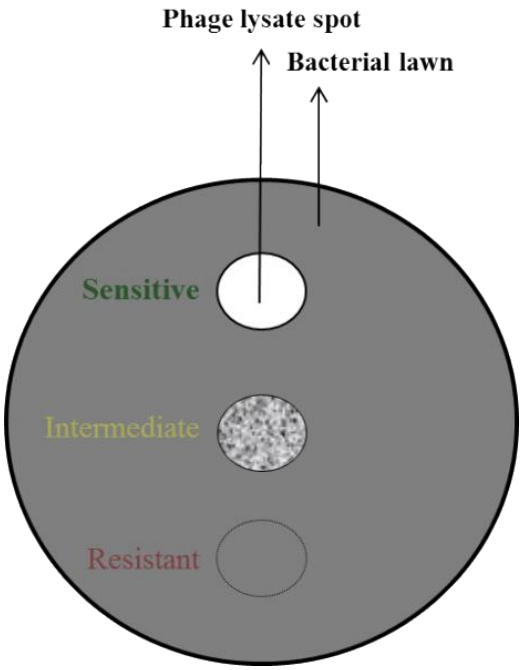

Figure 2.4: Representation of the spot test method for bacterial sensitivity screening.

2.2.6.2. Broth cultures

Alternatively, sensitivity screening was performed by monitoring optical density in broth cultures in 96-well microtitre plates. In the microplate wells a 1:100 dilution was prepared by adding 5 µl of an overnight culture to 195 µl of TSB. After 2 hours of incubation at 37 °C, the phage lysates at a desired MOI were added and the microplates were incubated for a further 24 hours. The incubation was followed on a plate reader (FLUOstar Omega, BMG LabTech, UK) where a growth curve is established at an optical density at 600 nm (OD_{600}). This approach allows observation of the phage-bacteria interaction over time and also allows for monitoring of the appearance of resistant mutants for each phage lysate.

2.2.7. Bacteriophage phage growth parameters

2.2.7.1. Theoretical Background

Bacteriophage propagation takes several distinct steps described by the one-step-growth curve and those can be measured (Figure 2.5). First, bacteriophage particles are required to adsorb to their host cell (A). Bacteriophages do not have specific structures or appendices for motility, consequently this adsorption step results from random phage-cell collision. Following that there is an eclipse stage (E) where replication of the viral particles takes place only and no infectious virus are completed yet. Mature viral particles start to accumulate inside the host cell and everything is ready to initiate the cell burst and release the phage progeny into the environment, named the latent period (L). After the cell burst there is an exponential release of phages and estimation of the number of phages released by a single host can be accomplished (B).

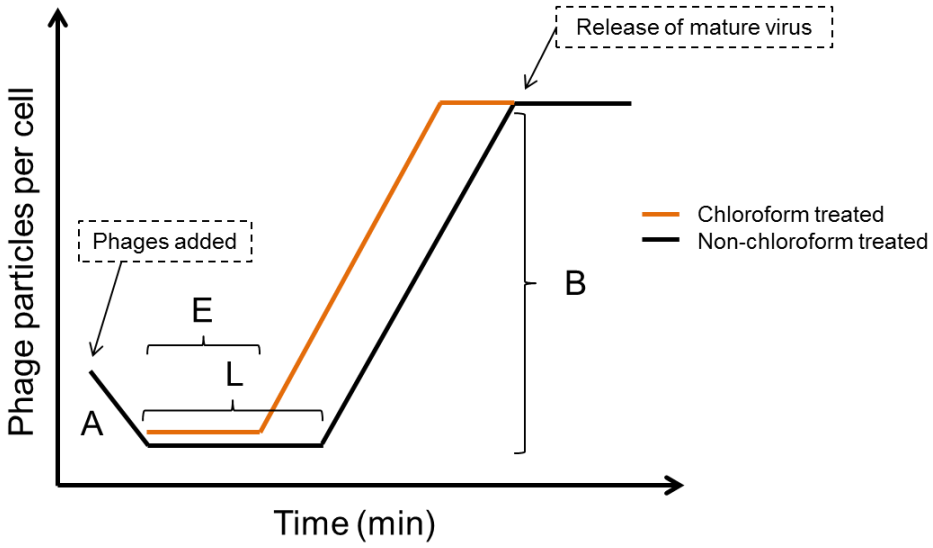

Figure 2.5: Bacteriophage growth parameters. A – adsorption, E – eclipse period, L – latent period and B – burst-size.

2.2.7.2. Bacteriophage adsorption

The experiment was carried out at 37 °C under constant shaking (60 rpm) and a phage inoculum with a multiplicity of infection (MOI) of 0.01. The number of free phages was calculated from the pfu of chloroform-treated samples within 5 min after inoculation. The adsorption rate assumes first-order kinetics and was calculated in terms of the percentage of free phage loss by fitting the phage decay curve (normalised as a percentage) to the rate equation:

$$\ln (\%\ \text{phage})_t = \ln (\%\ \text{phage})_o - k't \qquad (2.3)$$

Where k' is the pseudo-first order rate constant for free phage loss:

$$k' = k[\text{bacteria}] \qquad (2.4)$$

From this, the percent phage remaining at any time *t* can be easily calculated.

2.2.7.3. One-step growth curve

Bacteriophage growth cycle parameters - the latent period (L), eclipse period (E), and burst size (B) - were determined from the dynamic change in the number of free and total phages. Hence, one-step growth curves were measured as described by Pajunen *et al.* (225) with some modifications: 10 ml of a mid-exponential-phase culture was harvested by centrifugation (7,000 x g, 10 min, 4 °C) and resuspended in 5 ml of broth to obtain an optical density at 600 nm (OD_{600}) of 1.0. To this suspension, 5 µl of phage solution was added to obtain a multiplicity of infection (MOI) of 0.001. Phages were

allowed to adsorb for 5 min at room temperature. The mixture was than centrifuged as described above, and the pellet was resuspended in 10 ml of fresh TSB medium. Two samples were taken every 5 min over a period of 1 h at 37 °C under constant shaking. The first samples were plated immediately without any treatment, and the second set of samples was plated after treatment with 1 % (v/v) chloroform to release intracellular phages.

2.3. Measurement of phage zeta potential and size

2.3.1. Theoretical background dynamic light scattering

Dynamic light scattering (DLS) is one of the most commonly used methods to measure the size of particles. A monochromatic laser light irradiates onto a suspension and fluctuations in the intensity of the scattered light can be measured as a function of time. Fluctuations over time happen as particles are undergoing Brownian motion (defined as the random motion of particles in a suspension). Hence, smaller particles will move more than larger particles causing the intensity of the scattered light to become higher. The recorded intensity data goes through an autocorrelator and the size distribution of particles in the sample can be determined.

2.3.2. Theoretical background of electrophoretic mobility

The zeta-potential of suspended particles describes the difference of potential between the bulk of the conducting medium where they are dispersed and the stationary layer of fluid surrounding the particles. The zeta-potential is associated with the electrophoretic mobility of the particles. When phages are exposed to an external electrical field they will migrate towards an electrode of the opposite charge at a certain velocity. The

velocity is the particle electrophoretic mobility. Using appropriate equipment the magnitude of the particle electrophoretic motility is measured and zeta-potential is calculated automatically using the Henry's function:

$$u_E = \frac{2\varepsilon z f(ka)}{3\eta} \quad (2.5)$$

Where u_E is the electrophoretic mobility (μm cm $V^{-1}s^{-1}$), ε is the dielectric constant, z is the Zeta potential (mV), $f(ka)$ is the Henry's function, and η is the viscosity (cP).

2.3.3. Methodology

The particle size and electrophoretic mobility of phages were measured by dynamic light scattering (DLS) using a Zetasizer Z/S system (Malvern, United Kingdom) at 37 °C. Cuvettes, called capillary cells (Figure 2.6), are provided with two electrodes and hold approximately 1 ml of sample. Cuvettes were filled with the sample and were carefully inspected to avoid air bubbles. Phage lysates were diluted in distilled water (dH_2O) to a final concentration of 10^5 pfu/ml. For dilutions dH_2O was required as the presence of ions in the dispersing medium disturbs the quality and outcome of results. Measurements were repeated at least three times.

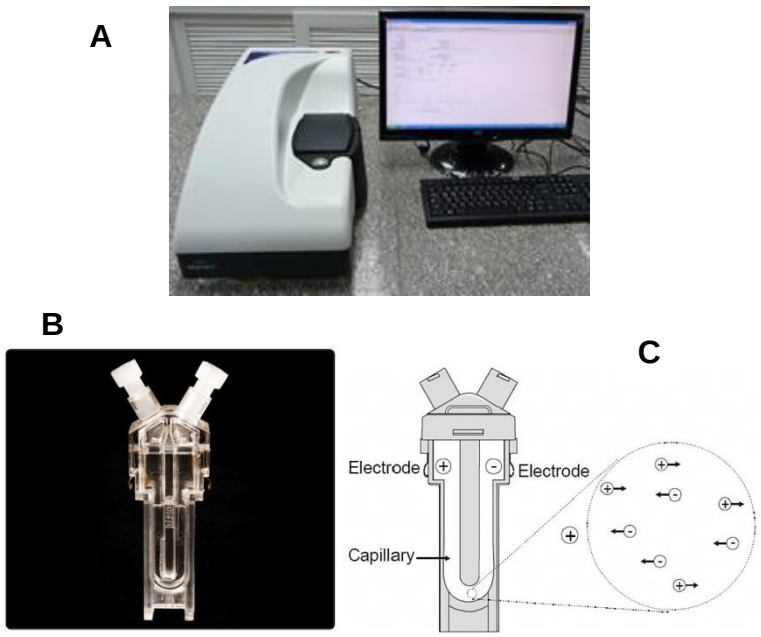

Figure 2.6: Image of Zetasizer Z/S system (A) and of a disposable capillary cell DTS1070 (B) and the schematic representation of particles moving in the capillary cell (C).

2.4. Bacteriophage DNA extraction

Bacteriophage DNA was isolated using a DNA extraction kit according to the manufacturer's instructions when titres of phages lysates were high ($\geq 10^{10}$ pfu/ml) or performing a PEG-precipitation for rapid concentration of the phage particles followed by a phenol-chloroform extraction for lower phage lysate titres followed by a (see below).

2.4.1. Bacteriophage Concentration and Purification

Prior to DNA extraction bacteriophage lysates were concentrated using centrifugal concentrators until the desirable volume. When necessary, further concentration and purification of the lysate was achieved by cesium chloride (CsCl) gradient centrifugation.

2.4.1.1. PEG-precipitation

Bacteriophage lysates purification was performed by adding 1 M NaCl and left at 4 °C overnight. The following day the solution was centrifuged (4000 x g, 1 hour) and the supernatant was carefully transferred to a new tube. 10 % (w/v) polyethylene glycol (PEG) m.w.8000 was added to the lysate and left at 4 °C overnight. On the next day, the solution was centrifuged (4000 x g, 30 min) to obtain a PEG-phage pellet. The pellet was resuspended gently in 1 ml of SM buffer and vortexed thoroughly.

2.4.2. Cesium chloride gradient

A CsCl gradient composed of three different solutions densities – 1.35, 1.50 and 1.7 g/ml - was prepared in a 36.5 ml ultracentrifuge tube (Beckman Coulter, Seton Scientific, UK). For the preparation of CsCl solution at a given density, ρ (g/ml), we used the following formula to calculate the final CsCl concentration, *c* (g/ml) (226):

$$c = 0.0478\rho^2 + 1.23\rho - 1.27 \quad (2.6)$$

Subsequently, a layer of the phage lysate was added (2-5 ml) and finally mineral oil was used to fill up the unused space of the tube (Figure 2.7). This process was performed very gently in order to avoid disturbance and mixture of the different layers. After ultracentrifugation at 25,000 rpm for 3 hours at 4 °C the phage band was collected. To collect the phage band, a whitish band observed when the tube contents were UV illuminated, a sterile needle-syringe was used. Following collection of the phage suspension, dialysis was performed in order to remove the CsCl. Briefly, phage suspension was introduced into dialysis cassettes, which in turn were introduced in 500 volumes of dialysis buffer (10 mM sodium phosphate, pH 7) for 30 min. After

performing the process three times the concentrated and purified phage suspension was collected.

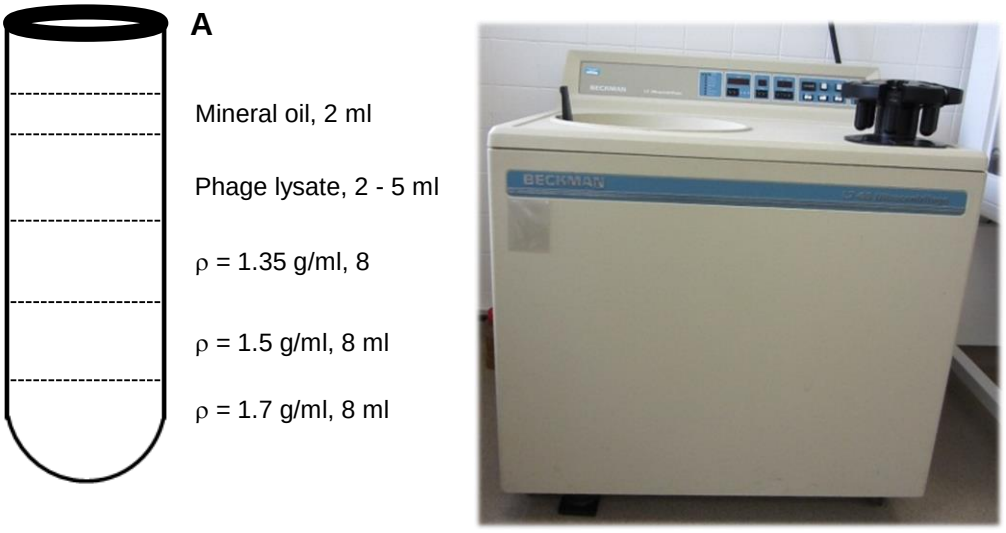

Figure 2.7: A - Schematic diagram for the set-up of CsCl density-gradient ultracentrifugation tubes, B – Image of the ultracentrifuge and JA-25.50 rotor (Beckman Coulter, USA).

2.4.3. Phenol-chloroform DNA extraction

Phenol/chloroform extraction was performed according to Pickard (227). 1.8 ml aliquots of phage lysate were treated with 18 µl of DNase I (1 mg/ml) and 8 µl of RNase A (10 mg/ml). The mixture was incubated at 37 °C for 60 min. Subsequently, 18 µl of proteinase K (10 mg/ml), 46 µl of 20 % sodium dodecyl sulphate (SDS) and 1 mM EDTA Na_2 were added to the samples and incubated at 65 °C for a further 60 min. Samples were aliquoted into 1.5 ml phase-lock gel eppendorf tubes and an equal volume of phenol:chloroform:isoamyl alcohol (25:24:1) was added to remove proteinaceous material. Extraction was repeated twice and between each step, the upper, aqueous phase layer was transferred into a new phage-lock gel tube and centrifuged (5 min, 8,000 x g). The aqueous top phase was retained and a final extraction with chloroform:isoamyl alcohol (24:1) was carried out by centrifugation (5 min, 6,000 x g). The supernatant was transferred to a new sterile 1.5 ml eppendorf tube

and DNA was precipitated by adding 45 µl of 3M sodium acetate and 500µl of 100 % isopropanol. The mixture was incubated at -20 °C overnight. The following day the samples were centrifuged (20 min, 8,000 x g) and supernatant was removed. The DNA pellet was washed with 1 ml of 70 % ethanol (v/v) and incubated at room temperature for 20 min. Centrifugation was performed for 20 min at 8,000 x g and the supernatant was removed. Pellets were rinsed with 70 % ethanol twice. Phage DNA was re-suspended in 200 µl of TE buffer (Tris-EDTA buffer solution, pH 8.0) and incubated at 65 °C for 10 min. After incubation the DNA was rehydrated at 4 °C overnight. Nucleic acid concentration and quality was measured with a NanoDrop spectrophotometer (Thermo Scientific, UK).

2.5. Agarose Gel Electrophoresis

Agarose gel electrophoresis was performed for uncut and digested DNA. A 1 % agarose gel was prepared using 1x TAE buffer. 2 % of ethidium bromide dye (10 mg/ml) was mixed with the agarose prior to pouring into the gel mould. The molecular weight DNA marker was prepared by mixing 1 µl of 6 x loading dye, 1 µl marker DNA and 4 µl of sterile deionised water. DNA samples were prepared by mixing 2 µl of 6X loading dye with 10 µl of DNA. The gel was run at 100 volts. The bands were visualised under UV light and a gel image was taken.

2.6. Restriction Fragment Length Polymorphism (RFLP)

Bacteriophage DNA was digested using the restriction enzymes *XbaI, XhoI* and *EcoRI* (FastEnzyme, Fermentas, UK). Digestion was carried out according to manufacturers' instructions. Bacteriophage K (GeneBank - AY176327) was used as a positive control

for the digestions performed. In order to find suitable restriction enzymes we used the NEBcutter tool (New England Biolabs, http://tools.neb.com/NEBcutter2/).

2.7. Multilocus sequence typing (MLST)

2.7.1. Theoretical background

Multilocus sequence typing (MLST) was proposed in 1998 as a universal and standardised sequencing-based method to characterise pathogenic bacteria (228). It examines the nucleotide sequence of multiple loci coding encoding housekeeping genes (generally seven loci). Housekeeping genes are genes required for the cell to normally function, for that reason they are present within all isolates within a species core genome. They are not under a high selective pressure; however there is enough variability within the nucleotide sequences that allows them to be put into different groups. The alleles of the sequenced genes are compared and their combination allows the assignment to a specific sequence type (ST). MLST databases showing the housekeeping gene sequence and ST's are available for a wide number of bacterial species, including for *S. aureus*. From the user point of view it is an extremely easy tool, one can upload directly the sequenced loci, wait for the software to compare them with the already available alleles and assign the isolate to a specific clonal group (229, 230).

2.7.2. Methodology

2.7.2.1. *S. aureus* DNA extraction protocol

Chromosomal DNA was extracted using the bacterial DNA extraction kit QIAamp DNA Mini Kit, according to manufacturers' instructions. However, the method was modified

for *S. aureus* by the inclusion of a cell wall lysis step. Briefly, bacterial cells were harvested (10 min, 5000 x g) and resuspended in an enzymatic lysis buffer (20 mM Tris [pH 8.0], 2 mM $EDTAN_2$, 1.2 % Triton x-100, immediately before use 20 µg/ml lysostaphin) for 30 min at 37 °C.

2.7.2.2. PCR conditions

Primers designed for the seven loci were purchased from Eurofins (UK) (Table 4). PCRs were carried out with 50 µl reaction volumes containing 2 µl of chromosomal DNA (approximately 0.5 µg), 5 µl of each primer working solution (100 pmol/µl), 0.25 µl (5 u/µl) of *Taq* DNA polymerase, 10 µl of 10X green buffer (supplied with the *Taq* polymerase), and 1 µl (10 mM) deoxynucleoside triphosphates. PCR was performed in a S1000^{TM} thermal cycler with an initial 4 min denaturation at 95 °C, followed by 30 cycles of denaturation at 95 °C for 30 sec, annealing at 55 °C for 30 sec, extension at 72 °C for 30 sec, followed by a final extension step of 72 °C for 10 min.

Following PCR run, all the reaction products went through a clean-up step to remove excess of primers, dNTTPs and salts that can interfere with the sequencing. The clean-up step was performed using a PCR clean-up kit, according to manufacturers' instructions. All the reactions were confirmed by electrophoresis in an agarose gel and sent for sequencing at Source Bioscience (Nottingham, UK).

2.7.2.3. Sequencing, analysing and alignment

All the fragments were sequenced by Sanger sequencing. Once the nucleotide sequences for the seven loci were available, each of them was inserted in FASTA format in the MEGA 5.0 software, where they were aligned with the reference alleles

for each locus and analysed. Afterwards, the sequences were submitted to the *S. aureus* database (http://saureus.mlst.net) to get the corresponding ST.

Table 2.1: The seven loci and the primers used for PCR.

loci	Function coded	Sequencing primers
arc	Carbamate kinase	arc up - 5' TTG ATT CAC CAG CGC GTA TTG TC -3' arc dn - 5' AGG TAT CTG CTT CAA TCA GCG -3'
aro	Shikimate dehydrogenase	aro up - 5' ATC GGA AAT CCT ATT TCA CAT TC -3' aro dn - 5' GGT GTT GTA TTA ATA ACG ATA TC -3'
glp	Glycerol kinase	glp up - 5' CTA GGA ACT GCA ATC TTA ATC C -3' glp dn - 5' TGG TAA AAT CGC ATG TCC AAT TC -3'
gmk	Guanylate kinase	gmk up - 5' ATC GTT TTA TCG GGA CCA TC -3' gmk dn - 5' TCA TTA ACT ACA ACG TAA TCG TA -3'
pta	Phosphate acetyltransferase	pta up - 5' GTT AAA ATC GTA TTA CCT GAA GG -3' pta dn - 5' GAC CCT TTT GTT GAA AAG CTT AA -3'
tpi	Triosephosphate isomerase	tpi up - 5' TCG TTC ATT CTG AAC GTC GTG AA -3' tpi dn - 5' TTT GCA CCT TCT AAC AAT TGT AC -3'
yqi	Acetyl coenzyme A acetyltransferase	yqi up- 5' CAG CAT ACA GGA CAC CTA TTG GC -3' yqi dn- 5' CGT TGA GGA ATC GAT ACT GGA AC -3'

2.8. Bacteriophage DNA sequencing, analysis, and assembly

DNA sequencing libraries were prepared using the Nextera XT DNA kit (Illumina, San Diego, CA, USA) according to the manufacturer's protocol. Individually tagged libraries were sequenced as a part of a flow cell as 2- by 250-base paired-end reads using the Illumina MiSeq platform (Illumina, San Diego, CA, USA) at The Danish National High-Throughput DNA-Sequencing Centre. Reads were analysed, trimmed, and assembled using 6.5.1 CLC Genomic Workbench as described before by Kot *et al.* (231). Genes were predicted and annotated using the RAST server (232).

2.9. Antibiotic Minimum Inhibitory Concentration (MIC)

Antibiotic MICs were determined according to the Clinical and Laboratory Standards Institute (CLSI) guidelines (233). The medium used for the assay was TSB and

Staphylococcus aureus ATCC 29213 was used as quality control strain. The determination of the MICs was performed by the broth micro-dilution method as described in the same guidelines. Briefly, 96-well microplates, each containing a volume of 200 µl with 1:2 dilution of the antibiotic (64 to 0.0625 µg/ml range) were inoculated with an initial standard inoculum of a 10^5 cfu/ml of an overnight culture. A 0.5 McFarland scale was used for inoculum standardisation. Incubation at 37 °C with shaking (90 rpm) followed for 18 hours. The MIC for each isolate was scored by direct visualisation. A negative control containing only broth was added and the experiments were run in triplicate.

2.10. Microscopy

2.10.1. Transmission electron microscopy (TEM)

2.10.1.1. Theoretical background

Electron microscopes are equipped with a beam of electrons, generated at high accelerating voltages, allowing them to achieve higher resolutions and magnifications than those obtained with light microscopes. The wavelength of an electron beam is greatly shorter than that of light, resulting in a much higher resolution. For observation of viral particles, such as bacteriophages, the transmission electron microscope (TEM) has been used for more than 70 years (234) and is the most common and widely used microscopy technique. In fact, electron microscopy still remains the basis for identification and classification of phage particles. A hot tungsten filament in an electron gun allows electrons to be pulled from the filament in an accelerated manner establishing a fine electron beam. This electron beam passes through an anode followed by an electromagnetic condenser lens that focuses the beam on the specimen. The beam passes thought the specimen and image is formed caused by the

interaction of the electrons transmitted through the specimen. A vacuum system is included in these microscopes to remove air, as gas molecules could interact and consequently scatter the electron beam, resulting in a poor resolution of the image. Figure 2.8 shows a diagram of the electron microscope. Samples are negatively stained and embedded with heavy metal salts, such as uranyl acetate (UA) or phosphotungstic acid (PTA). The heavy ions interact with the electron beam when this last one passes through the specimen producing a phase contrast image.

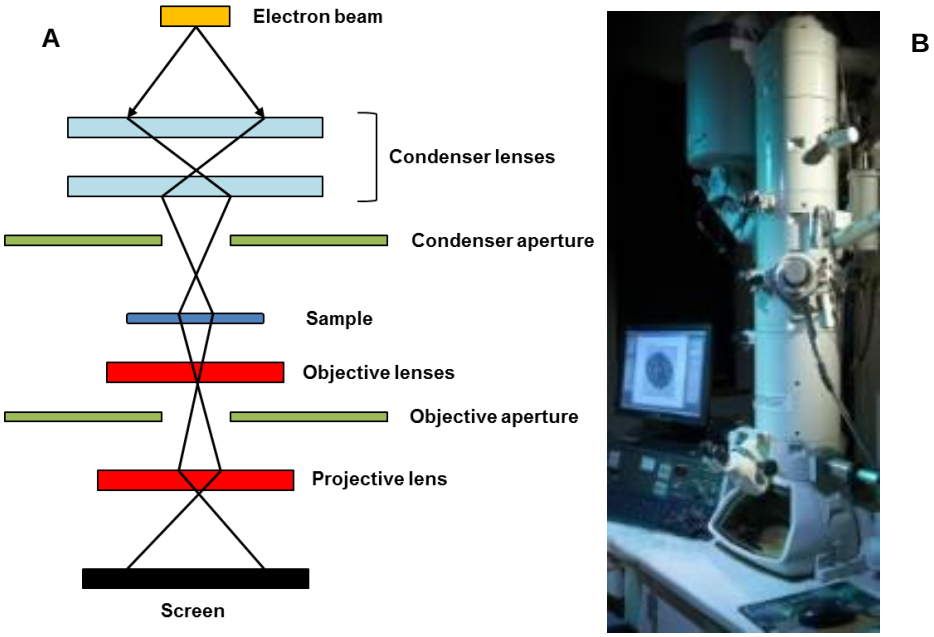

Figure 2.8: Representative diagram (A) and image (B) of the transmission electron microscope.

2.10.1.2. Sample preparation

Bacteriophage lysates were purified through PEG-precipitation (mentioned above in section 2.2.). Following purification, bacteriophage solution, containing ~1x10^9 pfu/ml, were deposited onto carbon-coated copper grids. To improve phage adsorption the grids were previously made hydrophilic by a 30 min exposition to UV light (235). A drop of phage suspension was placed on the grid and phages were allowed to adsorb for 1

min. The excess of suspension was drained off with filter paper and a drop of distilled water was placed on the grid and blot dried straight after. This was repeated another time. Finally, a drop of 1 % uranyl acetate (pH 4) was dropped on the grid for 30 sec and blot dried to negatively stain the phage particles. The sample grids were left to dry for 3 hours before observation on the electron microscope. Visualisation was performed using a transmission electron microscope (JEM1200EXII; JEOL, Bath, United Kingdom) operated at 120 kV.

2.10.2. Confocal laser scanning microscopy

2.10.2.1. Theoretical background

Confocal laser scanning microscopy is considered nowadays part of the gold-standard methodology for biofilm studies and analysis. It is described as an advanced and more versatile microscope technique overcoming some of the limitations of the conventional fluorescence microscopy, including visualisation of thick samples or *in vivo* studies, which patent was created in 1955 by Marvin Minsky (236). In a conventional optical light microscope, the sample is placed on the stage and despite light being shed to a point on the specimen the entire sample gets illuminated. This results in an image of low resolution. A confocal microscope comprises confocal apertures, named pinholes, that permit only light from the plane of focus to reach the detector and only a single point in the specimen is illuminated at a time (Figure 2.9), blocking the scattered light and the out-of-focus light observed in the conventional microscope, and resulting in an image of high quality. This allows for the collection of sections of the X-Y plane (a stack) that after collection of several stacks it can be put together to reconstruct a three-dimensional image of the specimen. Sections in the X-Z plane can also be acquired.

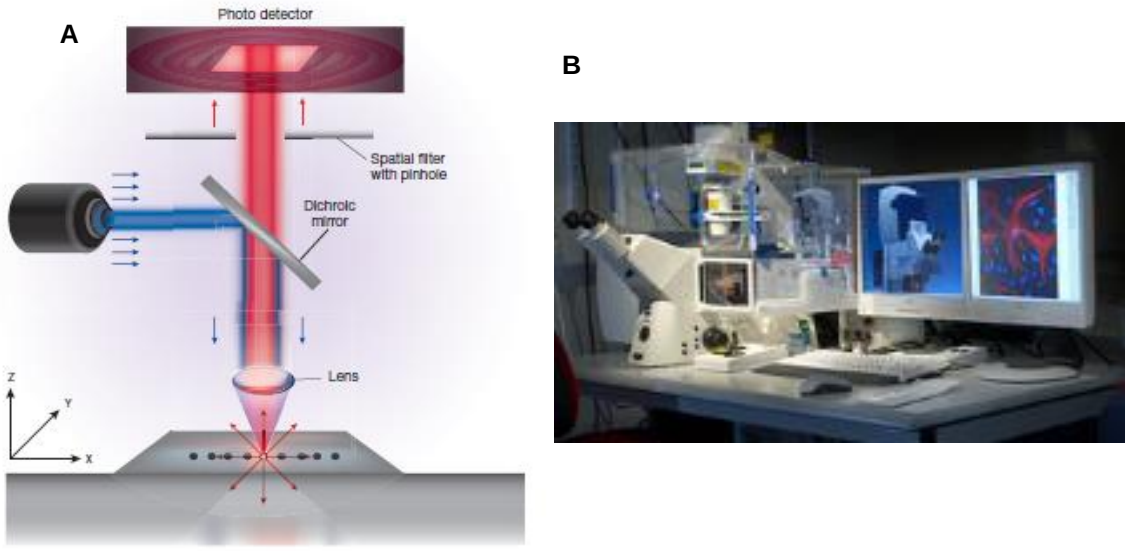

Figure 2.9: Representative diagram (A) and image (B) of the confocal microscope. (A) is reprinted from reference (236) and used with permission.

The fluorescence confocal microscope is used with samples stained with dyes, more specifically fluorophores, that get excited by the light source and the resulting emitted fluorescence is detected and collected to produce a detailed image of the specimen. In a laser scanning confocal microscope the excitation light is a laser beam. The laser is set at the required wavelength to excite the fluorophore. For the presented work two fluorescence DNA stains were used: SYTO 9 and propidium iodide. The first one stains all bacterial cells, independently of the integrity of the cell membrane and is excited at 480/500 nm, hence emits green light. Propidium iodide stains only bacteria with their cell membrane damaged and upon excitation at 490/635 nm, emits red light (Figure 2.10).

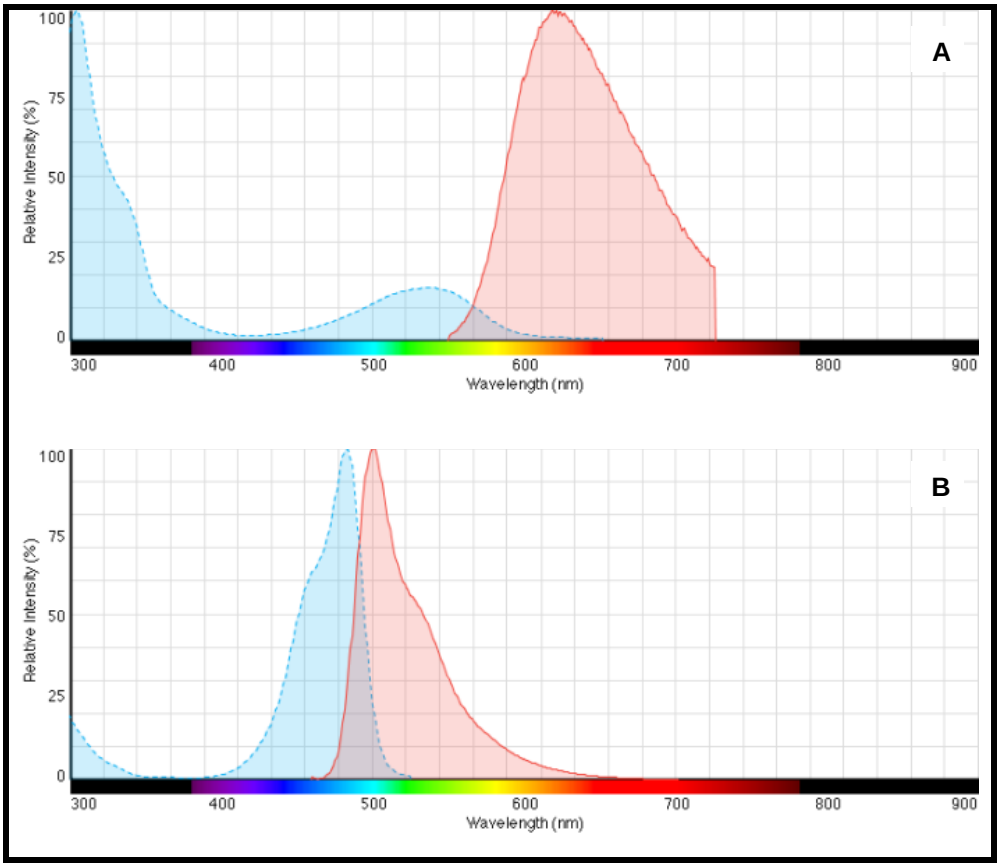

Figure 2.10: Fluorescence Ex/Em light spectra of propidium iodide (A) and SYTO 9 (B) nucleic acid stains (237).

2.10.2.2. Sample preparation

Biofilms were established on the surface of stainless steel pegs. Disks were carefully removed and the biofilm surface was washed twice with PBS. Biofilm cell viability was determined using LIVE/DEAD staining following the manufacturer's instructions. The disks were immersed in the staining solution and incubated at room temperature for 15 min in the dark. After staining, the disks were gently rinsed with PBS and this was repeated six times more. The biofilm images were acquired in a Zeiss LSM510META confocal scanning laser microscope. Biofilms were observed using the 20x objective (20x/0.5 W) or the 60x water-immersion objective (60x/1.2 W). Images were acquired with 1024 x 1024 resolution in at least three different regions of the biofilm surface. In order to determine the biofilm height for each region analysed the top and bottom layer

of the biofilm was determined and the average and maximum height of biofilm was calculated. Manipulation of the images and 3D reconstructions were performed using LSM Image Browser and Imaris 7.4.2 softwares.

2.11. *In vitro* Biofilm Methods

2.11.1. Biofilm formation for *S. aureus* isolates

The biofilm assay was performed similarly to previously described methods (238) but with some modifications in order to optimise the system. Biofilm formation was performed in 96-well polystyrene tissue culture microplates to achieve an improved cell attachment. TSB supplemented with 1 % D-(+)-glucose (TSBg) and 1 % NaCl (TSBg-NaCl) was used to perform this assay, as this helps to improve biofilm formation (227, 239). An overnight culture was diluted to a titre of 10^8 cfu/ml. Briefly, in the microplate wells a 1:100 dilution was performed by adding 5 µl of the bacterial suspension to 195 µl of TSBg-NaCl, making a starting inoculum of 10^6 cfu/ml. 200 µl of broth was added to a set of wells as a negative control. All wells were replicated three times. Afterwards, microplates were incubated at 37 °C for 48 h with no shaking for biofilm formation. Microplates were carefully wrapped with a layer of moistened blue paper towel roll and plastic to prevent the media in the microplates evaporating. During the incubation time (~24 h after incubation), 50 µl of fresh TSBg-NaCl was added to all control and test wells.

2.11.2. Biofilm formation for *P. aeruginosa* isolates

The biofilm assay for formation of *P. aeruginosa* biofilms was based on the previously described methods of Pires *et al.* (240) with some modifications when appropriate.

Formation of the biofilms was carried out in 96-well polystyrene tissue culture microtitre plates. An overnight culture was diluted to a titre of 10^8 cfu/ml. Briefly, in the microplate wells a 1:100 dilution was performed by adding 5 µl of the bacterial suspension to 195 µl of 50 % LBg media, making a starting inoculum of 10^6 cfu/ml. 200 µl of broth was added to a set of wells as a negative control. All wells were replicated three times. Afterwards, microplates were incubated at 37 °C for 48 h with constant shaking (120 rpm) for 48 hours. Microplates were carefully wrapped with a layer of moistened blue paper towel roll and plastic to prevent the media in the microplates evaporating. At 24 hours, 50 µl of fresh 50 % LB was added to all control and test wells.

2.11.3. Biofilm treatment with phage mixture

Biofilm formation was carried out as described above. Once biofilms were established and washed once with PBS, 100 µl of phage mixture in PBS was added to a set of wells. Two different MOIs were set up for the single or mixed phage. 100 µl of PBS were added to both the positive and negative controls. All the experiments were performed three times. After static incubation at 37 °C, microplates were washed and stained with crystal violet, as described below, at predetermined time points. Optical density readings of the staining intensity at 600 nm (OD_{600}) were performed and recorded using a plate reader.

2.11.4. Biofilm staining with crystal violet

Following incubation, medium was poured off and wells were carefully washed twice with sterile phosphate-buffered saline (PBS) solution to remove any planktonic cells. Microplates were allowed to dry for 1 hour at 50°C.To determine total biofilm biomass, microplate wells were stained with 0.1 % crystal violet (CV). After staining, the wells were washed twice with PBS solution and dried. Biofilm formation was determined by

visual comparison of the stained wells and photographed. CV was then dissolved, the wells were washed with PBS twice and 95 % ethanol was added. This was left for 30 min to dissolve the stain, following a 10-fold dilution the absorbance was measured by the FLUOstar plate reader at 600 nm.

2.11.5. XTT Reduction Assay

This assay determines the number of viable cells present in a biofilm by using XTT (a complex salt) which can only be reduced by metabolically active cells. This reduction of XTT turns the solution orange, and so the concentration of the dye is proportional to the number of metabolically active cells in the biofilm. Hence, biofilm cellular activity was determined by the XTT reduction assay. Medium from each well was poured off carefully and washed twice with sterile PBS. Following this 1 ml of XTT solution was added to each well and the microtitre plates were then incubated in the dark for 3 hours at 37 °C with constant shaking (120 rpm). Absorbance was then measured using the FLUOstar plate reader at 490 nm.

2.11.6. Colony and plaque counting

This assay determines the number of viable cells and phages particles within the biofilm. 200 µl of PBS buffer was added to the wells where biofilms have been grown and the bottom and walls of the wells were scraped with a loop. The contents of each well was recovered with a pipette after five times pipetting up and down for complete disruption and detachment of cells to the surface. Serial dilutions were performed in ferrous ammonium sulphate (FAS), a virucide (241) that ensures the inactivation of free phages prior to viable bacterial counts. The mechanism of activity of FAS has not yet been clarified and it has been suggested that the oxidative damage is not the mode of

action (242). A FAS stock solution was prepared, immediately before use, in 10 ml distilled water and filter sterilised (0.22 µm pore size) and was used at a working concentration of 10 mM. After standing at room temperature for 15 min, dilutions were plated out and bacterial colonies enumerated. For enumeration of phages present in the biofilm, an aliquot of 100 ml of the disrupted suspension was used to produce serial dilutions in PBS. Titres were determined using the method previously described in this chapter in Section 2.2.5.

2.11.7. Minimal Biofilm Eradication Concentration (MBEC)

Established biofilms were formed as described already in sections 2.11.1 and 2.11.2 in 96-well microtitre plates. Medium was gently removed and the wells were washed twice with PBS. 1:2 serial dilutions of the antibiotic was performed and 200 µl was added to the biofilm wells and the microtitre plate incubated for 24 hours. PBS only was added to biofilm wells as a negative control. MBECs were determined from the lowest concentration that was able to reduce the biofilm compared to the control after staining with crystal violet. All tests were performed in triplicate.

2.12. Data Analysis

Comparisons between the different time points and the positive controls were made by performing *Student's t* test, and a *P*-value of 0.05 was considered statistically significant for all cases. All tests were performed with a confidence level of 95 %. Spread of data at the 95 % confidence interval (CI) was estimated using the Winpepi freeware statistical analysis program (243). Graph plotting and analysis were performed with SigmaPlot 10.0 and OriginPro 8 Softwares.

2.13. List of materials and reagents used

Table 2.2: List of reagents and materials.

Material / Reagent	Supplier / Catalogue number
Agarose	Sigma / A9539
Bacteriological agar n^{o} 1	Sigma / A5306
$CaCl_2$	Sigma / C1016
Centrifugal concentrators	Fisher / 10550243
Cesium chloride	Sigma / 289329
Chloroform	Sigma / C7559
Chloroform:isoamyl alcohol (24:1)	Sigma / C0549
Crystal Violet	Sigma / C6158
D-(+)-glucose	Sigma / G8270
Deoxynucleoside triphosphates	Promega / U1511
Dialysis cassettes (Slide-A-Lyser, Fisher, UK)	Fisher / 10625655
DNA extraction kit QIAamp DNA Mini Kit	Qiagen / 51304
DNA ladder (1 kb)	New England Biolanbs / N3232S
DNA ladder (100 bp)	New England Biolabs / N3231S
DNase I	Qiagen / AM2222
EDTA Na_2	Sigma / E5134
Ethanol	Sigma / 51976
Ethidium bromide	Sigma / E1510
FAS	Sigma / 215406
FastDigest EcoRI	Fisher / 15302495
FastDigest XbaI	Fisher / 15342535
FastDigest XhoI	Fisher / 15362535
Gelatine	Sigma / 48723
Glycerol	Sigma / G5516
Helmanex III	Sigma / Z805939-1EA
Isopropanol	Sigma / I9030
LA	Sigma / L2025
LB	Sigma / L3022
LIVE/DEAD	Life technologies / L-7007
Loading dye, blue (6x)	New England Biolabds / B7021S

Table 2.3: List of reagents and materials (continuation of Table 2.2).

Material / Reagent	Supplier / Catalogue number
Lysostaphin	Sigma - L7386
$MgSO_4$	Sigma / M7506
MinElute Gel Extraction Kit	Qiagen / 28604
Mineral Oil	Sigma / M5904
Mucin	Sigma / M2378
NaCl	Sigma / S7653
PCR clean-up kit	Fisher / 10405703
Phase-lock gel Eppendorf tubes	5 PRIME / 2302800
Phenol:chloroform:isoamyl alcohol (25:24:1)	Sigma / P3803
Polyallomer ultracentrifuge tubes (50 ml)	Beckman Coulter
Polyethylene glycol (PEG) m.w.8000	Sigma / 1546605
Polystyrene tissue culture microplates (96-well)	Fisher / TKT-180-090X-F96
Proteinase K	Qiagen / 19131
QIAamp MinElute Virus Spin Kit	Qiagen / 57704
RNase A	Qiagen / 19101
Sodium dodecyl sulphate	Sigma / 436143
Sodium phosphate	Sigma / S8282
Taq DNA polymerase	Promega / M8305
TE buffer (Tris-EDTA buffer solution, pH 8.0)	Sigma / 93283
Thermal cycler	biorad S1000TM
Tris Acetate-EDTA buffer	Sigma / T8280
Triton x-100	Sigma / X100
TSA	Sigma / 22091
TSB	Sigma / 22092
Uranyl acetate	Sigma / 73943
XTT solution	Sigma / X4626
YPD media	Sigma / Y1375

Chapter Three:

PROSPECTING AND CHARACTERISING NEW BACTERIOPHAGES

3.1. Chapter summary

This chapter is focused on the isolation and characterisation of lytic bacteriophages and is divided into two main sections: a first section describing bacteriophages that effectively infect *Staphylococcus aureus* clinical isolates and a second section, where bacteriophages able to infect *Pseudomonas aeruginosa* clinical strains are described. In both sections, after isolating the phages, the best candidates are identified and characterised in order to establish a therapeutic and safe cocktail showing broad host range coverage against clinically relevant members of the two bacterial species. The work focus on *S. aureus* has been published in a scientific journal (244).

3.2. Background

The first stage for the establishment of a bacteriophage therapeutic is the isolation and respective characterisation of the phages as candidates for formulation. Isolation and characterisation play a crucial role for the success and effectiveness of bacteriophage therapy and negligence of steps, such as ineffective phage selection or poor phage stability, has been responsible for several failures in the past (this has been reviewed in Chapter One). This was promptly noted by d'Hérelle who published in 1938 a guide to the isolation and preparation of phage therapy (245), after testing several commercially available, but ineffective, phage formulations.

For phage isolation, although a relatively easy step when compared to discovery of other alternatives, it is important to consider the ecology of the bacterial species to be targeted in order to maximise the recovery of suitable viral particles. For example, phages against bovine mastitis causing *S. aureus* have been sampled from farmyard slurry and effluent (246) and phages targeting the marine pathogen *Vibrio vulnificus* have been isolated from estuarine sediment known to be a habitat for the pathogen

(247). Once environmental samples are obtained and prior to direct inspection for phage, the best approach for isolation of promising phages is by performing bacterial enrichments using preferably, some of the relevant clinical isolates causing the infection. Sample enrichments, in a situation when small numbers of the targeted phage are present, will allow them to propagate when samples are incubated making them easily detected. As mentioned elsewhere, any method used for phage isolation will always influence the type of phage to be selected (248). For enrichment-based methods phages that proliferate faster in the bacterial strains used for the enrichments will have a selective advantage over phage strains that despite their slower growth could potentially infect and be effective against other clinical strains.

The next crucial step is the characterisation of the phage, where determination of host range, level of virulence, morphology and lack of toxin-encoding genes or lysogeny determinants are to be evaluated. For the determination of the host range of the phages selected, they are going to be used to challenge a collection of bacterial clinical isolates and their efficiency of plating (EOP) evaluated. Ideally this collection should be as representative as possible with the most prevalent isolates of the targeted infection aimed. Usually, phages showing a broader host range will prevail and be chosen over phages with narrower host coverage ranges. Often, formulations composed of several phages (cocktails) are employed not only because bacterial resistance is less likely to emerge, but also because the combination has a broader therapeutic range.

Ideally phages that show a high level of virulence infecting their bacterial hosts are preferred. Phage virulence refers to phages infecting in an efficient fashion and being responsible for a quick bacterial extinction. This can be due to efficiency in recognising the cell wall receptor (adsorption) or in injecting the genome inside or being able to proliferate more rapidly and in high numbers (burst size).

The determination of phage morphology is achieved by TEM analysis and viral particles can be classified taxonomically. Most likely particles will belong to the capsid

lipid-free *Caudovirales* order due to a biased isolation method where chloroform is often used. Also, it is most likely phages will carry a linear dsDNA genome, a feature of phages of *Caudovirales* order.

The improvement and the technical advances in DNA sequencing have allowed this technology to become more efficient and more affordable making it easily accessible and it is common nowadays (in 2015) to include genome data when new phages are isolated. The availability of the genomes allow us to better predict the phage behaviour and, in case of commercial and therapeutic uses, to look for a lysogenic phage life-style or any unwanted toxin and resistance factor that would be enough to exclude the phage from future therapeutic use. However, phage genomes still contain many "cryptic" regions, where the great majority of putative coding genes lack known function. Phage genomics is still at a relatively early stage and more intense genome sequencing and characterisation of their gene products is required to increase our knowledge of the as yet largely hidden phage metagenome.

3.3. Methods

3.3.1. Bacterial strains used for the study

In this chapter several bacterial strains including *P. aeruginosa, S. aureus* and coagulase-negative *staphylococci* were used in order to isolate, proliferate and efficacy evaluation of lytic phages. Their provenances are listed in Table 3.1, Table 3.2 and Table 3.3, respectively.

Table 3.1: List of human bacterial *P. aeruginosa* strains isolated from acute and chronic sites of infection, with their respective country of origin and related information.

	Isolate	ST	Country	Source
	PAO1	-	Standard Laboratory Reference Strain	(249)
Acute Infections	PA45311	-	Bristol, UK	nd
	PA45291	-	Bristol, UK	nd
	PA45235	-	Bristol, UK	nd
	PA45379	-	Bristol, UK	nd
	PA45321	-	Bristol, UK	nd
Chronic Infections	BC00918	-	Genova , Italy	CF, Male, 23
	BC01026	-	Australia	nd
	BC00909	-	Paris, France	CF, Male, 25
	BC00888	1517	Utrecht, The Netherlands	CF, M, 11/01/2007
	BC00907	1528	Paris, France	CF, Female, 24
	BC00917	1544	Genova , Italy	CF, Male, 29 years
	BC00920	1547	Lisbon, Portugal	CF, Male, 32 years
	BC00921	1535	Lisbon, Portugal	CF, Female, 37 Years
	BC00922	155	Lisbon, Portugal	CF, Female, 8 Years
	BC00923	1548	Lisbon, Portugal	CF, Female, 19 years
	BC00931	-	Bordeaux, France	CF, Female
	BC00932	1529	Bordeaux, France	CF, Male
	BC00933	1530	Bordeaux, France	CF, Female
	BC00934	1552	Bordeaux, France	CF, Male
	BC00935	-	Bordeaux, France	CF, Male

CF, cystic fibrosis; n.d. no data available

Table 3.2: List of human bacterial *S. aureus* isolates with their respective sequence type (ST) and their country of origin.

Isolates	ST	Country
WBG8343	1	Australia
MSSA H476	1	England
HT2001749	1	USA
H148	3	UK
BK519	5	USA
CDC980193-USA800	5	USA
Mu3	5	Japan
963Small	5	USA
97.1948.S.	5	Scotland
C56	6	UK
C2	7	UK
CDC201114-USA300	8	USA
15981	8	Spain
HT20030203	8	USA
HT20030206	8	USA
C125	8	UK
Fra97392	8	France
EMRSA6	8	UK
99st22111	8	-
H169	9	UK
D316	11	UK
D329	12	England
H117	12	UK
H402	13	UK
C154	14	UK
C357	15	UK
H291	18	UK
H42	20	UK
HO50960412	22	UK
H182	22	England
C720	22	England
C13	22	Eire
C49	23	UK
D279	25	UK
Not116	27	UK
H118	28	UK
SwedenAO17934/97	30	Sweden
Cuba4030	30	Cuba
C390	31	UK
H399	33	UK
C160	34	UK
Btn766	36	UK
MRSA 252	36	England
H325	36	UK
EMRSA16	36	UK
H137	38	UK
H137MRSA	38	UK
C253	40	UK
C427	42	UK
Fin76167	45	Finland
C316	49	UK
H417	50	UK
C3	51	UK
D49	53	UK
D98	54	UK
D318	57	UK
D535	59	UK
HT20050306	59	Australia
H40	60	UK
D473	69	UK
CDC201078-USA700	72	USA
HT20040991	80	Algeria
SwedN8890/99	80	Sweden
BK1563	88	USA
HT20020635	93	Australia
HT2001634	93	Australia
Cuba4005	94	Cuba
D302	97	UK
Not38	101	UK
D472	109	UK
H560	121	UK
D139	145	UK
D22	182	UK
Can6428-011	188	Canada
D470	207	UK
98/10618	217	UK
CDC12	225	USA
Germany131/98	228	Germany
CDC16	231	USA
99.3759V	235	Scotland
SwedenON408/99	246	Sweden
KD121618	250	Switzerland
KD12943	257	UK
Not271	264	UK
Not380	266	UK
Not98-53	280	UK
CAN6820-0616	289	Canada
Fin62305	296	Finland
Not266	301	UK
Btn2164	312	UK
Btn2299	322	UK
Btn2289	322	UK
515/09[†]	398	n.d.
Not161	517	UK
Not290	529	UK

[†] bovine mastitis isolate; n.d. no data available.

Table 3.3: List of bacterial coagulase-negative *staphylococci* strains.

Species	Isolates
S. xylosus	ATCC 29971
S. sciuri subsp. *sciuri*	ATCC 29062
S. chromogenes	CCM 3387
S. hyicus	CCM 29368
S. arlettae	N910 254
S. vitulinus	ATCC 51145
S. simulans	N920 197
S. epidermidis	ATCC 14990

3.3.2. Genome search of antibiotic resistance determinants and virulence factors

Phage genomes were searched for antimicrobial resistance determinants (98 % ID threshold) using the web-tool Resfinder that uses the BLAST algorithm (250). The antibiotic resistance genes search was focused on the main antibiotics (Table 3.4). The web-tool VirulenceFinder (251) was used for the search of genes potential coding for virulence factors (98 % ID threshold) found in *E. coli*, *Enterococcus* spp and *S aureus*.

Table 3.4: Antibiotics to which resistance genes determinants were searched with ResFinder web-tool.

Antibiotic
Nitroimidazole
Oxazolidinone
Fusidic Acid
Fluoroquinolone
Fosfomycin
MLS - Macrolide, Lincosamide and Streptogramin B
Beta-lactam
Aminoglycoside
Chloramphenicol
Rifampicin
Sulphonamide
Tetracycline
Trimethoprim
Glycopeptide

3.4. Results

3.4.1. *S. aureus* phages isolation and characterisation

3.4.1.1. Bacteriophage isolation and plaque morphology

A total of 21 phages were isolated from sewage samples after enrichments with the *S. aureus* strains listed on Table 3.2. Plaque morphology of *S. aureus* phages observed is circular with regular borders and generally small, between 0.5 mm to 1.5 mm diameter, and without halo zones, although some present a small halo surrounding plaques. Halos are caused by the diffusion of enzymatic molecules produced by the phage. Table 3.5 describes the morphology of plaques produced by the phages isolated for this work and Figure 3.1 shows examples of plaques.

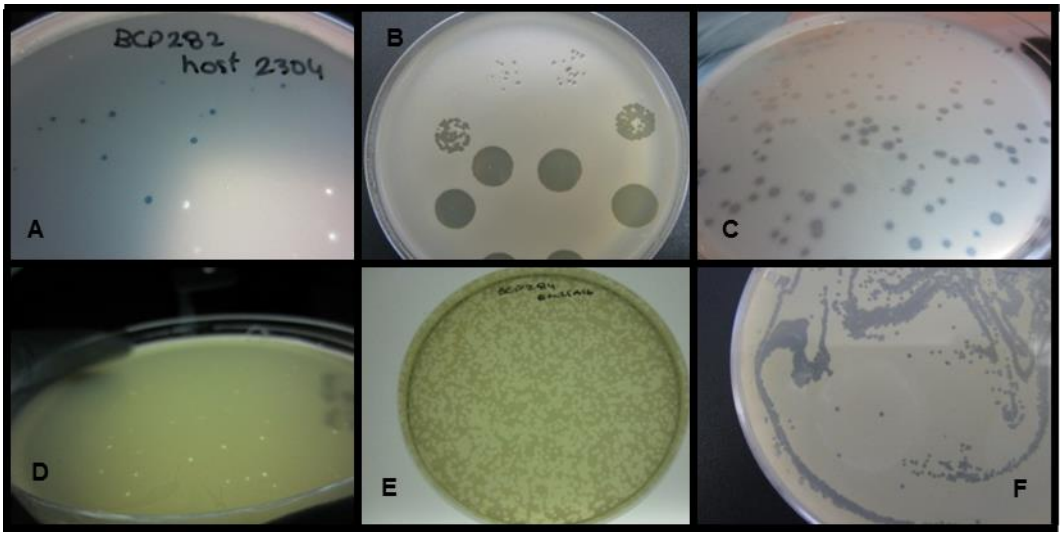

Figure 3.1: Examples of *S. aureus* isolated phage plaques (clear spots caused by bacterial lysis). A – BCP282; B – DRA88; C – BCP285; D – BCP286; E – BCP284; F – phage K.

Table 3.5: Phages isolated with respective *S. aureus* bacterial hosts and plaque morphology.

Isolated phage	*S. aureus* host	Plaque morphology ~ mm (∅); halo
DRA88	BC0691	<0.5
DRA145	Not290	<0.5
DRA147	D551	0.5
DRA189	BC1009	1.5
DRA226	D551	0.5 – 1.0
DRA278	H560	1.0
DRA279	H560	1.0
DRA280	H560	1.0
DRA281	BTN2306	2.0
DRA282	BTN2306	2.0
DRA283	EMRSA3	0.5
DRA284	EMRSA16	1.0
DRA285	BTN766	1.5; halo
DRA286	98/10618	0.5; halo
DRA287	HT20010254	1.0; halo
DRA288	EMRSA16	1.0
DRA289	98/10618	1.0
DRA290	BTN766	1.5
DRA291	FFP221	<0.5
DRA292	FFP221	<0.5
DRAE2260	E2260	0.5
Phage K	EMRSA16	1.0

3.4.1.2. Host range determination and selection of phage cocktail

The lytic phages previously isolated for *S. aureus* were evaluated regarding their host range of infectivity in order to select the phages showing the broadest range of host infectivity. Phages were tested against a small but diverse *S. aureus* collection of 23 clinical isolates, including geographical as well as antibiotic resistance profile diversity, the latter including examples of methicillin sensitive *S. aureus* (MSSA) and methicillin-resistant *S. aureus* (MRSA). An isolate of *S. epidermidis* was also included in the collection. Phage K is a polyvalent phage of the staphylococcal genus and we observed 71 % (CI 95 %, 51 % to 86 %) of coverage of the tested isolates. The majority of the isolated phages present a broad host range, varying between 29 % (CI 95 %, 14 % to 49 %; 7 isolates out of 24 were susceptible) for DRA283 to 75 % (CI 95

%, 55 % to 89 %; 18 isolates out of 24 were susceptible) of host coverage for BCP287. Others showed a narrower host range, such as phage DRAE2260 that was only able to infect three strains of the collection (12.5 %, CI 95 %, 3.2 % to 30.3 %) and phage DRA279 only infecting one of the isolates (4 %, CI 95 %, 2 % to 18 %). Phages DRA145, DRA147 and DRA226 showed to have an even higher narrow host range and were not able to infect any of the *S. aureus* isolates. Apart from phage K, that produced small plaques in the bacterial lawn of the *S. epidermidis* isolate and *S. aureus* HT20040991, any other of the isolated phages were able to infect them.

For the phage cocktail composition phages DRA88, DRA288 and K were selected in order to obtain the best combination possible to achieve a broad host range of infectivity and prevent the emergence of resistant mutants. The latter result is presented in Chapter Four.

3.4.1.3. Genome restriction analysis

Isolation of phage genomic DNA and the subsequent enzymatic restriction digest analysis was carried out to determine whether phages were genetically closely related (Figure 3.2). The restriction analysis was performed with *XbaI* and *EcoRI* endonucleases. Phage K was the positive control for the restriction analysis. DNA extraction straight after phage propagation resulted in low DNA yield and presence of smears, possibly due to the presence of proteins and RNA. High DNA yield and greatly improved purity was achieved only with CsCl gradients. The restriction profiles produced by two enzymes yielded a large number of fragments that showed a similar pattern for all the three phages on a 1 % agarose gel. Although similar, it is possible to visualise the presence or lack of some bands, for example the band pattern of the *XbaI* digest in the region of 2027 bp and 564 bp was different for all phages. This suggests

that DRA88, DRA288 and phage K are different phage particles, however very closely related.

Table 3.6: Sensitivity screening of isolated phages against 23 *S. aureus* isolates and one *S. epidermidis* isolate [†].

Bacterial Isolates	Bacteriophages (DRA)																					
	88	145	147	189	226	278	279	280	281	282	283	284	285	286	287	288	289	290	291	292	E2260	K
159181	S	R	R	S	R	S	I	S	S	S	I	S	S	S	S	S	S	S	S	S	R	I
C316	S	R	R	R	R	R	R	R	R	R	I	R	R	R	S	I	I	I	S	R	R	S
D329	S	R	R	S	R	S	I	S	S	S	S	S	S	S	S	S	S	S	S	S	I	S
H137	I	R	R	I	R	I	I	I	I	I	I	I	I	I	I	I	I	I	S	I	R	I
H560	S	R	R	S	R	S	S	S	S	S	S	S	S	S	S	S	S	S	S	S	R	S
Btn766	S	R	R	S	R	S	I	S	S	S	S	S	S	S	S	S	S	S	I	S	R	S
HT20030203	I	I	I	I	R	R	I	I	R	R	S	R	R	R	S	I	I	I		I	S	S
HT20030206	I	I	I	R	R	R	R	R	R	R	I	R	R	R	S	R	R	R		R	S	S
HT20040991	R	R	R	R	R	R	R	R	R	R	R	R	R	R	R	R	R	R	R	R	R	I
HT20020635	I	R	R	R	R	R	R	R	R	R	R	R	R	R	R	I	R	R	I	R	R	S
ATCC14990	R	R	R	R	R	R	R	R	R	R	R	R	R	R	R	R	R	R	R	R	R	I
HO50960412	S	R	R	I	R	S	I	S	S	S	I	S	S	S	S	S	S	S	I	S	R	I
H182	S	R	R	I	R	S	I	S	S	S	I	S	S	S	S	S	S	S	I	S	R	S
C720	S	R	R		R	S	I	S	S	S	I	S	S	S	S	S	S	S	I	S	R	R
98/10618	S	R	R	I	R	S	I	S	S	S	I	S	S	S	S	S	S	S	S	S	R	S
MRSA 252	S	R	R	S	R	S	I	S	S	S	I	S	S	S	S	S	S	S	S	S	R	S
H325	S	R	R	S	I	S	I	S	S	S	I	S	S	S	S	S	S	S	S	S	R	S
WBG8343	I	R	R	R	R	R	R	R	R	R	R	R	R	R	S	R	R	R	R	R	R	S
MSSA H476	S	R	R	S	R	S	I	S	S	S	I	S	S	S	S	S	S	S	S	S	R	S
Mu3	R	R	R	R	R	I	I	I	I	I	I	I	I	I	I	I	I	I	I	I	R	S
963Small	S	R	R	S	R	S		S	S	S	S	S	S	S	S	S	S	S	S	S	R	S
97.1948.S.	R	R	R	R	R	R	R	R	R	R	R	R	R	R	R	R	R	R	R	R	R	R
515/09	S	R	R	S	R	I	I	S	I	I	S	S	S	S	S	S	S	S	I	S	R	S
KD121618	I	R	R	S	R	I	I	S	I	I	S	S	S	S	S	S	S	S	I	I	S	S
Hit (%)	58	0	0	42	0	50	4.2	58	50	50	29	58	58	58	75	58	58	58	42	54	13	71

[†] Bacterial isolates were susceptible (clear spot; S; green), intermediate (turbid spot; I; yellow), or resistant (no disturbance of bacterial lawn; R; red) to phage infection.

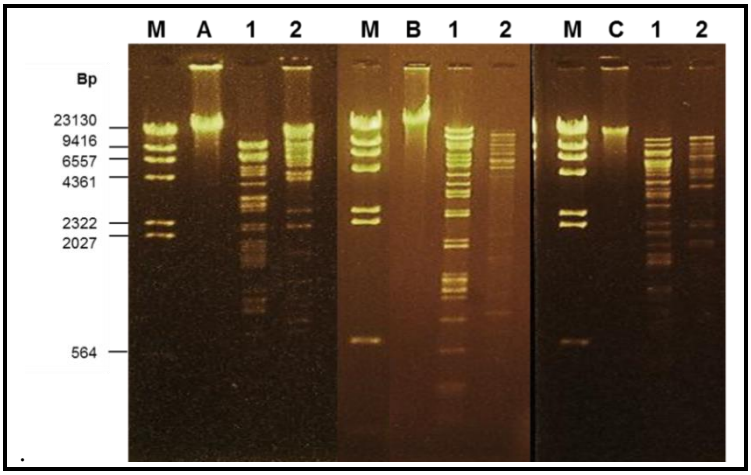

Figure 3.2: Restriction analysis of phages K, DRA88 and DRA288. Lane identification is as follows: M – marker λ/HindIII; A, B and C – undigested DNA of phages K, DRA88 and DRA288, respectively; 1 – DNA digested with *XbaI*; 2 – DNA digested by *EcoRI*.

3.4.1.4. Bacteriophage morphology

The isolated phages DRA88 and DRA288 were further characterised regarding their morphology. Images of the phages were produced using transmission electron microscopy (TEM). The results revealed that both phages showed a similar morphology, with an icosahedral head of ~78 nm and ~85 nm in diameter, a long contractile tail of ~179x18 nm and ~208x16 nm with tail fibres, for DRA88 and DRA288 respectively (Figure 3.3). The protein neck connecting the capsid and the tail of ~9x10 nm and ~7x10 nm, for DRA88 and DRA288, respectively, is revealed on the images. Therefore, both phages can be classified as belonging to the *Myoviridae* family and sub-family *Spounaviridae* (order *Caudovirales*), according to the classification system of Ackermann (144). It was observed for phage DRA88 that, besides single dispersed particles, there was also various particles aggregated through contact of their tail fibres (Figure 3.10). Phage K was also observed under TEM, revealing viral particles also belonging to the *Myoviridae* family and previously documented (221).

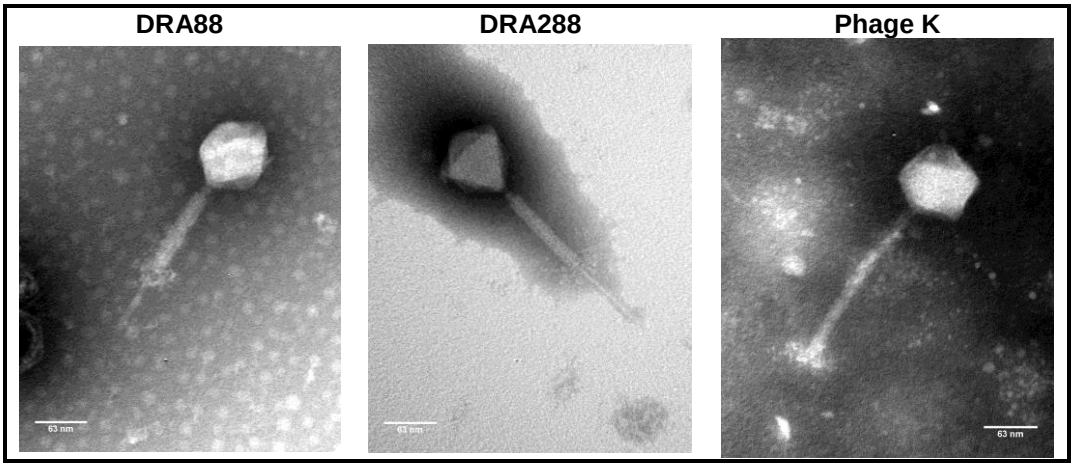

Figure 3.3: Electron micrograph images of phage DRA88, phage DRA288 and phage K negatively stained with 1 % uranyl acetate. DRA88 and DRA288 are showing the tail in a contracted position. Scale is indicated by the bars.

3.4.1.4.1. Contamination with prophages

Although the phages were always passed through several rounds of purification when we were observing them under the electron microscope two different viral particles were being revealed for DRA88: a *Myoviridae* in higher proportion (described in the section above) and a *Siphoviridae* in a lower ratio. This was also observed when plating the phage onto bacterial lawns, where besides the expected phage plaques it also revealed very small diameter plaques were appearing on the agar lawn, usually a sign of the presence of more than one phage type. The bacterial strain *S. aureus* EMRSA 16 was been used as host for phage propagation and this strain is known to harbour four prophages in its genome. Perhaps, one of the prophages was being induced when DRA88 infects the bacterial cell and consequently excised from the chromosome. To confirm this, *the S. aureus* prophage-free strain RN4220 was used as a host and several purification passages were performed to ensure purity and the lysate was observed by TEM (Figure 3.4). This time it was not fond *Siphoviridae* particles in the sample, but only the *Myoviridae* particles. Hence, *S. aureus* EMRSA16 was ignored as a host for phage replication being replaced by *S. aureus* RN4220.

However, phage DRA288 was not able to infect this strain and for that reason was pulled out from the further studies.

3.4.1.5. Host range determination of phage mixture

Phage DRA88, phage K and their combination were assessed regarding their host infectivity range against a larger and more representative collection of 95 *S. aureus* isolates (Table 3.7) assigned to 14 different multilocus sequence typing (MLST) types (Table 3.3, Figure 3.5). DRA88 presented a host infectivity coverage of 60 % (95 % CI, 50 % to 69 %; 57 isolates out of 95 were susceptible). Phage K showed host coverage of 64.2 % (95 % CI, 54 % to 73 %; 61 isolates out of 95 were susceptible). These two phages when in combination gave a total coverage of 73.7 % (95 % CI, 64 % to 82 %) of the *S. aureus* isolates. Infectivity of both phages was also assessed on a group of coagulase-negative isolates, where DRA88 did not infect efficiently any of the isolates. Phage K also showed weak infectivity; however, two of the isolates - *S. simulans* and *S. hyicus* – were sensitive revealing a lytic spot on the agar lawn (Table 3.8).

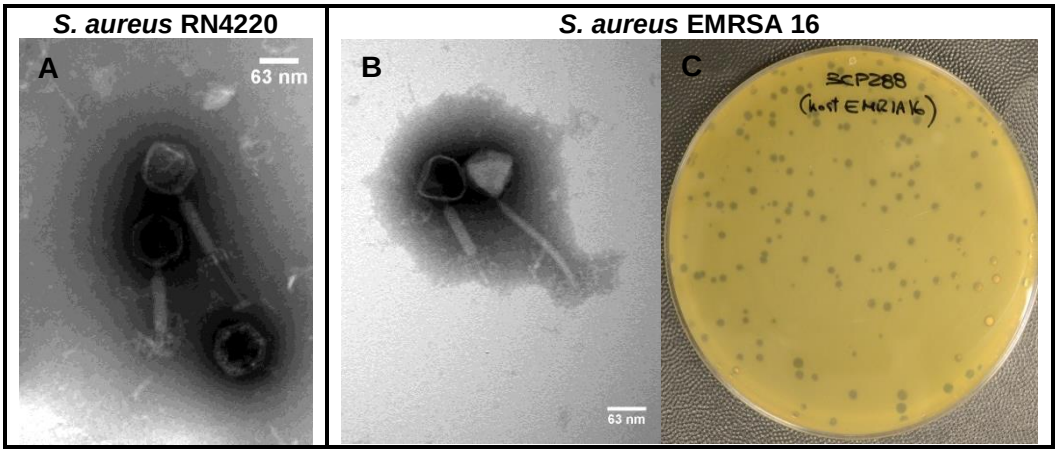

Figure 3.4: Electron micrograph images of phage DRA88 when growing (A) in the *S. aureus* RN4220 host (only *Myoviridae* particles are observed) and when growing in (B) *S. aureus* EMRSA 16 host (particles of *Myoviridae* and *Siphoviridae* can be observed). Samples were negatively stained with 1 % uranyl acetate. Scale is indicated by the bars. (C) A bacterial lawn of *S. aureus* EMRSA 16 on an agar plate show the heterogeneous plaques produced by the two different phage particles.

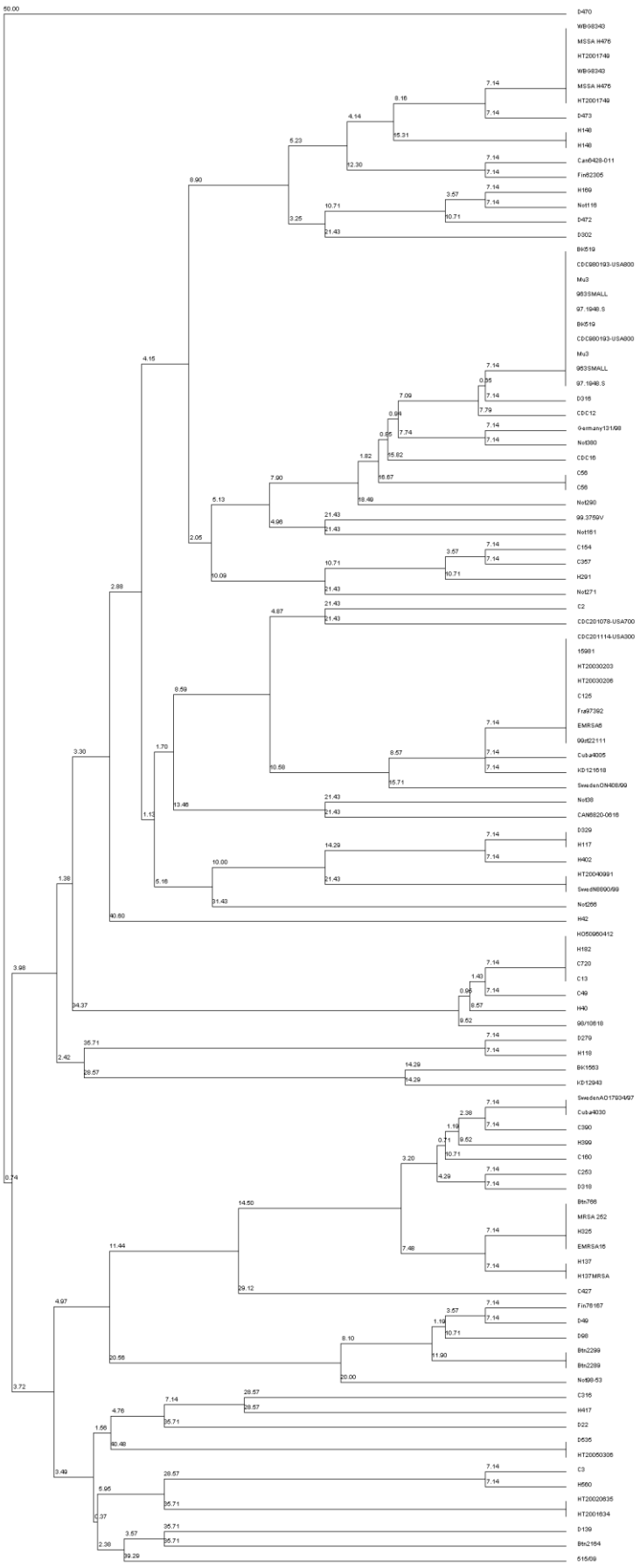

Figure 3.5: Neighbour joining tree of the *S. aureus* clinical isolates used in this study. The tree was computed by using concatenated nucleotide sequences of seven housekeeping genes and was constructed using the tool provided by the MLST database (http://saureus.mlst.net/sql/uniquetree.asp?). Bootstrap values are indicated above the branches.

Table 3.7: Sensitivity screening of phage mixture against 95 *S. aureus* isolates[†].

Bacterial Isolates	Phage K	DRA88	Phage mixture
CDC201114-USA300	S	S	S
CDC201078-USA700	I	I	I
CDC980193-USA800	S	S	S
WBG8343	S	I	S
MSSA H476	S	S	S
HT2001749	S	I	S
H148	S	S	S
Mu3	S	R	S
963Small	S	S	S
97.1948.S.	R	R	R
C56	S	S	S
C2	I	I	I
15981	I	S	S
HT20030203	I	S	S
HT20030206	S	I	S
C125	I	I	I
Fra97392	I	R	I
EMRSA6	I	I	I
99st22111	S	S	S
H169	S	S	S
D316	I	I	I
D329	S	S	S
H117	S	S	S
H402	S	S	S
C154	S	S	S
C357	S	S	S
H291	S	I	S
H42	S	S	S
HO50960412	I	S	S
H182	S	S	S
C720	R	S	S
C13	S	S	S
C49	S	S	S
D279	I	I	I
Not116	S	S	S
H118	S	I	S
SwedenAO17934/97	S	I	S
Cuba4030	I	I	I
C390	S	S	S
H399	S	S	S
C160	I	I	I
Btn766	S	S	S
MRSA 252	S	S	S
H325	S	S	S
EMRSA16	S	S	S
H137	I	I	I
H137MRSA	S	S	S
BK519	I	S	S

Bacterial Isolates	Phage K	DRA88	Phage mixture
C253	I	I	I
C427	S	S	S
Fin76167	S	S	S
C316	S	S	S
H417	S	S	S
C3	S	S	S
D49	S	S	S
D98	I	I	I
D318	S	S	S
D535	I	I	I
HT20050306	I	I	I
H40	S	S	S
D473	I	I	I
HT20040991	S	R	S
SwedN8890/99	I	I	I
BK1563	I	S	S
HT20020635	S	I	S
HT2001634	I	S	S
Cuba4005	S	S	S
D302	S	S	S
Not38	S	S	S
D472	S	S	S
H560	S	S	S
D139	I	I	I
D22	I	I	I
Can6428-011	S	S	S
D470	I	I	I
98/10618	S	S	S
CDC12	S	S	S
Germany131/98	S	S	S
CDC16	S	S	S
99.3759V	S	I	S
SwedenON408/99	I	I	I
KD121618	S	I	S
KD12943	I	I	I
Not271	I	I	I
Not380	I	S	S
Not98-53	I	S	I
CAN6820-0616	I	I	I
Fin62305	S	I	S
Not266	S	S	S
Btn2164	S	S	S
Btn2299	I	I	S
Btn2289	S	S	S
515/09	S	S	S
Not161	S	I	S
Not290	S	S	S

[†] Bacterial isolates were susceptible (clear spot; S; green), intermediate (turbid spot; I; yellow), or resistant (no disturbance of bacterial lawn; R; red) to phage infection.

Table 3.8: Sensitivity screening of phage mixture against coagulase-negative *staphylococci* isolates[†].

Species	Bacterial Isolates	Phage K	DRA88	Phage Mixture
S. xylosus	ATCC 29971	I	I	I
S. sciuri subsp. Sciuri	ATCC 29062	I	I	I
S. chromogenes	CCM 3387	I	I	I
S. hyicus	CCM 29368	S	I	S
S. arlettae	N910 254	I	I	I
S. vitulinus	ATCC 51145	I	I	I
S. simulans	N920 197	S	I	S
S. epidermidis	ATCC 14990	I	R	I

[†] Bacterial isolates were susceptible (clear spot; S; green), intermediate (turbid spot; I; yellow), or resistant (no disturbance of bacterial lawn; R; red) to phage infection.

3.4.1.6. Genomic characterisation of DRA88 and comparison with phage K

To gain a more complete understanding of phage DRA88, its DNA was extracted and genome sequencing was performed. Upon assembly and annotation, it was found that phage DRA88 has a large double-stranded DNA (dsDNA) genome with terminal redundancy, which suggests that phage DRA88 has a headful packaging system (252). The genome comprises 141,907 bp and can be grouped into class III of staphylococcal phages (>125 kbp) (253); 204 putative coding regions and four tRNA genes were identified (Figure 3.6). The gene coding potential, with 1.44 genes per kb, exhibits a high gene density. The majority of genes, 145 (71 %), are found in the forward strand, and 59 (29 %) are found in the opposite strand. tRNA genes are all located in the reverse strand of the genome. Regarding the G+C % content, it is 30.4 %, a lower percentage than the one found in the *S. aureus* host, 32.9 %. The amino acid sequence was found to share strong similarities (>95 %) with those of several other phages, such as JD007 and GH15, previously sequenced (254, 255). A comparison between phage DRA88 and phage K was performed using the BLASTN algorithm

(256). The DRA88 genome seems to be organised into functional modules - cell lysis, DNA replication, and structural elements - similar to the organisation of phage K and other staphylococcal *Myoviridae* phages belonging to the Twort-like viruses (253, 257, 258). Between these modules, we can find several putative coding regions that are not yet found in the NCBI database or have no attributed function (phage and hypothetical proteins). These unknown functions represent 84.81 % of the coding capacity. Three potential coding regions (ORF178, ORF192, and ORD195) did not have any identical match with phage genes in the NCBI database. DRA88 lysin and DNA polymerase are not interrupted by introns (255), in contrast to phage K but similarly to phage GH15. At the end of the genome (between ORF164 and ORF182), there is a large coding region with unidentified functions inserted into the DRA88 genome that is not observed in phage K. Also, DRA88 genome analysis did not reveal the presence of known virulence-associated and toxin proteins or antibiotic resistance determinants.

The genomic sequence of the phage DRA88 can be found in the NCBI GenBank database under accession number KJ888149.

3.4.1.7. Phage growth characteristics

The life cycle and adsorption affinity of phage DRA88 and phage K were assessed when growing in *S. aureus* RN4220 at 37°C.In order to identify the different stages of the phage infection process (Chapter Two, Figure 2.5) one-step growth studies were performed. Hence, after inoculation, the phage growth cycle parameters (L, latent; E, eclipse; B, burst size) were determined (Figure 3.8). In the system established, the eclipse and latent periods of DRA88 were 15 min and 25 min, respectively. DRA88 yielded a burst size of 76 PFU and phage K yielded a burst size of 125 PFU per infected cell after a 60 min incubation period. Such values identified are in conformity with the values that are normally observed for phages from the T7 group (259).

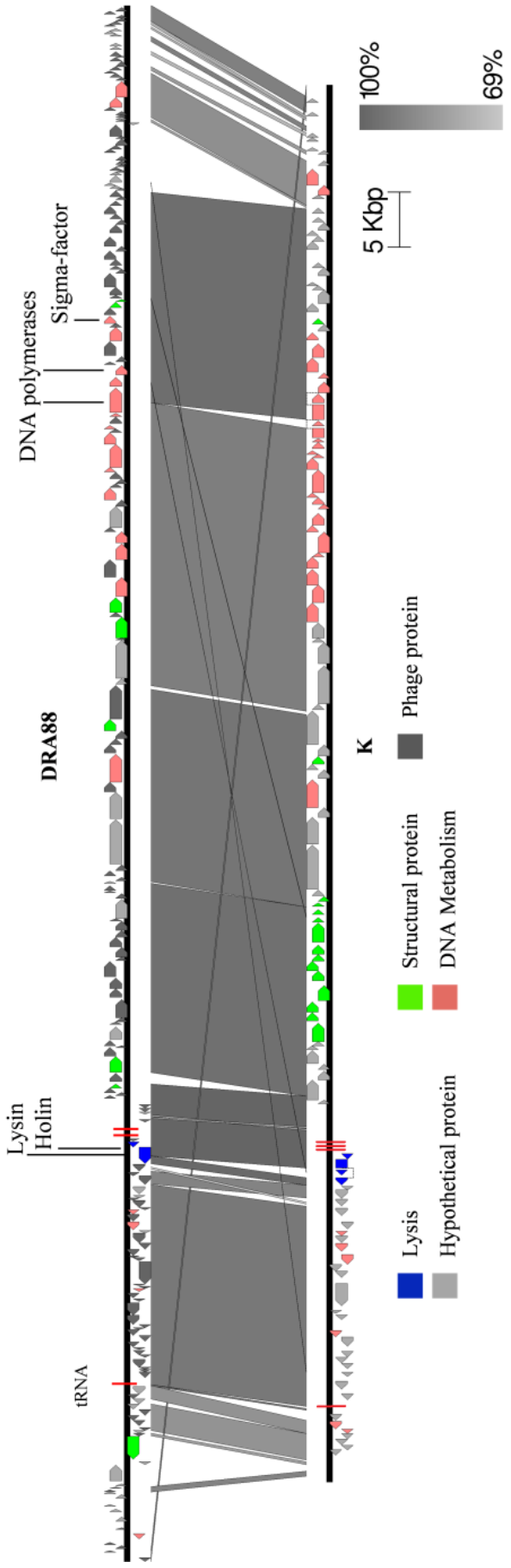

Figure 3.6: Comparative genomic analysis of phage DRA88 and phage K. Nucleotide sequences were compared using the Artemis comparison tool (ACT). Predicted open reading frames are denoted by arrows, tRNAs are indicated (vertical blue dashed line), and genes encoding proteins with at least 69 % amino acid identity between the two genomes are indicated by shaded regions

For estimation of the adsorption efficiency of phages to *S. aureus* RN4220 host, a study during cells early logarithmic growth phase was performed (Figure 3.7). From equation 1, the rate constants for the adsorption (loss of free phage) for phage K and DRA88 were calculated, k' = 0.352 min^{-1} and k' = 0.252 min^{-1}, respectively. Hence, although the phages were similar, after 5 min, 80.3 % of phage K and 71.6 % of DRA88 were adsorbed to the bacteria. After 10 min of incubation, values for free phages were below 5 % for both phage K and DRA88.

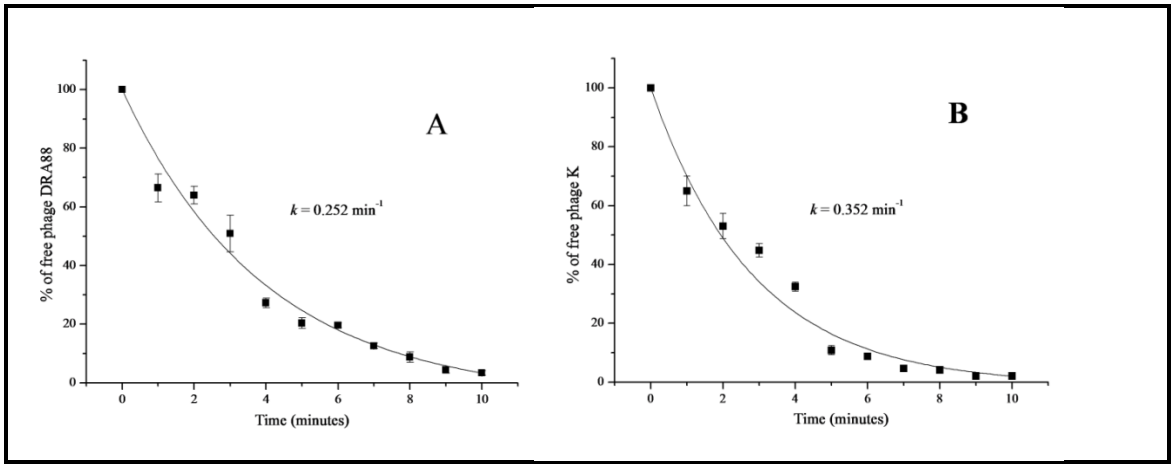

Figure 3.7: Percentage of free DRA88 (A) and phage K (B) phages after infection of actively growing *S. aureus* RN4220 at an MOI of 0.001 at several time points over 10 min. Rate constants for loss of phage are 0.352 min^{-1} for phage K and 0.252 min^{-1} for DRA88. Each data point is the mean of three independent experiments, and error bars indicate the means ± standard deviations. Reprinted from reference (244) and used with permission.

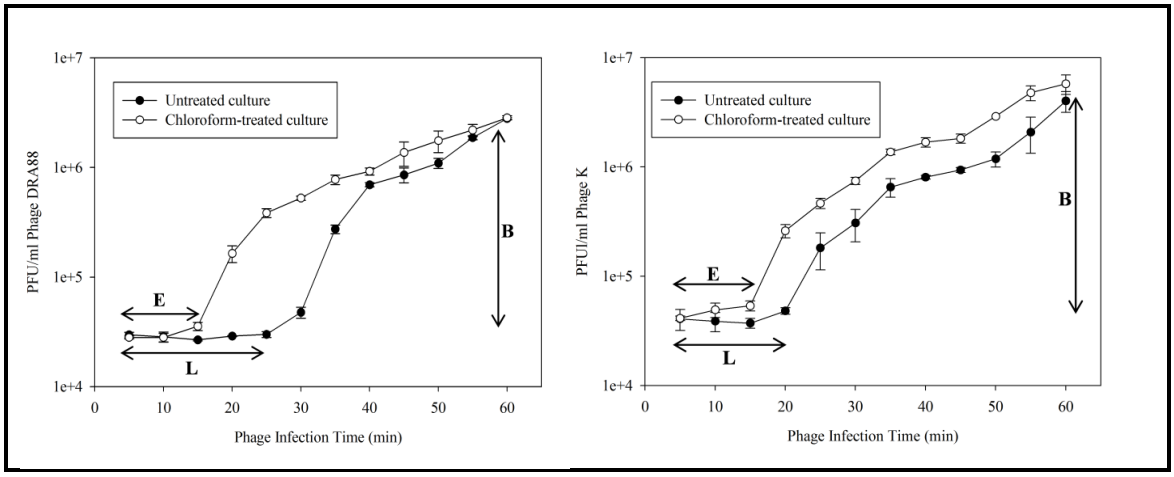

Figure 3.8: Curve for one-step growth of phage DRA88 (left) and phage K (right) in *S. aureus* RN4220 at 37°C. Shown are the PFU per infected cell in untreated cultures (●) and in chloroform-treated cultures (○) at several time points over 60 min. The phage growth parameters are indicated in the figure and correspond to eclipse period (E), latent period (L), and burst size (B). Each data point is the mean of three independent experiments, and error bars indicate the means ± standard deviations. Reprinted from reference (244) and used with permission.

3.4.1.8. Aggregation experiments

The zeta potential of phage DRA88 and phage K calculated from the electrophoretic mobility was, respectively, -17 mV and -26.3 mV. The particle size measured for phage K was 122 nm (121.5 nm, SD ± 2.7) (Figure 3.8A), however according to the TEM micrographs and the literature, phage K has an average size of 280 nm in length (146). Such discrepancy could be due to the contraction of the phage tails, which was often observed on the TEM, resulting in interference with the measurements. Dynamic light scattering (DLS) may show lower accuracy when measuring particles with an irregular shape, hence not uniform in all dimensions and this holds true for tailed phages. Regarding phage DRA88, that has a size of ~257 nm, we were not able to obtain an accurate size measurement (Figure 3.9B) and this might be related to the phenomenon of aggregation observed under TEM. When observing phage DRA88 under the electron

microscope, besides dispersed single phage particles it was also observed various aggregates were made through contact of their tail fibres (Figure 3.10). Also, several heads and tails were observed separately, suggesting that in a certain step of the sample preparation those were broken apart and might contribute to the size measurements discrepancy.

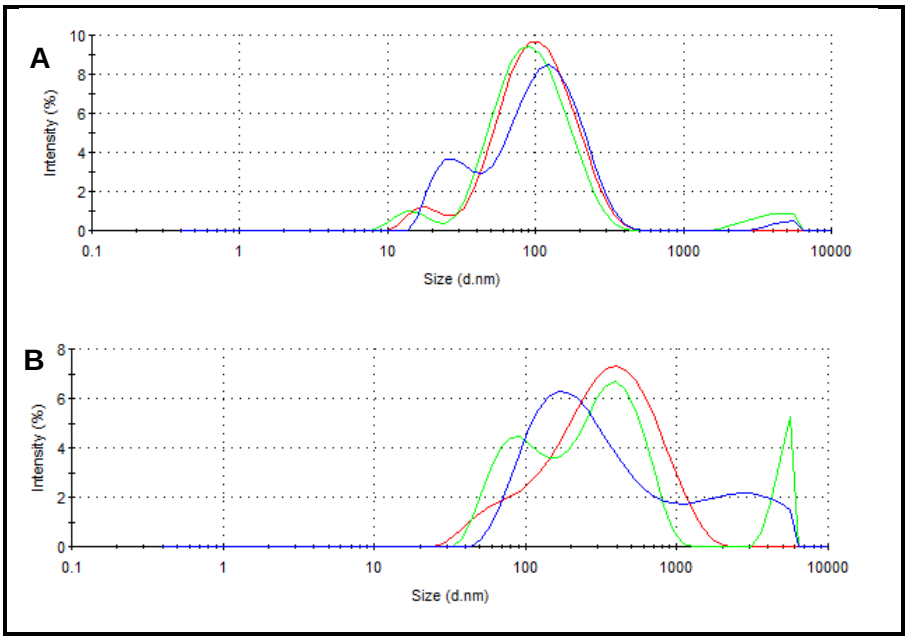

Figure 3.9: Size distribution intensity of phage particles in suspension at 37 ^{o}C revealed by DLS. A – phage K, B – phage DRA88.

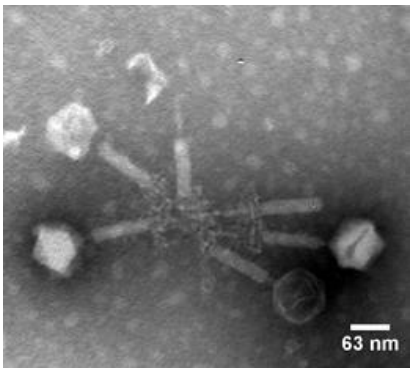

Figure 3.10: Electron micrograph images of phage DRA88 infecting S. aureus forming aggregates negatively stained with 1 % uranyl acetate. Scale is indicated by the bars. Reprinted from reference (244) and used with permission.

3.4.2. *P. aeruginosa* phages isolation and characterisation

3.4.2.1. Bacteriophage isolation and plaque morphology

A total of 17 phages were isolated from sewage and flood water samples after enrichments with the *P. aeruginosa* strains listed on Table 3.1. Phages showing clear isolated plaques were selected over phages where plaques showed turbidity. Regarding the plaque morphology of phages isolated for *P. aeruginosa* strains they were generally circular with both regular and irregular edges were identified, however showing larger diameters than ones observed for *S. aureus* phages (between 0.5 mm and 3.0 mm). Halos, caused by the diffusion of enzymatic molecules were frequently observed for these phages. Interestingly, phage DL64 produced a plaque that consisted of a clear small centre with a turbid halo and this one surrounded by a clear halo. Table 3.9 describes the morphology of the plaques produced by the isolated phages and Figure 3.11 shows examples of plaques.

Table 3.9: Phages isolated with respective *P. aeruginosa* bacterial hosts and plaque morphology.

Phage	*P. aeruginosa* host strain	Plaque morphology ~ mm (∅); halo
DL52	PA45291	1.0; halo
DL53	PAO1	0.5; halo
DL54	PAO1	1.0
DL55	PAO1	1.0; halo
DL56	PAO1	1.5, halo
DL57	BC00907	1.5
DL58	BC00907	1.0; halo
DL59	BC00907	2.0; halo
DL60	BC00907	1.0; halo
DL61	PA45321	3.0; halo
DL62	BC00918	2.5; halo
DL63	PA45291	1.0; halo
DL64	PAO1	1.5; halo
DL65	PA45291	2.0
DL67	PA45291	0.5; halo
DL68	PAO1	1.0; halo
DL69	PAO1	1.5

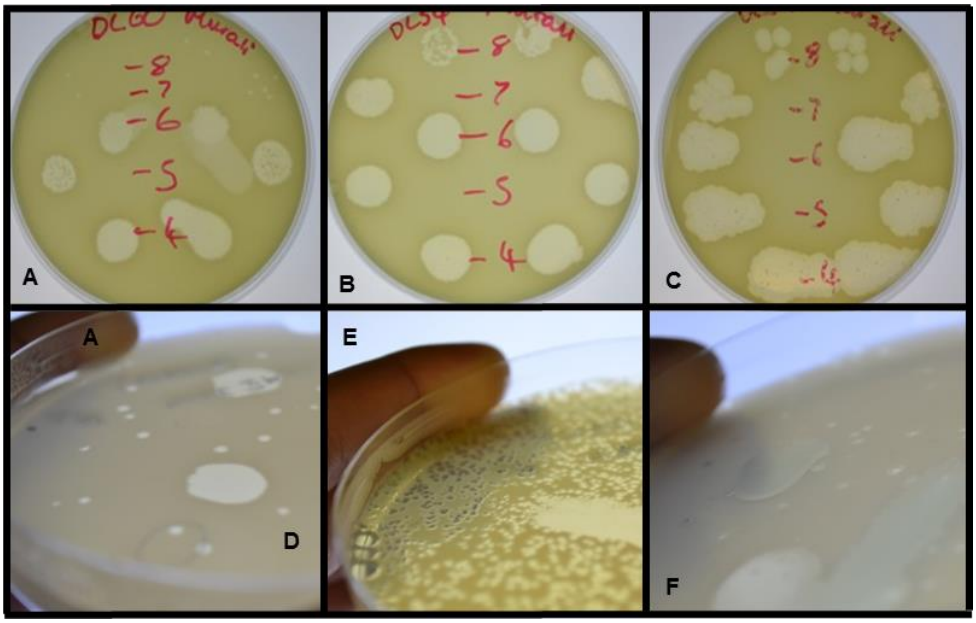

Figure 3.11: Examples of *P. aeruginosa* isolated phage plaques (clear spots caused by bacterial lysis). A – DL54; B – DL60; C – DL67; D – DL52; E – DL57; F – DL63.

3.4.2.2. Host range determination and selection of phage cocktail

The lytic phages previously isolated for *P. aeruginosa* were evaluated regarding their host range of infectivity. Phages were tested against a *P. aeruginosa* collection of geographically diverse clinical isolates coming from both acute and chronic situations listed in Table 3.10 in order to isolate phages with broad host ranges. For 11 phages the host coverage was <32 %, where phage DL63 was only infecting one out of 22 isolates tested (95 % CI, 5 %, 2 % to 20 %), the acute isolate PA45291. The remaining six phages showed a host cover ranging from 45 % for DL61 (95 % CI, 24 % to 65 %; 10 isolates out of 22 were susceptible) to 59 % for DL68 (95 % CI, 38 % to 78 %; 13 isolates out of 22 were susceptible).

Table 3.10: Sensitivity screening of isolated phages against *P. aeruginosa* clinical isolates[†].

P. aeruginosa isolates	Bacteriophages																
	DL52	DL53	DL54	DL55	DL56	DL57	DL58	DL59	DL60	DL61	DL62	DL63	DL64	DL65	DL67	DL68	DL70
BC00932	I	I	I	R	S	S	I	R	I	S	S	I	I	S	S	S	S
BC00931	I	R	R	I	R	R	I	R	I	R	I	R	I	I	I	S	I
BC00923	R	R	I	R	R	R	I	R	I	R	R	I	R	R	I	R	R
PAO1	S	S	S	S	S	R	S	S	S	R	S	R	S	S	S	S	S
BC01026	I	I	I	R	R	R	R	R	R	I	S	I	S	I	I	S	S
BC00935	S	S	S	S	R	I	S	S	S	I	I	R	S	S	S	S	S
BC00934	R	I	S	R	R	I	S	R	S	I	I	R	I	I	I	S	S
PAB45379	I	R	I	I	R	I	R	R	R	I	S	I	R	I	I	I	I
BC00907	S	S	S	S	R	S	S	S	S	I	S	I	S	S	S	S	S
PAB45235	R	R	R	R	R	R	I	I	R	I	I	I	S	I	I	I	I
PAB45321	R	R	R	I	I	R	I	R	I	I	R	R	R	S	S	R	R
PAB45291	S	I	S	S	R	R	S	I	S	R	S	S	S	S	S	S	S
BC00909	R	R	R	R	R	R	R	R	R	S	S	I	R	I	I	I	R
BC00918	R	R	R	R	R	R	R	R	R	R	S	R	R	R	R	R	R
BC00917	R	R	I	R	R	R	R	R	R	I	I	R	S	S	S	S	S
BC00920	S	S	S	R	R	R	S	S	S	S	I	I	S	S	S	S	S
BC00921	R	R	R	R	R	R	I	R	I	R	R	R	R	S	S	R	R
PAB45311	I	I	R	R	I	I	R	R	R	I	R	R	R	S	S	R	R
BC00922	I	I	I	I	I	I	R	R	R	I	S	I	S	I	I	I	I
BC00888	I	R	I	I	I	R	R	R	R	I	R	R	S	I	I	S	S
BC00933	S	I	S	R	R	R	I	I	I	I	R	R	S	I	I	S	S
BC00920	I	R	R	R	R	I	I	I	I	I	S	I	S	S	S	S	S
Hit %	30	20	35	20	10	10	30	20	30	15	50	5	60	55	55	65	60

[†] Bacterial isolates were susceptible (clear spot; S; green), intermediate (turbid spot; I; yellow), or resistant (no disturbance of bacterial lawn; R; red) to phage infection.

Determination of the host range allowed us to formulate a phage combination that would give the highest percentage of coverage. For that reason six phages were selected to make part of the phage cocktail – DL52, DL54, DL60, DL62, DL64 and DL68 – giving a total coverage of 90 % (95 % CI, 62 % to 94 %; 18 isolates out of 22 were susceptible). All the phages selected to establish the cocktail were able to infect *P. aeruginosa* PAO1 (Table 3.11.), for that reason for further studies the strain was used as host for phage propagation.

Table 3.11: Sensitivity screening of phage cocktail against *P. aeruginosa* clinical isolates[†].

P. aeruginosa isolates	DL52	DL54	DL60	DL62	DL64	DL68	Cocktail
BC00932	I	I	I	S	I	S	S
BC00931	I	R	I	I	I	S	S
BC00923	R	I	I	R	R	R	I
PAO1	S	S	S	S	S	S	S
BCO1O26	I	I	R	S	S	S	S
BC00935	S	S	S	I	S	S	S
BC00934	R	S	S	I	I	S	S
PAB45379	I	I	R	S	R	I	S
BC00907	S	S	S	S	S	S	S
PAB45235	R	R	R	I	S	I	S
PAB45321	R	R	I	R	R	R	I
PAB45291	S	S	S	S	S	S	S
BCOO909	R	R	R	S	R	I	S
BC00918	R	R	R	S	R	R	S
BC00917	R	I	R	I	S	S	S
BC00920	S	S	S	I	S	S	S
BC00921	R	R	I	R	R	R	I
PAB45311	I	R	R	R	R	R	I
BC00922	I	I	R	S	S	I	S
BC00888	I	I	R	R	S	S	S
BC00933	S	S	I	R	S	S	S
BC00920	I	R	I	S	S	S	S
Hit %	30	35	30	50	60	65	90

[†] Bacterial isolates were susceptible (clear spot; S; green), intermediate (turbid spot; I; yellow), or resistant (no disturbance of bacterial lawn; R; red) to phage infection.

3.4.2.3. Morphology of phages

The six *P. aeruginosa* phages were also characterised regarding their morphology and for this samples were prepared to be observed under the electron microscope. The results found two different types of morphology. DL52, DL60 and DL68 phages have an icosahedral head of ~60 nm, ~76 nm and ~72 nm in diameter, respectively. Long contractile tails, with tail fibres, of approximately ~123x18 nm, ~95x19 nm and ~177x23 nm, respectively (Figure 3.12) were also observed. Phages DL54, DL62 and DL64 have an icosahedral head of approximately ~45 nm, ~63 nm and ~65 nm in diameter, respectively and a short tail of ~12x9 nm and ~13x9 nm with no tail fibres visible. For

DL64 the tail was clearly visible, however fibres protruding from the capsid are observed. Therefore, according to the system of Ackermann (144) such traits allow classification of the first group of phages as belonging to the *Myoviridae* family and the second group as belonging to the *Podoviridae* family, both from the order *Caudovirales*. The samples of the observed *Myoviridae* phages showed the presence of many disintegrated phages, where several free capsids and free tails could be observed. Samples of phages DL54 and DL60 showed the presence of phage aggregates.

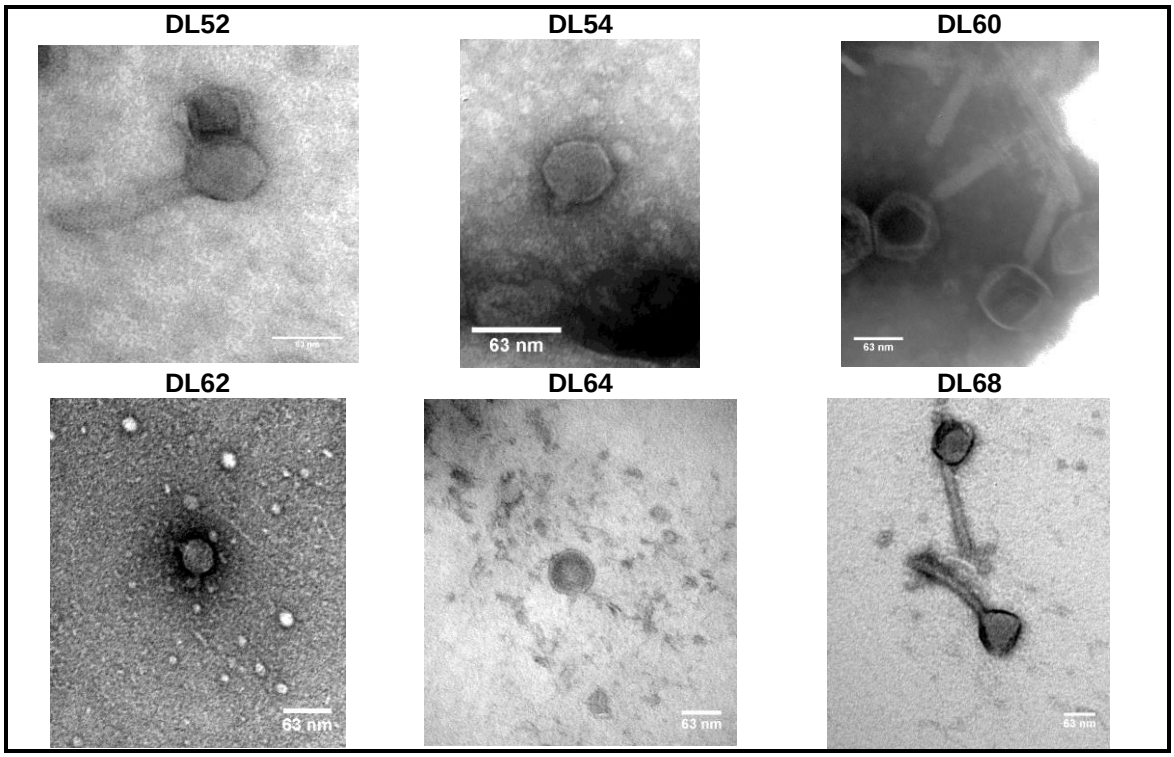

Figure 3.12: Electron micrograph images of phage L52, DL54, DL60, DL62, DL64 and DL68 infecting *P. aeruginosa* negatively stained with 1 % uranyl acetate. Scale is indicated by the bars.

3.4.2.4. Genome analysis

DNA from the six *P. aeruginosa* phages was extracted and genome sequencing was performed in order to achieve more information about the phages. Table 3.12 summarises the key features of the six genomes.

The genome sizes observed for phages DL52, DL60 and DL68 were larger, comprising 65,867 bp, 66,103 bp and 66,111 bp, respectively. Figure 3.13 shows a comparison between these *Myoviridae* phages, performed using the BLASTN algorithm (256). This comparison shows that they are 90 % identical in their nucleotide sequence and in particular DL52 and DL60 are 96 % identical. Genes are arranged in a typically compact manner with a coding percentage ranging from 89.7 % to 91.6 %. For all the phages tRNAs genes are absent. *P. aeruginosa* shows a G+C % content of 66.6 % and for all the phages their content was much lower (between 52.4 % – 62.2 %). Phages DL52 and DL60 show strong similarities to phage PB1 (>96 %) and phage LBL3 (>92 %), that recently have been sequenced (260). Phage DL68 shares high similarities with phage KPP12 DNA (96 %) (261), but is still strongly related with PB1 and LBL3 phages (>90 %). Hence, the three phages can be put in the PB1-like lytic virus group. It has been documented that these phages use the bacterial lipopolysaccharide as a receptor to attach to the cell (262) and we can assume that the same attachment mechanism might be employed by these three phages. In accordance with other related phages such as PB1 (260), RNA polymerases are absent in all three phages, which is commonly observed in this type of phages where their transcription relies entirely on the host machinery. All three phages carry a DNA polymerase III alpha-subunit that catalyses the polymerisation reaction of the host DNA polymerase III holoenzyme, which is the main observed DNA polymerase within bacteria (263). The presence of phage-encoded DNA primase and helicase suggests that viral dsDNA elongation is performed by the phage and independent of the host replication machinery.

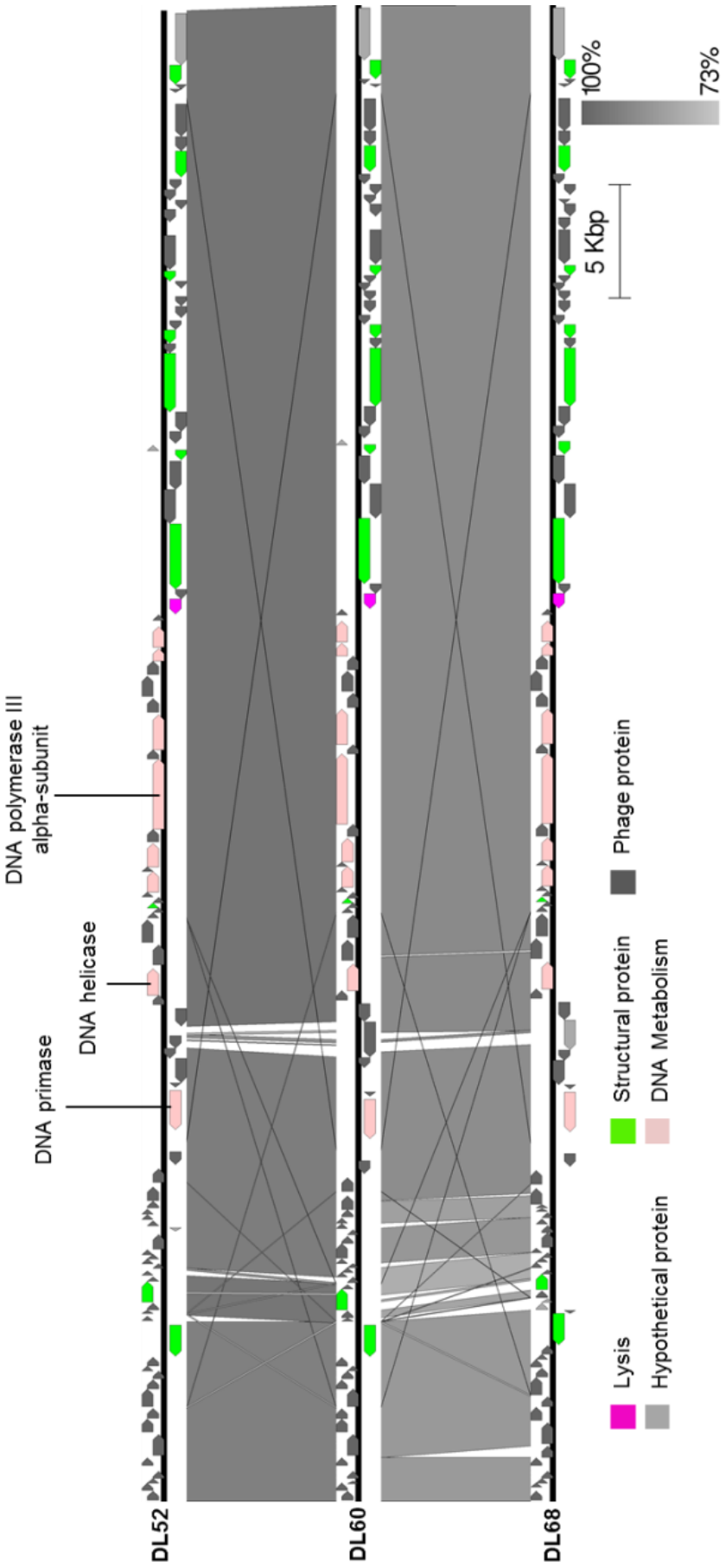

Figure 3.13: Comparative genomic analysis of the annotated *Myoviridae* phages DL52, DL60 and DL68. Nucleotide sequences were compared using the Artemis comparison tool (ACT). Predicted reading frames are denoted by arrows and genes encoding proteins with at least 73 % amino acid identity between the genomes are indicated by shaded regions.

For the three phages the majority of genes are found rightward orientated (57.8 %, 59.6 % and 57.6 %, for DL52, DL60 and DL68, respectively), while the others are leftward orientated (42.2 %, 40.4 % and 42.4 %, for DL52, DL60 and DL68, respectively).

The genome size observed for the *Podoviridae* phages DL54 and DL62 was similar, comprising 45,673 bp and 42,508 bp, respectively. Phage DL64 genome was much larger comprising 72,378 bp (Figure 3.14). A comparison between the nucleotide sequence of DL54, DL62 and DL64 showed no similarities shared between them. DL54 show share strong similarities (>98 %) with other lytic *Podoviridae* infecting *P. aeruginosa*, such as phiIBB-PAA2 and LUZ24 (264, 265). Phage LUZ24 has two tRNA genes present in its genome, however for DL54 tRNA genes were not observed in the genome sequence (265). It is possible to recognise a conserved coding region responsible for phage assembly (large subunit of the terminase and upstream of the portal, capsid and scaffolding protein genes) and a region for DNA metabolism similarly, where the DNA polymerase was fragmented into three parts by an endonuclease gene, as observed for phage LUZ24 (265). The DNA primase/helicase gene can also be found in the middle of the DNA polymerase. The two main modules are separated by several potential coding genes for phage proteins with unknown roles. The majority of genes, 50 (70.4 %), are found in the leftward orientated strand, and 21 (29.6 %) are found in the opposite strand.

The search using the BLASTN algorithm in the NCBI database showed that phage DL62 is closely related to phiKMV-like phages (>95 %), such as phiKMV and LUZ19 (266, 267) and these phages are grouped into the T7-like phages genus in the subfamily of the *Autographivirinae*. Genomes of T7-types have been previously sequenced for phages of *Klebsiella pneumonia* for example (268), where genes are arranged into three clusters: early genes (cluster I), DNA metabolism (class II) and structural proteins for phage assembly and for host lysis (class III) (266). Such genome

organisation is easily observed for phage DL62. However, differences can be found, such as the RNA polymerase that in T7-like phages is present in the cluster I of early genes and both in DL62 and phiKMV phages is present within the class II cluster. Typically there is the presence in the genome of a gene pairing lysin-holin in order to breakdown the bacterial cell. Phage DL62 carries a lysin (ORF51) found within cluster III, possibly with muraminidase activity, and the position and small size (66 residues) of ORF52 might code for the holin (269, 270). Like phiKMV (266), phage DL62 has a higher G+C % content (62.2 %) when in comparison to the other phages of the cocktail, being close to the G+C % content of the bacterial host (65 %) (271) and in accordance with the homologue phiKMV phage (272). Genes were all found in the forward strand, but the first gene is located in the reverse strand.

Lastly phage DL64 showed a unique genome sequence. The most striking feature of the genome is the presence of two genes (ORF41 and ORF42) homologous to rIIA-like and rIIB-like proteins from phage N4 that, although not yet clear, might play a role in the phenomenon of lysis inhibition and in other functions, such as interference in cell metabolism (273). Lysis inhibition is defined as a delay of the phage in producing the enzyme holin while phage particles are being produced resulting in their accumulation inside the host. Phage DL64 genome can be grouped in the N4-like phages, such as LIT1 (98 %) and LUZ7 (73 %) that have been previously sequenced (274) and many others on which work has not yet been published. N4-like phages use three distinct RNA polymerases during their lytic infection cycle: a giant virion-encapsulated RNA polymerase that is co-injected with the phage genome into the host upon infection, a heterodimeric phage RNA polymerase transcribed from the middle region and a DNA-binding protein that is able to arrest the host RNA polymerase to transcribe late phage proteins (275). Although, the BLAST search in the database only predicted one RNA polymerase, we can presume that ORF15 might code for the giant RNA polymerase, as it is positioned in the early gene regions and its large size (3398 residues).

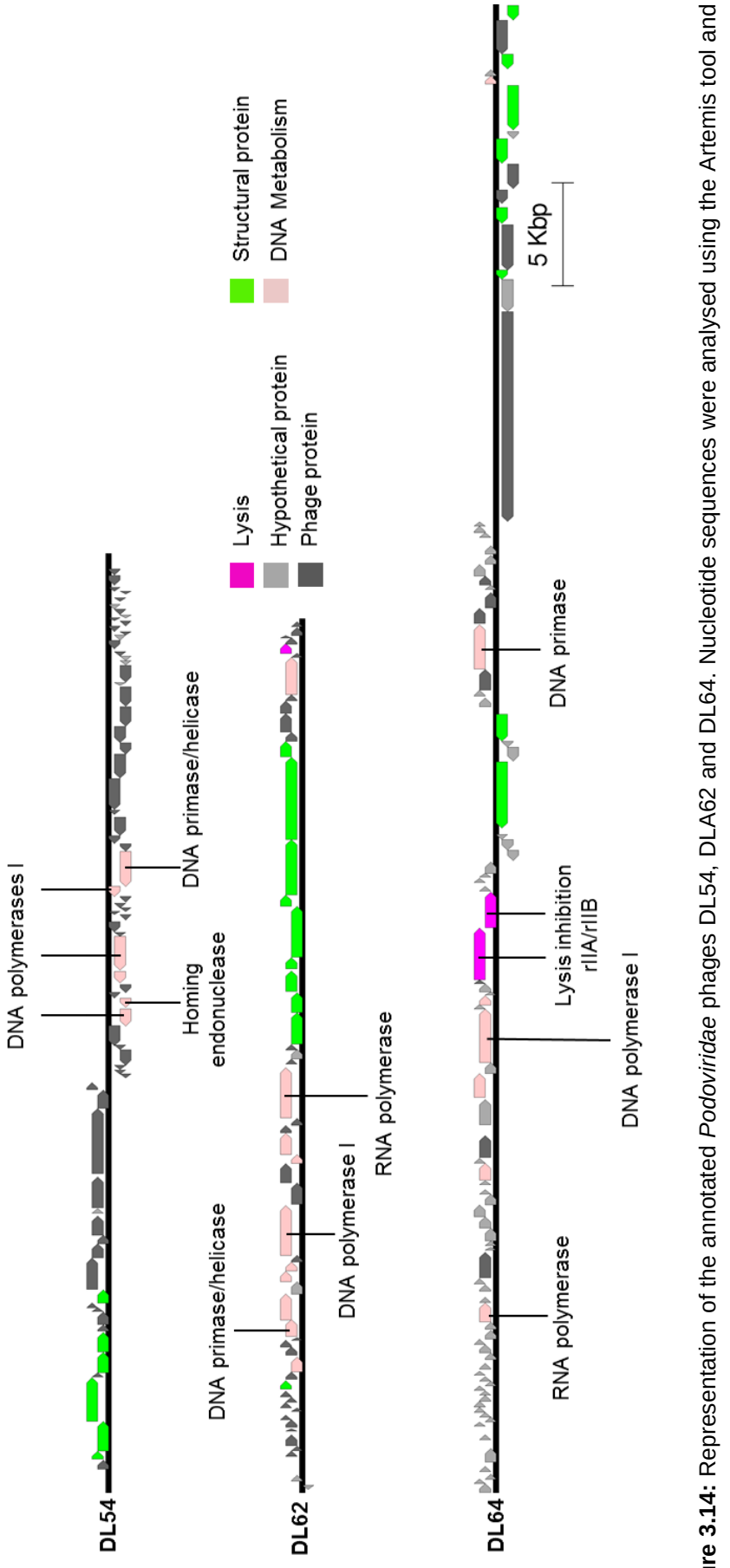

Figure 3.14: Representation of the annotated *Podoviridae* phages DL54, DLA62 and DL64. Nucleotide sequences were analysed using the Artemis tool and predicted reading frames are denoted by arrows.

It is suggested that the DNA-binding protein coding gene might be ORF66 positioned strictly upstream of the predicted RNA polymerase 1 (ORF67) with 88 residues. N4 phage codes for three tRNAs, however no tRNAs were predicted for phage DL64 and phages LUZ7 and LIT1 (274). No potential coding gene was predicted for the lytic enzyme for DL64, but also for LUZ7 and LIT1, and it is suggested that these phages might code for a novel type of endolysin or execute a different lysis mechanism (274). A DNA polymerase I and DNA helicase and primase are included in the genome of phage DL64, suggesting a host independency for DNA replication. The genome organisation seems to be divided into two large clusters positioned on different strands and in their middle two small clusters are present which are transcribed from opposite directions. This can also be observed for phages LUZ7 and LIT1 (274). Hence, the first larger cluster includes transcription, DNA replication and lysis inhibition, a first small cluster that comprises a DNA primase, a second small cluster for structural proteins followed by the second large cluster for DNA package. The great majority of the genes, 70 (77.8 %), are found in the leftward strand, and the other 20 genes (22.2 %) in the opposite strand.

Table 3.12: Summary of general genome features of the phage cocktail.

Phage	Taxonomic Family	Genome size	Nr. of predicted ORFs	G+C %	Gene Density (genes per kb)	Coding%
DL52	*Myoviridae*	65,867	90	54.9	1.366	89.7
DL54	*Podoviridae*	45,673	71	52.4	1.554	92.4
DL60	*Myoviridae*	66,103	89	54.9	1.346	89.8
DL62	*Podoviridae*	42,508	55	62.2	1.293	94.4
DL64	*Podoviridae*	72,378	90	55.0	1.243	92.5
DL68	*Myoviridae*	66,111	92	55.7	1.391	91.6

The gene coding potential of these phages ranges from 1.243 to 1.391 genes per kb. Phage DL54 stands out from the other phages exhibiting the highest gene density of 1.554 genes per kb. Although for the great majority of potential coding regions (more than 60 % for all cases) no known function has yet been found. The six DNA

sequences were searched for the presence of antimicrobial resistance genes and for any known virulence factors using the BLASTN algorithm (250). The antibiotic resistance genes search was focused on the main antibiotic classes (Table 3.4). The virulence genes search was performed against known virulence factors found in *E. coli*, *Enterococcus* spp and *S. aureus*. Results from this search revealed that all six phages do not carry any potential genes coding for known antibiotic resistance or virulence factors. The genomic sequences of the six phages are deposited in the NCBI GenBank database under accession numbers KR054028-KR054033.

3.5. Discussion

The work of this chapter resulted in the isolation and characterisation of two groups of lytic bacteriophages against two of the main bacterial targets involved in serious and common infectious diseases. Therefore, 21 phages infecting *S. aureus* clinical isolates and another group of 17 phages infecting *P. aeruginosa* clinical isolates were isolated. Such isolation and initial characterisation was indispensable for the selection, establishment and further characterisation of broad phage cocktails targeting each one of the different clinical isolates. For both cases, phages were easily isolated from environmental samples enriched with selected strains.

Plaques produced by the isolated *S. aureus* phages were generally small and halos, if present, were difficult to visualise. On the other hand the average size of plaques produced by *P. aeruginosa* phages was greater and halos could be easily observed. This plaque morphology difference could be related to some intrinsic characteristics of phage diffusion, the permeability of the agar and the time spent by the phage when infecting a host bacteria (276). The presence of halos surrounding the clear plaque spot is a good indication that the phage can be efficient in dispersing biofilms, as they are caused by the diffusion of enzymatic molecules, perhaps EPS depolymerases, produced by the phage. These proteins are then much smaller than a whole phage, hence diffusing at a higher rate into the bacterial lawn and causing the degradation of bacterial produced polymers. Plaque assays are extremely valuable as a first selection method, as we can identify phages that produce a lysogenic cycle or that are not efficient in adsorbing to the host cells. It also indicates phages producing biofilm matrix degrading enzymes and evaluates if the phage lysate contains more than one phage type (277). The latter feature was useful when trying to obtain a pure lysate of the *S. aureus* phages DRA88 and DRA288. When using a host harbouring prophages it was noticed that plaque assays were resulting in heterogeneous plaque morphologies as well as TEM analysis of the lysate, where *Siphoviridae* particles could be observed.

The majority of prophages found in the *S. aureus* host have been identified as belonging to the *Siphoviridae* family (278). Hence, it can be suggested that some prophage was being excised by the host chromosome. It is important to be aware of prophage induction that is an event, even when growing bacteria *per se*, likely to happen and even if occurring at low frequencies, for example prophage excision has been documented during the course of a chronic lung infection in CF patients (279). Such induction can be caused by external stress factors or be triggered in a spontaneous way (280). One might think that is a minor issue, however if considered for therapeutic uses, a scale-up of all the manufacturing process will take place causing the amount of induced prophages to drastically increase, then the implications are significant. If we take into consideration that prophages are strongly related to the horizontal transfer of many virulent genes, such as genes for enterotoxin A (281), the Panton-Valentine leucocidin (282) or the shiga-toxin (283) and that obviously has been contributing to bacterial population evolution, then phage therapeutics should be carefully designed. Firstly, bacterial hosts should be free of prophages, eliminating the possibility to have excised temperate prophages within the therapeutic lysate. This can be achieved by genetically modifying the host's chromosome or by using a "surrogate" strain for phage propagation. The last one has been described where phages targeting *S. aureus* were propagated in a food-grade bacteria, *S. xylosus* (284). Secondly, the bacteria to be targeted in the clinical site most likely will carry several prophages in their chromosomes able to be induced and released into the surrounding environment and have a role in the introduction or increase of their pathogenicity. This could be worrying and could be the opening of Pandora's Box. Hence, phages used for therapeutics should be highly virulent, proliferating and killing the bacterial hosts before any prophage has time to excise and assemble. This has however already been observed by the use of antibiotics in animal feed (285), hence being able to prevent such phenomenon would bring great leverage for the safe use of bacteriophages in the clinic. Another event of concern which is related to phage, most particularly in the case

of *S. aureus* bacteria, is the occurrence in their genome of *S. aureus* pathogenicity islands (SaPIs). SaPIs are responsible for carrying genes coding for superantigens: causing superantigen-induced diseases, such as toxic shock syndrome (TSS). These SaPIs are genetic elements mobilised between bacteria populations by means of a phage (also called helper-phages). Phages described so far as SaPI helper-phages all belong to the *Siphoviridae* family (286, 287). Hence, a potential way to avoid such events to occur is the avoidance of phages sharing the morphology of the *Siphoviridae* family.

The composition of the phage cocktails was based on the best combination possible to achieve the broadest host range infectivity. The combined host range infectivity of the *S. aureus* cocktail was 73.7 % when assessed against a genetically diverse collection of *S. aureus* isolates. Such broad infectivity range was due to the polyvalent performance of both DRA88 and its close related phage K. Phage K is a well-known staphylococcal phage that most likely was first isolated by André Gratia almost 100 years ago (288), the phage attaches specifically to the cell wall teichoic acid (289), providing a broad spectrum host range and it can be assumed that phage DRA88, given its similarities with phage K and its wide host range, might use the same cell wall receptor. Based on TEM analysis and like phage K, DRA88 belongs to the *Myoviridae* tailed-phage family. Adsorption experiments showed that both phages attach to cells in a rapid and similar fashion, which is in accordance with several *S. aureus*-infecting *Myoviridae* phages (290, 291).

The phage cocktail targeting *P. aeruginosa* isolates was composed of a larger number of phages, six in total and as single phages that were not shown to be polyvalent, at least, with regards to the bacterial collection assessed. It is known that *P. aeruginosa* bacterial cells related to a inherited hypermutability behaviour, for example, causing strains to be highly diverse in their gene content (292). The phage bacterial receptor used by the phages might not be highly conserved and then be subject to more

fluctuation. Usually phages targeting gram-negative bacteria use either an outer membrane protein, such as a porin, or a sugar moiety of the lipopolysaccharide (LPS) (293). It is documented that PB1-like phages use the LPS to attach to the cell, giving to these phages a wide infectivity range. However, only DL68 was observed to be polyvalent, DL52 and DL60 showed narrow host ranges and this might suggest that even using the LPS for bacterial recognition and initial attachment these phages might require a second surface component for the establishment of an irreversible adsorption, a process observed for several other phages (294) and could explain the narrow host range. Hence, a combination of several phages isolated was made in order to give the best and broadest host coverage range, resulting in infection of 82 % of the isolates tested. TEM analysis revealed two types of morphology, DLA52, DL60 and DL68 belong to the *Myoviridae* family and DL54, DL62 and DL64 belong to the *Podoviridae* family.

An interesting observation for phage DRA88, but also phages DL54 and DL60 was the possible formation of phage aggregates. Phage aggregation is observed occasionally in nature (295, 296) and is dependent on pH, ionic strength, and the composition of ions. Such phenomena could have been influenced by uranyl acetate (pH 4) used to stain the phages for TEM observation. DLS measurements for DRA88 (in dH2O, ~pH 7) were unsuccessful, possibly due to the several sizes found in the sample (singles and multiple aggregates); hence, we suspect that phage DRA88 is prone to forming aggregates. When phage interacts with bacterial cells, aggregation could impede phage access to the cells and hence decrease the rate of adsorption. Phage aggregation can be inhibited by optimisation of growth medium composition or by stabilising in nano-emulsions, resulting in phages that more efficiently attach to bacterial cells (297–299); consequently, this could affect estimation of the PFU, which then may not directly correspond with the number of infective particles (MOI).

At the genome level, DRA88 was revealed to be a large double stranded DNA (dsDNA) phage, usually a common characteristic of *Myoviridae staphylococcal* phages (257), carrying a high gene density and low G+C % content. DRA88 genome exhibits a high degree of relatedness to several other phages belonging to the Twort-like group, including phage K. Regarding *P. aeruginosa* phages, all phages were revealed to have medium length dsDNA genomes. Phages in this study shared similarities with previously sequenced phages and it was possible to identify four distinct groups of phages within the cocktail: PB1-like, LUZ24-like, phiKMV-like and N4-like phages, which have been considered ideal for use in phage therapy and some of them can be found in commercial mixtures already (300), such as the “pyophage” from the Eliava Institute (301). DL52, DL60 and DL68 were shown to be homologues of each other and several other phages belonging to the PB1-like group of phages, which used for *in vivo* therapy assays has been proved successful in a keratitis mice model for a member of this group (261). DL62 phage was revealed to be the smallest genome comprising of potential coding regions showing a high degree of relatedness with phages of the phage group phiKMV-like, where recently a member of this group was assessed for *in vivo* therapy against hemorrhagic pneumonia in a mink model (302).

Interestingly, phage DL68 appears to carry the rIIA/rIIB lysis inhibition cassette, in fact widely distributed among genomes of phages infecting different host genera (303, 304), which enables a delay in the host lysis, but consequently results in a high increase in the burst size of the phage. This feature provides phages of this type with a competitive advantage over others. It should be important if this type of phage is integrated within a therapeutic cocktail product to always perform its propagation separately; otherwise such a phage might take over the phage population. However, the role of such a cassette remains uncertain and several additional roles have been attributed to it, such as being involved in the host resistance mechanism of the abortive infection system (305).

No virulence or antibiotic resistance factors were identified in the genome, according to the data available at the moment, suggesting that either *S. aureus* or *P. aeruginosa* phage preparations could be safely used to treat infections related to these bacteria. However, the majority of putative coding regions of the DRA88 genome and for the *P. aeruginosa* phages do not have any function attributed yet, which is generally applies to the several phages being sequenced at the moment (306). Consequently, there is an urgent need for a more comprehensive investigation of phage genomes in order to understand phage gene products. Considering phage therapy as a therapeutic approach option, it is extremely important that we expand our knowledge regarding phage genes and proteins and their respective functions and potentialities, as they can be involved in phage-host interaction and even code for novel virulence determinants (307).

Phage therapy has been developing recently under small carefully controlled steps, in contrast to the scenario observed early in the century, where the misinformation on phage nature led many clinical trials to unsuccessful outcomes. Still, there are numerous technical opportunities to improve and understand the phage therapy product, such as phage selection criteria, the standards for phage purity and the recent advance in sequencing and bioinformatics analysis, which ultimately will facilitate their regulatory approval.

Annexe

Table 3.13: General features of putative ORFs from *S. aureus* phage DRA88 with best matches in the NCBI database.

ORF	bp		Strand	Gene Length	Representative similarity to proteins in database	% Identity	E-value	Accession no.
	Start	Stop						
1	20	358	-	339	Phage protein	99	2E-70	YP_007002124
2	852	977	+	126	Phage protein	95	3E-03	YP_007002125
3	1183	1467	+	285	Phage protein	96	8E-60	YP_241032
4	1542	1733	+	192	Phage protein	100	6E-37	YP_241033
5	2064	2552	-	489	HNH homing endonuclease # Phage intron	94	5E-91	YP_241035
6	2950	3081	+	132	Phage protein	98	4E-20	YP_007112858
7	3670	4071	+	402	Hypothetical protein	94	1E-72	YP_007112856
8	4568	4789	+	222	Hypothetical protein	99	2E-44	YP_007112855
9	5049	5213	+	165	Hypothetical protein	100	4E-29	YP_007112853
10	5770	6120	+	351	Hypothetical protein	31	2E-06	YP_004301348
11	6189	6353	+	165	Hypothetical protein	42	1E-04	YP_001504239
12	6366	6539	+	174	Phage protein	93	9E-28	YP_007002137
13	6683	6808	+	126	Phage protein	93	8E-18	YP_007002138
14	6910	7077	+	168	Hypothetical protein	37	2	YP_007112846
15	7370	8818	+	1449	Hypothetical protein	48	6E-21	WP_016279792
16	8837	9127	-	291	Hypothetical protein	83	3E-54	YP_007002140
17	9328	11421	-	2094	Tail fiber protein	71	6E-61	WP_019168862
18	11463	11699	-	237	Phage protein	82	4E-40	YP_007002141
19	11715	11960	-	246	Hypothetical protein	96	4.9E-48	YP_007002142
20	11960	12205	-	246	Phage protein	94	1E-43	YP_007002145
21	12393	12878	-	486	Phage protein	94	1E-77	AEJ79651
22	12871	13311	-	441	Phage protein	94	6E-85	YP_007002150
23	13325	13867	-	543	Phage protein	100	4E-113	YP_007002151
24	13879	14367	-	489	Phage protein	93	10E-110	YP_007002152
25	14382	14834	-	453	Hypothetical protein	43	2E-02	WP_016184223
26	14851	15255	-	405	Phage protein	99	2E-81	YP_007002153
27	15258	15959	-	702	Hypothetical protein	99	2E-166	YP_008853985
28	16748	17296	-	549	Phage protein	100	2E-98	YP_024439
29	17300	17518	-	219	Phage protein	100	3E-43	YP_241058
30	17519	17713	-	195	Phage protein	98	5E-37	YP_241059
31	17703	18440	-	738	Phage protein	99	2E-161	YP_007112830
32	18629	18856	-	228	Phage protein	90	4E-40	YP_007002161
33	18858	19247	-	390	Phage protein	100	7E-90	YP_007002162
34	19341	19514	-	174	Phage protein	100	8E-34	YP_007002163
35	19555	20037	-	483	Phage protein	98	2E-107	YP_007002164
36	20087	20629	-	543	Phage protein	94	2E-114	YP_007002165
37	20629	21159	-	531	Phage protein	98	1E-110	YP_007002166
38	21162	21326	-	165	Phage protein	100	7E-29	YP_007002167
39	21329	21616	-	288	Phage protein	49	2E+00	YP_007002168
40	21616	22461	-	846	Phage protein	98	0	YP_007002169
41	22474	23592	-	1119	Phage protein	98	0	YP_241071
42	23745	23960	-	216	Phage protein	96	1E-41	YP_007002171
43	24064	24480	-	417	Phage protein	99	4E-83	YP_007002172
44	24612	24914	-	303	Phage DNA-binding protein	100	6E-64	YP_024448
45	24914	25102	-	189	Phage protein	100	2E-34	YP_007002174
46	25146	25307	-	162	Phage protein	100	3E-29	YP_241076
47	25307	27358	-	2052	Phage protein	100	0	YP_007002176
48	27438	27701	-	264	Phage protein	99	9E-54	YP_007002177

49	27718	27891	-	174	Phage protein	100	8E-32	YP_007112812
50	27898	28476	-	579	Phage protein	100	1E-111	YP_007112811
51	28469	29062	-	594	Phage protein	82	6E-111	YP_007112810
52	29055	29951	-	897	Phage protein	100	0	YP_007112809
53	29951	30175	-	225	hypothetical protein	100	8E-17	YP_007112808
54	30244	30984	-	741	Phosphate starvation-inducible protein PhoH,predicted ATPase	100	0	YP_024453
55	31036	31650	-	615	Phage protein	100	4E-143	YP_024454
56	31666	32091	-	426	Phage ribonuclease H	100	3E-94	YP_024455
57	32081	32272	-	192	Phage protein	100	3E-37	YP_241086
58	32295	32936	-	642	Phage protein	100	5E-123	YP_024456
59	32926	33156	-	231	Phage protein	100	1E-46	YP_241088
60	33159	33386	-	228	hypothetical protein	100	8E-45	YP_241089
61	33501	34193	-	693	hypothetical protein	99	2E-141	YP_024457
62	34391	35185	-	795	Phage protein	100	6E-178	YP_007112798
63	35185	35493	-	309	Phage protein	99	2E-64	YP_007002193
64	35607	36227	-	621	Phage protein	61	5E-41	YP_024458
65	36290	37780	-	1491	Phage lysin, N-acetylmuramoyl-L-alanine amidase	100	0	YP_024461
66	37780	38283	-	504	Phage holin	100	5E-116	YP_007112795
67	38368	38553	-	186	Phage protein	100	1E-33	YP_241098
68	40100	40318	-	219	Phage protein	100	4E-30	YP_241099
69	40796	41005	-	210	hypothetical protein	100	2E-42	YP_241100
70	41018	41350	-	333	Phage protein	100	10E-59	YP_007002199
71	41363	41689	-	327	Phage protein	100	7E-71	YP_007002200
72	42249	42515	+	267	Phage protein	100	3E-41	AFV80863
73	42493	42771	+	279	Phage protein	100	2E-60	YP_241104
74	42768	43178	+	411	Phage protein	100	2E-91	YP_241105
75	43193	43546	+	354	Phage terminase, large subunit	100	2E-76	YP_024465
76	43784	44554	+	771	Phage protein	95	2E-142	YP_007677505
77	44621	46081	+	1461	Phage terminase, large subunit	100	0	AFN38730
78	46095	46895	+	801	Phage protein	99	6E-165	YP_007002206
79	46882	47055	+	174	Phage protein	97	5E-16	YP_240894
80	47052	47531	+	480	Phage protein	100	7E-98	YP_024467
81	47648	48775	+	1128	hypothetical protein	100	3E-140	YP_007112782
82	49013	49201	+	189	Phage protein	100	1E-17	YP_007002210
83	49219	49590	+	372	Phage protein	100	5E-72	YP_024470
84	49594	51285	+	1692	Phage protein	100	0	YP_007002212
85	51479	52252	+	774	Phage protein	100	0	YP_024472
86	52271	53230	+	960	Phage protein	98	3E-137	YP_007002214
87	53346	54737	+	1392	Phage major capsid protein	100	0	YP_007002215
88	54829	55125	+	297	Phage protein	100	8E-26	YP_007002216
89	55138	56046	+	909	Phage protein	100	0	YP_024475
90	56060	56938	+	879	Phage protein	100	0	YP_007002218
91	56938	57558	+	621	Phage protein	100	8.0E-148	YP_007002219
92	57577	58413	+	837	Phage protein	100	0	YP_024478
93	58415	58630	+	216	Phage protein	100	2E-45	YP_240909
94	58657	60420	+	1764	hypothetical protein	99	0	ABL87117
95	60493	60921	+	429	Phage protein	100	1E-99	YP_024480
96	61008	61148	+	141	Phage protein	100	8E-23	YP_007112766
97	61191	61643	+	453	Phage protein	93	2E-97	YP_007002226
98	61866	62018	+	153	hypothetical protein	29	2	WP_007845149
99	62086	62397	+	312	Phage protein	100	6E-66	YP_007002227
100	62529	62987	+	459	Phage protein	99	2E-104	YP_007002228
101	63031	63567	+	537	Phage protein	100	6E-124	YP_024484
102	63623	67678	+	4056	Hypothetical protein	99	0	YP_007002230
103	67757	70183	+	2427	Hypothetical protein	100	0	YP_007112760
104	70197	71084	+	888	Phage protein	99	0	YP_007002232
105	71084	73630	+	2547	Glycerophosphoryl diester phosphodiesterase	99	0	YP_007112758

106	73737	74528	+	792	Phage protein	100	0	YP_024489
107	74528	75052	+	525	Phage protein	100	3E-121	YP_240925
108	75052	75756	+	705	Phage protein	100	5E-171	YP_024491
109	75771	76817	+	1047	Phage baseplate	100	0	YP_024492
110	76838	79903	+	3066	Phage protein	89	0	YP_007112753
111	80014	80535	+	522	hypothetical protein	100	4E-122	YP_024494
112	80557	84015	+	3459	hypothetical protein	100	0	YP_007112751
113	84064	84222	+	159	Phage protein	87	2E-22	YP_240931
114	84223	86154	+	1932	Phage capsid and scaffold	71	0	ACB89087
115	86168	86542	+	375	Phage protein	83	2E-69	YP_024497
116	86549	87925	+	1377	Phage capsid and scaffold	97	0	YP_007112747
117	88015	89763	+	1749	DNA helicase, phage-associated	98	0	YP_024499
118	89775	91388	+	1614	Phage protein	99	0	YP_007002246
119	91381	92823	+	1443	DNA helicase, phage-associated	99	0	YP_024501
120	92902	93927	+	1026	Phage recombination exonuclease	96	0	YP_007002248
121	93927	94304	+	378	Phage protein	93	3E-80	YP_024503
122	94304	96223	+	1920	Hypothetical protein	96	0	YP_024504
123	96223	96819	+	597	Phage protein	98	5E-140	YP_007112958
124	96834	97901	+	1068	DNA primase / DNA helicase 3.6.1.-), phage-associated	99	0	YP_024506
125	97967	98305	+	339	Phage protein	98	6E-48	YP_240943
126	98305	98757	+	453	Phage protein	95	7E-81	YP_007002254
127	98744	99352	+	609	Phage protein	100	8E-147	YP_240945
128	99369	99761	+	393	Ribonucleotide reduction protein NrdI	99	9E-88	YP_007002257
129	99776	101890	+	2115	Ribonucleotide reductase of class Ib (aerobic),alpha subunit (EC 1.17.4.1)	99	0	YP_007002258
130	101904	102953	+	1050	Ribonucleotide reductase of class Ib (aerobic),beta subunit (EC 1.17.4.1)	99	0	YP_007112951
131	102971	103300	+	330	Phage protein	98	5E-71	YP_007112950
132	103284	103604	+	321	Phage oxidoreductase	100	3E-68	YP_024513
133	103811	104407	+	597	Phage protein	100	2E-140	YP_007002262
134	104417	104722	+	306	Phage integration host factor	99	1E-65	YP_024515
135	104798	107029	+	2232	DNA polymerase I	100	0	YP_007002264
136	107195	108004	+	810	HNH homing endonuclease	100	0	YP_024518
137	108238	109098	+	861	DNA polymerase I	100	0	YP_240958
138	109167	109409	+	243	Phage protein	98	5E-33	YP_240959
139	109426	109908	+	483	Phage protein	100	1E-114	YP_024519
140	109995	111266	+	1272	Phage protein	99	0	YP_024520
141	111326	112582	+	1257	Phage recombinase	100	0	YP_024521
142	112586	112939	+	354	Phage protein	100	2E-65	YP_240963
143	112926	113588	+	663	Putative sigma factor	100	10E-156	YP_024522
144	113715	114347	+	633	Phage protein	100	2E-149	YP_024523
145	114371	114883	+	513	Phage major tail protein	99	5E-113	YP_007002272
146	114898	115107	+	210	Phage major tail protein	99	2E-39	YP_240967
147	115220	115480	+	261	Phage protein	100	8E-55	YP_007002274
148	115484	116239	+	756	Phage protein	99	2E-162	YP_024525
149	116232	117482	+	1251	Phage protein	100	0	YP_007002276
150	117496	117864	+	369	Phage protein	99	3E-71	YP_007112931
151	117851	118162	+	312	Phage protein	100	6E-68	YP_024528
152	118226	118762	+	537	Phage protein	99	2E-116	YP_007002279
153	118755	119522	+	768	Phage protein	100	0	YP_024529
154	119500	119946	+	447	Phage protein	100	1E-102	YP_024530
155	119946	120809	+	864	Phage protein	99	0	YP_240976
156	121181	121912	+	732	Phage protein	100	1E-172	YP_024531
157	121930	122388	+	459	Phage protein	100	2E-105	YP_007002284
158	122453	122896	+	444	Phage protein	100	7E-90	YP_024533
159	122913	123617	+	705	Phage protein	98	2E-164	YP_007002286
160	123680	124078	+	399	Phage protein	100	7E-80	YP_007002287
161	124225	124467	+	243	Phage protein	96	5E-47	YP_240982
162	124472	125029	+	558	Phage protein	100	5E-129	YP_007112919

163	125065	125241	+	177	Phage protein	100	2E-32	YP_240984
164	125234	125482	+	249	Hypothetical protein	95	2E-46	YP_007112917
165	125496	125708	+	213	Hypothetical protein	99	2E-41	YP_007002292
166	125789	126433	+	645	Hypothetical protein	97	8E-112	YP_007002293
167	126449	126697	+	249	Hypothetical protein	95	4E-27	YP_007002294
168	126709	126885	+	177	Phage protein	100	2E-31	AFN38398
169	126878	127174	+	297	Phage protein	98	1E-61	YP_007002295
170	127222	127404	+	183	Phage protein	98	2E-32	YP_240988
171	127417	127785	+	369	Phage protein	99	6E-69	YP_007002297
172	127798	128145	+	348	Phage protein	99	3E-76	YP_007002298
173	128493	128798	+	306	Phage protein	88	7E-61	YP_007002300
174	128813	129163	+	351	Phage protein	97	6E-74	YP_240993
175	129163	129765	+	603	Phage protein	96	2E-138	YP_240994
176	129784	129972	+	189	Phage protein	85	2E-20	YP_007002303
177	129977	131029	+	1053	Phage protein	58	6E-52	WP_002508231
178	131026	131202	-	177	Hypothetical protein	-	-	not available
179	131329	131487	+	159	Phage protein	89	4E-12	YP_007002320
180	131503	131727	+	225	hypothetical protein	96	4E-44	YP_007002321
181	131740	131940	+	201	Phage protein	98	3E-40	YP_241008
182	131941	132231	+	291	Phage protein	100	5E-59	YP_007002323
183	132324	132617	+	294	Phage protein	100	9E-64	YP_007002324
184	132614	133522	+	909	Ribose-phosphate pyrophosphokinase	84	7E-180	YP_024538
185	133540	135009	+	1470	Nicotinamide phosphoribosyltransferase	97	0	ACB89165
186	135088	135333	+	246	Phage protein	99	7E-51	YP_241013
187	135353	135745	+	393	Phage protein	94	3E-79	YP_007002328
188	135747	135944	+	198	Phage protein	98	6E-36	YP_007002329
189	136010	136321	+	312	Phage protein	97	2E-52	YP_241016
190	136324	136833	+	510	Phage protein	98	2E-115	YP_241017
191	136835	137173	+	339	Phage protein	84	9E-61	YP_007002334
192	137170	137286	+	117	Hypothetical protein	-	-	not available
193	137300	137701	+	402	Phage protein	57	2E-44	YP_024544
194	137300	138142	+	843	Hypothetical protein	36	2E+00	WP_017622020
195	138245	138469	+	225	Hypothetical protein	-	-	not available
196	139106	139254	+	149	Hypothetical protein	36	5E+00	WP_022070173
197	139308	139601	+	294	Hypothetical protein	49	7E-09	ACB89175
198	139598	139783	+	186	Hypothetical protein	49	4E-05	YP_241023
199	140019	140183	+	165	Phage protein	89	2E-24	ACB89176
200	140183	140470	+	288	Phage protein	96	3E-59	YP_241025
201	140470	140763	+	294	Phage protein	96	5E-61	ACB89178
202	140767	141024	+	258	Phage protein	100	1E-45	YP_241027
203	141132	141371	+	240	Phage protein	96	6E-47	ACB89180
204	141382	141726	+	345	Phage protein	83	2E-39	YP_007112864

Table 3.14: General features of putative ORFs from *P. aeruginosa* phage DL52 with best matches in the NCBI database.

ORF	bp		Strand	Gene Length	Representative similarity to proteins in database	% Identity	E-value	Accession no.
	Start	Stop						
1	65	466	+	402	Phage protein	96	8E-87	YP_001294433
2	498	821	+	324	Phage protein	100	3E-74	YP_001294432
3	818	1021	+	204	Phage protein	100	1E-30	YP_009009036
4	1027	1338	+	312	Phage protein	96	7E-64	YP_002154157
5	1587	1934	+	348	Phage protein	97	1E-74	YP_001294430
6	2038	2970	+	933	Phage protein	99	0	YP_002455942
7	3072	3659	+	588	Phage protein	99	3E-142	YP_009009031
8	3677	4114	+	438	Phage protein	97	3E-81	YP_001294427
9	4200	4979	+	780	Phage protein	100	0	YP_001294426
10	4982	5383	+	402	Phage protein	90	9E-71	YP_001294425
11	5428	5778	+	351	Phage protein	99	7E-66	YP_001294424
12	5778	5996	+	219	Phage protein	100	5E-45	YP_001294423
13	5993	6376	+	384	Phage protein	98	3E-65	YP_001294422
14	6414	7796	-	1383	Phage terminase, large subunit	100	0	YP_001294421
15	7998	8186	+	189	Phage protein	98	1E-22	YP_001294420
16	8307	8453	+	147	Phage protein	100	9E-12	YP_001294419
17	8465	8767	+	303	Phage protein	95	3E-60	YP_001294418
18	8814	9731	+	918	Phage tail length tape-measure protein	99	6E-123	YP_002456023
19	9734	9922	+	189	Phage protein	97	4E-38	YP_001294508
20	10002	10187	+	186	Phage protein	98	3E-34	YP_001294507
21	10312	10512	+	201	Phage protein	98	3E-39	YP_001294505
22	10509	10724	+	216	Phage protein	99	8E-42	YP_001294504
23	10721	10924	+	204	Phage protein	61	6E-18	YP_001294503
24	10908	11120	+	213	Phage protein	90	1E-40	YP_001294502
25	11149	11796	+	648	Phage protein	93	2E-135	YP_001294501
26	11940	12098	-	159	hypothetical protein	-	-	not available
27	12185	12409	+	225	Phage protein	93	1E-42	YP_002154315
28	12465	12692	+	228	Phage protein	75	4E-32	YP_006200849
29	12702	12923	+	222	Phage protein	81	2E-33	YP_007002628
30	12971	13288	+	318	Phage protein	93	5E-69	YP_002456011
31	13298	13906	+	609	Phage protein	91	2E-106	YP_002456010
32	14098	14712	+	615	Phage protein	99	7E-92	YP_002154310
33	14880	15452	-	573	Phage protein	98	1E-119	YP_001294493
34	16425	18164	-	1740	DNA primase, phage associated	99	0	YP_002456007
35	18312	18497	-	186	Phage protein	100	6E-14	YP_001294490
36	18503	19579	-	1077	Phage protein	99	0	YP_002364381
37	19576	20025	-	450	Phage protein	97	2E-102	YP_007238225
38	20025	20579	-	555	Phage protein	91	3E-29	WP_023104124
39	20999	21784	-	786	Phage protein	99	1E-180	YP_002456002
40	21952	22374	+	423	Phage protein	99	2E-96	YP_002456001
41	22361	23548	+	1188	DNA helicase, phage-associated	99	0	YP_002456000
42	23710	24600	+	891	Phage protein	100	2E-68	YP_002154209
43	24705	25706	+	1002	Phage protein	99	0	YP_002455998
44	25796	26026	+	231	Phage protein	97	1E-35	YP_002455997
45	26026	26244	+	219	Phage protein	97	2E-30	YP_002154206
46	26228	26446	+	219	Phage tail assembly	97	2E-44	YP_001294479
47	26446	26706	+	261	Phage protein	94	2E-50	YP_002455994

48	26718	26924	+	207	Phage protein	96	6E-39	YP_001294477
49	26924	27841	+	918	Thymidylate synthase thyX	100	0	YP_001294476
50	27843	28034	+	192	Phage protein	100	4E-35	YP_001294475
51	28037	29077	+	1041	3'-phosphatase, 5'-polynucleotide kinase, phage-associated	94	0E+00	YP_002455989
52	29153	29707	+	555	Phage protein	99	1E-132	YP_001294473
53	29707	32814	+	3108	DNA polymerase III alpha subunit	99	0	YP_002455987
54	32807	33217	+	411	Phage protein	100	3E-81	YP_001294471
55	33214	34773	+	1560	DNA helicase, phage-associated	99	0	YP_001294470
56	34868	35488	+	621	Phage protein	100	3E-120	YP_002154195
57	35577	36476	+	900	Phage protein	100	0	YP_002154194
58	36533	37138	+	606	Phage protein	100	2E-100	YP_001294467
59	37135	37689	+	555	Phage DNA-binding protein	98	1E-128	YP_002154192
60	37744	38655	+	912	DNA ligase, phage-associated	96	0	YP_002154191
61	38935	39186	+	252	Phage protein	-	-	not available
62	39210	39872	-	663	Lytic enzyme	-	-	not available
63	39872	40300	-	429	Phage protein	-	-	not available
64	40302	43196	-	2895	Phage tail fibers	-	-	not available
65	43201	44715	-	1515	Phage protein	-	-	not available
66	44712	45965	-	1254	Phage protein	-	-	not available
67	46022	46453	-	432	Phage baseplate	-	-	not available
68	46433	46666	-	234	hypothetical protein	-	-	not available
69	46743	47276	-	534	Phage protein	-	-	not available
70	47276	48139	-	864	Phage protein	-	-	not available
71	48139	50721	-	2583	Phage internal (core) protein	-	-	not available
72	50725	51153	-	429	Phage protein	-	-	not available
73	51163	51756	-	594	Phage tail fiber protein	-	-	not available
74	51765	52169	-	405	Phage protein	-	-	not available
75	52304	52807	-	504	Phage protein	-	-	not available
76	52817	53245	-	429	Phage protein	-	-	not available
77	53594	53917	-	324	Phage protein	-	-	not available
78	53917	54369	-	453	Phage tail fiber protein	-	-	not available
79	54427	55941	-	1515	Phage protein	-	-	not available
80	56536	57087	-	552	Phage protein	-	-	not available
81	57095	57493	-	399	Phage protein	95	2E-85	YP_001294443
82	57490	57957	-	468	Phage protein	99	6E-76	YP_001294442
83	57972	58409	-	438	Phage protein	100	4E-103	YP_001294441
84	58511	59659	-	1149	Phage capsid and scaffold	99	0E+00	YP_002455954
85	59669	60304	-	636	Phage protein	100	2E-145	YP_001294439
86	60308	61744	-	1437	Phage protein	100	0E+00	YP_001294438
87	62259	62396	-	138	Phage protein	98	3E-21	YP_002455951
88	62393	62599	-	207	Phage protein	99	1E-39	YP_001294436
89	62619	63455	-	837	Phage minor capsid protein	100	0	YP_002455949
90	63455	65752	-	2298	Phage-related protein	99	0	YP_001294434

Table 3.15: General features of putative ORFs from *P. aeruginosa* phage DL54 with best matches in the NCBI database.

ORF	bp		Strand	Gene Length	Representative similarity to proteins in database	% Identity	E-value	Accession no.
	Start	Stop						
1	1147	1605	+	459	Phage protein	99	1E-105	YP_008857869
2	1637	2035	+	399	Phage baseplate hub	99	5E-90	YP_001671940
3	2035	3483	+	1449	Phage terminase, large subunit	100	0	YP_001671939
4	3483	5603	+	2121	Phage portal (connector) protein	100	0	YP_008857866
5	5633	5848	+	216	Phage protein	100	3E-43	YP_001671937
6	5848	6840	+	993	Phage capsid and scaffold	100	1E-164	YP_009125634
7	6859	7812	+	954	Phage capsid and scaffold	100	0	YP_001671935
8	7861	8181	+	321	Phage protein	100	3E-71	YP_001671934
9	8185	8811	+	627	Phage protein	100	1E-139	YP_001671933
10	8822	9013	+	192	Phage protein	100	4E-34	YP_001671932
11	8997	9245	+	249	Phage protein	100	1E-27	YP_001671931
12	9235	9882	+	648	Phage tail fibers	100	3E-152	YP_001671930
13	9891	11432	+	1542	Phage protein	100	0	AGC35290
14	11429	12118	+	690	Phage protein	100	2E-142	YP_001671928
15	12115	12549	+	435	Phage protein	99	3E-102	YP_001671927
16	12530	13471	+	942	Phage protein	99	2E-151	YP_008857854
17	13601	13831	+	231	hypothetical protein	100	1E-43	YP_009125623
18	13856	15370	+	1515	Phage protein	100	0	YP_008857852
19	15521	18688	+	3168	Phage protein	100	0	YP_001671923
20	18700	19587	+	888	Phage protein	95	0	YP_008857850
21	19602	19958	+	357	Phage protein	97	2E-76	YP_009007837
22	20165	20371	-	207	Phage protein	100	2E-22	YP_001671920
23	20358	20567	-	210	Phage protein	100	3E-42	YP_008857847
24	20571	20789	-	219	Phage protein	100	8E-44	YP_001671918
25	20786	21547	-	762	Phage protein	100	0	YP_001671917
26	21540	21779	-	240	Phage protein	99	2E-50	YP_009125613
27	21733	22713	-	981	Phage protein	100	0	YP_008857844
28	22694	23524	-	831	DNA polymerase I	99	0	YP_009007830
29	23609	24058	-	450	Phage-associated homing endonuclease	100	7E-106	YP_001671913
30	24058	24342	-	285	Phage protein	98	4E-58	YP_009125609
31	24314	24724	-	411	Phage protein	99	4E-92	YP_009007827
32	24795	25349	-	555	Helix-destabilising protein	100	1E-115	YP_001671910
33	25419	27056	-	1638	DNA polymerase, phage-associated	100	0	YP_001671907
34	27057	27254	-	198	Phage protein	98	2E-37	YP_008857837
35	27259	27768	-	510	Phage protein	86	2E-105	YP_008857836
36	27845	28123	-	279	Phage protein	99	7E-57	AGC35267
37	28114	28275	-	162	Phage protein	100	1E-28	AGC35266
38	28265	28456	-	192	Phage protein	98	4E-37	YP_001671901
39	28437	28670	-	234	Phage protein	100	2E-32	YP_008857832
40	28706	29002	-	297	Phage protein	98	4E-56	YP_009007816
41	28984	29493	-	510	DNA polymerase, phage-associated	99	2E-121	YP_009007815
42	29477	31186	-	1710	DNA primase/helicase, phage-associated	100	0	AGC35261
43	31187	31564	-	378	Phage protein	100	3E-87	YP_008857828
44	31564	31962	-	399	Phage protein	100	2E-91	YP_001671895
45	31962	32846	-	885	Phage protein	99	0	YP_001671894

46	32977	33198	-	222	Phage protein	100	4E-44	YP_001671893
47	33208	34740	-	1533	Phage protein	100	0	YP_008857824
48	34752	35927	-	1176	Phage protein	99	0	YP_008857823
49	35903	36472	-	570	Phage protein	100	6E-136	YP_001671890
50	36465	37265	-	801	Phage protein	98	0	YP_009125589
51	37262	38218	-	957	Phage protein	99	0	YP_008857820
52	38237	39199	-	963	Phage protein	98	0	YP_008857819
53	39270	39398	-	129	hypothetical protein	98	2E-20	YP_009125586
54	39410	40234	-	825	Phage protein	100	1E-170	YP_009007804
55	40244	40462	-	219	hypothetical protein	96	4E-43	YP_009125584
56	40469	40687	-	219	hypothetical protein	49	4E-13	YP_009125583
57	40689	40901	-	213	Phage protein	83	4E-32	AGC35246
58	41032	41457	-	426	Phage protein	96	2E-95	YP_001671885
59	41457	41708	-	252	hypothetical protein	60	9E-14	AGC35244
60	41705	41875	-	171	Phage protein	100	3E-31	AGC35243
61	41875	42141	-	267	Phage protein	97	2E-55	YP_001671884
62	42146	42391	-	246	Phage protein	100	5E-52	YP_008857811
63	42400	42546	-	147	Phage protein	100	4E-27	NP_775198
64	42533	42688	-	156	hypothetical protein	100	2E-28	YP_008857809
65	42699	42974	-	276	Phage protein	100	2E-59	YP_008857808
66	42976	43209	-	234	hypothetical protein	100	1E-47	YP_001671880
67	43341	43523	-	183	Phage protein	100	7E-33	YP_001671879
68	43703	43843	-	141	Phage protein	100	8E-24	NP_775190
69	43840	44028	-	189	Phage protein	98	9E-35	YP_008857803
70	44131	44613	-	483	Phage protein	98	1E-107	YP_008857802
71	44617	44922	-	306	Phage protein	100	7E-57	YP_008857801

Table 3.16: General features of putative ORFs from *P. aeruginosa* phage DL60 with best matches in the NCBI database.

ORF	bp		Strand	Gene Length	Representative similarity to proteins in database	% Identity	E-value	Accession no.
	Start	Stop						
1	53	466	+	414	Phage protein	99	1E-91	YP_002455947
2	498	821	+	324	Phage protein	98	9E-73	YP_002455946
3	793	909	+	117	Phage protein	92	1E-14	YP_001294431
4	1027	1338	+	312	Phage protein	100	3E-68	YP_002455944
5	1587	1934	+	348	Phage protein	97	1E-74	YP_002455943
6	2038	2967	+	930	Phage protein	95	0E+00	YP_001294429
7	3069	3656	+	588	Phage protein	98	8E-140	YP_009009031
8	3672	4109	+	438	Phage protein	89	7E-73	YP_001294427
9	4195	4974	+	780	Phage protein	99	0	YP_002154152
10	4977	5378	+	402	Phage protein	99	6E-61	YP_001294425
11	5423	5773	+	351	Phage protein	98	9E-65	YP_001294424
12	5773	5991	+	219	Phage protein	99	4E-44	YP_001294423
13	5988	6371	+	384	Phage protein	98	2E-82	YP_002455935
14	6408	7790	-	1383	Phage terminase, large subunit	100	0	YP_001294421
15	7967	8113	+	147	Phage protein	100	9E-12	YP_001294419
16	8126	8428	+	303	Phage protein	100	7E-63	YP_001294418
17	8475	9392	+	918	Phage tail length tape-measure protein	99	2E-123	YP_002456023
18	9395	9583	+	189	Phage protein	98	8E-38	YP_001294508
19	9670	9921	+	252	Phage protein	94	5E-50	YP_002154231
20	9918	10118	+	201	Phage protein	97	7E-38	YP_001294505
21	10115	10330	+	216	Phage protein	100	2E-42	YP_001294504
22	10339	10518	+	180	Phage protein	98	2E-33	YP_001294503
23	10515	10727	+	213	Phage protein	96	1E-42	YP_001294502
24	10755	11402	+	648	Phage protein	99	1E-143	YP_001294501
25	11399	11725	+	327	Phage protein	99	4E-72	YP_002154225
26	11791	12015	+	225	Phage protein	93	1E-42	YP_002154315
27	12069	12296	+	228	Phage protein	68	1E-25	WP_041598427
28	12306	12527	+	222	Phage protein	85	9E-36	YP_007002628
29	12575	12892	+	318	Phage protein	93	8E-69	YP_002456011
30	12902	13507	+	606	Phage protein	98	7E-116	YP_002456010
31	13700	14314	+	615	Phage protein	99	1E-93	YP_002154219
32	14485	15057	-	573	Phage protein	99	3E-120	YP_001294493
33	16029	17759	-	1731	DNA primase, phage associated	99	0	YP_001294491
34	17907	18092	-	186	Phage protein	93	7E-06	YP_001294490
35	19171	19620	-	450	Phage protein	99	6E-103	YP_007002619
36	19644	21194	-	1551	Phage protein	93	8E-157	YP_006200837
37	21205	21990	-	786	Phage protein	97	1E-176	YP_002456002
38	22158	22580	+	423	Phage protein	99	5E-96	YP_002456001
39	22567	23754	+	1188	DNA helicase, phage-associated	98	0	YP_002456000
40	23915	24817	+	903	Phage protein	99	4E-68	YP_007238220
41	24922	25923	+	1002	Phage protein	97	0	YP_002455998
42	26012	26242	+	231	Phage protein	97	2E-35	YP_001294481
43	26242	26460	+	219	Phage protein	99	3E-30	YP_007002611
44	26444	26662	+	219	Phage tail assembly	99	1E-44	YP_001294479
45	26662	26925	+	264	Phage protein	95	4E-52	YP_001294478
46	26937	27143	+	207	Phage protein	96	9E-40	YP_001294477
47	27143	28060	+	918	Thymidylate synthase thyX	97	0	YP_002455991
48	28062	28253	+	192	Phage protein	98	2E-34	YP_001294475
49	28256	29305	+	1050	3'-phosphatase, 5'-polynucleotide kinase, phage-associated	89	0	YP_002455989

50	29380	29934	+	555	Phage protein	100	4E-134	YP_001294473
51	29934	33041	+	3108	DNA polymerase III alpha subunit	99	0	YP_001294472
52	33034	33444	+	411	Phage protein	97	2E-78	YP_002154288
53	33441	35000	+	1560	DNA helicase, phage-associated	99	0	YP_001294470
54	35083	35715	+	633	Phage protein	100	5E-113	YP_002455984
55	35804	36700	+	897	Phage protein	100	0E+00	YP_002154194
56	36757	37362	+	606	Phage protein	100	2E-100	YP_001294467
57	37359	37928	+	570	Phage DNA-binding protein	88	3E-114	YP_002154192
58	37983	38894	+	912	DNA ligase, phage-associated	97	0	YP_002455980
59	39174	39425	+	252	Phage protein	100	2E-39	YP_002154190
60	39453	40115	-	663	Lytic enzyme	99	1E-159	YP_009124368
61	40115	40543	-	429	Phage protein	-	-	not available
62	40546	43440	-	2895	Phage tail fibers	-	-	not available
63	43445	44959	-	1515	Phage protein	-	-	not available
64	44956	46209	-	1254	Phage protein	-	-	not available
65	46266	46697	-	432	Phage baseplate	-	-	not available
66	46677	46916	+	240	hypothetical protein	-	-	not available
67	46987	47520	-	534	Phage protein	-	-	not available
68	47520	48383	-	864	Phage protein	-	-	not available
69	48383	50965	-	2583	Phage internal (core) protein	-	-	not available
70	50969	51397	-	429	Phage protein	-	-	not available
71	51407	52000	-	594	Phage tail fiber protein	-	-	not available
72	52009	52413	-	405	Phage protein	-	-	not available
73	52548	53051	-	504	Phage protein	-	-	not available
74	53061	53489	-	429	Phage protein	-	-	not available
75	53491	53841	-	351	Phage protein	-	-	not available
76	53838	54161	-	324	Phage protein	-	-	not available
77	54161	54613	-	453	Phage tail fiber protein	-	-	not available
78	54671	56185	-	1515	Phage protein	-	-	not available
79	56780	57331	-	552	Phage protein	-	-	not available
80	57339	57737	-	399	Phage protein	-	-	not available
81	57734	58201	-	468	Phage protein	100	1E-76	YP_001294442
82	58216	58653	-	438	Phage protein	100	4E-103	YP_001294441
83	58755	59903	-	1149	Phage capsid and scaffold	99	0	YP_001294440
84	59913	60548	-	636	Phage protein	99	6E-145	YP_002455953
85	60552	61979	-	1428	Phage protein	97	0E+00	YP_002455952
86	62492	62632	-	141	Phage protein	93	2E-19	YP_002455951
87	62629	62835	-	207	Phage protein	97	1E-38	YP_001294436
88	62855	63691	-	837	Phage minor capsid protein	98	0	YP_001294435
89	63691	65988	-	2298	Phage-related protein	99	0	YP_001294434

Table 3.17: General features of putative ORFs from *P. aeruginosa* phage DL62 with best matches in the NCBI database.

ORF	bp		Strand	Gene Length	Representative similarity to proteins in database	% Identity	E-value	Accession no.
	Start	Stop						
1	160	369	-	210	hypothetical protein	53	3	XP_005307517
2	577	861	+	285	hypothetical protein	-	-	not available
3	1769	2053	+	285	Phage protein	100	0	NP_877440
4	2053	2280	+	228	Phage protein	97	0	NP_877441
5	2291	2830	+	540	Phage protein	100	0	YP_001671945
6	2999	3118	+	120	Phage protein	97	0	AIK67566
7	3197	3565	+	369	Phage protein	100	0	YP_001671946
8	3552	3779	+	228	Phage protein	96	0	YP_009125704
9	3958	4131	+	174	Phage protein	72	0	YP_002117787
10	4131	4412	+	282	Phage protein	76	0	YP_008431317
11	4412	4672	+	261	Phage protein	60	0	YP_002727828
12	4674	4961	+	288	Phage protein	98	0	YP_001671951
13	5040	5459	+	420	Phage tail fibers	98	0	YP_001522798
14	5528	5887	+	360	Phage protein	100	0	YP_001671953
15	5890	6615	+	726	Phage DNA-binding protein	60	0	YP_001671954
16	6695	7114	+	420	Phage protein	96	0	YP_656507
17	7080	7427	+	348	Phage protein	97	0	YP_002117736
18	7417	7545	+	129	Phage protein	100	0	YP_001522803
19	7613	8437	+	825	DNA primase/helicase, phage-associated	99	0	YP_001671958
20	8406	9674	+	1269	DNA helicase, phage-associated	100	0	YP_009125717
21	9664	10275	+	612	Putative protein	-	-	not available
22	10275	10772	+	498	DNA ligase, phage-associated	-	-	not available
23	10793	11221	+	429	DNA ligase, phage-associated	-	-	not available
24	11224	11553	+	330	Phage protein	-	-	not available
25	11550	13976	+	2427	DNA polymerase I, phage-associated	-	-	not available
26	14032	15081	+	1050	Phage protein	-	-	not available
27	15081	16022	+	942	Phage protein	-	-	not available
28	16012	16452	+	441	Phage endonuclease	-	-	not available
29	16449	17495	+	1047	Phage exonuclease	-	-	not available
30	17505	17876	+	372	Phage protein	-	-	not available
31	17869	18219	+	351	Phage protein	-	-	not available
32	18228	20675	+	2448	Phage RNA polymerase	-	-	not available
33	20849	21100	+	252	Phage protein	-	-	not available
34	21100	21573	+	474	Putative protein	-	-	not available
35	21539	21814	+	276	Phage protein	-	-	not available
36	21826	23358	+	1533	Phage collar	-	-	not available
37	23362	24330	+	969	Phage capsid and scaffold	-	-	not available
38	24383	25390	+	1008	Phage capsid and scaffold	-	-	not available
39	25487	26041	+	555	Phage tail fibers	-	-	not available
40	26044	28524	+	2481	Phage tail fibers	-	-	not available
41	28524	29069	+	546	Phage internal (core) protein	99	0	AIK67602
42	29069	31765	+	2697	Phage baseplate hub; Phage lysozyme	100	0	YP_008431349
43	31769	35782	+	4014	Phage internal (core) protein	99	0	YP_009125740
44	35784	36539	+	756	Phage tail fibers	100	0	YP_001671983
45	36539	36997	+	459	Phage protein	99	0	YP_002117765
46	36990	37898	+	909	Phage protein	98	0	YP_009125743
47	37902	38507	+	606	Phage protein	100	0	YP_009125744
48	38507	38812	+	306	Phage protein	100	0	YP_001522834
49	38822	40627	+	1806	Phage terminase, large subunit (T7-like direct terminal repeats)	100	0	YP_009125746

50	40624	40824	+	201	Phage protein	98	0	NP_877483
51	40821	41303	+	483	Phage lysin	99	0	YP_008431358
52	41261	41590	+	330	Phage protein	98	0	YP_008431359
53	41565	41678	+	114	Phage protein	100	0	YP_009125750
54	41680	42093	+	414	Phage protein	98	0	YP_009125751
55	42112	42357	+	246	Phage protein	96	0	YP_001671994

Table 3.18: General features of putative ORFs from *P. aeruginosa* phage DL64 with best matches in the NCBI database.

ORF	bp		Strand	Gene Length	Representative similarity to proteins in database	% Identity	E-value	Accession no.
	Start	Stop						
1	71924	72355	-	432	hypothetical protein	98	2E-97	YP_003358483
2	71712	71924	-	213	hypothetical protein	99	1E-42	YP_009031858
3	71455	71715	-	261	hypothetical protein	67	4E-06	AIZ94839
4	71081	71347	-	267	hypothetical protein	66	6E-19	AFO70586
5	70216	70878	-	663	hypothetical protein	91	5E-132	AFO70587
6	69542	69796	-	255	hypothetical protein	99	4E-49	YP_003358398
7	68943	69134	-	192	hypothetical protein	100	4E-39	AIZ94844
8	68686	68928	-	243	hypothetical protein	90	2E-44	YP_003358400
9	68459	68689	-	231	hypothetical protein	99	1E-46	YP_003358401
10	68208	68459	-	252	hypothetical protein	96	3E-52	AIZ94847
11	67908	68204	-	297	hypothetical protein	93	2E-62	YP_003358403
12	67622	67924	-	303	hypothetical protein	88	5E-58	YP_003358404
13	67415	67618	-	204	hypothetical protein	93	2E-33	YP_003358405
14	67167	67385	-	219	hypothetical protein	97	8E-30	AFO70508
15	66937	67170	-	234	hypothetical protein	100	2E-44	AIZ94852
16	66719	66940	-	222	hypothetical protein	100	7E-43	YP_003358408
17	66462	66647	-	186	hypothetical protein	98	8E-35	YP_003358409
18	66080	66370	-	291	hypothetical protein	100	1E-60	YP_009031789
19	65560	65895	-	336	hypothetical protein	85	9E-58	AIZ94764
20	65159	65560	-	402	Phage protein	99	4E-94	AIZ94765
21	64908	65159	-	252	hypothetical protein	98	8E-52	AIZ94766
22	64468	64908	-	441	hypothetical protein	99	1E-103	AIZ94950
23	64081	64428	-	348	hypothetical protein	100	5E-80	AIZ94951
24	63137	64069	-	933	RNA polymerase, phage-associated	98	0	AFO70518
25	62864	63124	-	261	hypothetical protein	95	2E-52	AIZ94862
26	62258	62572	-	315	hypothetical protein	88	8E-61	AIZ94863
27	61953	62225	-	273	hypothetical protein	97	6E-43	AFO70520
28	60677	61918	-	1242	Phage protein	100	0	AIX13178
29	60427	60579	-	153	hypothetical protein	100	1E-27	AIZ94866
30	60130	60354	-	225	hypothetical protein	97	1E-16	YP_003358421
31	59500	60126	-	627	hypothetical protein	-	-	not available
32	58949	59503	-	555	hypothetical protein	-	-	not available
33	58368	58949	-	582	hypothetical protein	-	-	not available
34	57853	58368	-	516	hypothetical protein	-	-	not available
35	57632	57856	-	225	hypothetical protein	-	-	not available
36	57203	57388	-	186	hypothetical protein	-	-	not available
37	56342	57175	-	834	ATP-dependent Clp protease ATP-binding subunit ClpX	-	-	not available
38	56103	56345	-	243	hypothetical protein	-	-	not available
39	55001	56071	-	1071	Phage protein	-	-	not available
40	53243	54472	-	1230	hypothetical protein	-	-	not available
41	51987	53153	-	1167	RecD-like DNA helicase YrrC	-	-	not available
42	51460	51987	-	528	hypothetical protein	-	-	not available
43	48845	51460	-	2616	DNA polymerase I	-	-	not available
44	48624	48848	-	225	hypothetical protein	-	-	not available
45	48194	48664	-	471	dCMP deaminase, Late competence protein ComEB	-	-	not available
46	48022	48162	-	141	hypothetical protein	-	-	not available
47	47621	48019	-	399	hypothetical protein	-	-	not available
48	47433	47624	-	192	Phage protein	-	-	not available
49	44913	47429	-	2517	Phage rIIA lysis inhibitor	-	-	not available

50	43162	44901	-	1740	Phage lysis inhibitor # T4-like rIIA-rIIB membrane associated #T4 GC1698	-	-	not available
51	42890	43114	-	225	hypothetical protein	99	3E-24	AFO70543
52	42489	42689	-	201	hypothetical protein	98	3E-39	AFO70544
53	42248	42439	-	192	hypothetical protein	100	6E-37	YP_003358443
54	41701	42255	-	555	hypothetical protein	100	1E-132	YP_003358444
55	41126	41638	+	513	hypothetical protein	100	4E-106	YP_003358445
56	40605	41129	+	525	hypothetical protein	100	7E-124	YP_003358446
57	40366	40608	+	243	hypothetical protein	100	3E-48	YP_003358447
58	36838	40059	+	3222	Putative tail fiber protein	98	0	YP_003358449
59	36128	36799	+	672	hypothetical protein	99	2E-160	AIZ94804
60	35832	36131	+	300	hypothetical protein	97	1E-60	AFO70552
61	34522	35835	+	1314	Phage tail fiber protein	100	0	AIZ94898
62	33725	34153	-	429	hypothetical protein	100	1E-98	YP_003358454
63	33348	33635	-	288	hypothetical protein	99	1E-61	YP_003358455
64	32336	33346	-	1011	Phage protein	100	0	YP_003358456
65	30153	32321	-	2169	DNA primase, phage associated	100	0	AFO70557
66	29370	30104	-	735	Phage protein	100	0	AFO70558
67	28597	29343	-	747	Phage protein	100	2E-155	YP_003358459
68	28228	28455	-	228	hypothetical protein	97	1E-45	YP_003358460
69	27788	28231	-	444	Phage protein	100	1E-87	YP_003358461
70	27240	27800	-	561	hypothetical protein	100	9E-126	YP_003358462
71	26791	27228	-	438	hypothetical protein	-	-	not available
72	26329	26733	-	405	hypothetical protein	-	-	not available
73	25688	25924	-	237	hypothetical protein	-	-	not available
74	25374	25691	-	318	hypothetical protein	-	-	not available
75	25161	25364	-	204	hypothetical protein	-	-	not available
76	14949	25145	+	10197	Phage protein	-	-	not available
77	13383	14948	+	1566	hypothetical protein	-	-	not available
78	12916	13383	+	468	N4 gp52-like protein	-	-	not available
79	10713	12935	+	2223	Phage protein	-	-	not available
80	9880	10656	+	777	N4 gp54-like protein	-	-	not available
81	9022	9687	+	666	Phage protein	-	-	not available
82	7766	8965	+	1200	Phage protein	-	-	not available
83	6529	7731	+	1203	MJ0042 family finger-like protein	-	-	not available
84	6191	6529	+	339	hypothetical protein	-	-	not available
85	3941	6121	+	2181	Phage portal protein	-	-	not available
86	3487	3873	-	387	Deoxyuridine 5'-triphosphate nucleotidohydrolase	-	-	not available
87	3184	3483	-	300	hypothetical protein	-	-	not available
88	2418	3152	+	735	N4 gp67-like protein	-	-	not available
89	769	2421	+	1653	Phage protein	-	-	not available
90	44	772	+	729	N4 gp69-like protein	-	-	not available

Table 3.19: General features of putative ORFs from *P. aeruginosa* phage DL68 with best matches in the NCBI database.

ORF	bp		Strand	Gene Length	Representative similarity to proteins in database	% Identity	E-value	Accession no.
	Start	Stop						
1	66	467	+	402	Phage protein	100	0	YP_002364325
2	636	821	+	186	Phage protein	98	0	YP_002364324
3	818	1021	+	204	Phage protein	97	0	YP_007002562
4	1027	1338	+	312	Phage protein	100	0	YP_006200780
5	1587	1934	+	348	Phage protein	99	0	YP_002364322
6	1954	2454	+	501	Phage protein	100	0	YP_002364321
7	2557	3489	+	933	Phage protein	100	0	YP_002364320
8	3591	4178	+	588	Phage protein	82	0	YP_009009031
9	4195	4632	+	438	Phage protein	100	0	YP_006200775
10	4719	5498	+	780	Phage protein	100	0	YP_002364316
11	5501	5899	+	399	Phage protein	97	0	YP_002154151
12	5943	6293	+	351	Phage protein	99	0	YP_009124329
13	6293	6508	+	216	Phage protein	100	0	YP_002418812
14	6508	6891	+	384	Phage protein	99	0	YP_007002551
15	6928	8310	-	1383	Phage terminase, large subunit	100	0	YP_002418810
16	8315	8437	-	123	Phage protein	78	0	YP_002154146
17	8480	8770	+	291	hypothetical protein	-	-	not available
18	8800	8955	+	156	hypothetical protein	57	0	ERY56378
19	9011	9313	+	303	Phage protein	98	0	YP_002364309
20	9368	10054	+	687	Phage capsid and scaffold	99	0	YP_006200858
21	10057	10245	+	189	Phage protein	88	0	YP_006200857
22	10332	10583	+	252	Phage protein	100	0	YP_006200856
23	10580	10780	+	201	Phage protein	100	0	YP_002418895
24	10777	10992	+	216	Phage protein	99	0	YP_006200854
25	10989	11198	+	210	Phage protein	100	0	YP_002364393
26	11230	11874	+	645	Phage protein	100	0	YP_006200852
27	11875	12204	+	330	Phage protein	97	0	YP_002154316
28	12266	12490	+	225	Phage protein	97	0	YP_009124310
29	12544	12765	+	222	Phage protein	100	0	YP_002364388
30	12818	12946	+	129	Phage protein	98	0	YP_002364387
31	12980	13129	+	150	Phage protein	98	0	YP_002364387
32	13140	13835	+	696	Phage protein	100	0	YP_002364386
33	14025	14636	+	612	Phage protein	100	0	YP_002364385
34	14804	15373	-	570	Phage protein	100	0	YP_002364384
35	16337	18076	-	1740	DNA primase, phage associated	99	0	YP_009124396
36	18224	18409	-	186	Phage protein	100	0	YP_001294490
37	18415	19491	-	1077	Phage protein	100	0	YP_002364381
38	19488	19940	-	453	Phage protein	99	0	YP_002364380
39	19964	21268	-	1305	hypothetical protein	100	0	WP_023099019
40	21279	22064	-	786	Phage protein	100	0	YP_002364378
41	22233	22655	+	423	Phage protein	100	0	YP_001294485
42	22642	23829	+	1188	DNA helicase, phage-associated	100	0	YP_002418875
43	23991	24875	+	885	Phage protein	99	0	YP_002364375
44	24980	25981	+	1002	Phage protein	98	0	YP_002418873
45	26069	26299	+	231	Phage protein	100	0	YP_002364373
46	26299	26517	+	219	Phage protein	100	0	YP_002154206
47	26501	26719	+	219	Phage tail assembly protein	100	0	YP_002418870
48	26752	26982	+	231	Phage protein	100	0	YP_002418869
49	26990	27196	+	207	Phage protein	100	0	YP_002364369
50	27196	28113	+	918	Thymidylate synthase thyX	100	0	YP_006200825

51	28115	28306	+	192	Phage protein	100	0	YP_006200824
52	28309	29328	+	1020	3'-phosphatase, 5'-polynucleotide kinase, phage-associated	96	0	YP_007238211
53	29405	29959	+	555	Phage protein	100	0	YP_007002604
54	29959	33066	+	3108	DNA polymerase III alpha subunit	99	0	YP_006200821
55	33059	33469	+	411	Phage protein	100	0	YP_007002602
56	33466	35025	+	1560	DNA helicase, phage-associated	100	0	YP_002364362
57	35120	35740	+	621	Phage protein	100	0	YP_002154286
58	35829	36728	+	900	Phage protein	100	0	YP_006200817
59	36782	37387	+	606	Phage protein	100	0	YP_001294467
60	37384	37938	+	555	Phage DNA binding protein	99	0	YP_006200815
61	37993	38904	+	912	DNA ligase, phage-associated	100	0	YP_002154282
62	39184	39435	+	252	Phage protein	100	0	YP_002364356
63	39460	40122	-	663	Lytic enzyme	100	0	YP_006200812
64	40122	40550	-	429	Phage protein	99	0	YP_002154188
65	40552	43446	-	2895	Phage tail fibers	98	0	YP_009124366
66	43451	44965	-	1515	Phage protein	97	0	YP_006200809
67	44962	46215	-	1254	Phage protein	100	0	YP_009008971
68	46272	46835	-	564	Phage baseplate	99	0	YP_001294458
69	46993	47526	-	534	Phage protein	99	0	YP_002364349
70	47526	48389	-	864	Phage protein	100	0	YP_002154273
71	48389	50965	-	2577	Phage internal (core) protein	100	0	YP_002154272
72	50969	51397	-	429	Phage protein	100	0	YP_002154180
73	51407	52000	-	594	Phage tail fiber protein	100	0	YP_002154179
74	52009	52413	-	405	Phage protein	100	0	YP_002154269
75	52548	53051	-	504	Phage protein	100	0	YP_002418842
76	53061	53492	-	432	Phage protein	98	0	YP_002418841
77	53494	53844	-	351	Phage protein	100	0	YP_002154266
78	53841	54164	-	324	Phage protein	100	0	YP_002154265
79	54164	54616	-	453	Phage tail fiber protein	100	0	YP_002154264
80	54675	56189	-	1515	Phage protein	100	0	YP_007002577
81	56205	56729	-	525	Phage protein	100	0	YP_007238183
82	56783	57334	-	552	Phage protein	100	0	YP_002154170
83	57342	57530	-	189	Phage protein	100	0	YP_002364335
84	57737	58204	-	468	Phage protein	99	0	YP_002154168
85	58219	58656	-	438	Phage protein	100	0	YP_002154167
86	58758	59906	-	1149	Phage capsid and scaffold	100	0	YP_002364332
87	59916	60551	-	636	Phage protein	100	0	YP_002364331
88	60555	61988	-	1434	Phage protein	100	0	YP_002364330
89	62502	62642	-	141	Phage protein	100	0	YP_002418828
90	62639	62845	-	207	Phage protein	100	0	YP_002418827
91	62864	63700	-	837	Phage minor capsid protein	100	0	YP_002364327
92	63700	65997	-	2298	Phage-related protein	99	0	YP_002364326

Chapter Four:

ASSESSMENT OF PHAGE LYTIC ACTIVITY AND BIOFILM REMOVAL

4.1. Chapter summary

This chapter focuses on the efficacy assessment of the phage cocktails, isolated and characterised in the previous chapter, against *P. aeruginosa* and *S. aureus* bacterial strains on three *in vitro* models. Planktonic growth bacterial cultures were the first model where the phage efficacy was tested. The strains used for the planktonic growth represent clinical strains that frequently caused formation of biofilms, strongly related to infection initiation and maintenance. Firstly, an *in vitro* static model for biofilm production was evaluated and the phage efficacy tested. Finally, efficacy was assessed on an *in vitro* biofilm flow model, where implementation and optimisation of the system were executed. The different models performed represented, in a progressive fashion, a closer scenario to what is observed in nature when an infection occurs. Part of the biofilm work presented for *S. aureus* have been published in a scientific journal (244).

4.2. Background

Following isolation and characterisation of lytic phages, the next logical step is the analysis of their lytic performance when growing with the target bacterial strains. Commonly, phages are introduced into planktonic bacterial cultures and their growth is evaluated throughout a pre-determined period of time. This allows a monitoring of the phage efficacy and evaluates how frequently bacterial cells are able to counteract the presence of the phage by emergence of bacterial phage resistant mutants. The latter, can often be delayed by including a cocktail of phages, allowing the optimisation of the best combination of phages to tackle the bacteria of interest.

Several studies documenting phage isolation and their evaluation on planktonic bacterial cultures can be found in the literature. However, evaluation of the phage lytic activity against planktonic cultures only is, to some extent, a very limited approach. As

discussed in Chapter One, bacterial biofilm communities are the rule rather than the exception and likewise, bacterial infections, especially wound infections, get initiated by the formation of a biofilm. Within a biofilm, bacterial cells behaviour is switched and they are strongly protected from the external environment. For that reason, the outcome when phage are infecting bacteria in a broth culture it is often different to the one observed when infecting the same strain when growing as a biofilm. Cerca and colleagues (238) showed that phage K was able to reduce a planktonic culture of *S. epidermidis* in a period of two hours, however for biofilm it was only possible to observe a reduction in biomass 24 hours after infection. This is mainly due to the presence of the protective and cell aggregating *S. epidermidis* extracellular polysaccharide, poly-*N*-acetylglucosamine (PNAG) expressed by the cells in the biofilm, but also to the low metabolic activity of biofilm cells. Therefore, to more accurately reflect their potential *in vivo*, when assessing the lytic effect of phage it is recommended to study this in biofilm models of infection.

To understand the crucial role that biofilms have in nature, in the hospital, in the industry and the environment, several *in vitro* models for biofilm formation have been developed over the years and each one of them is allied with certain advantages and of course limitations (for review see 308). Although in many instances these systems lack versatility and are difficult to set up they remain a powerful tool for studying factors that affect biofilm formation. In this study we have employed two biofilm models to study biofilm reduction and dispersion by phage attack. *In vitro* biofilm models can be subdivided into closed and open systems, such as the microtitre plate model and the Robbins device, respectively. Microtitre plate based systems might be the most widespread used model for studying biofilms (308). In this closed system biofilms are formed on the bottom and the walls of a microtitre plate and are ideal systems for screening purposes, where multiple parameters are able to be studied, protocols are straightforward and small volumes of reagents are employed. For results assessment,

evaluation of biofilm biomass by crystal violet assay and microbial physiology activity by XTT or resazurin assay can be easily performed.

The Robbins device, developed by Jim Robbins at the University of Calgary and later modified by McCoy and colleagues (309) and called The Modified Robbins Device (MRD), is one of the classical models employed for the study of biofilms (310). It consists of a device that contains multiple individual ports placed in a linear fashion with each port holding a plug. On the bottom of each plug, a disk can be found that is in contact with the lumen of the device. Media and cells are passed through the device entering in contact with to the disks and biofilms are formed. Often, Robbins devices are coupled to a chemostat so that bacterial cells growing at a defined growth rate and nutrient conditions are used as feeding inoculum for the formation of a biofilm (311). It has been widely used to study oral biofilms (312) and used as "artificial throat" for the study of biofilm formation on laryngeal shunt prostheses (313).

Table 4.1: Description of the main advantages and disadvantages of the *in vitro* biofilm model systems used in the assessment of phage lytic and dispersal activity.

Biofilm device	Advantages	Disadvantages	Reference
Microtitre plate	• High throughput. • Cheap. • Allows testing of different parameters and materials.	• Direct observation of wells under a microscope is difficult. • Operates in a closed system.	(314)
Modified Robbins device	• Precise hydrodynamic conditions. • Operates at continuous culture conditions.	• Low throughput. • Time consuming.	(310)

4.3. Methods

4.3.1. Optimisation and setup of the *in vitro* biofilm model using the Modified Robbins Device

4.3.1.1. Continuous-culture

Continuous culture is an approach that provides us the possibility to study bacteria under conditions that more closely resemble the manner they grow in nature. The basis of the chemostat approach was first described by Monod (315). Hence, when assuming steady-state conditions, the bacterial culture grows at a constant rate (parameters, such as cell number, volume and temperature are kept constant) and the dilution rate (*D*) equals the specific growth rate (*μ*) of the organism. Consequently, the bacterial growth stage can be easily manipulated and provide a system with defined growth rates and constant nutrient conditions for biofilm formation over time that will more closely resemble the situation in human bacterial infections.

In a continuous culture bacterial growth occurs in an equilibrium fashion, where the influx of the fresh medium that allows production of new biomass is compensated by the efflux of waste medium, which is a mixture of living cells and cell debris.

The rate of medium flow (*F*) into the chemostat is related to its volume (*V*) and is defined by the dilution rate (*D*):

$$D = \frac{F}{V} \qquad (4.1)$$

The change in biomass (x) over time during the steady state growth is expressed as:

$$\frac{dx}{dt} = \mu x - Dx \quad (4.2)$$

However, under the steady state the biomass concentration is kept constant:

$$\frac{dx}{dt} = 0, \text{hence } \mu x - Dx = 0 \text{ or } \mu = D \quad (4.3)$$

Hence, the growth rate can be manipulated as a function of the dilution rate:

$$Rate\ of\ biomass\ accumulation = Rate\ of\ biomass\ production - Rate\ of\ biomass\ loss \quad (4.4)$$

The rate of accumulation is expressed as the derivative of the concentration of biomass, with respect to time (*t*), multiplied by the volume of the reactor:

$$Rate\ of\ biomass\ accumulation = V.\frac{d[biomass]}{dt} \quad (4.5)$$

The rate of biomass loss is equal to the outlet flow rate (*F*) multiplied by the concentration of biomass

$$Rate\ of\ biomass\ loss = F.[biomass] \quad (4.6)$$

The rate of biomass production can be expressed by the logistic curve of growth, where the growth parameters are bacterial specific growth rate (*a*, h^{-1}) and the carrying

capacity (*k*), defined as the maximum number of bacteria that is reached in the stationary phase, all multiplied by the volume to obtain the correct units:

$$Rate\ of\ biomass\ production = V.a.[biomass].\left(1 - \frac{[biomass]}{k}\right) \quad (4.7)$$

Putting all the parameters together and replacing equation 4.4:

$$V.\frac{d[biomass]}{dt} = V.a.[biomass].\left(1 - \frac{[biomass]}{k}\right) - F.[biomass] \quad (4.8)$$

Divided by the volume

$$\frac{d[biomass]}{dt} = a.[biomass]\left(1 - \frac{[biomass]}{k}\right) - D.[biomass] \quad (4.9)$$

$$D = a.\left(1 - \frac{[biomass]}{k}\right) \quad (4.10)$$

In order to calculate the growth parameters, the bacterial growth curve should be fitted to a logistic curve that describes the sigmoidal growth curve of the bacterial. Figure 4.1 shows the fitting of the planktonic bacterial growth of both S*. aureus* 15981 and *P. aeruginosa* PAO1 to the sigmoidal logistic function and the growth parameters. The specific growth rate of both strains was very similar (S*. aureus* 15981 = 0.49; *P. aeruginosa* PAO1 = 0.51) and hence a dilution rate of 0.1 h^{-1} was selected to perform both chemostat cultures and the growth was slow and close to achieve the stationary-

phase. Before starting the flow system, the pumps (Ismatec, UK) were calibrated in order to obtain the desired flow rate.

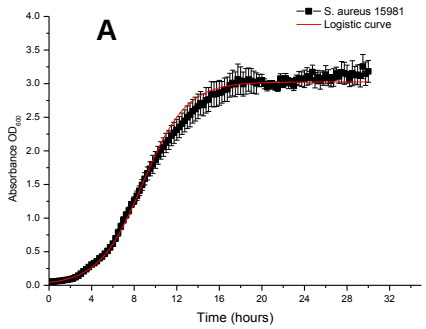

Equation	y = a/(1 + b*exp(-k*x))	
Adj. R-Square	0.99756	
Value		Standard Error
a	0.48648	0.00452
k	3.02571	0.01449

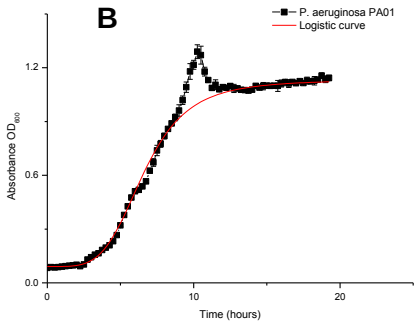

Equation	y = a/(1 + b*exp(-k*x))	
Adj. R-Square	0.99477	
Value		Standard Error
a	0.51341	0.01923
k	1.11965	0.00907

Figure 4.1: Bacterial planktonic growth fitting of (A) *S. aureus* 15981 and (B) *P. aeruginosa* PAO1 to the sigmoidal logistic curve. The sigmoidal logistic curve equation is indicated and the parameter *a* and *k*, for calculation of the dilution rate are also indicated.

4.3.1.2. Chemostat setup

A chemostat system was used to generate a continuous bacterial culture in order to provide inoculum for use in the Modified Robbins Device (MRD) as described by Jass and colleagues (311) with some modifications regarding the equipment and facilities available. The chemostat vessel consisted of a 500 ml glass double wall vessel (Tyler Research Corporation, Canada) agitated at 300 rpm with a polysulfone cap provided with fittings for tubing. For monitoring the temperature (37 °C±0.2) a standard temperature probe was fitted to the polysulfone cap and for pH (7.0±0.1) the monitoring was performed indirectly, by taking hourly samples and monitoring pH. All the fittings

added (tubing and temperature probe) were carefully insulated with Blu-Tack in order to avoid contamination from the outside. A 10 ml sample of an overnight culture with 10^8 cfu/ml was used to inoculate 500 ml of sterile half strength nutrient broth (TSB or LB) within the chemostat. Following inoculation, the stirred chemostat was operated as a batch culture for four hours to allow the establishment of the culture. The medium volume inside the chemostat was maintained at 500 ml and perfused with sterile growth medium at a certain dilution rate (Figure 4.2), determined in the previous section for the bacteria being studied. The chemostat was run over 48 hours for the culture to achieve the steady-state, meaning a constant population size of $3.01x10^7$ cfu/ml for *S. aureus* 15981 and $3.62 x10^7$ cfu/ml for *P. aeruginosa* PAO1.

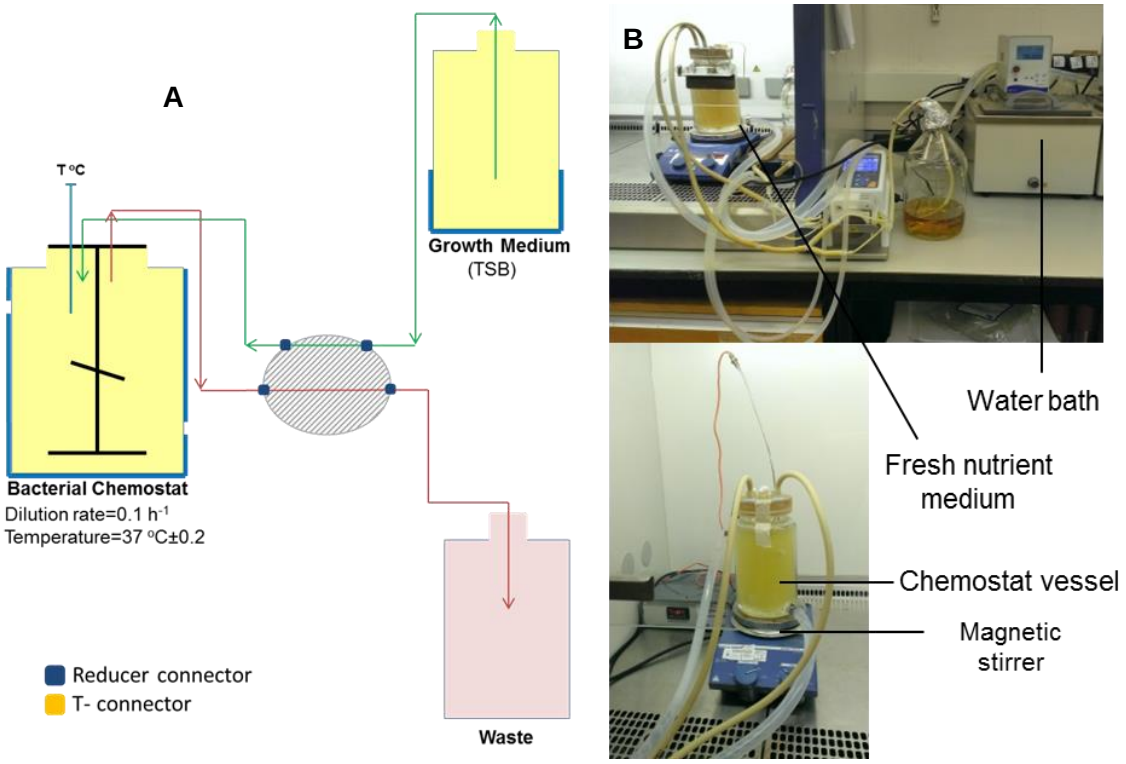

Figure 4.2: A – Diagram of the chemostat setup. Green lines represent the inlet tubing and red lines represent the outlet tubing. B – Images showing the chemostat system running.

4.3.1.3. Biofilm formation on the Robbins Device.

A Robbins device was used to study biofilm formation. The device provided quantifiable samples of biofilm that were monitored over time. It consists of hollow rectangular stainless steel tubes with 12 evenly spaced sampling ports. Each port allowed the insertion of a sampling stud that contained a stainless steel disk that lay flush to the inner surface of the lumen being subjected to the flow media and bacteria (Figure 4.3). Every stud was dipped into a sterile solution of mucin (100 µg/ml) to improve attachment of bacterial cells (316). The MRD was fitted into a thermal liquid regulated container (Tyler Research Corporation, Canada) that maintained the internal lumen temperature at 37 ^{o}C.

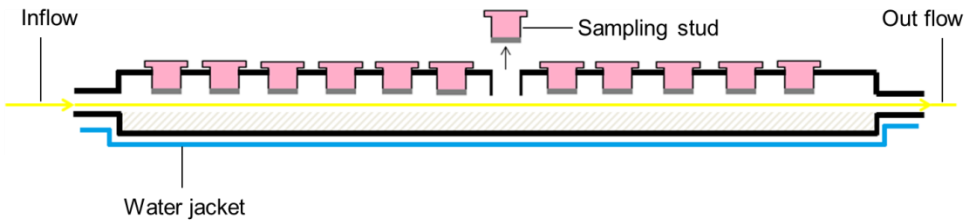

Figure 4.3: Diagram of the Robbins device. The stainless steel tube has 12 sampling ports that can easily be removed by pulling them up. The device is kept in a thermal liquid regulated container (blue line) and the nutrient media flows across the lumen of the device (yellow line), entering into contact with the surface of the studs.

Culture growing under steady-state was pumped through the MRD, via the effluent tubing (flow rate = 250 µl/min) of the chemostat and biofilms were allowed to develop on the surface of the stainless steel disks (Figure 4.4) exposed to the culture for 24 hours. Over this period the culture feed was replaced by fresh half strength media supplemented with 0.1 % D-(+)-glucose (TSBg or LBg) for another 24 hours. At this time point, biofilms had been growing for 48 hours and fresh media feeding was paused in order to inoculate into the system 10 ml (10^{7} pfu/ml) of phage in an oil-in-water nano-emulsion suspension and the control. Such emulsion was used to promote

the lytic activity of the phage particles, as they provide a more stable environment for adsorption to the cells to occur (299). Once the suspension was inside the MRD, which time taken was estimated by calculating the velocity (min) of the suspension according to equation (14), the inlet and outlet tubing of the MRD were clamped for a period of 20 min and phages were allowed to adsorb to the bacteria in the biofilms.

$$Flow\ rate = Velocity.tubing\ area \tag{4.11}$$

One hour later the inlet and outlet tubing of the MRD were clamped again and four random studs were removed in order to sample the biofilm communities formed. The removed studs were replaced with new sterile studs. The stainless steel disks were unscrewed from the studs and then three were processed for viable bacterial and phage counts and the fourth was prepared for analysis in the confocal laser scanning microscope (CLSM), which theoretical background and sample preparation have been previously described in Chapter Two, Section 2.10.2.2. Studs were removed from the MRD at predetermined time intervals: 0, 24 and 48 hours. Figure 4.5 and 4.6 show a diagram and images of the model system setup.

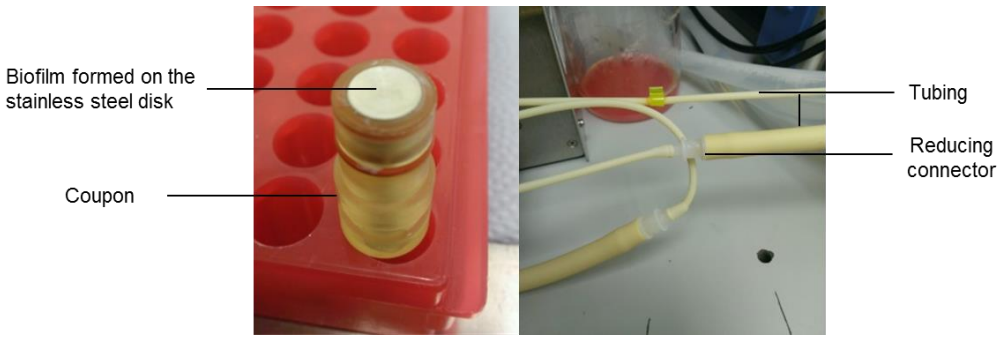

Figure 4.4: Left - Image showing a stud upside down, where a biofilm can be observed grown on the surface of the stainless steel disk. Right – Image showing the different types of connectors used to link all the tubing system.

4.3.1.4. Bacteria and phage viable counts on MRD disks

Disks were carefully detached using tweezers from the stud and rinsed twice by dipping the disk in 1 ml in of PBS to remove planktonic and loosely adherent cells. The disk was placed in 1 ml PBS contained in 1 ml centrifuge tube and sonicated for 6 min (60W) before vortexing for 2 min to ensure complete detachment of the biofilm from the disk. For enumeration of viable bacterial cells, serial dilutions were performed in FAS virucide, and numbers determined using the method previously described in Chapter Two, Section 2.11.6. For enumeration of phages present in the biofilm, 100 µl of the disrupted biofilm suspension was used to perform serial dilutions and titration was performed by using the method previously described in Chapter Two, Section 2.2.5.

All the manipulation was performed inside a flow cabinet to prevent introduction of contamination. The flow system was connected through a long life thermoplastic Marprene tubing (Watson Marlow, UK), where a three port tubing of 0.89 mm in diameter was used for the pump and 6.4 mm in diameter for the rest of the tubing.

4.3.1.5. Cleaning and sterilisation of the system

For cleaning the system, a 1 % Helmanex III solution was passed through the system for 2 hours under flow rate of 2 ml/min. Following this time period the flow was reduced to 500 µl/min and it was left overnight, approximately 18 hours. On the following day, distilled water was passed through the system which was left to dry overnight at 50 °C. Prior to the experiment, tubing, equipment and connectors (Figure 4.4) were autoclaved in autoclaving wrap bags (Westfield Medical, UK) to ensure that the system would be sterile.

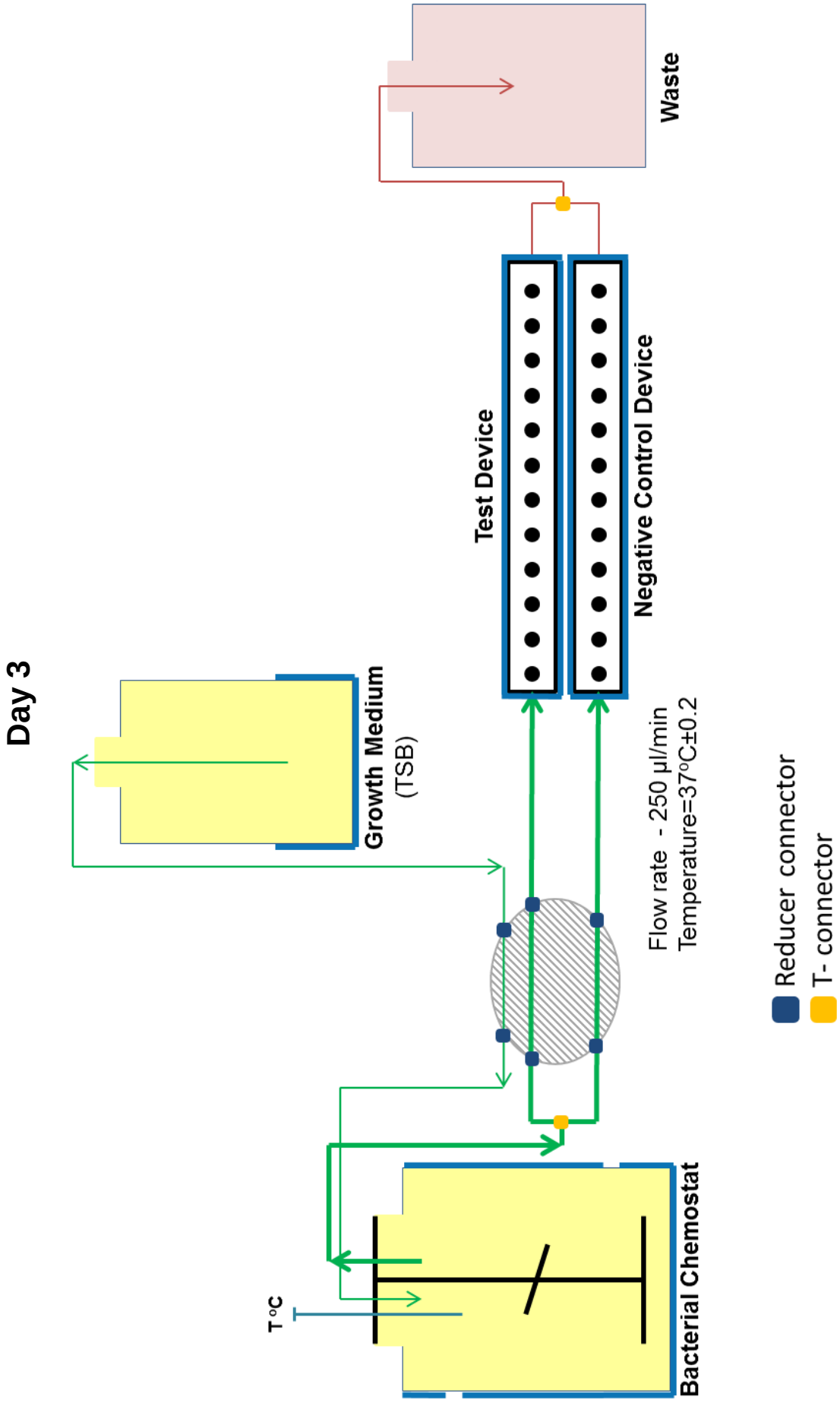
Day 3
Waste
Test Device
Negative Control Device
Growth Medium
(TSB)
Flow rate - 250 µl/min
Temperature=37°C±0.2
Reducer connector
T- connector
T °C
Bacterial Chemostat

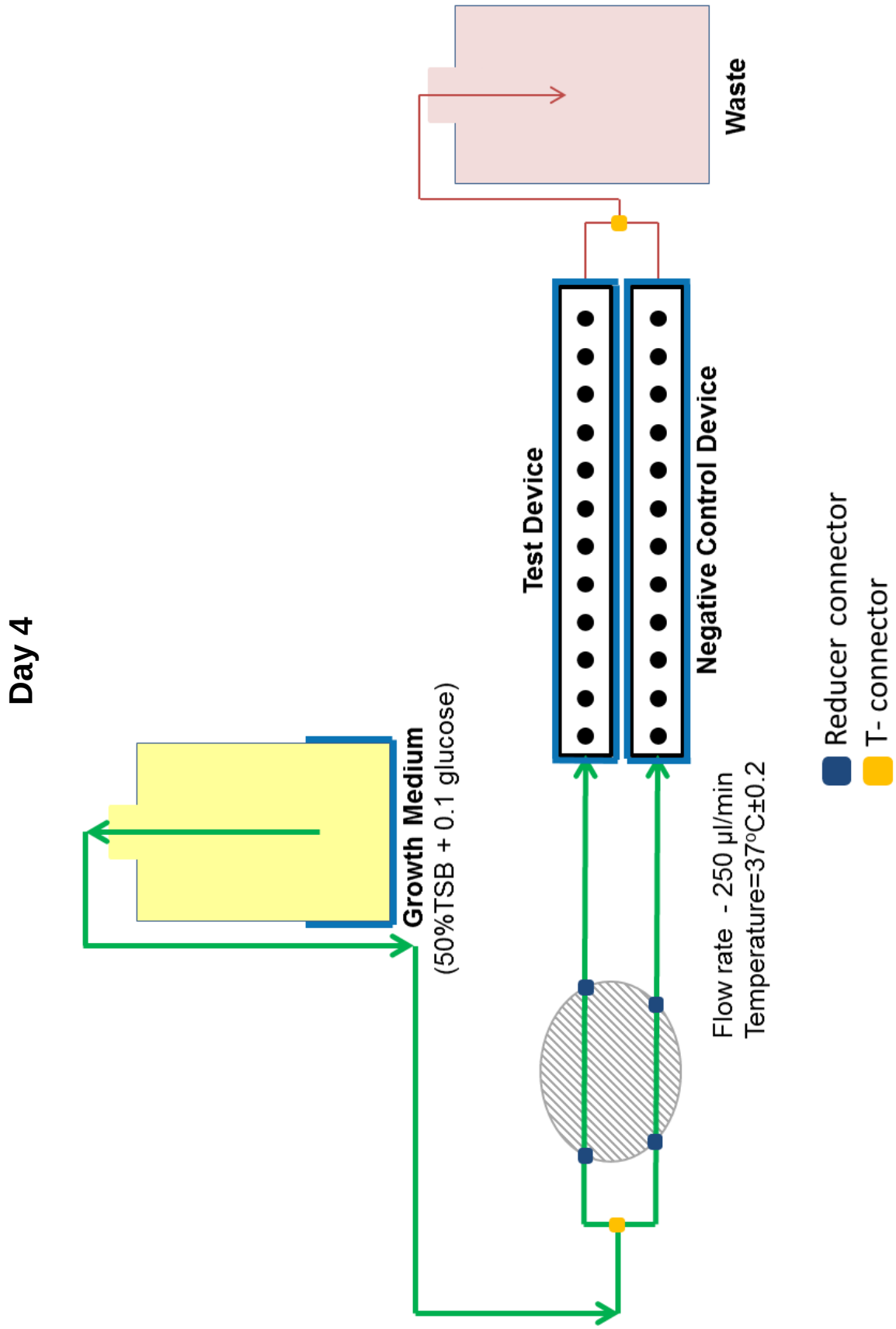
Day 4
Waste
Test Device
Negative Control Device
Growth Medium
(50%TSB + 0.1 glucose)
Flow rate - 250 µl/min
Temperature=37°C±0.2
Reducer connector
T- connector

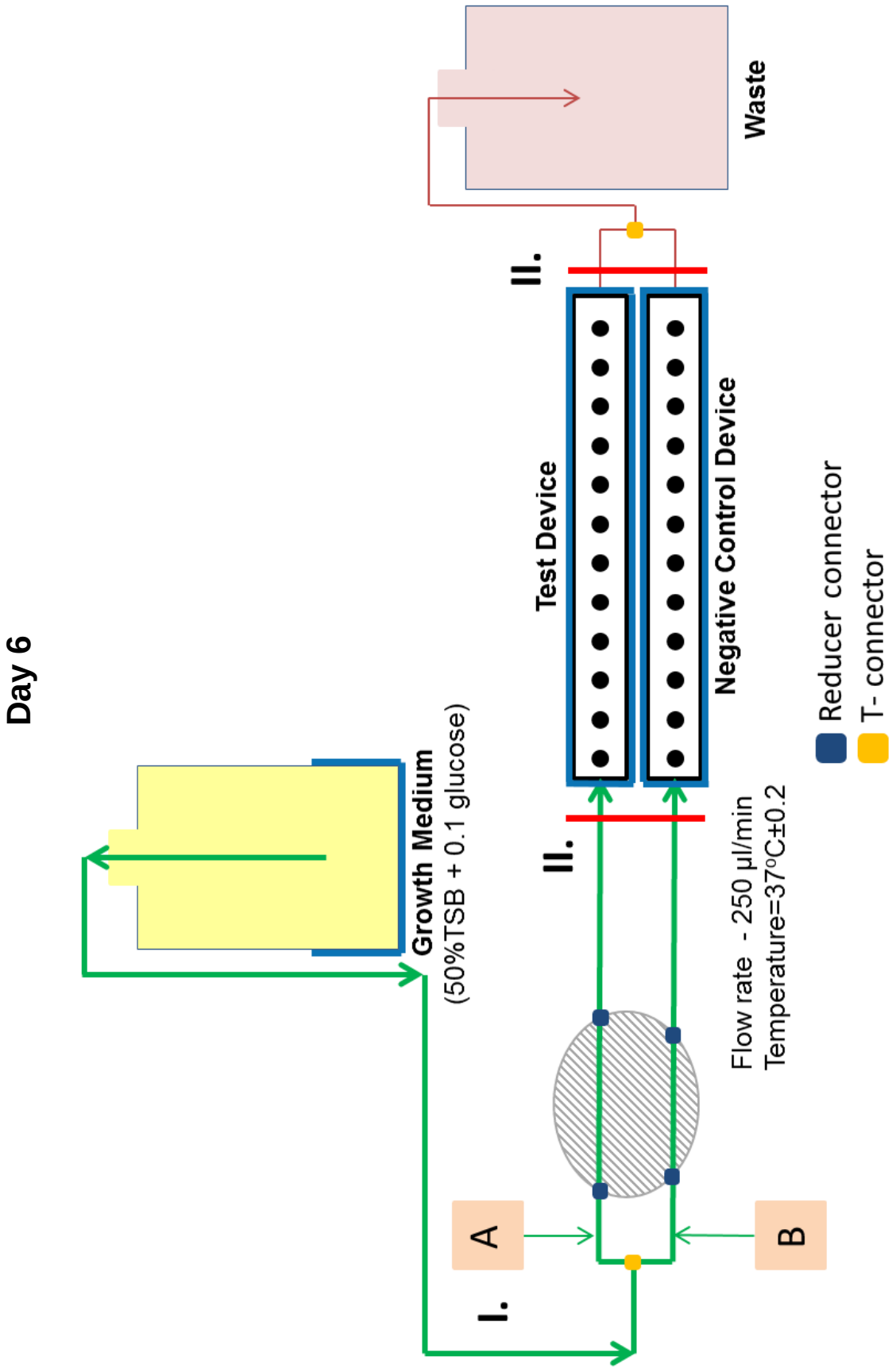
Day 6
Waste
II.
Test Device
Negative Control Device
Reducer connector
T- connector
Growth Medium
(50%TSB + 0.1 glucose)
II.
Flow rate - 250 µl/min
Temperature=37°C±0.2
A
B
I.

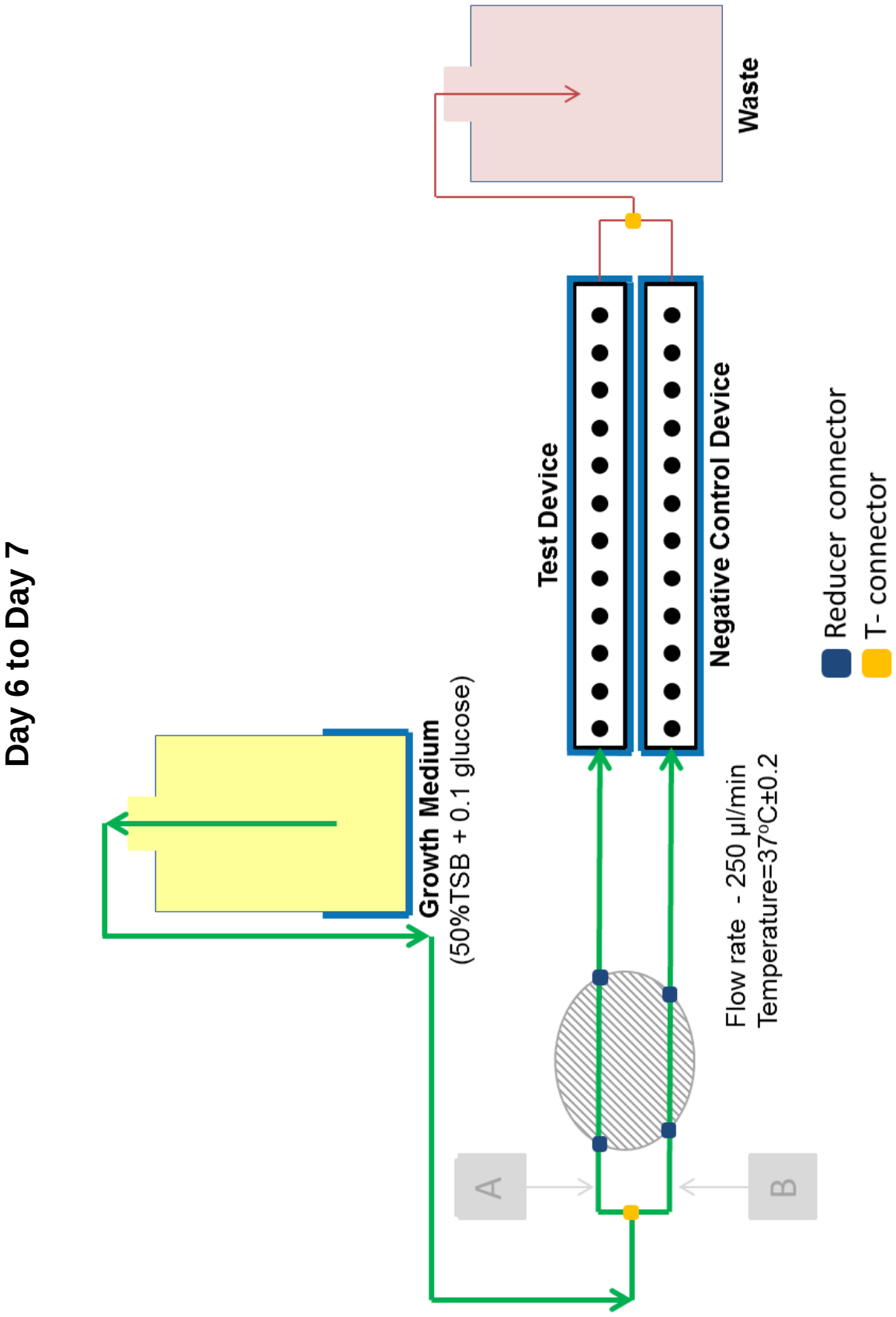
Day 6 to Day 7
Waste
Test Device
Negative Control Device
Reducer connector
T- connector
Growth Medium
(50%TSB + 0.1 glucose)
Flow rate - 250 µl/min
Temperature=37°C±0.2
A
B

Figure 4.5: The above pages show a diagram of the Robbins Device system for biofilm production and phage treatment. Green lines represent the inlet tubing and red lines represent the outlet tubing. Blue lines represent the temperature regulated devices. On day 5 the treatment was performed. Inoculation of the phage (A) and control (B) suspensions. I and II represent the inlet and outlet clamping for 20 min for phage adsorption.

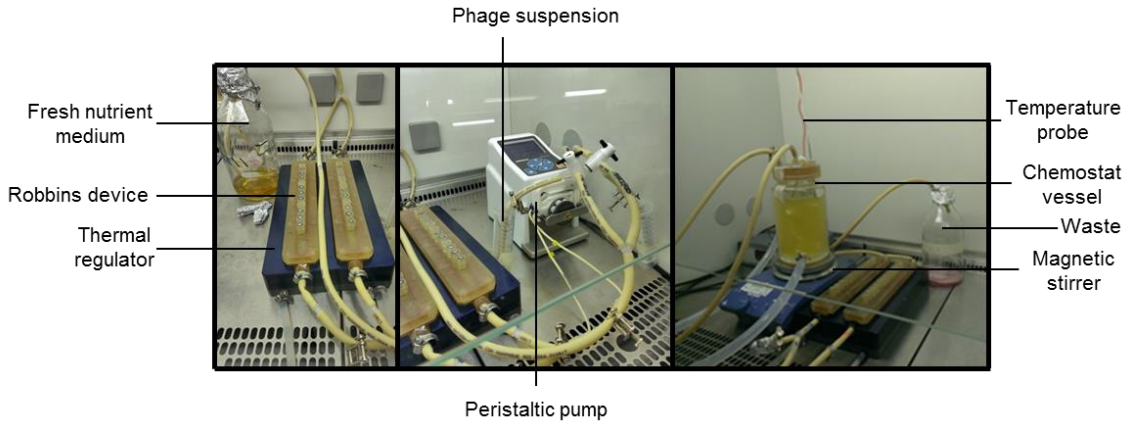

Figure 4.6: Images of the Robbins device biofilm model system running.

4.4. Results

4.4.1. Selection of phage cocktail

In order to select bacterial isolates prone to form thick biofilms that could after be used to test the *S. aureus*-phage mixture efficacy, a collection of isolates (listed previously in Table 3.3 from Chapter Three) was screened. 48 hour-old biofilms were grown and stained with crystal violet for biomass assessment (Figure 4.7). Isolate 15981 was used as a control as its ability to produce biofilm has been used in other studies documented in the literature (317). Surprisingly, all the isolates tested showed a good biofilm formation. Some of the strains, such as HT20020635, HT20040991 and Mu3, despite the strong biofilm produced, were rejected for further biofilm work because all phages from the cocktail were not able to infect them. In order to test the phage cocktail both in antibiotic sensitive and resistant strains, the MSSA isolate 15981 and two MRSA isolates MRSA252 and H325 were selected for further studies.

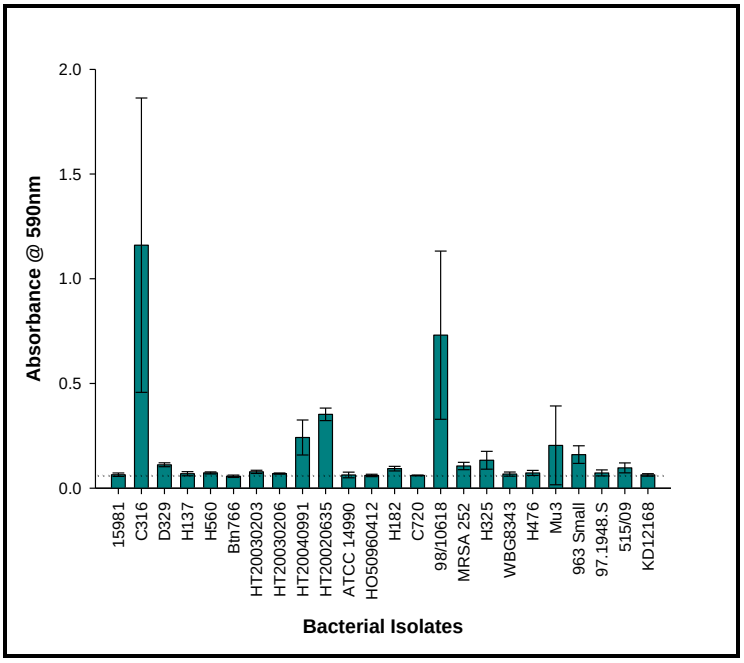

Figure 4.7: Biofilm forming ability screening (Crystal violet stain). A 48-hour biofilm was performed for each of the 23 isolates and 15981 was the positive control. All experiments were performed four times. Dotted line represents the results obtained with the biofilm producing strain 15981 (positive control) and error bars indicate the mean ± standard deviation.

The selection of the phage cocktail against *S. aureus* isolates included the assessment of the isolated phages when growing together with the bacterial isolates under planktonic growth conditions. Phage K and DRA88 showed to be the only phages where bacterial growth inhibition was observed, at least in the first 18 hours of incubation and were selected. The mutant cells observed for phage DRA88 when treating MRSA 252 (Figure 4.9B) were recovered and another screening was performed in order to find a phage that would infect these mutant cells and improve the performance of the cocktail. Figure 4.8 shows that phage DRA288 was the only phage able to infect these mutant cells. However, due to contamination issues described in Chapter Three, Section 3.3.1.4.1, phage DRA288 had to be removed from the cocktail.

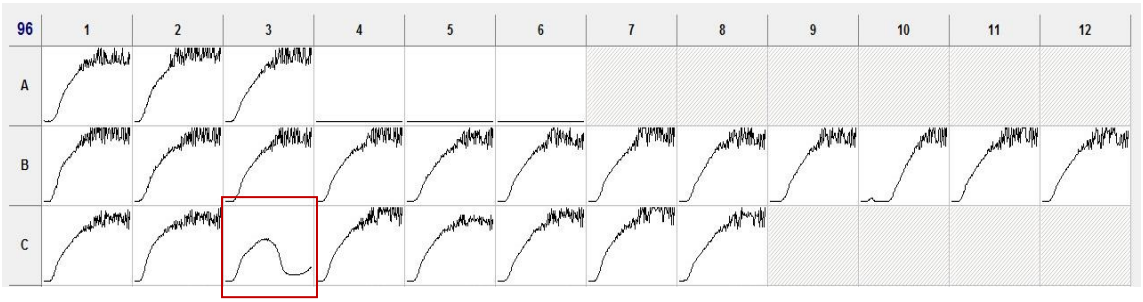

Figure 4.8: Phage sensitivity screening for MRSA 252 resistant mutant of DRA88 in a 96-well microplate over 24 hours. Assays were performed in a plate reader and OD_{590} was read over time. *A1 – A3*: positive control; *A4 – A6*: negative control. Resistant mutant growing with *B1* – DRA145; *B2* – DRA147; *B3* – DRA189; *B4* – DRA226; *B5* – DRA278; *B6* – DRA279; *B7* – DRA280; *B8* – DRA281; *B9* – DRA282; *B10* – DRA283; *B11* – DRA284; *B12* – DRA285; *C1* – DRA286; *C2* – DRA287; *C3* – DRA288 (□); *C4* – DRA289; *C5* – DRA290; *C6* – DRA291; *C7* – DRA292; *C8* – DRAE2260.

4.4.2. Phage lytic assessment in planktonic bacterial cultures

4.4.2.1. *S. aureus* phage cocktail assessment in broth bacterial cultures

The efficacy of single phage DRA88 and phage K and their combination into a phage cocktail was assessed when treating bacterial broth cultures. Suspensions from single and combined phages at a multiplicity of infection (MOI) of 0.1 were introduced to the bacterial culture that had been growing for two hours under planktonic conditions and this was allowed to grow for 22 hours further (Figure 4.9). In general, use of single phage treatment resulted in less success that when phages were combined. This was clearly observed for *S. aureus* isolate 15981. For all three *S. aureus* bacterial cultures – 15981, MRSA 252 and H325 – treated with the phage mixture, cell growth was not observed when compared to the bacteria not treated. Actually, an efficient inhibition and prevention of bacterial growth can be observed for both 15981 and H325. However, the same was not observed for the MRSA 252 isolate, where bacterial growth occurred following 18 hours of treatment (time point = 20 hours).

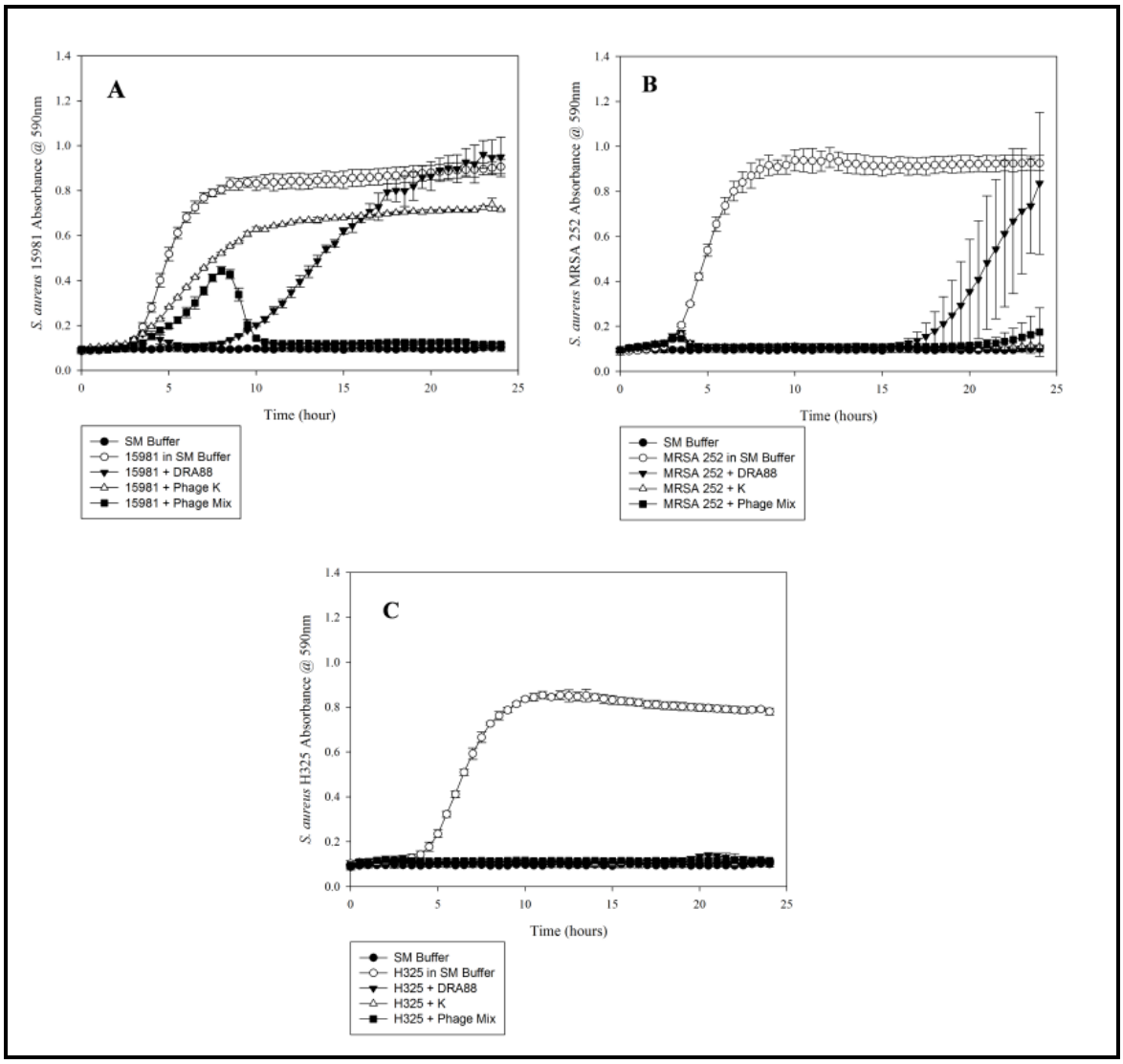

Figure 4.9: Dynamic of *S. aureus* bacteria with single phage and phage mixture in liquid cultures over 24 hours of incubation at 37°C. Absorbance readings at 590 nm were taken in a microtitre plate reader. *S. aureus* isolates 15981 (A), MRSA 252 (B), and H325 (C) growing with only SM buffer (○), with single DRA88 (▼), with single phage K (Δ), and with the phage mixture in SM buffer (■) and also a negative-control SM-only buffer (●) are shown in the figure. Assays were performed three times, and OD_{590} was expressed as the mean ± standard deviation. Reprinted from reference (244) and used with permission.

4.4.2.2. *P. aeruginosa* phage cocktail assessment in broth bacterial cultures

The efficacy of each of the single six phages and their combination into a cocktail was assessed when treating a bacterial broth culture of *P. aeruginosa* PAO1. Suspensions containing the phages were prepared to achieve a MOI of 0.1 in the culture and introduced after 2 hours of incubation of the latter. Growth continued for a further 22 hours. Figure 4.10 shows that for all single phage suspensions it was observed that eventually there was a regrowth of the PAO1 culture between 8 hours and 13 hours after phage treatment (time points: 10 h – 15 h). On the other hand, by using the suspension of the phage cocktail no regrowth and a full inhibition of the bacterial culture was observed when compared to the bacteria growing without phage.

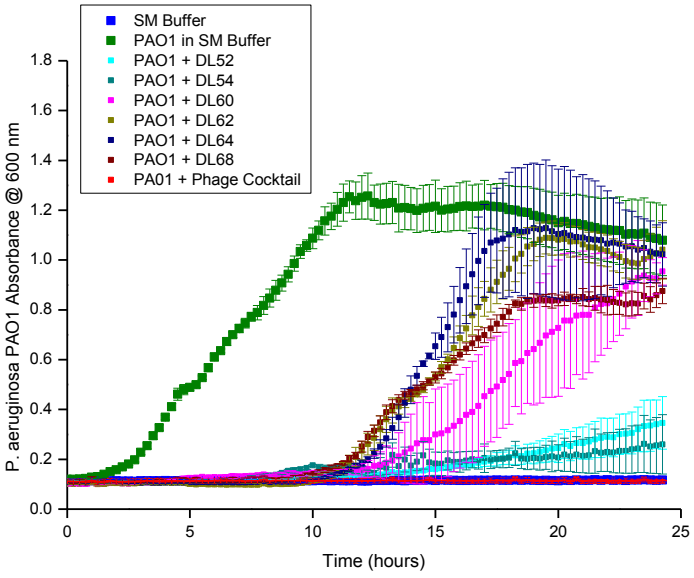

Figure 4.10: Dynamic of *P. aeruginosa* PAO1 bacteria with single phage and phage cocktail in liquid cultures over 24 hours of incubation at 37°C. Absorbance readings at 600 nm were taken in a microtitre plate reader. *P. aeruginosa* PAO1 isolate growing with only SM buffer (■), with single DL52 (■), DL54 (■), DL60 (■), DL62 (■), DL64 (■) DL68 (■) and with the phage cocktail in SM buffer (■) and also a negative-control SM-only buffer (■) are shown in the figure. Assays were performed three times, and OD_{600} was expressed as the mean ± standard deviation.

4.4.2.3. Bacterial mutants'

The efficacy of the phage cocktail regarding its concentration and the time point when applied to a bacterial broth culture of *P. aeruginosa* PAO1 was assessed. Phage suspensions were prepared to achieve MOIs ranging from 0.01 to 100 of phage to bacteria. The bacterial broth cultures were phage treated at 0 hours, 2 hours and 4 hours of incubation time and growth continued for further 22 hours. Figure 4.11 shows that the bacterial culture where the phage cocktail was added at the start of the incubation time, only MOI 100 and 10 resulted in bacterial growth inhibition, lower MOIs resulted in bacterial regrowth (time point = 15 hours).

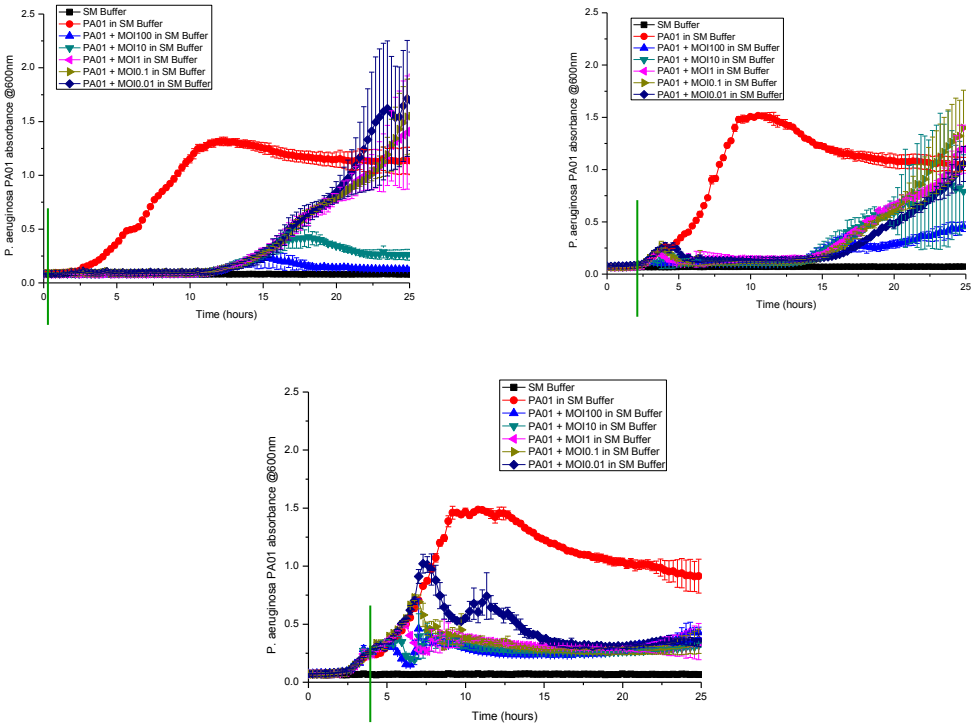

Figure 4.11: Dynamic of *P. aeruginosa* PAO1 bacteria with phage cocktail at different MOIs and added at different time points to the liquid cultures over 24 hours of incubation at 37°C. Green line indicates when the phages were added, 0, 2 or 4 hours. Absorbance readings at 600 nm were taken in a microtitre plate reader. Assays were performed three times, and OD_{600} was expressed as the mean ± standard deviation

When the phage cocktail was added 2 hours after incubation all MOIs resulted in bacterial regrowth (time point = 15 hours), where MOI 100 shown to slow down this regrowth. For the bacterial suspension treated 4 hours after incubation a more successful inhibition of the bacterial regrowth by the cocktail was observed for all MOIs, although complete elimination of the bacteria was not observed during the incubation time assayed.

4.4.3. Phage lytic assessment on an *in vitro* biofilm model (closed system)

4.4.3.1. *S. aureus* biofilm eradication

For this experiment 48 hour-old biofilms produced by three *S. aureus* isolates were established in 96-well microtitre plates. Although all isolates were strong biofilm producers, MRSA 252 and H325 isolates produced biofilms with more fragile structures when compared to isolate 15981. This could be observed when performing the mechanical washing steps as these biofilms were more susceptible to disruption. The established biofilms were treated with either single or combined phage suspensions at an MOI of 10 and the biofilm was assessed by crystal violet staining and intensity measured in a plate reader at OD_{600} (Figure 4.12 and 4.14). Results showed a clear reduction following phage inoculation compared to the non-phage inoculated wells ($P < 0.05$). A decrease in biofilm biomass from the mixture compared with the single phages after 48 hours of treatment was observed for all cases; although this reduction was not significant, it could be easily observed by eye (along with the CV stained wells). Established biofilms were also treated only with the phage combination, but this time employing two different MOIs, 1 and 10, and the biofilm biomass was assessed at the time points 0, 2, 4, 24 and 48 hours (Figure 4.13). For *S. aureus* 15981 biofilms treated with a MOI of 10, at 4 hours after phage inoculation, there were already 50 % biofilm

biomass reduction ($P < 0.05$). After 48 hours of treatment, the biomass of the biofilm was almost completely disrupted (MOI of 10, P = 4.82×10^{-3}; MOI of 1, P = 1.47×10^{-5}). For *S. aureus* MRSA 252, biofilms were eliminated by more than 50 % (MOI of 10, P = 0.003; MOI of 1, P = 0.012) after 48 hours of treatment. Biofilms produced by H325 were not initially as strong as the other isolates, however it was still possible to observe a reduction of the biofilm over 48 hours when the phage suspension at a MOI 10 was inoculated (P = 0.049). For the MOI 1, a reduction of the biofilm biomass was observed after 24 hours of treatment, however, at 48 hours ($P = 0.034$) a regrowth of the biofilm was observed.

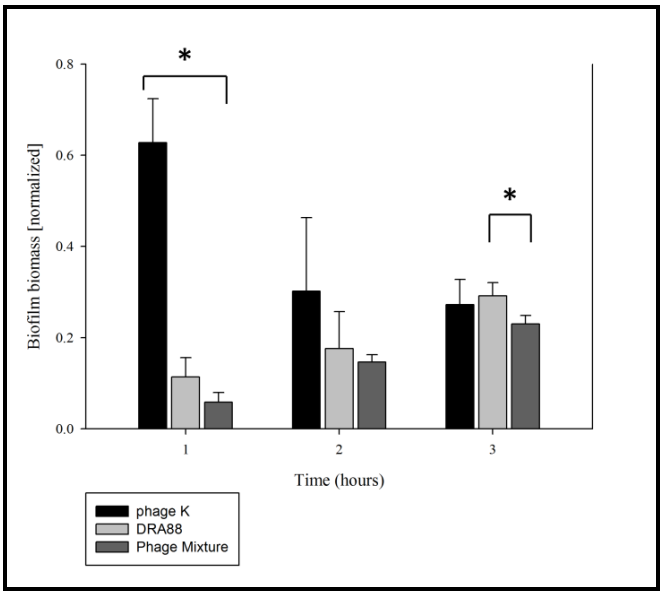

Figure 4.12: Normalised biofilm biomass treated with single phage K, DRA88, and the phage mixture after 48 hours at an MOI of 10 (OD590 reading after CV staining). *S. aureus* isolates: 1, 15981; 2, MRSA 252; 3, H325. Mean values (standard deviations) for the three strains treated with phage K were 0.63 (± 0.10), 0.30 (± 0.16), and 0.27 (± 0.06); those for DRA88 were 0.11 (± 0.04), 0.18 (± 0.08), and 0.29 (± 0.03); and those for the phage mixture were 0.06 (± 0.02), 0.15 (± 0.02), and 0.23 (± 0.02). Assays were performed three times, and the means ± standard deviations are indicated. Statistical significance of biofilm reduction was assessed by performing Student's *t* test. *P* values are indicated (*, 0.05). Reprinted from reference (244) and used with permission.

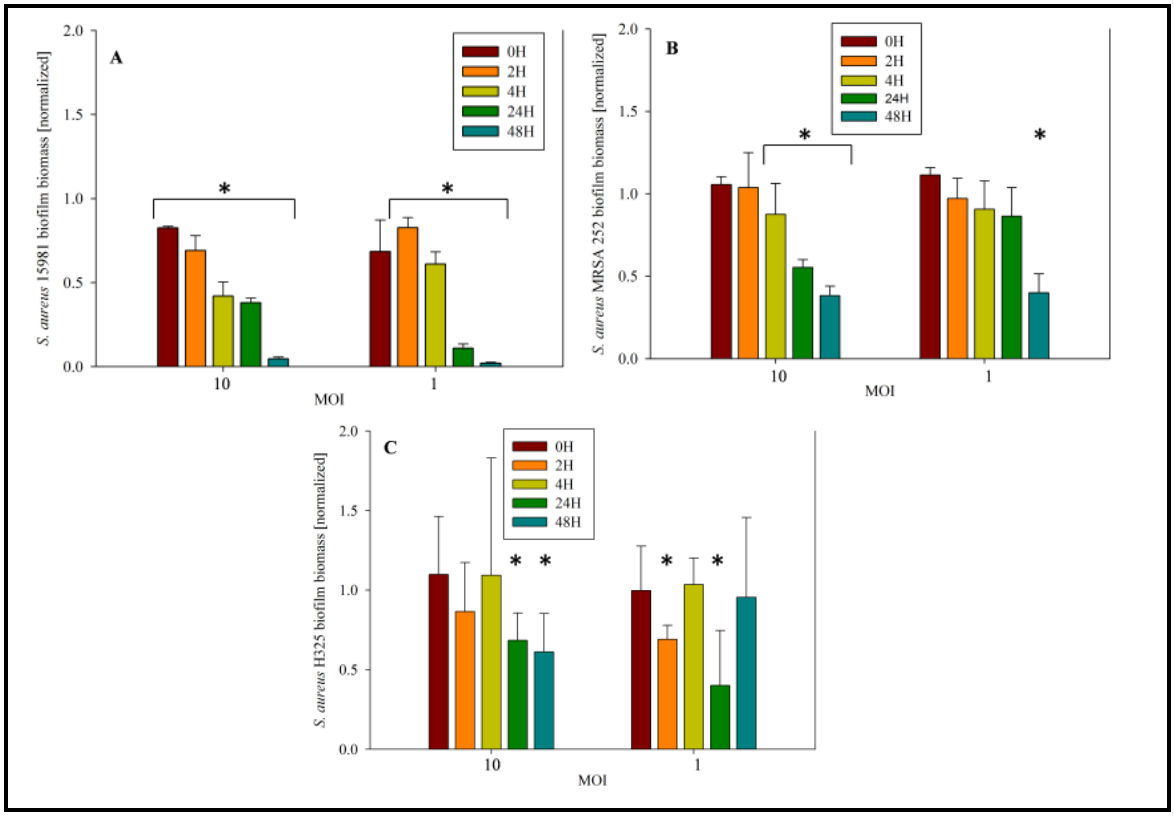

Figure 4.13: Normalised biofilm biomass treated with the phage mixture over 48 hours at two different MOIs (OD590 reading after CV staining). *S. aureus* isolates: 15981 (A), MRSA 252 (B), and H325 (C). Assays were performed three times, and the means ± standard deviations are indicated. Statistical significance of biofilm reduction was assessed by performing Student's *t* test. *P*-values are indicated (*, 0.05). Reprinted from reference (244) and used with permission.

	S. aureus 15981		*S. aureus* MRSA 252		*S. aureus* H325	
Biofilm Treatment	**0 Hour**	**48 hours**	**0 hours**	**48 hours**	**0 hours**	**48 hours**
PBS	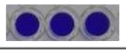	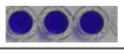	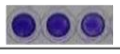	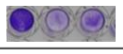	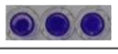	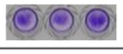
Phage K	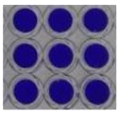	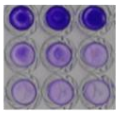	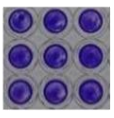	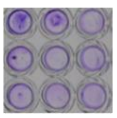	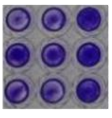	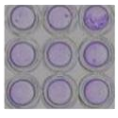
DRA88						
Phage Combination						

Figure 4.14: Visualisation of wells stained with 0.1 % crystal violet after 48 hours of phage treatment at an MOI of 10. Shown are the biofilm wells treated with PBS, phage K, DRA88, and phage mixture at 0 h (A) and 48 h after (B). Experiments were performed in triplicate. Reprinted from reference (244) and used with permission.

4.4.3.2. *P. aeruginosa* biofilm eradication

The literature provides several protocols for growth of *P. aeruginosa* biofilms in microtitre plates (308) and the main parameter changing is the medium used for the growth. Therefore, a preliminary assessment was performed in order to choose the best medium and conditions to achieve the production of a strong biofilm by *P. aeruginosa* PAO1 strain. LB and YPD medium supplemented with D-(+)-glucose (LBg and YPDg) at four different strengths were prepared: 20 %, 50 %, 80 % and 100 % and biofilms were established in a 96-well microtitre plate (Figure 4.15). For YPD it was observed an improvement in biofilm formation with the increase in medium strength. However and interestingly, LB medium at 50 % of its strength was seen to allow the formation of a stronger biofilm, showing almost twice biofilm biomass density than when using YPD ($P < 0.05$). For this reason LB at 50 % was selected to perform further experiments.

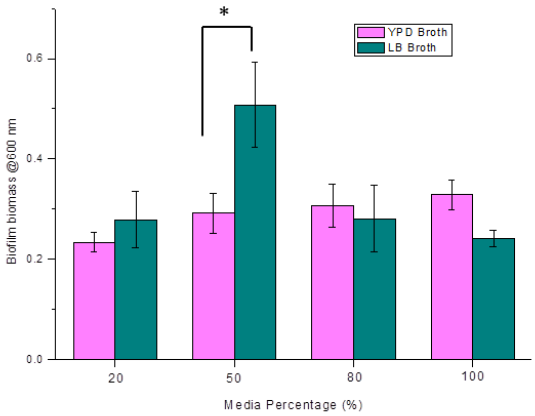

Figure 4.15: Biofilm biomass produced by *P. aeruginosa* PAO1 on a 96-well microtitre plate when grown in different concentrations of LB and YPD nutrient media over 48 hours. Shown are the OD_{600} readings after crystal-violet staining. Statistical significance comparing both media was assessed by performing Student's *t* test. *P*-value is indicated (*, 0.05).

Hence, 48 hour-old biofilms produced by the *P. aeruginosa* PAO1 were established in 96-well microtitre plates. Washing steps were performed carefully, as although the biofilms were stronger than the ones produced by *S. aureus*; the mechanical wash step was still able to disrupt biofilms that were very viscous, due to high polysaccharides content. Established biofilms were treated with the phage cocktail at two different MOIs, 1 and 10, and their biomass density assessed at the time points 0, 2, 4, 24 and 48 hours, by crystal violet staining followed by OD_{600} measurements (Figure 4.16). A clear reduction of 80 % of the biofilm biomass was observed only in the first 4 hours of phage treatment for MOI 1 and more than 95 % for MOI 10 ($P < 0.05$). At 24 hours, although biofilm biomass was still lower than that observed for the PBS control biofilm wells for both MOI cases (MOI of 10, $P = 0.015$; MOI of 1, $P = 0.003$) (Figures 4.16A and 4.17), there was biofilm regrowth compared to the time point at 4 hours and by the end of the experiment at 48 hours, the biofilm biomass measured was greater than the biomass of the control biofilms. In parallel, an XTT assay was performed to evaluate the metabolic activity of the cells in the biofilm when treated with a phage cocktail suspension at MOI 10 during 48 hours. A decrease of the metabolic activity in the first 4 hours of treatment ($P < 0.05$) could again be observed (Figure 4.16B and 4.17), which was followed by a regrowth in the next incubation hours. Although in this case, by 48 hours the regrowth biofilm did not surpass the biomass of the biofilms inoculated only with PBS, showing lower numbers ($P < 0.05$). In another similar experiment, biofilms were disrupted and both bacterial and phages numbers were estimated. The same behaviour was observed, where in the first 4 hours of treatment there was a clear reduction of the viable number of cells, followed by a regrowth measured at 24 hours. By 48 hours a cell number reduction of ~1log could be observed, however this was also observed for the disrupted control biofilm and could not be related to the phage, but was, perhaps, due to a saturation of the biofilm environment (Figure 4.16C). Regarding the phage numbers in the biofilm, it was observed that at time point 4 hours a decrease in their concentration, most likely due to many of the phages being

adsorbed to the cells and not present in the surrounding environment. At 24 hours and 48 hours, the number of phages present in the biofilm increased to ~2logs (Figure 4.16D).

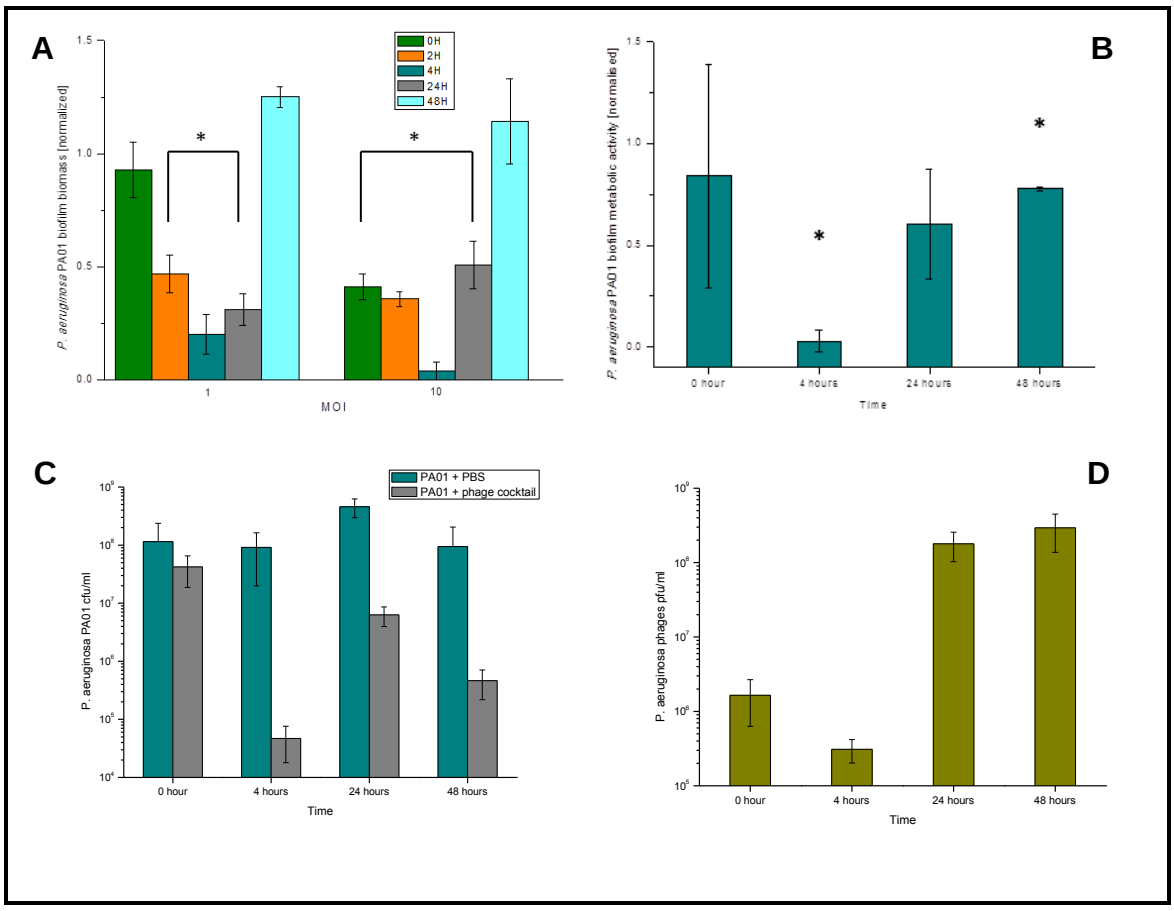

Figure 4.16: *P. aeruginosa* PAO1 biofilm treated with the phage cocktail over 48 hours. (A) Normalised biofilm biomass treated with the phage cocktail at two different MOIs (OD_{600} reading after CV staining). (B) Normalised cell metabolic activity in the biofilm treated with the phage cocktail at MOI 1 (OD_{600} reading after XTT assay). (C) and (D) show the estimation of numbers of viable bacterial cells and phage particles in the biofilms treated with the phage cocktail. Assays were performed three times, and the means ± standard deviations are indicated. Statistical significance of biofilm reduction was assessed by performing Student's *t* test. *P*-values are indicated (*, < 0.05).

***P. aeruginosa* PAO1**	**Crystal violet staining**		**XTT assay**	
	PBS	Phage cocktail	PBS	Phage cocktail
MOI 10				
MOI 1				

Figure 4.17: Visualisation of wells stained with 0.1 % crystal violet after 24 hours of phage treatment, at an MOI of 10 and 1. Also, wells where the XTT reaction was performed can be observed after 4 hours of phage treatment at MOI 10. Experiments were performed in triplicate.

4.4.3.3. Biofilm eradication by synchronised use of phage and antibiotic

The synchronised effect of biofilm reduction when using the phage cocktail and an antibiotic was explored for *S. aureus* and *P. aeruginosa*. The antibiotics used for this study were vancomycin for *S. aureus* 15981 and ofloxacin for *P. aeruginosa* PAO1. Vancomycin, a bactericidal antibiotic drug for *S. aureus* (318), inhibits the cell wall synthesis by preventing the peptide subunits NAG and NAM from being incorporated into the peptidoglycan. Ofloxacin stops the DNA replication of Gram-positive and Gram-negative bacteria, by inhibiting DNA supercoiling of DNA gyrase and making it a powerful bactericidal (319). A preliminary test was performed to assess the minimum inhibitory concentration (MIC) of these antibiotics when cultures were growing under planktonic conditions. Results showed the MIC of vancomycin for *S. aureus* 15981 was 1 µg/ml and for *P. aeruginosa* PAO1 it was 0.25 µg/ml. Later, 48 hour-old biofilms were established in 96-well microplates and in a gradient scale were treated with different MOIs of phage cocktail (100 to 0.01) and antibiotic concentrations (128 µg/ml to 2 µg/ml) over 24 hours (Figure 4.18). Regarding the biofilm produced by *S. aureus* 15981 a more successful eradication of the biofilm was observed when treatment was done only by phage at MOI 10, followed by biofilms treated with MOI 10 an antibiotic concentrations between 16 µg/ml and 2 µg/ml were used, with biofilm biomass reduction in the range 46 % and 65 %. In general, any other case where the combined use of phage and antibiotic was employed resulted in a lower disruption of the biofilm

or an enhancement of the biofilm growth. For the biofilm produced by *P. aeruginosa* PAO1 the major biofilm disruption was achieved when using only ofloxacin.

Table 4.2: Antibiotic MIC performed by the microdilution method.

Antibiotic	Isolate	MIC (µg/ml)
Vancomycin	*S. aureus* 15981	1
Ofloxacin	*P. aeruginosa* PAO1	0.25

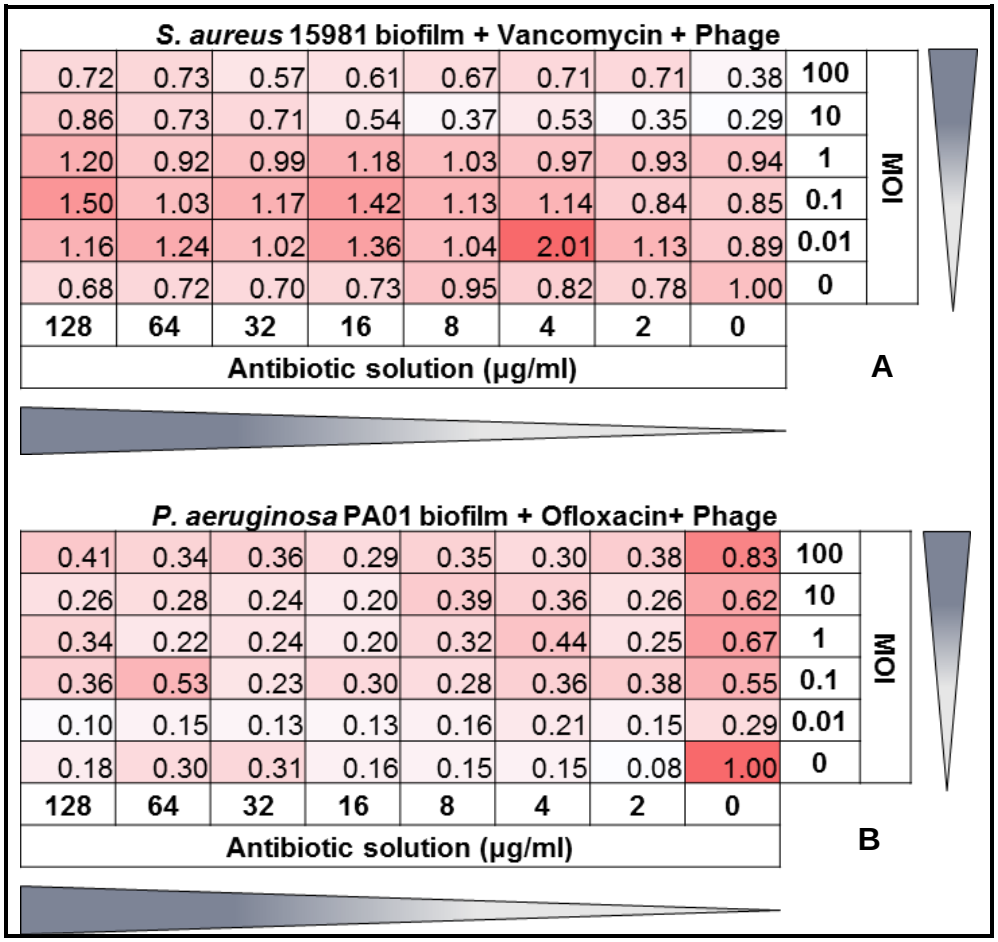

Figure 4.18: Biofilm biomass treated with gradient concentrations of antibiotic and phage cocktail over 24 hours. Results were normalised against the PBS treated biofilm (OD_{600} reading after CV staining). Lighter pink indicates higher levels of biofilm disruption (lower biofilm biomass) and darker pink lower levels of biofilm disruption (higher biofilm biomass). A – *S. aureus 15981* treated with phage mixture and vancomycin. B – *P. aeruginosa* PAO1 treated with phage cocktail and ofloxacin. Experiments were performed three times.

4.4.4. Phage lytic assessment on an *in vitro* biofilm model (open system)

A flow system for biofilm formation was performed in order to assess the quantitative and structurally changes produced by phage cocktail treatment over a period of 48 hours. A bacterial culture growing under continuous constant conditions in a chemostat, with a dilution rate of 0.5, was used to feed a Robbins device for 24 hours. Over this time, flowing bacterial cells were allowed to attach to the surface of the stainless steel coupons. After 24 hours, the chemostat was replaced by fresh half strength media supplemented with 0.1 % of D-(+)-glucose for biofilm growth and maturation over 48 hours. Figure 4.19 shows the biomass recovered from the biofilm grown on the coupons at different time points. By 48 hours the biofilm produced was stronger and similar to the one observed at 72 hours. For that reason, an incubation time of 48 hours was found optimal to perform in the further studies.

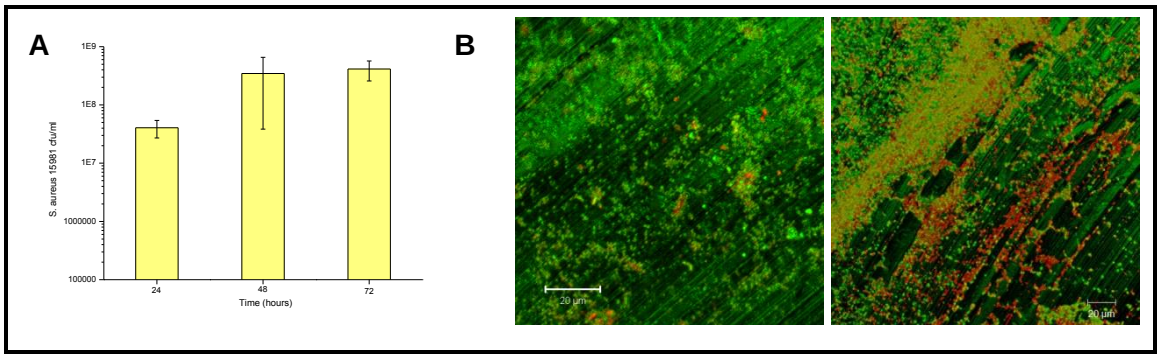

Figure 4.19: *S. aureus* 15981 biofilm increase on the surface of stainless steel coupons over 72 hours. (A) number of viable cells recovered from the disruption of the biofilm. Assays were performed three times, and the means ± standard deviations are indicated. (B) Image of biofilms at 24 hours (left) and 48 hours (right) stained with LIVE/DEAD stain at a magnification of 20x. Live (green) and dead (red) bacterial cells can be observed on the surface of the stainless steel disk.

4.4.4.1. *S. aureus* 15981 biofilm eradication and dispersion

A 48 hour-old biofilm of *S. aureus* 15981 grown from a steady-state culture and allowed to develop under dynamic conditions was treated with an emulsion suspension of the phage mixture at a MOI 0.1 and assessed regarding its eradication and dispersion by counting the number of viable cells present and by visualisation of a stained specimen under confocal microscopy. Results showed a clear dispersion and reduction of biofilms attached to the stainless steel coupons compared to the ones treated with a PBS in emulsion suspension only (Figure 4.20C) and by 48 hours of phage treatment such difference was significantly different (Figure 4.20A, $P = 0.003$). A reduction of the biofilm structure of the control experiment from the first day of treatment to the end can be observed, whether by colony counting the disrupted biofilms or by direct visualisation using the confocal microscope. The biofilm height measured for the phage treated biofilm was 19.64 µm, SD±4.83 at 0 hours and 12.02 µm, SD±1.34 at 48 hours; for the PBS treated biofilm 21.98 µm, SD±4.67 compared to 15.82 µm, SD±2.64. Disrupted biofilms were also used to enumerate phages and it was observed a ~2log increase in their number over the 48 hours of treatment (Figure 20B). Such observation supports the fact that biofilms reduction and dispersion was a consequence of the phage addition and infection. Control biofilms were also screened for the absence of phages and rules out any possible contamination. Also, the phage injected into the system was at a concentration of 10^7 pfu/ml, however phages recovered by the disruption of the biofilms were in the order of 10^5 pfu/ml, mainly caused by the dilution effect, but also many phages will not attach efficiently to the bacterial cells and be washed out from the system.

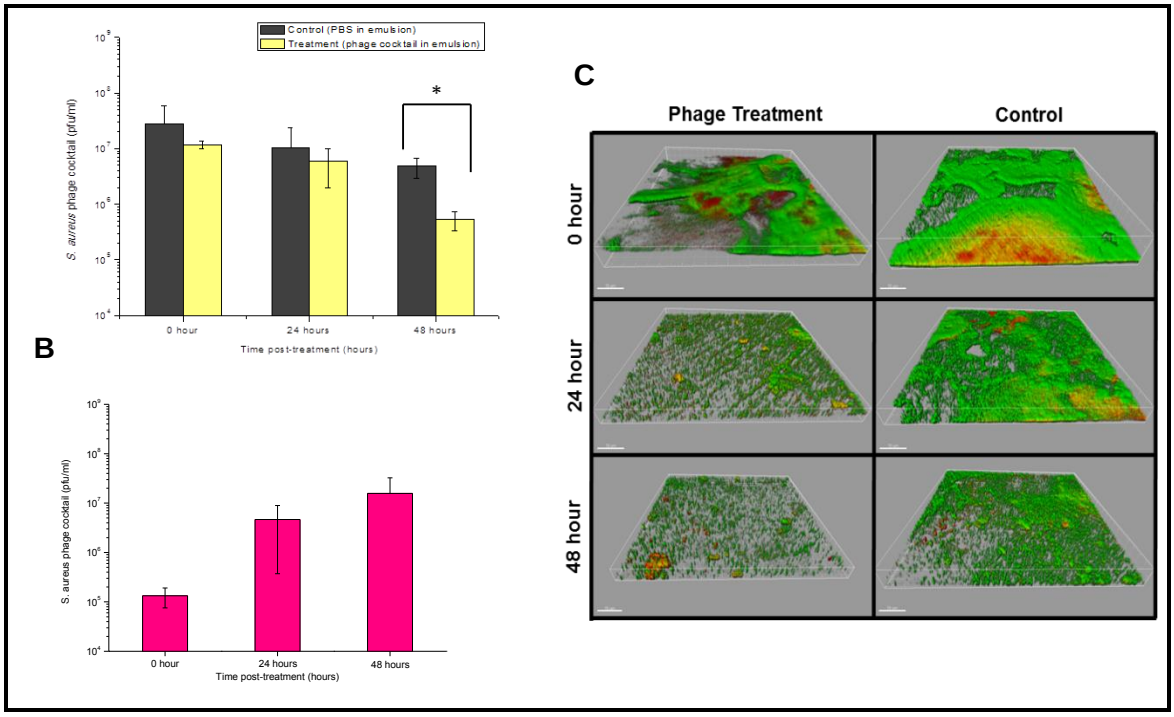

Figure 4.20: *S. aureus* 15981 48 hour-old biofilm grown under flow conditions in the Robbins device and treated with a phage in emulsion suspension or PBS in emulsion suspension (control) for 48 hours. A - Number of viable cells recovered from the disruption of the biofilms, B – Number of phage particles recovered from the disputed biofilms, C – 3D images of the biofilms observed under the confocal microscope stained with LIVE/DEAD stain at a magnification of 20x. Live (green) and dead (red) bacterial cells can be observed on the surface of the stainless steel disk. Enumeration assays were performed three times, and the means ± standard deviations are indicated. Statistical significance of biofilm reduction was assessed by performing Student's *t* test. *P*-values are indicated (*, < 0.05).

4.4.4.2. *P. aeruginosa* PAO1 biofilm eradication and dispersion

A continuous growing culture of *P. aeruginosa* PAO1 was also established to allow the production of a 48 hour-old biofilm under dynamic flowing conditions. The biofilm was then treated with an emulsion suspension of the phage cocktail at an MOI 0.1 and the biofilm was monitored and assessed regarding its eradication and dispersion using the same approaches used for the *S. aureus* biofilm previously described.

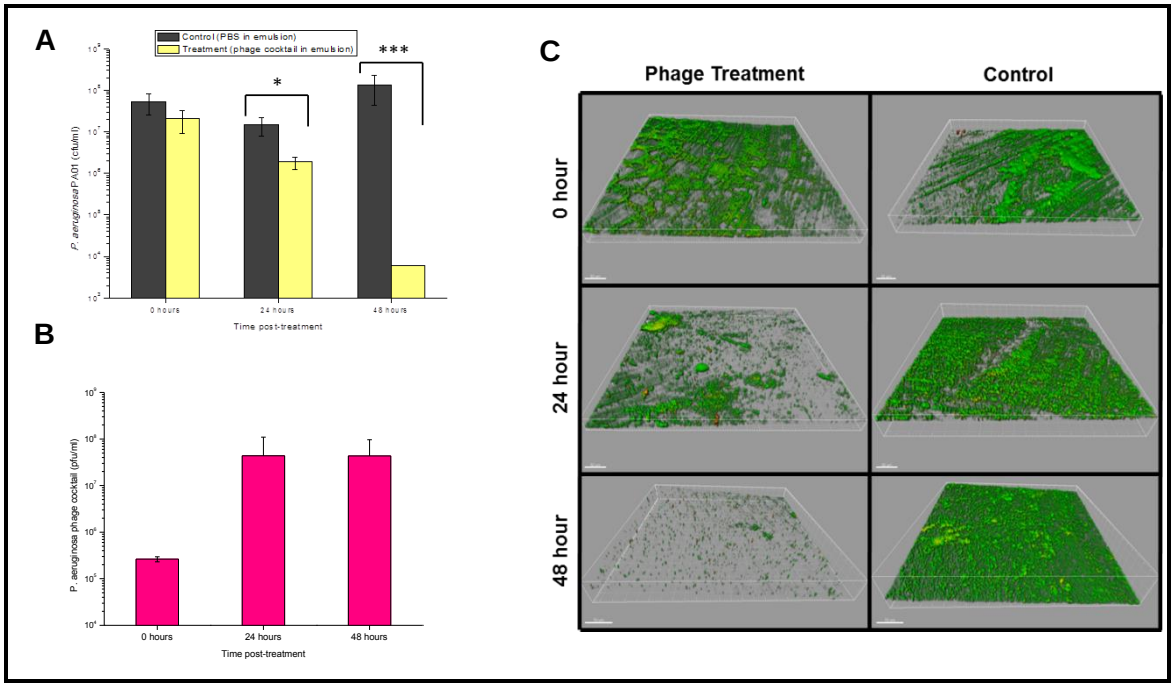

Figure 4.21: *P. aeruginosa* PAO1 48 hour-old biofilm grown under flow conditions in the Robbins device and treated with a phage in emulsion suspension or PBS in emulsion suspension (control) for 48 hours. A - Number of viable cells recovered from the disruption of the biofilms, B – Number of phage particles recovered from the disputed biofilms, C – 3D images of the biofilms observed under the confocal microscope stained with LIVE/DEAD stain at a magnification of 20x. Live (green) and dead (red) bacterial cells can be observed on the surface of the stainless steel disk. Enumeration assays were performed three times, and the means ± standard deviations are indicated. Statistical significance of biofilm reduction was assessed by performing Student's *t* test. *P*-values are indicated (*, < 0.05; ***, < 0.001).

Results showed a clear reduction of the biofilm and by 24 hours of phage treatment this reduction was significantly different from the PBS treated biofilms (Figure 4.21A, P = 0.003) and by 48 hours such reduction was even more evident (P = 0.00008). Under the confocal microscope the biofilm reduction and dispersion was also observed (Figure 4.21C) and by 48 hours the presence of a biofilm on the stainless steel disks was barely visible with only a few dispersed bacterial aggregates. The biofilm height measured for the phage treated biofilm was 29.01 µm, SD±3.04 at 0 hours and 10.87 µm, SD±2.00 at 48 hours; for the PBS treated biofilm 25.57 µm, SD±4.03 compared to

25.22 μm, SD±1.83. Such results are reinforced by the observation of an increase in the number of phages present in the disrupted biofilms by ~3logs (Figure 4.21B). Also, here the initial concentration of phage particles recovered from the disrupted biofilms was lower than the amount injected.

4.5. Discussion

In this chapter the phage lytic potential of the phage cocktails, isolated and characterised in Chapter Three, targeting *S. aureus* and *P. aeruginosa* isolates was investigated in three *in vitro* model systems: planktonic growth, biofilm growth in a static system and biofilm growth in a dynamic flow system.

The planktonic growth of phages with the bacterial isolates showed a different outcome when the same isolates were plated on an agar plate and the phage suspension spotted on. The bacterial lawn on a plate mimics a static environment, where under planktonic conditions bacteria and phage are in a dynamic environment. In this environment, adsorption of phage to bacteria is more challenging to occur and results from occasional random encounters. Moreover, planktonic conditions allow observing the bacteria-phage dynamic over time and where mutational events in both bacteria and phage particles are likely to occur. This makes it possible to select phages that are able to overcome the evolution of phage resistance in the bacterial population.

Several studies have demonstrated that the use of a phage cocktail brings not only advantages regarding how broad a cocktail can be, but also in terms of preventing or delaying mutations in the population that can result in phage resistant clones and failure of the therapeutic (320, 321). When a bacterial population is growing with a single phage type, this can be translated in a one-to-one race and perhaps only a single mutation maybe needed to confer resistance to the phage. On the other hand, a phage cocktail where different receptors and pathways for infection are used, poses a more problematic situation for bacterial cells. The probability for a mutation to occur in a natural isolate is in the order of 10^{-8} (322) and as a result there is the need for bacteria undergo multiple mutations to achieve resistance. Bacterial broth cultures growing with the phage cocktails showed an elimination of bacterial cells growth and suppression of resistant mutants for both *S. aureus* and *P. aeruginosa* strains tested. However, for *S. aureus* MRSA 252 that was not entirely correct; after 18 hours of

growth bacterial cells were able to counteract the infectivity of the phage present in the culture, possibly due to the presence of phage-receptor-mutated clones. Such situations can be overcome or delayed by including additional phage types to the therapeutic mixture, which is a task to undertake that is easier (more rapid and likely to succeed) than the discovery of a new antibiotic. However, the likely scenario *in vivo* is that reducing the initial bacterial load could be enough to bring the bacterial numbers under control so that an antibiotic drug or the action of the immune system could clear the infection in an effective way (323). Such bacterial mutation emergence can be, however, manipulated by studying and optimising the optimal phage concentration to treat the culture. The results of testing a range of different phage cocktail MOIs added to a planktonic culture, where the arms race between bacteria and phage can be easily observed, suggest better results in suppressing the regrowth by adding lower phage concentrations. This has been previously observed (324, 325). More successful results were achieved by adding phages later on to the growing planktonic culture; this might be related to a slower metabolic state of bacteria when compared to the growth at the start of the incubation time, suggesting a lower chance for bacteria mutational events or instead be related at some extent to the existence of a resistant sub-population or to a random fluctuation model followed by the interaction of phage and bacteria and the appearance of resistant bacteria (326).

More than 60 % of all infections are related to the formation of biofilms, as previously discussed in Chapter One. Hence, although assessment of phage lytic activity on bacterial planktonic growth reveals to be a significant assay it is important that biofilm model studies are investigated when testing a new antibacterial therapeutic and phage cocktails are required to go through those studies. Some studies already on *S. aureus* and *P. aeruginosa* strains suggest the significant potential use of phages to reduce and/or eliminate biofilms produced by those strains. This is the case for phage K, where biofilms produced by *S. aureus* isolates showed a significant decrease in their

biofilm biomass when treated with phage (220, 238). Also, cocktails of isolated phages have been successfully tested on biofilms produced by *P. aeruginosa* isolates, such as PAO1 (240), and also assessed for prevention of biofilm formation on indwelling medical devices, such as catheters (216). In this chapter, it is shown that phage cocktails were able to significantly reduce the biofilm biomass produced by *S. aureus* and *P. aeruginosa*. The first biofilm model system was performed under static conditions on a polystyrene surface for 48 hours and phages were added to the formed biofilms. For the isolate *S. aureus* 15981 the eradication effect started promptly after addition of the phage mixture and after 48 hours of treatment the biofilm was almost completely disrupted. To date very few studies have been performed regarding phage cocktail treatments, especially to treat *S. aureus* biofilms and in particularly those formed by MRSA isolates. Kelly and colleagues (220) have shown the efficacy of using a cocktail of phage K and its derivatives on the eradication of *S. aureus* biofilms produced by non-human clinical isolates. In this chapter, prevalent *S. aureus* human clinical isolates, that also included MRSA types, were used for the biofilm assessment of the phage mixture. For *P. aeruginosa* PAO1 the biofilm biomass disruption after addition of the phage cocktail was quickly observed in the first six hours of treatment. 24 hours later, although the biofilm biomass was still lower than the biofilm PBS-treated, it was clearly higher than the previous endpoint. By 48 hours the biofilm showed a completely regrowth with a biomass higher than the non-treated biofilms. Biofilm destruction was shown not only by the crystal violet biomass staining, but also when assaying the metabolic activity and the number of viable cells of the biofilm, and after 24 hours the reduction was followed by regrowth. This was not caused by a lack of phage particles, because phages were recovered from the disrupting of the biofilms. A decrease in phage numbers can be observed in the first 4 hours of treatment, where phages by then have been able to not only disrupt the biofilm matrix releasing bacterial cells, but by infecting the cells. By 24 hours of treatment a clear proliferation of the phages was observed. Similarly, for *S. aureus* H325 a regrowth of the biofilm was

observed after 24 hours of treatment when using the lower MOI. Such regrowth has also been observed elsewhere (240) and it might be a consequence of a longer interaction of the phage with the bacteria, also helped by a slower metabolic activity of the bacteria in the biofilm where phages proliferation is slowed down, resulting in the emergence of phage resistant clones in the bacterial population (327). For all cases the higher MOI showed to be more rapid in reducing the biofilm biomass and also better preventing the biofilm regrowth, observed for *S. aureus* H325 and *P. aeruginosa* PAO1.

Comparing the effect of the phage cocktails on broth cultures to biofilms, a more positive and rapid effect was observed on eliminating the bacterial load of broth cultures than that on biofilm, which was disrupted at a slower pace. This scenario was hypothesised to be due to the metabolic state of the cells. In a biofilm, cells can be in a low metabolic activity state and phages cannot proliferate as efficiently and as quickly when compared to actively growing cells (238). This has been also been shown for antibiotic drugs where bacteria in biofilms can be much more resilient than those in planktonic culture (208). Such an observation was explained as not mainly due to a low penetration of the antibiotic through the EPS matrix, but mainly due to the low metabolic activity of cells and oxygen limitation, particularly the inner areas of the biofilm, impairing the action of the drug (328). This was actually observed, when treating the biofilms produced by *S. aureus* 15981 with vancomycin, only a concentration 128 times higher than the effective concentration used in the planktonic state were able to disrupt around ~30 % of the biofilm biomass. For some other cases, the biofilm biomass showed an increase when compared to biofilms also receiving phage treatment suggesting that the addition of the antibiotic might have resulted in antibiotic resistance development. In a study it was shown that this increase in antibiotic resistance was due to a lower penetration of the drug to the insides of the biofilm and cells were gradually exposed to the antibiotic molecule, which triggered stress-induced changes in their metabolic and transcriptional processes and so

selected for resistance, however interestingly such low penetration was not found to be attributed to the production of the slime polysaccharide matrix (329). The biofilm produced by *P. aeruginosa* PAO1 treated with ofloxacin on the other hand was almost completely disrupted by using four times higher the concentration for the MICs. Phage treated biofilms showed greater disruption when treated with lower MOIs, following the same trend observed for the biofilm studies shown in Figure 4.16A, perhaps a high selective pressure (MOI100) gives an advantage to the already resistant types in population, that will multiply using the resources made available after elimination of the sensitive cells (by the phage). When applying a low selective pressure (MOI0.1), sensitive cells are slowly eliminated and resources are shared for longer among resistant and sensitive cells. It can be hypothesised thus in such scenario, resistant cells do not multiply as quickly and phages meanwhile have the opportunity to undergo evolutionary changes able to counteract resistance.

Bacteria are able to adapt to different habitats and *S. aureus* and *P. aeruginosa* are no different (as previously described in Chapter One). Such flexibility is made possible through phenotypic changes employed by the bacteria, usually by expression or loss of cellular components, allowing them to better adapt (330). Some of these changes will have a direct effect on bacterial attachment to surfaces, how biofilm communities are formed and how resilient they are to external stresses, such as phages and antibiotics (331). For this reason, when studying biofilms it is important to provide a controlled bacterial culture when colonising to produce biofilms on surfaces (311). The *in vitro* closed biofilm system of microtitre plates misses out such controlled environment, where the inoculated bacterial cells proliferate and grow as agglomerates that eventually stack together forming a biofilm. However, the environment over 48 hours, even with the addition of fresh nutrient media, changes through the experiment perhaps reaching a saturated situation. This is in contrast to the situation of a biofilm model produced using a bacterial culture growing in a chemostat, in which levels of

bacterial cells, their products and waste and media components are constant. Such a controlled environment allows bacteria to grow at a constant growth rate. It is know that the bacterial growth rate interferes with the different expression of cell wall proteins and secretion of extracellular polysaccharides (332) that will ultimately be implicated in the adhesion process of bacterial cells to a surface (333). The key point is that the growth rate can be easily manipulated to achieve slow growth rates, where expression of cell wall proteins is enhanced and bacterial communities resemble at a higher level an *in vivo* situation. Also, the MRD provides biofilm produced under a dynamic environment; hence such communities are more likely to be better protected from external surfaces and better attached to the surface and cells to each other.

Biofilms produced on the MRD flow system were revealed to be strong structures composed of a majority of live cells, but where dead cells and possibly water channels could also be observed. The attachment to the coupons surface was improved by dipping those surfaces into a mucin solution, as mucin promotes biofilm formation (334). The mucus layer is largely composed of mucin oligosaccharides (335) that represent binding sites for the bacterial cells adhesins, similar to those in the airways of cystic fibrosis patients (336). Others workers have used media supplemented with human plasma solution to stimulate the growth of *S. aureus* biofilms (337). The results showed that *S. aureus* formed very robust and reproducible biofilms under static conditions; with strain 15981 producing the strongest, most stable biofilm in polystyrene plate wells. For this reason, this strain was selected for further study including its use in the dynamic flow model. The phage suspensions when applied to the formed biofilm were able to disrupt and disperse the bacterial cells. However, such disruption compared to the one observed for the static model took longer to occur. As mentioned above, this might be related to the structure of the biofilms produced from a continuous culture and matured under flow conditions that will resemble more a natural biofilm. It was also observed, however that the biofilm receiving the control treatment also

showed a gradual dispersion over the 48 hours of treatment. The presence of phages was ruled out after assessing those biofilms for the presence of study phage. Hence, such disruption might be related to the several sampling interruptions to the flow system, where the flow was paused. This somehow might have interfered with the structure of the biofilms. Lastly, a bubble trap was not used and therefore bubbles passing through the MRD could have caused biofilm disruption. This, on the other hand, was not observed for the control biofilm produced by *P. aeruginosa* PAO1 where a maturation of the biofilm was observed over the experiment. Interestingly, the biofilm disruption outcome observed by the 48 hours of treatment was almost complete and a regrowth of the biofilm, promoted by bacterial resistance to phage, was not observed. It has been noted that *P. aeruginosa* biofilms produced by a chemostat culture coupled with a flow device system was shown to have greatly upregulated the expression of a large number of cellular proteins when compared to planktonic growth (338). Hence, this result suggests a more promising and successful use of the *P. aeruginosa* phage cocktail as a therapeutic weapon. Also, emphasizing the importance of testing the phage cocktails in different biofilm models, as expression of polysaccharides, cell signalling and ultimately resilience to external stresses is strongly affected by a myriad of factors and strategies, where the success of a therapeutic might be strongly dependent.

The studies performed in this chapter suggest that the use of phage cocktails, in this case for *S. aureus* and *P. aeruginosa* could provide practical alternatives to antibiotic treatments for combating such biofilm related infections and in particular the devastating effects of biofilm related MRSA and CF infections. Even with the contribution of these studies to the effectiveness of bacteriophage therapy to fight established bacterial infections, there is still a long way to go and several barriers to address.

Chapter Five:

ASSESSMENT OF PHAGE EFFECT ON THE SURVIVAL OF *GALLERIA MELLONELLA*

5.1. Chapter summary

In the previous chapter the phage cocktails were characterised and their lytic and biofilm eradication potential were assessed on *in vitro* models. In this chapter the phage cocktails targeting *S. aureus* and *P. aeruginosa* are used on an *in vivo Galleria mellonella* infection model, where both phage treatment and protection are studied.

5.2. Background

In vitro studies provide a valuable first understanding of the efficacy of a phage cocktail, however in accordance with what happens to any other prospective therapeutic product it is even more important to assess this efficacy on *in vivo* infection models. *In vivo* models comprise advanced multifactorial environments that might reveal unpredicted interactions not observed in a modest *in vitro* model system. In an *in vivo* model, factors such as the distribution pattern of phages, the target bacteria itself establishing an infection and interacting with the host, the phages needing to get access to the cells, the presence of an active immune system and phage loss by excretion, all influence the final therapeutic efficacy of the phage product.

Mammalian models, such as mouse models have been extensively used to test phage efficacy (339–341), however such models are associated with significant cost, appropriate infrastructures and ethical issues. Insect infection models on the other hand are valuable alternatives showing reliable results. Insects are provided with advanced systems for fighting antimicrobial disease. Although these are much simpler than the mammalian systems, they are still complex (342), making them similar to mammals and pertinent models to test new antimicrobials. When facing a bacterial invasion, the haemocyte cells in the haemolymph are able to phagocytise the invaders. At the moment six types of haemocytes have been reported (343). Furthermore, there

are the production of a humoral immune response involving the synthesis of antimicrobial peptides, such as lysozyme (344), and a heat-shock protein (345). Also processes, such as haemolymph clotting, wound healing and melanisation are strategies employed by the insect to overcome a threat. The last one relates to the activation of the prophenoloxidase cascade, performed by serine-proteases. When activated, phenoloxidase initiates the biosynthesis of quinolones to melanin pigment, which is deposited on the insect cells and around the invading pathogen as a defensive strategy (346, 347).

Regarding *Galleria mellonella* (the greater wax moth), this infection model brings several advantages. The caterpillar larvae are easy to handle and it is possible to perform several injections with fair accuracy (about 2 cm long and 250 mg on average), they are able to live in a wide range of temperatures, including 37 °C, making it possible to perform studies that simulate mammalian situations. They are susceptible to numerous human pathogens making it possible to get positive correlation with an infection in mammals (348). Purchase of the worms is cheap and they are easily stored at 4 °C in a cold room, hence there is no need for an animal facility. When testing a new antimicrobial, record of larvae survival numbers is possible by direct observation. When dead, larvae show lack of movement and turn black due to deposition of melanin on the tissues. Finally, the use of *G. mellonella* larvae for research testing is ethical approval-free, making it a very appealing model for a first attempt before testing on a more complex *in vivo* model (349).

The wax moth larva *G. mellonella* as a model has been used already to examine several host-pathogen interactions, including bacterial virulence studies for *S. aureus* (350), *P. aeruginosa* (348) and *Bacillus cereus* (351), but fungus virulence has also been studied, such as *Candida albicans* (352). Also experimental antimicrobial agent assessment using *G. mellonella* infection models was studied previously (353, 354)

and phage therapy has recently been reported, where infections caused by *Burkholderia cepacia* and *Cronobacter sakazakii* were studied (355, 356).

5.3. Materials and Methods

5.3.1. Bacterial strains and preparation of inoculum

Phage therapy was assessed on two infection models using *S. aureus* MRSA 252 and *P. aeruginosa* PAO1 strains. Clinical isolates were also used in further tests and included *S. aureus* H560, 15981, H137, HT2004-0991 and 97.1948.S, the first two have a MSSA genotype and the other three are MRSA isolates. Regarding *P. aeruginosa* two clinical isolates were used, PA45291 and BC00907, isolated from bacteraemia and cystic fibrosis samples, respectively. Bacteria were grown overnight in TSB or LB, depending if the bacteria were *S. aureus* or *P. aeruginosa*, and on the following day a 1:100 dilution was performed in order to establish a subculture. The subculture was incubated until mid-log phase once they achieved an OD ~1.0 and washed once in PBS. Cells were resuspended in PBS to give a final concentration of $1x10^8$ cfu/ml and diluted accordingly in PBS to the required inoculum size for each experiment. The cell number was always confirmed by a standard colony assay on agar plates.

5.3.2. Phage cocktail preparation and titration

Phage cocktails were prepared for use against *S. aureus* (phage strains DRA88 and Phage K) and *P. aeruginosa* (phage strains DL52, DLA54, DL60, DL62, DL64 and DL68). The phage strains had shown lytic efficacy against all *S. aureus* and *P.aeruginosa* as previously described in Chapters III and IV. Phage suspensions were propagated on the respective host, i.e*. S. aureus* RN4220 and *P. aeruginosa* PAO1 and PEG-precipitated (phage propagation and PEG-precipitation were previously described in Chapter Two Section 2.2.4. and Section 2.4.1.1.). All the necessary dilutions were performed in SM buffer. For the titration of the bacteriophage content in

the haemolymph, a similar methodology to the propagation was followed. The several dilutions were mixed with the host bacterial cells and 3 ml of soft agar was added and poured onto agar plates. After an overnight incubation, plaques were counted to determine phage titre.

5.3.3. *G. mellonella* phage therapy assay: treatment and protection

Larvae of *G. mellonella* were obtained from Livefood UK Ltd (Somerset, UK). Larvae were stored at 4 °C used within 1 week of receipt. A modified methodology developed by Peleg *et al.* (357) was used to infect each larvae. Briefly, larvae were surface sterilised before injection with a Fat Aid pre-injection swab containing 70 % ethanol. A pair of tweezers was used to immobilise the larvae and with a 26 gauge syringe 10 µl of required bacterial inoculum was delivered into the larval haemolymph behind the last proleg (Figure 5.1). For the treatment model, phage suspension was delivered behind the last proleg on the opposite side to the infection two hours post-infection. For the protection experiment phage suspension was given two hours pre-infection. All experiments used 15 larvae per treatment. For all the experiments a positive control group, where the larvae were infected and treated with PBS solution, and two negative control groups were also included: one group injected with PBS only, assessing the impact of any negative effect from the injection procedure, and one group injected with phage suspension only, assessing toxicity of the phage cocktail. Larvae were placed into petri dishes and incubated at the desired temperature, being examined regularly and recorded as dead when they did not move in response to touch. Kaplan-Meier survival curves were plotted using OriginPro 8.0 Software and statistical analysis was performed by using the Log-rank (Mantel-Cox) statistical test with 95 % confidence interval.

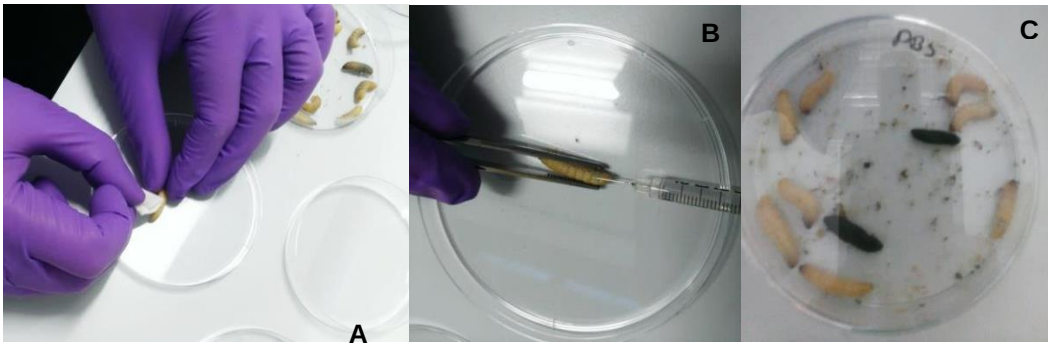

Figure 5.1: A – Surface sterilisation of larvae before injections; B – Injection of larvae in the last proleg; C – Mixture of dead (black) and alive larvae on the petri dish.

5.3.4. Heat-killed bacteria experiment

Bacteria were grown overnight in TSB and on the following day a 1:100 dilution was performed in order to establish a subculture. The subculture was incubated until mid-log phase once they achieved an OD ~1.0 and washed once in PBS. Bacterial cells were killed by heat at 95 °C for 10 min.

5.3.5. Bleeding larvae haemolymph

In order to follow the kinetics of bacteria and phage in the larvae haemolymph larvae were bled out. Experimental groups were established and the proper injections made and every 0, 8 and 24 hours the concentration of phages and bacteria was measured. To bleed the larvae, tweezers were used to make an incision and the content of the larvae was collected to a centrifuge tube. Three larvae were used for each time point. Recovered volumes of haemolymph ranged from 20 to 40 µl. All phage dilutions were performed in SM buffer and bacterial dilutions were performed in FAS virucide as described in Chapter Two, Section 2.11.6, in order to degrade all the phages in the haemolymph that could interfere with the bacterial numbers. To rule out the possibility

of PAO1 cells evolving phage resistance during the *in vivo* infection, re-isolated PAO1 cells were subjected to plaque assay to confirm susceptibility.

5.4. Results

5.4.1. Survival curves for *S. aureus* infection and phage treatment

The effect of *S. aureus* MRSA 252 on the survival of the larvae was shown to be dose dependent, where a lower survival rate was observed for the higher inoculum of *S. aureus*. We injected three groups of larvae with OD 1, 0.5 and 0.1, corresponding to approximately $4.5x10^6$, $2.25x10^6$ and $4.5x10^5$ cells injected per larvae (Figure 5.2). The survival rates at 48 hours after larvae infection were 40 %, 60 %, 93.33 %, respectively. At 72 hours post-infection survival rates were reduced to 33.33 %, 40 %, 73.33 %, respectively. Larvae were also injected with the phage cocktail at a concentration of 10^6 virus per larvae in order to investigate if there was a toxic or antigenic reaction by the larvae defence mechanisms. Survival numbers remained at 100 % throughout all experiments. For the treatment experiments, larvae were infected with *S. aureus* MRSA 252 and 2 hours later the phage cocktail was injected. Figure 5.3 shows the survival rates for larvae infected at OD 0.1 (5.3.A) and OD 1 (5.3.B) that received phage treatment at MOI 1. Surprisingly, we did not observe an improvement of larvae survival for the group receiving phage treatment. Larvae treated with phage showed a more rapid killing than the ones not receiving treatment. For an OD 1 24 hours post-infection, phage treated larvae showed a survival rate of 66.67 % vs 73.33 % for the positive non-treated control group. For the OD 0.1, the group receiving treatment showed a survival rate of 86.67 % compared to 100 % survival of the non-treated group. The same effect was also observed for an OD 0.5 when treated with two different MOIs – 10 and 1. Figure 5.4 shows the survival rates, where only 40 % of larvae treated with MOI 10 were alive after 24 hours post-infection and after 48 hours both MOIs had resulted in 60 % death of larvae compared to the non-treated group with 70 % of larvae alive.

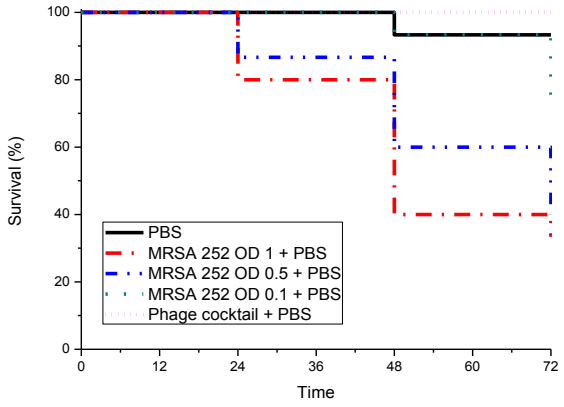

Figure 5.2: Survival of *G. mellonella* larvae infected with different inoculum concentrations of *S. aureus* MRSA 252 and with phage cocktail only. OD, optical density.

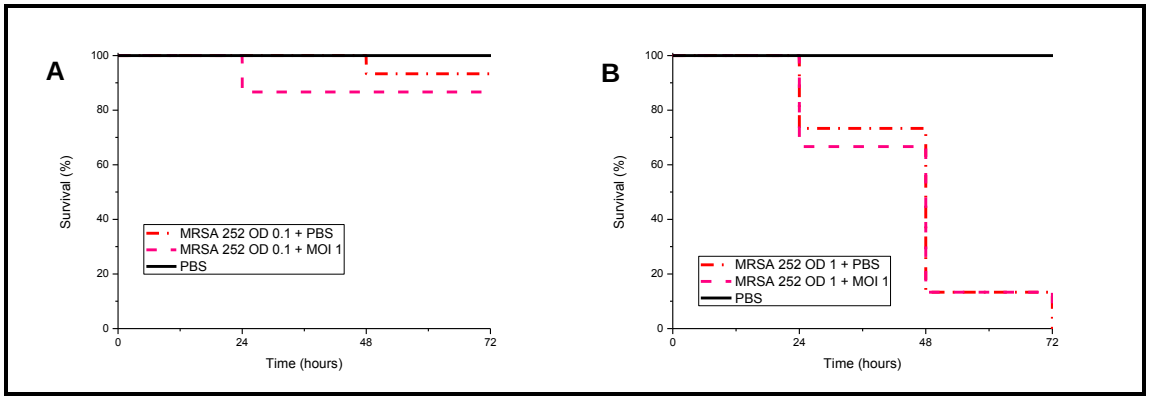

Figure 5.3: Survival of *G. mellonella* larvae infected with different inoculum concentrations of *S. aureus* MRSA 252, treated 2 hours post-infection with phage cocktail at MOI 1. A – OD 0.1, B – OD 1.0. OD, optical density.

5.4.2. Effect of heat-killed *S. aureus* MRSA 252 cells on larvae survival

Previously it was shown that heat-killed *S. aureus* bacteria did not result in larvae killing (350), however because we are using a different *S. aureus* strain we wanted to verify if the more rapid death of larvae was only due to a strong immunogenic response to bacterial cell lysis by the phage, but also due to the bacterial cell wall itself. *S. aureus* MRSA 252 subculture (~OD 0.5) was inactivated by heat and injected in the larvae. Two other groups were set up with *S. aureus* MRSA 252 (~OD 1.0), the positive control

group (bacterial cells and PBS) and the treatment group (bacterial cells and phage treatment). After 48 hours post-infection, the group injected with the bacteria killed by heat remained with a 100 % survival rate (Figure 5.4). The inactivation of the bacteria is not causing the larvae killing.

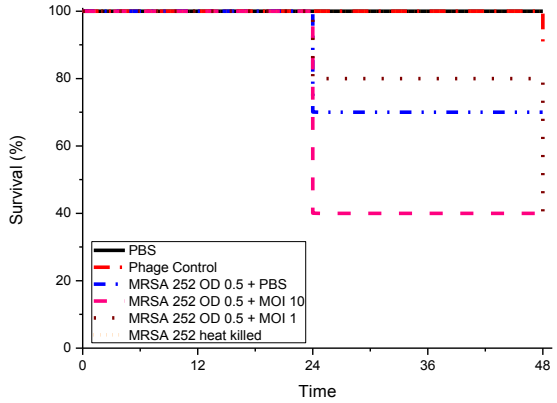

Figure 5.4: Survival of *G. mellonella* larvae infected with different inoculum concentrations of *S. aureus* MRSA 252, treated 2 hours post-infection with phage cocktail at MOI 1 and infected with *S. aureus* MRSA 252 heat killed. OD, optical density.

5.4.3. Effect of *ex-vivo* phage lysed MRSA 252 cells on larvae survival

To investigate if the more rapid death of larvae was due to a strong immune response to bacterial cell debris, composed of exotoxins and surface proteins, and resultant from the phage lytic cycle infection, *S. aureus* MRSA 252 cultures in mid-log phase showing approximate ODs of 1.0, 0.5 or 0.1 were incubated with the phage cocktail at MOI 1 and incubated for approximately 4 hours until when the culture was not showing signs of turbidity. Other *S. aureus* MRSA 252 mid-log phase cultures at the same ODs, but not challenged by the phage were also performed. Groups of larvae were injected either with the lysed cultures or active culture. Treatment groups were also performed (bacterial cells and phage cocktail). In this experiment, bacterial injections and phage administration were performed one after the other. For all the three experiments 72

hours post infection (Figure 5.5), larvae infected with bacterial cells lysed showed survival rates higher than 80 % (OD 1.0 – 93.33 %, OD 0.5 – 93.33 %, OD 0.1 – 86.67 %). Survival rates for larvae receiving a phage treatment after infection were lower than 47 % for all cases (OD 1.0 – 33.33 %, OD 0.5 – 46.67 %, OD 0.1 – 33.33 %). Hence, bacterial debris caused by the lysis of bacterial cells did not cause the low survival rates observed when treatment is applied *in vivo*.

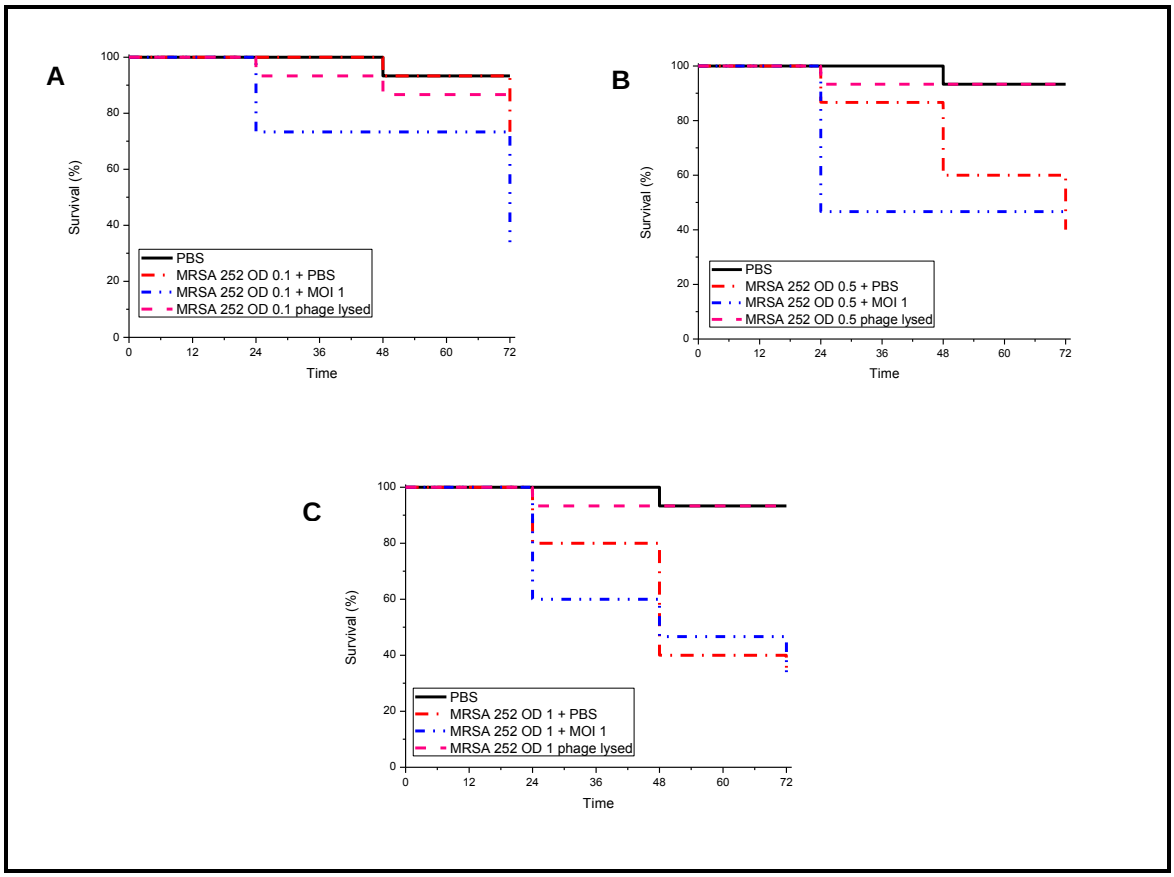

Figure 5.5: Survival of *G. mellonella* larvae infected with different inoculum concentrations of *S. aureus* MRSA 252, treated 2 hours post-infection with phage cocktail at MOI 1 and infected with *S. aureus* MRSA 252 lysate. A – OD 0.1, B – OD 0.5 and C – OD 1.0. OD, optical density.

5.4.4. Clinical isolates of *S. aureus*

To verify if the observed rapid killing effect on larvae infected with *S. aureus* MRSA 252 and treated with phage may also be observed for other *S. aureus* bacteria we infected larvae with a group of five clinical isolates (MSSA and MRSA included) and treated

them with phage at MOI 1. After 24 hour of larvae infection for all the phage treated groups mortality rates were 100 %. For larvae infected with clinical isolates H137 (MRSA) and 15981 (MSSA) observed survival was 30 % and 50 %, respectively, when not treated with phage (Figure 5.6). The clinical strains all showed higher virulence in comparison to MRSA 252.

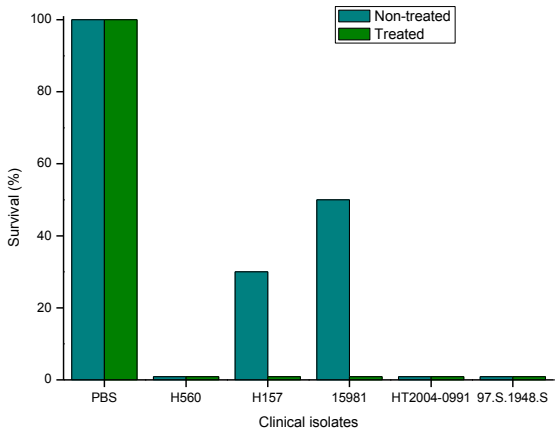

Figure 5.6: Percentage of *G. mellonella* survival infected with *S. aureus* clinical strains at 24 hours in treated and non-treated groups.

5.4.5. Phage treatment of *S. aureus* infection at different temperatures

Another strategy was used in order to test if the strong immune response to the bacterial debris was caused by phage cell lysis, we established parallel experiments run at two different temperatures – 26 °C and 37 °C. The lower temperature should slow down the proliferation of the bacteria as well as the immune response to the infection and cell debris. The phage MOIs administered were also lowered for both experiments – 0.1, 0.01 and 0.001 – resulting in lower cell burst. Hence, larvae infected with *S. aureus* MRSA 252 at OD 1 and incubated at 26 °C or 37 °C for infection to establish and treated after 2 hours with the different phage MOIs. Larvae were infected with *S. aureus* MRSA 252 (~OD 1.0) and survival of larvae was followed over 48 hours. The uninfected groups (PBS only) did not result in larvae death, although in some

cases 10 % mortality was observed, probably by chance. For the group studied at 26 °C, for all infected larvae, a lower mortality rate was observed than the one observed for the group kept at 37 °C (Figure 5.7AB). For example, after 48 hours the survival rate at 26 °C for infected larvae not treated was 55 % compared to no survival at 37 °C.

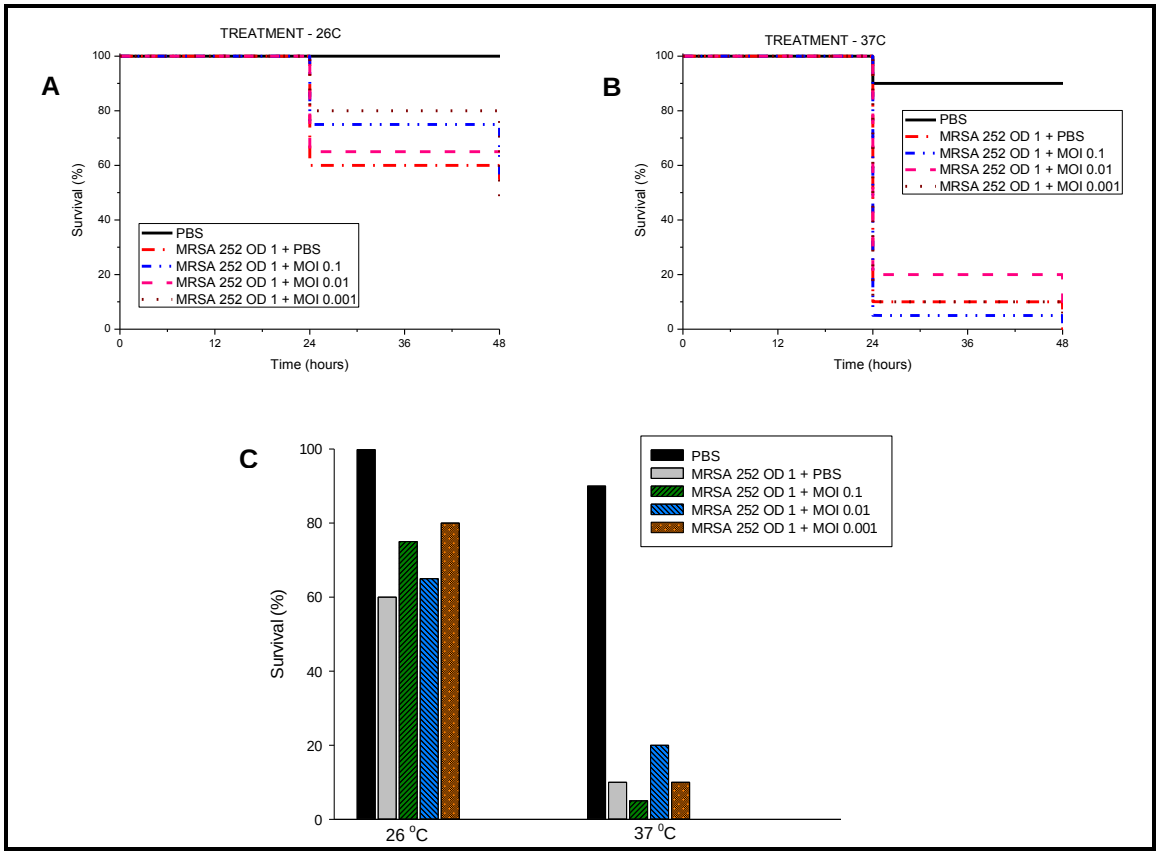

Figure 5.7: Survival of *G. mellonella* larvae infected with *S. aureus* MRSA 252 at OD~1.0 treated 2 hours post-infection with phage cocktail at MOI 0.1, 0.01 and 0.001, incubated at two different temperatures (A – 26 °C, B – 37 °C). C - C. Percentage of *G. mellonell**a*** survival at 24 hours. OD, optical density.

At 26 °C we observed that the phage cocktail showed some success at maintaining larvae survival. After 24 hours untreated larvae showed a survival rate of 60 % and when treated with phage there was a survival improvement; 75 %, 65 % and 80 % for MOIs 0.1, 0.01 and 0.001, showing better protection was observed at lower phage concentrations (Figure 5.7C). For the experiment run at 37 °C, after 24 hours there was

10 % survival for the untreated larvae and 20 % for the larvae treated with MOI 0.01. MOIs 0.1 and 0.001 showed a 5 % and 10 % survival rate (Figure 5.7C), however the survival curves were not statistically significant different ($P > 0.05$).

5.4.6. Phage protection of *S. aureus* infection at different temperatures

A similar experiment performed to study the phage cocktail treatment efficacy was performed to assess the infection protection efficacy on the larvae. For this purpose, larvae were administered phage at varying MOIs - 0.1, 0.01 and 0.001 – and incubated, one group at 26 °C and other at 37 °C. Here the viral particles were allowed to distribute along the host system. Two hours later, all larvae were infected with *S. aureus* MRSA 252 and their survival was observed over 48 hours. For this experiment the uninfected groups (PBS only) also did not result in larvae death, although 10 % mortality was observed for group kept at 37 °C. For the group kept at 26 °C (Figure 5.8A) only the larvae receiving a prophylactic phage dose of MOI 0.1 showed a more successful reduced mortality rate when compared to the non-treated group, 80 % vs 50 % at 24 hours ($P = 0.02$) (Figure 5.8C). The other two phage doses didn't show any protection effect, both 45 % of survival rates. For the group incubated at normal mammalian temperature all three prophylactic phage doses showed an improvement of larvae survival compared to the non-treated group (Figure 5.8B). At 24 hours, the untreated group only showed 10 % larvae survival compared to 20 %, 15 % and 25 % for MOIs 0.1, 0.01 and 0.001, respectively (Figure 5.8C). Still, the survival curves were not statistically significant different ($P > 0.05$).

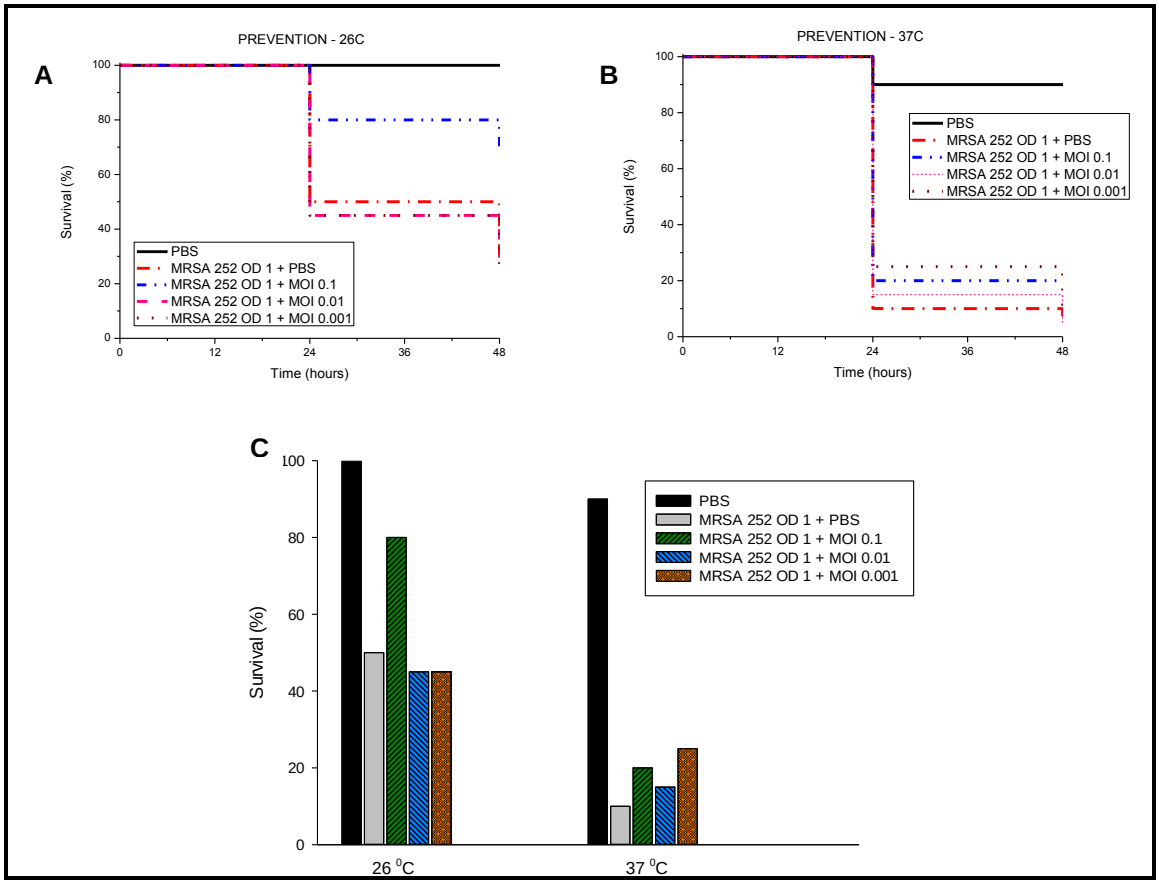

Figure 5.8: Survival of *G. mellonella* larvae infected with phage cocktail at MOI 0.1, 0.01 and 0.001 and infected with *S. aureus* MRSA 252 at OD 1 two hours after incubated at two different temperatures (A – 26 °C, B – 37 °C). C - Percentage of *G. mellonella* survival at 24 hours. OD, optical density.

5.4.7. Survival curves for *P. aeruginosa* infection and phage treatment

In this study phage and infection interactions were examined under a treatment model. Larvae were infected with either 10 or 100 cells of *P. aeruginosa* PAO1, confirmed by a colony plate assay, and left to allow an infection to establish for two hours. Varying MOIs of phage were then administered and death was observed over 48 hours. No mortality was recorded in the PBS controls and non-treated larvae died quicker when infected with 100 cells vs 10 cells. Administration of phage prolonged the survival of the larvae in a dose dependent manner, but no survival was eventually seen in all groups by 30 hours (Figure 5.9). At 24 hours there was 100 % mortality in the infected non-

treated larvae, but 40 % survival for those infected with 10 cells and treated with an MOI of 10 compared with 20 % survival with those infected with 100 cells at the same MOI (Figure 5.9C). A statistically significant difference was observed between the treated and non-treated survival curves ($P < 0.0001$).

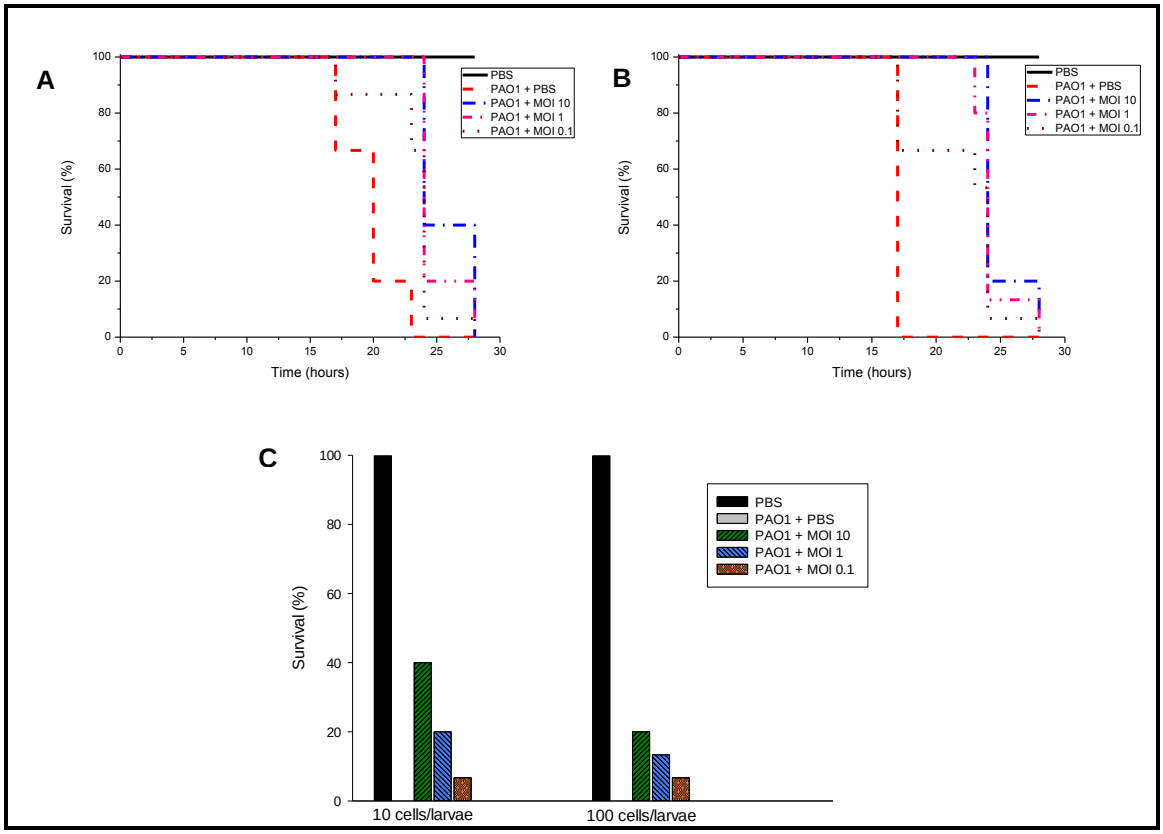

Figure 5.9: Kaplan-Meier survival curves of *G. mellonella* infected with (A) 100 cells or (B) 10 cells of *P. aeruginosa* PAO1 and treated with phage at varying multiplicities of infection two hours post-infection. C. Percentage of *G. mellonella* survival at 24 hours.

5.4.8. Phage protection from *P. aeruginosa* infection

A phage protection model was also performed to assess its efficacy on larvae survival. Larvae were given varying prophylactic doses of phage two hours prior to infection with *P. aeruginosa* PAO1. Similarly to the treatment experiment, larvae infected with 100 cells died quicker than those infected with 10 cells when given PBS two hours before

infection (Figure 5.10). At 24 hours, survival rates ranged from 80 % in larvae given an MOI of 100 to 35 % in those given an MOI of 0.1 (Figure 5.10C). Survival ranged from 90 % to 60 % in *Galleria* given MOIs of 100 and 1, respectively. A statistically significant difference was observed between the treated and non-treated survival curves ($P < 0.0001$).

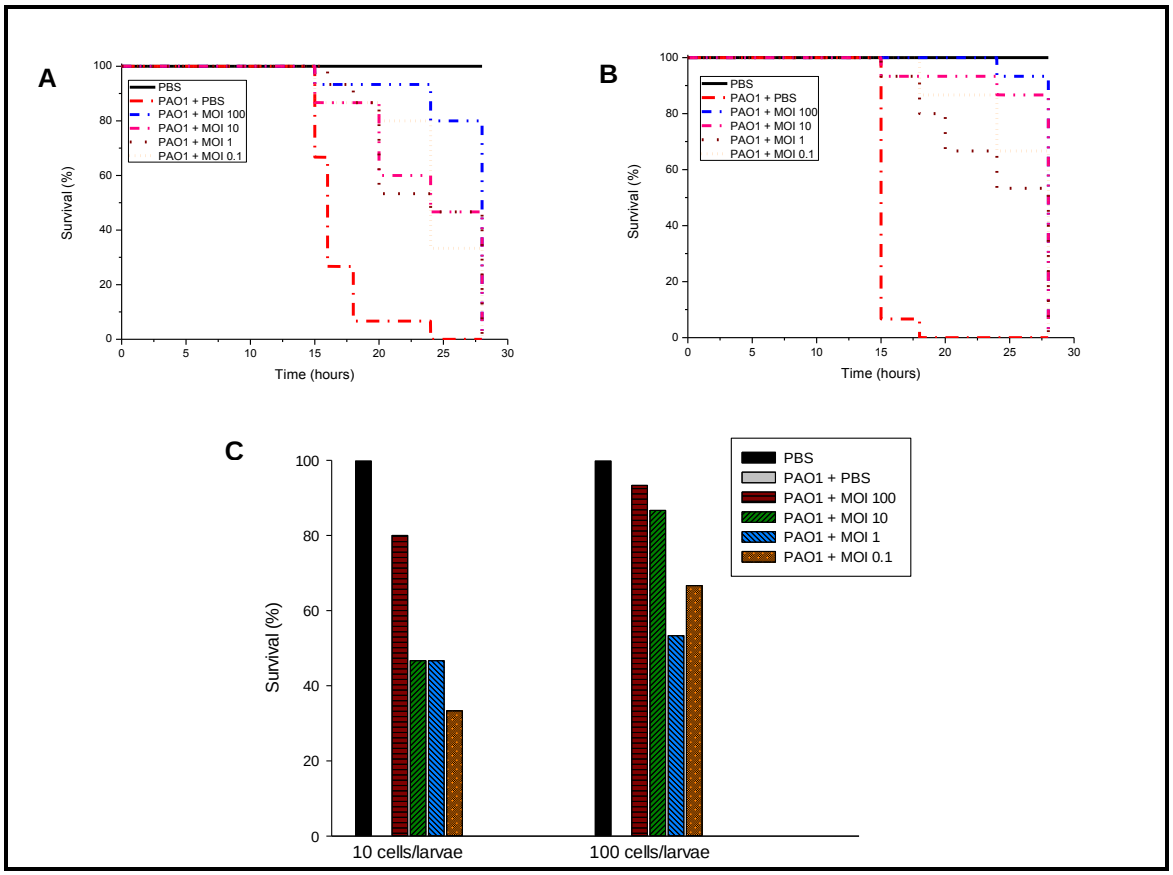

Figure 5.10: Kaplan-Meier survival curves of *G. mellonella* infected with (A) 100 cells or (B) 10 cells of *P. aeruginosa* PAO1 and pre-treated with phage at varying multiplicities of infection two hours pre-infection. C. Percentage of *G. mellonella* survival at 24 hours.

5.4.9. Clinical isolates of *P. aeruginosa*

To validate the model of phage therapy with *P. aeruginosa* we decided to test the protection assay with two clinical strains isolated from cystic fibrosis patients experiencing acute and chronic episodes of *P. aeruginosa* infections. With the

PA45291 acute strain all infected larvae were dead by 24 hours whereas a 60 % survival was observed at 28 hours in the group which were pre-injected with phage at an MOI 10 ($P < 0.0001$). When larvae were infected with the BC09007 chronic strain there was little death at 24 hours (90 % survival) for the infected non-protected larvae, but 100 % survival in the phage protected group. By 40 hours all larvae were dead (Figure 5.11).

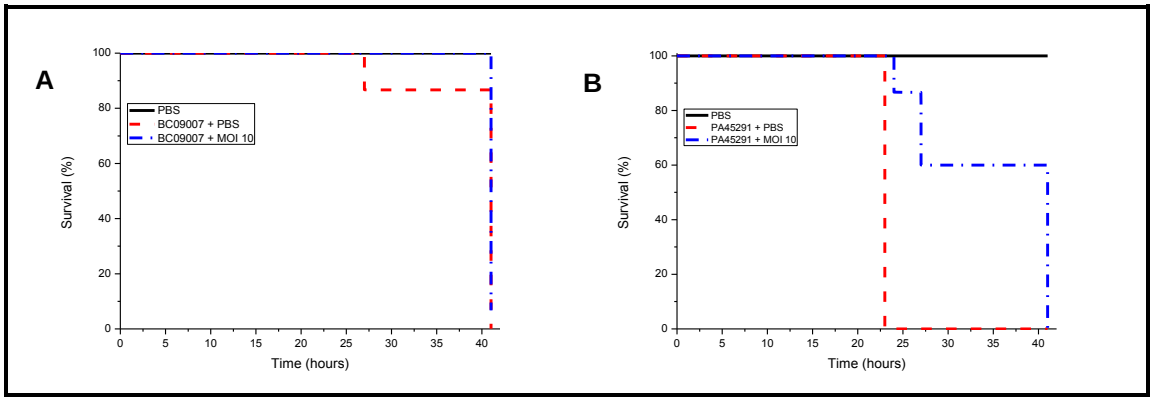

Figure 5.11: Survival curves of *G. mellonella* infected with 10 cells of (A) acute *P. aeruginosa* PA45291 or (B) chronic P. aeruginosa BC09007 and pre-treated with phage at an MOI 10 two hours pre-infection.

5.4.10. Comparison of single and double phage treatment of *P. aeruginosa* infection

To verify if the unsuccessful treatment or infection protection by the phage was the cause of larvae death at the end of experiments where all larvae eventually died, we administered a second dose of phage two hours after the first treatment dose. The first dose showed an MOI 100 compared to the bacterial inoculum injected in the larvae and the second dose had the same concentration, although at the moment of the second dose (four hours after infection) the concentration of bacteria most probably had triplicated. We observed no difference on the survival rates of the larvae challenged with one and two phage treatments, both showing at 26 hours and 48 hours post-

infection 73.33 % and 6.67 % survival compared to no survival in the non-treated group (Figure 5.12). This suggests that the cause of larvae death was not a lack of phage.

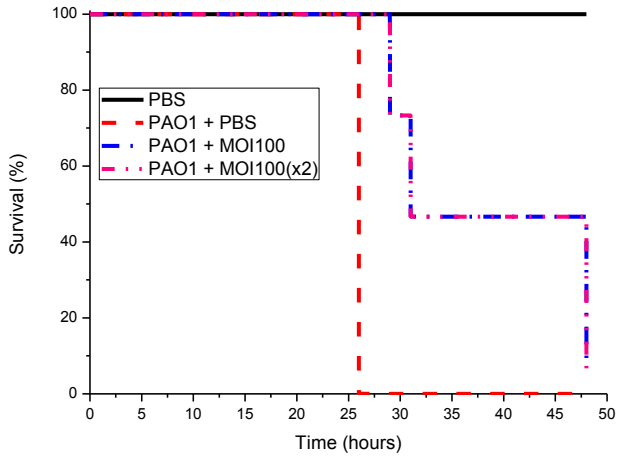

Figure 5.12: Survival curves of *G. mellonella* infected with 100 cells *P. aeruginosa* PAO1 and single or double treated with phage at an MOI 100 with two interval from each injection.

5.4.11. Kinetics of *P. aeruginosa* infection and effect of phage treatment

In order to understand the kinetics of a *P. aeruginosa* infection within *G. mellonella* (Figure 5.13), larvae were infected with 100 cells using the protection model of infection. Bacteria and phage were quantified at three set time points by bleeding the haemolymph of the larvae. No endogenous *P. aeruginosa* cells or phage particles with lytic activity against *P. aeruginosa* PAO1 were detected in the uninfected controls for all the time points. For the larvae which were given only *P. aeruginosa* PAO1, control group, the numbers of cells isolated from the haemolymph increased over the duration of the experiment. By 24 hours all larvae were dead and numbers of *P. aeruginosa* were in the order of 10^8 cfu/larvae. The second group of larvae were given a prophylactic dose of phage 2 hours before the infection and phage and bacteria were then quantified over the course of infection. Numbers of *P. aeruginosa* PAO1 were comparable to that of the non-treated larvae after 8 hours infection, but were three orders of magnitude lower at 24 hours compared with the group lacking phage

prophylaxis. These larvae were alive at 24 hours. Numbers of phage increased over the duration of the infection reaching a peak titre at 24 hours of 10^8 pfu/larvae. Bacterial colonies from both groups were grown and challenged with the phage cocktail *in vitro* under planktonic conditions (Figure 5.14). PAO1 from lab stock was used as a control. We observed that bacteria recovered from the treated group had possibly undergone a mutation that had improved their fitness, resulting in a faster growth. The bacteria recovered from the untreated group showed a similar growth curve as PAO1 from the stock. However, all three cultures when growing in the presence of the phage showed no signs of resistance.

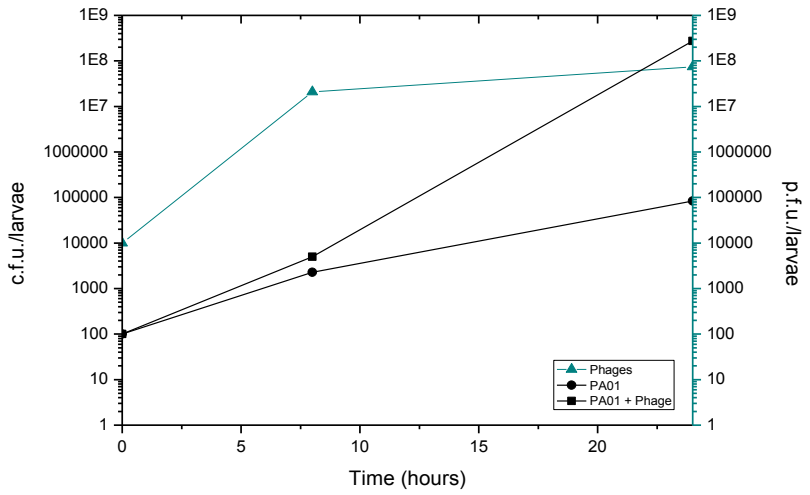

Figure 5.13: *in vivo* kinetics of P. aeruginosa infection within *G. mellonella* with and without phage treatment.

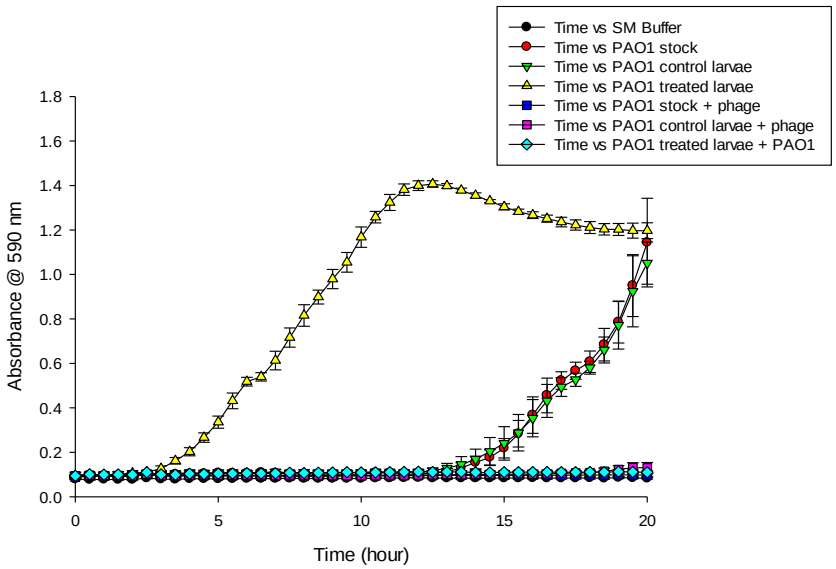

Figure 5.14: Dynamics of bacterial colonies recovered from non-treated and phage treated *G. mellonella* larvae when grown with the phage cocktail in planktonic cultures.

5.5. Discussion

Antibiotic resistance among human bacterial isolates is a worrying fact nowadays that is commonly seen and is becoming the rule rather than the exception. *S. aureus* and *P. aeruginosa* are at the top of the list with resistance profiles for more than one antibiotic class. Both bacteria are known to cause systemic infections (358, 359) that usually end up in the patient's death if not effectively treated (360). Phage therapy is considered an encouraging novel therapeutic alternative to antibiotics, especially for those bacteria showing increased resistance to the main antibiotics available. As with any other therapeutic product, phage therapy is required to be assessed on *in vivo* models. However, as a first line assessment, using *in vivo* models might provide some hurdles, such as the lack of appropriate facilities and obtaining ethical approval. The *G. mellonella* infection model usually provides an additional intermediate step between *in vitro* and *in vivo* mammalian studies.

Two models of infection were performed for both *S. aureus* and *P. aeruginosa* – infection treatment and infection protection by use of phage cocktails. For the first situation, infection was allowed to establish for 2 hours prior to administration of phage, for the second situation phages were administered 2 hours prior infection.

The strain *P. aeruginosa* PAO1 proved to be more virulent than the strain *S. aureus* MRSA 252 in the *G. mellonella* model, where only 10 cells per larvae were required to result in death in 24 hours. For the *S. aureus* strains an inoculum of 10^5-10^6 cells/per larvae was required for an infection to be established and cause larvae death, which is in accordance to previous studies (354). Similar numbers have been recorded for *Helicobacter pylori* infections on *G. mellonella*, with a requirement of 10^6-10^7 cells, and *Acinetobacter baumannii* requiring at least 10^4 cells per larvae (361, 362). A low infectious dose will result in reduced endotoxin and other bacterial debris being released upon phage infection into the host, causing a quieter activation of the immune

responses. This may be the explanation for the outcomes observed for larvae infected with *S. aureus*. When phages were added at MOI 1 or 10 larvae death was more rapid, suggesting that the burst of the bacteria in such a short time was causing a greater immune response not manageable by the host. Five different clinical isolates were also tested, with the treatment model, and the same pattern was always observed. However, when using *S. aureus* MRSA 252 such faster death was not observed when administering MOIs lower than 1 and it was even more successful when the incubation temperature was at 26 °C. At this low temperature also the bacteria replicate slower and probably are less virulent (350). Therefore, phage proliferation would consequently occur more slowly as would the release of bacterial debris and endotoxin-like material. If this is the scenario occurring then the host is not confronted with such a massive quantity of cell debris and antigenic material and activation of the host defences develops at a slower pace. The *G. mellonella* model is considered a model for studying systemic infections, therefore these results are important in case of a human bacteraemia, and where the event of an anaphylactic shock is an event to avoid as will result ultimately in the patient's death. The situation certainly is different if dealing with a local infection, such as a burn wound, where the infection is restrained and easier to handle and resolve. Endotoxins apart from their high toxicity are known to be highly immunogenic. Usually endotoxin refers to the gram-negative lipopolysaccharide (LPS) and gram-positive bacteria do not have LPS. However, gram-positive bacteria produce several cellular toxins such as exotoxins (previously discussed in Chapter One), especially in their log-phase when they are actively growing. This is clearly the case with several *S. aureus* strains which produce a number of exotoxins. These exotoxins are highly immunogenic in mammals and so it can be hypothesised that this is the phenomenon that we are observing when the bacteria lyse (363). When performing lysis *ex vivo*, however the same mortality effect was not observed. This might suggest the production of an intermediate compound during the lysis that is released causing the massive shock, which when lysis is performed *ex vivo* is not present anymore (due

to lack of stability, for example). Another hypothesis is that the immune system is to deal with the invasion as soon as the lysate is injected. When performing both infection and treatment injection perhaps the bacteria had time to spread along the host, phage particles then would have to find the bacteria. During the time for phage to attach to bacteria, the bacterial cells themselves are proliferating, increasing the number of cells as well the amount of cell debris (upon cell burst). A heat-inactivated bacterial inoculum was also given to a group of larvae, in order to rule out the contribution of the antigenic cell wall of live bacteria to the strong immune response observed. However, as expected, such contribution was not observed. Heat causes changes to the surface of the bacteria making them less susceptible and less immunogenic (364). In conclusion, the results suggest the existence of a thin equilibrium when using *G. mellonella* infected by *S. aureus* cells and treated with phage, where a high number of phage particles in relation to bacterial cells cause the death of the host, but a low number of phage particles is not enough to protect the host from the pathogenic bacteria. It was also noticed that, although the ODs injected were always approximately equal to 1 the survival rates for larvae was very variable, sometimes displaying a 50 % death during the first 24 hours and at other time only at 48 hours. This was not seen for *P. aeruginosa* strains injected into the model. Such a fact may be related to the injection procedure where 10 µl is difficult to accurately administer. Hence, if we administered a couple of extra µl, the cell concentration will greatly differ for *S. aureus* strains. For example, in the case of *P. aeruginosa* strains – 10 µl contain 10 cells and 12 µl will have 2 more cells. For *S. aureus* strains - 10 µl contain $1x10^6$ and 12 µl have $2x10^5$ more bacteria. This applies to the phage injections as well. In conclusion, to accurately perform experiments for *S. aureus*, where we clearly need to have a perfect equilibrium between amount of phage and bacterial cells, the *G. mellonella* model might not be suitable for assessing phage treatment for a *S. aureus* systemic infection.

Regarding *P. aeruginosa*, experiments were shown to be more successful in terms of phage therapy. At all MOIs of phage there was a prolonged survival of the larvae regardless whether 10 or 100 bacterial cells were used as the inoculum, although the survival rates were higher when administering the lower inoculum. Probably the 10-fold higher inoculum of 100 cells vs 10 cells had meant that the infection had become more firmly established within the two hour time frame therefore reducing the efficacy of the phage to prolong survival. The protection assay showed the ability of phage to protect from infection using a prophylactic administration of phage two hours prior to infection. When compared with the treatment model, prophylactic administration of phage resulted in greater survival after 24 hours at all comparable MOI values. Presumably this increased efficacy was the result of phage being able to distribute throughout the haemolymph over the two hour period prior to infection, whereas in the treatment model the bacteria will have had opportunity to establish and begin to express toxins. Interesting was the observation of greater survival among larvae which received the higher inoculum of 100 cells, compared with 10 cells. This may have been due to the higher number of bacterial cells resulting in an increased chance of bacteria and phage interaction resulting in a more rapid amplification of the phage. For all *P. aeruginosa* experiments eventually larvae succumbed to the infection resulting in death by 30 hours post-infection. For this reason, the kinetics of bacterial cells throughout the infection as well as the phage numbers (in the treated experiments) was explored *in vivo*. The most striking observation was the comparison between numbers of *P. aeruginosa* cells in the phage treated and untreated larvae. At 24 hours the phage had kept the number of bacterial cells to 1000-fold less than the non-treated larvae, but even in the presence of high titres of phage there had still been active growth, and therefore infection, from the *P. aeruginosa* over the duration of the experiment. The death observed could suggest a lack of available phage to target the remaining bacterial cells. However, the kinetics assay showed that this was not the case due to the high titre of phage within the haemolymph, although the MOI had shifted from 100

to less than 1 by 24 hours. Such hypothesis was also ruled out by an experiment where larvae were given a second dose of phage four hours after an initial dosing, but there was no difference when compared with the single dose control. One possibility for the continual survival of PAO1 in the presence of a high titre of phage was the evolution of phage resistance within the larvae. This was ruled out after observation of no bacterial growth when co-cultivating *P. aeruginosa* single colonies, recovered at 24 hours after phage treatment, and a suspension of phage cocktail. A final explanation for the survival would be the unavailability of *P. aeruginosa* cells due to intracellular localisation. *P. aeruginosa* is known to have the ability to invade epithelial cells which might protect them from attack by the phage (365) and in these experiments only bacterial numbers were examined within extracted haemolymph. This highlights one of the limitations of phage therapy on pathogens which are able to exist and replicate in an intracellular environment. Phages, unlike some antibiotics, are not diffusible across membranes and perhaps combination therapy with antibiotics which can enter host cells such as a fluoroquinolone or tetracycline would have aided in clearance. This potential intracellular survival strategy would also explain why the protection model showed improved survival compared with the treatment model where the *P. aeruginosa* will have had time to establish within cells before larvae received a dose of the phage. However, there must have been a degree of extracellular replication of cells within the haemolymph to allow for the observed propagation of the phage over time. Another possibility could be the escape of bacterial cells close to tissue being protected from the phage infection (246). Finally, the effectiveness of the phage model on clinical isolates of *P. aeruginosa* was also assessed regarding phage protection. An acute and a chronic CF infection causing isolates were used. Here, the acute isolate resulted in rapid death of larvae within 24 hours and the chronic isolate was less virulent at 24 hours compared with the acute and PAO1 strains, but 100 % mortality was then seen by 40 hours.

In conclusion we present data for the use of the *G. mellonella* as a simple, robust and cost-effective model for initial examination *P. aeruginosa* targeted phage therapy, but perhaps more complex in the case of a *S. aureus* infection.

Chapter Six:

CONCLUSIONS AND FURTHER WORK

6.1. Conclusions

The aim of this thesis was to select suitable, safe and efficacious phage candidates against *S. aureus* and *P. aeruginosa* clinical strains and to validate their ability to reduce and control bacterial biofilms produced by the bacteria aforementioned. With those aims, this thesis was divided into two main chapters.

The first one (Chapter Three) describes the whole process of phage isolation, after which phages shown to be lytic with broad host ranges were selected and their detailed characterisation was performed. The sensitivity assays against clinical isolates proved to be valuable not only to discard phages employing lysogenic cycles, but also to better select phages able to infect as broader range of isolates as possible, whether because the phage strategy to infect the cell is fairly conserved within the bacterial group (*S. aureus* phages) or because the combination between several phages covers the majority of the clinical isolates (*P. aeruginosa* phages), a feature required for a phage therapeutic cocktail as in an infection situation where immediate treatment is required, and the pathogen might not be fully identified. To characterise the phages regarding their morphology, TEM analysis was performed as this also helped to discard *Siphoviridae* type phages that were to be avoided in the case of *S. aureus* phages and also to assure the purity of the phage suspension. For further characterisation, a whole genome sequencing and analysis of the isolated phages was performed as this is a prerequisite in a post-genomic era when isolating and studying phages that are potentially to be applied therapeutically. Genome sequencing can reveal not only what genes are present and their function, but also their organisation into the genome. This is then valuable for comparisons with previously isolated and studied phages, allowing identification of the morphology and to allocate them into an existing group or in the case of a unique phage, create a new taxonomic group. Also, it tells us of the presence of factors enabling the phage to produce a lysogenic infection which in the case of this thesis would rule out the phage for therapeutic use, and to a certain level, the presence

of toxin or antibiotic resistance genes can be evaluated. Genome sequencing can be of value in the future for development and production of phage-based products such as lysins or depolymerases, and also for genetic modification of phages. Phages DRA88, a *Myoviridae*, together with phage K formed the cocktail to target *S. aureus* strains. Regarding *P. aeruginosa* strains, a cocktail made of six phages was established, where DL52, DL60 and DL68 belong to the *Myoviridae* family and all belonging to the same group (PB1-like group) sharing high similarities, and DL54, DL62 and DL64 belong to the *Podoviridae* family, but all three in different groups. No virulence or toxin factors were identified; however genes with no attributed function remain as the majority of the genome. Hopefully, with the availability nowadays of an easy access to sequencing (fast and relatively cheap) a growing number of phage sequences have been generated and this will help to better understand phages and their relationships. With continuous and deeper study of phage genes and protein structure, these unknown gene functions can be identified.

The following chapter (Chapter Four) assessed the ability of the selected cocktails to inhibit or reduce bacterial growth while this takes place under planktonic conditions, but it goes further exploring the lytic aptitude for reducing and dispersing biofilm communities, whether those were performed under static conditions or dynamic ones. Such reduction was observed whether the isolates carried antibiotic resistance factors or not. The growth of phage with bacteria under planktonic conditions allows observing of their dynamics and how fast resistance can be achieved by the bacteria to the phages. However, the bacterial biofilm mode of living is the rule in nature and obviously the same is observed when, for example, a wound infection occurs, and therefore the biofilm mode must be included when studying lytic phages. The two biofilm models established allowed the observation that both cocktails were efficient in bringing down established biofilm communities, however at a slower pace than the one observed for planktonic cultures and even slower when comparing the static to the dynamic biofilm

systems, where the last one was shown to be removed at a slower speed. The flow model was performed to achieve a more realistic resemblance to an *in vivo* situation. Both cocktails proved to powerfully reduce the number of bacterial cells attached to the stainless steel surfaces, although the effect was more significant in the case of the *P. aeruginosa* cocktail when treating the PAO1 biofilm.

These two chapters were then followed by Chapter Five, where the phage cocktails, already assessed for their suitability and efficacy for potentially treating infectious diseases caused by biofilm production, are assessed for the ability to treat systemic infections from *S. aureus* and *P. aeruginosa* in an *in vivo* larvae infection model. Here, the phage cocktails were not assessed for biofilm removal, but rather for a bacteraemia where the infection is established and spread through the system of the larvae. For the case of *S. aureus,* the high level of bacterial cells that had to be injected to cause a lethal infection was so high that it enabled us to observe a positive phage influence towards the treatment of the larvae. And often the opposite was observed, when the phages were applied a higher mortality was observed, most probably due to the high number of cells being burst in a short period of time. This relates to the fact that when treating bacteraemia, the endotoxin release should be taken into account and carefully considered for *in vivo* animal models to avoid an anaphylactic shock in the patient. Perhaps phage therapy would have a better outcome when treating localised infections and maybe other approaches should be used when treating systemic infections, for example the use of genetically modified phages that kill the bacterium but do not cause it to burst. In the case of *P. aeruginosa* it was possible to observe that the phage extended the survival of the larvae, although not being able to fully treat and allow the larvae to recover from the infection. Hence, the *G. mellonella* model can be considered a very good model before going to higher animal systems to study bacterial infections that only need a low infectivity dose.

This work shows how phages can be employed as an alternative to reduce and treat bacterial infections, especially those ones growing under a biofilm community and showing antibiotic resistant profile. However, not all the isolates have been tested with these phage cocktails and there might be a situation where the phage cocktail might not be enough for complete infection removal, and synchronisation with other alternatives, such as bacteriocins for example, is the key. Even an antibiotic drug will help by bringing the bacterial cell numbers down to a level where the immune system can deal with and resolve the infection.

The main focus of this thesis was the reduction and control of biofilms involved in infections; however it could even be extended to treat decontamination of hospital equipment or indwelling devices that would benefit from an additional method of sterilization. Such use of phages might reduce the need for antibiotic drugs in the case of treatment of human diseases as well as reduce the amount of chemicals and detergent used to treat wastewater and decontaminate medical devices.

6.2. Further work

The work presented in this thesis can be seen as a starting point for several other lines of investigation to achieve a deeper understanding of the potential of phage to treat bacterial infections.

Regarding the *S. aureus* cocktail, considering that both phages are highly similar it would be worthwhile to isolate and add another phage type, perhaps targeting those isolates resistant to the other two phages. Regarding *P. aeruginosa*, the phage cocktail can be further characterised, such as the growth parameters of each phage can be studied and the cocktail can be tested using clinical isolates, by performing treatment of planktonic cultures and biofilm communities.

It would be interesting to further analyse the aggregation phenomenon observed, by using long tailed phages, such as DRA88 (*Myoviridae*) and short tailed ones, such as DL62 (*Podoviridae*) using the DLS technique. This could be achieved by changing the buffer compositions, such as the concentration of ions, pH or temperature and measure their size in the suspension. To complement such a study, it would be interesting to perform plaque assays in order to estimate their titre and analyse if the composition of therapeutic phage suspension can have an effect on how efficiently phages can attach and infect bacterial cells.

Also, a preliminary study coupling the use of phage with antibiotic has been performed here, this can be taken further by performing a large screening involving several antibiotics, phages and clinical isolates. Not only antibiotics can be included in such a study, but other alternatives being investigated at the moment, such as antimicrobial peptides could be included in the study and possible bacterial biofilm reduction synchronisation effects explored.

The biofilms performed on the Modified Robbins Device can be better improved and several parameters can be investigated, for example by studying different clinical isolates, but also by using different growth media with a composition resembling more a realistic infection environment, for example a burn wound or a leg ulcer wound infection. Also, for better biofilm maturation it is recommended to allow the experiment to run for longer, perhaps two to four additional days, with the inclusion of a bubble trap at the start of the device, removing possible air bubbles that often are formed and once inside the lumen of the device can disrupt parts of the formed biofilms. Besides the Robbins Device, other dynamic systems can also be implemented to study the action of the phages on biofilms, such as the flow cell.

Finally, it should be noted that the next sensible step would be the performance of dual species biofilms with *P. aeruginosa* and *S. aureus*, the main bacteria present in biofilm wound infections, where the use of both phage cocktails could be employed and their

eradication efficacy explored. Further down the line and in a more complex way, isolation of phages to *Klebsiella pneumonia* and *Acinetobacter baumannii* would allow the study of the potential of multispecies phage cocktails to eliminate multispecies biofilms.

The sequencing of the phages genomes can allow a more thorough investigation and manipulation of the genomes could be an option to improve the polyvalent character of a phage, for example in the case of *P. aeruginosa*, it would benefit from having phages less host specific. Also, a screen looking for depolymerases enzymes within the genome could be employed and protein expression and purification of those enzymes could be used to study their effect on eliminating or dispersing biofilms by themselves.

Lastly, a sensible investigation step would be testing the phage cocktails on *in vivo* animal models, such as a murine model, where a thermal injury could be induced to establish then an infection and phage cocktail applied to the infected area. Monitoring of such experiment could give very promising results on the use of these phage cocktails to be used in a therapeutic way.

Bibliography

1. **Rice LB**. 2009. The clinical consequences of antimicrobial resistance. Curr. Opin. Microbiol. **12**:476–81.

2. **Taubes G**. 2008. The bacteria fight back. Science **321**:356–61.

3. **Ling LL, Schneider T, Peoples AJ, Spoering AL, Engels I, Conlon BP, Mueller A, Schäberle TF, Hughes DE, Epstein S, Jones M, Lazarides L, Steadman VA, Cohen DR, Felix CR, Fetterman KA, Millett WP, Nitti AG, Zullo AM, Chen C, Lewis K**. 2015. A new antibiotic kills pathogens without detectable resistance. Nature **517**:455–459.

4. **Bush K, Macielag M, Weidner-Wells M**. 2004. Taking inventory: antibacterial agents currently at or beyond phase 1. Curr. Opin. Microbiol. **7**:466–76.

5. **Fair RJ, Tor Y**. 2014. Antibiotics and bacterial resistance in the 21st century. Perspect. Medicin. Chem. **6**:25–64.

6. **Siegel RE**. 2008. Emerging gram-negative antibiotic resistance: daunting challenges, declining sensitivities, and dire consequences. Respir. Care **53**:471–9.

7. **Spellberg B, Blaser M, Guidos RJ, Boucher HW, Bradley JS, Eisenstein BI, Gerding D, Lynfield R, Reller LB, Rex J, Schwartz D, Septimus E, Tenover FC, Gilbert DN**. 2011. Combating antimicrobial resistance: policy recommendations to save lives. Clin. Infect. Dis. **52 Suppl 5**:S397–428.

8. **ECDC/EMEA**. 2009. The bacterial challenge : time to react. European Center for Disease Prevention and Control (ECDC) & European Medicines Agency (EMA).

9. **Nyquist AC, Gonzales R, Steiner JF, Sande MA**. 1998. Antibiotic prescribing for children with colds, upper respiratory tract infections, and bronchitis. JAMA **279**:875–7.

10. **Bergus GR, Levy BT, Levy SM, Slager SL, Kiritsy MC**. 1996. Antibiotic use during the first 200 days of life. Arch. Fam. Med. **5**:523–6.

11. **Blaser M**. 2011. Antibiotic overuse: Stop the killing of beneficial bacteria. Nature **476**:393–4.

12. **Aarestrup FM, Wegener HC, Collignon P**. 2008. Resistance in bacteria of the food chain: epidemiology and control strategies. Expert Rev. Anti. Infect. Ther. **6**:733–50.

13. **WHO**. 2003. Joint FAO/OIE/WHO Expert Workshop on Non-Human Antimicrobial Usage and Antimicrobial Resistance: Scientific assessmentWorld Health Organization. World Helalth Organization.

14. **Huh AJ, Kwon YJ**. 2011. “Nanoantibiotics”: a new paradigm for treating infectious diseases using nanomaterials in the antibiotics resistant era. J. Control. Release **156**:128–45.

15. **WHO**. Governing Body Documentation. Official Records.

16. **WHO**. 2001. Global Strategy for Containment of Antimicrobial Strategy for Containment of Antimicrobial Resistance. WHO Press.

17. **European Commission**. 2011. Communication from the Commission to the European Parliament and the Council - Action plan against the rising threats from Antimicrobial Resistance.

18. **European Council**. 2012. Council conclusions on the impact of antimicrobial resistance in the human health sector and in the veterinary sector – a “One Health” perspective. Eur. Counc. **32**:1–6.

19. **European Community**. 2003. Regulation (EC) No 1831/2003 of the European Parliament and of the Council of 22 September 2003 on additives for use in animal nutrition (Text with EEA relevance). Off. J. **L 268**:29–43.

20. **FDA**. Press Announcements - FDA takes steps to protect public health.

21. **Department of Health, Department for Environment Food and Rural Affairs**. 2013. UK Five Year Antimicrobial Resistance Strategy 2013 to 2018.

22. **Grice EA, Segre JA**. 2011. The skin microbiome. Nat. Rev. Microbiol. **9**:244–53.

23. **Shai A, Halevy S**. 2005. Direct triggers for ulceration in patients with venous insufficiency. Int. J. Dermatol. **44**:1006–9.

24. **Hermans MHE, Treadwell T**. 2010. An introduction to wounds, p. 83–114. *In* Percival; Steven; Cutting; Keith (ed.), Microbiology of wounds. CRC Press, New York.

25. **Wolcott R, Cutting KF, Dowd SE**. 2008. Surgical site infections: biofilms, dehiscence and delayed healing. US Dermatol 56–59.

26. **Turner KH, Everett J, Trivedi U, Rumbaugh KP, Whiteley M**. 2014. Requirements for Pseudomonas aeruginosa acute burn and chronic surgical wound infection. PLoS Genet. **10**:e1004518.

27. **Bowler PG, Duerden BI, Armstrong DG**. 2001. Wound microbiology and associated approaches to wound management. Clin. Microbiol. Rev. **14**:244–69.

28. **Dowd SE, Sun Y, Secor PR, Rhoads DD, Wolcott BM, James GA, Wolcott RD**. 2008. Survey of bacterial diversity in chronic wounds using pyrosequencing, DGGE, and full ribosome shotgun sequencing. BMC Microbiol. **8**:43.

29. **Agnihotri N, Gupta V, Joshi RM**. 2004. Aerobic bacterial isolates from burn wound infections and their antibiograms--a five-year study. Burns **30**:241–3.

30. **Bayram Y, Parlak M, Aypak C, Bayram I**. 2013. Three-year review of bacteriological profile and antibiogram of burn wound isolates in Van, Turkey. Int. J. Med. Sci. **10**:19–23.

31. **Djahmi N, Messad N, Nedjai S, Moussaoui A, Mazouz D, Richard J-L, Sotto A, Lavigne J-P**. 2013. Molecular epidemiology of Staphylococcus aureus strains isolated from inpatients with infected diabetic foot ulcers in an Algerian University Hospital. Clin. Microbiol. Infect. **19**:E398–404.

32. **Church D, Elsayed S, Reid O, Winston B, Lindsay R**. 2006. Burn wound infections. Clin. Microbiol. Rev. **19**:403–34.

33. **Frank DN, Wysocki A, Specht-Glick DD, Rooney A, Feldman RA, St Amand AL, Pace NR, Trent JD**. 2009. Microbial diversity in chronic open wounds. Wound repair Regen. **17**:163–72.

34. **Madsen SM, Westh H, Danielsen L, Rosdahl VT**. 1996. Bacterial colonization and healing of venous leg ulcers. APMIS **104**:895–9.

35. **Pallua N, Fuchs PC, Hafemann B, Völpel U, Noah M, Lütticken R**. 1999. A new technique for quantitative bacterial assessment on burn wounds by modified dermabrasion. J. Hosp. Infect. **42**:329–37.

36. **Morales E, Cots F, Sala M, Comas M, Belvis F, Riu M, Salvadó M, Grau S, Horcajada JP, Montero MM, Castells X**. 2012. Hospital costs of nosocomial multi-drug resistant Pseudomonas aeruginosa acquisition. BMC Health Serv. Res. **12**:122.

37. **Morell EA, Balkin DM**. 2010. Methicillin-resistant Staphylococcus aureus: a pervasive pathogen highlights the need for new antimicrobial development. Yale J. Biol. Med. **83**:223–33.

38. **Weber J, McManus A**. 2004. Infection control in burn patients. Burns **30**:A16–24.

39. **James GA, Swogger E, Wolcott R, Pulcini E deLancey, Secor P, Sestrich J, Costerton JW, Stewart PS**. 2008. Biofilms in chronic wounds. Wound Repair Regen. **16**:37–44.

40. **Williams P**. 1994. Host immune defences and biofilms, p. 93–96. *In* Bacterial biofilms and their control in Medicine and Industry. UK:BioLine, Cardiff.

41. **Peacock SJ, de Silva I, Lowy FD**. 2001. What determines nasal carriage of Staphylococcus aureus? Trends Microbiol. **9**:605–10.

42. **Liesse Iyamba JM, Seil M, Devleeschouwer M, Takaisi Kikuni NB, Dehaye JP**. 2011. Study of the formation of a biofilm by clinical strains of Staphylococcus aureus. Biofouling **27**:811–21.

43. **Daum RS, Spellberg B**. 2012. Progress toward a Staphylococcus aureus vaccine. Clin. Infect. Dis. **54**:560–7.

44. **Patti JM, Allen BL, McGavin MJ, Höök M**. 1994. MSCRAMM-mediated adherence of microorganisms to host tissues. Annu. Rev. Microbiol. **48**:585–617.

45. **O'Riordan K, Lee JC**. 2004. Staphylococcus aureus capsular polysaccharides. Clin. Microbiol. Rev. **17**:218–34.

46. **Arbeit RD, Karakawa WW, Vann WF, Robbins JB**. 1984. Predominance of two newly described capsular polysaccharide types among clinical isolates of Staphylococcus aureus. Diagn. Microbiol. Infect. Dis. **2**:85–91.

47. **Uhlén M, Guss B, Nilsson B, Gatenbeck S, Philipson L, Lindberg M**. 1984. Complete sequence of the staphylococcal gene encoding protein A. A gene evolved through multiple duplications. J. Biol. Chem. **259**:1695–702.

48. **Foster TJ**. 2005. Immune evasion by staphylococci. Nat. Rev. Microbiol. **3**:948–958.

49. **Patel AH, Nowlan P, Weavers ED, Foster T**. 1987. Virulence of protein A-deficient and alpha-toxin-deficient mutants of Staphylococcus aureus isolated by allele replacement. Infect. Immun. **55**:3103–10.

50. **Bera A, Biswas R, Herbert S, Götz F**. 2006. The presence of peptidoglycan O-acetyltransferase in various staphylococcal species correlates with lysozyme resistance and pathogenicity. Infect. Immun. **74**:4598–604.

51. **Gillet Y, Issartel B, Vanhems P, Fournet J-C, Lina G, Bes M, Vandenesch F, Piémont Y, Brousse N, Floret D, Etienne J**. 2002. Association between Staphylococcus aureus strains carrying gene for Panton-Valentine leukocidin and highly lethal necrotising pneumonia in young immunocompetent patients. Lancet **359**:753–9.

52. **Prevost G, Couppie P, Prevost P, Gayet S, Petiau P, Cribier B, Monteil H, Piemont Y**. 1995. Epidemiological data on Staphylococcus aureus strains producing synergohymenotropic toxins. J. Med. Microbiol. **42**:237–45.

53. **Micek ST, Dunne M, Kollef MH**. 2005. Pleuropulmonary complications of Panton-Valentine leukocidin-positive community-acquired methicillin-resistant Staphylococcus aureus: importance of treatment with antimicrobials inhibiting exotoxin production. Chest **128**:2732–8.

54. **Amagai M**. 1999. Autoimmunity against desmosomal cadherins in pemphigus. J. Dermatol. Sci. **20**:92–102.

55. **Ladhani S**. 2001. Recent developments in staphylococcal scalded skin syndrome. Clin. Microbiol. Infect. **7**:301–7.

56. **Ladhani S, Evans RW**. 1998. Staphylococcal scalded skin syndrome. Arch. Dis. Child. **78**:85–8.

57. **Melish M**. 1982. Staphylococci, streptococci and the skin: review of impetigo and staphylococcal scalded skin syndrome. Semin. Dermatol. 335–337.

58. **Gilbert RJ, Wieneke AA, Lanser J, Simkovicová M**. 1972. Serological detection of enterotoxin in foods implicated in staphylococcal food poisoning. J. Hyg. (Lond). **70**:755–62.

59. **Chesney PJ, Bergdoll MS, Davis JP, Vergeront JM**. 1984. The disease spectrum, epidemiology, and etiology of toxic-shock syndrome. Annu. Rev. Microbiol. **38**:315–38.

60. **Faulkner L, Cooper A, Fantino C, Altmann DM, Sriskandan S**. 2005. The mechanism of superantigen-mediated toxic shock: not a simple Th1 cytokine storm. J. Immunol. **175**:6870–7.

61. **Vergeront JM, Stolz SJ, Crass BA, Nelson DB, Davis JP, Bergdoll MS**. 1983. Prevalence of serum antibody to staphylococcal enterotoxin F among Wisconsin residents: implications for toxic-shock syndrome. J. Infect. Dis. **148**:692–8.

62. **Brosnahan AJ, Schlievert PM**. 2011. Gram-positive bacterial superantigen outside-in signaling causes toxic shock syndrome. FEBS J. **278**:4649–67.

63. **Laurent TC, Fraser JR**. 1992. Hyaluronan. FASEB J. **6**:2397–404.

64. **Zasloff M**. 2002. Antimicrobial peptides of multicellular organisms. Nature **415**:389–95.

65. **Bokarewa MI, Jin T, Tarkowski A**. 2006. Staphylococcus aureus: Staphylokinase. Int. J. Biochem. Cell Biol. **38**:504–9.

66. **Mölkänen T, Tyynelä J, Helin J, Kalkkinen N, Kuusela P**. 2002. Enhanced activation of bound plasminogen on Staphylococcus aureus by staphylokinase. FEBS Lett. **517**:72–78.

67. **Frimmersdorf E, Horatzek S, Pelnikevich A, Wiehlmann L, Schomburg D**. 2010. How Pseudomonas aeruginosa adapts to various environments: a metabolomic approach. Environ. Microbiol. **12**:1734–47.

68. **De Abreu PM, Farias PG, Paiva GS, Almeida AM, Morais PV**. 2014. Persistence of microbial communities including Pseudomonas aeruginosa in a hospital environment: a potential health hazard. BMC Microbiol. **14**:118.

69. **Pollack M**. 1995. Pseudomonas aeruginosa, p. 1820–2003. *In* G. L. Mandell, R. Dolan, and J. E. Bennett. Principles and practices of infectious diseases. Churchill Livingstone, New York.

70. **Morrison AJ, Wenzel RP**. 1984. Epidemiology of infections due to Pseudomonas aeruginosa. Rev. Infect. Dis. **6 Suppl 3**:S627–42.

71. **Van Delden C, Iglewski BH**. 1998. Cell-to-cell signaling and Pseudomonas aeruginosa infections. Emerg. Infect. Dis. **4**:551–60.

72. **Köhler T, Curty LK, Barja F, van Delden C, Pechère JC**. 2000. Swarming of Pseudomonas aeruginosa is dependent on cell-to-cell signaling and requires flagella and pili. J. Bacteriol. **182**:5990–6.

73. **Arora SK, Ritchings BW, Almira EC, Lory S, Ramphal R**. 1996. Cloning and characterization of Pseudomonas aeruginosa fliF, necessary for flagellar assembly and bacterial adherence to mucin. Infect. Immun. **64**:2130–6.

74. **Bucior I, Pielage JF, Engel JN**. 2012. Pseudomonas aeruginosa pili and flagella mediate distinct binding and signaling events at the apical and basolateral surface of airway epithelium. PLoS Pathog. **8**:e1002616.

75. **Jenkins ATA, Buckling A, McGhee M, ffrench-Constant RH**. 2005. Surface plasmon resonance shows that type IV pili are important in surface attachment by Pseudomonas aeruginosa. J. R. Soc. Interface **2**:255–9.

76. **Kintz E, Goldberg JB**. 2008. Regulation of lipopolysaccharide O antigen expression in Pseudomonas aeruginosa. Future Microbiol. **3**:191–203.

77. **Miki T, Hardt W-D**. 2013. Outer membrane permeabilization is an essential step in the killing of gram-negative bacteria by the lectin RegIIIβ. PLoS One **8**:e69901.

78. **Knirel YA, Bystrova O V, Kocharova NA, Zähringer U, Pier GB**. 2006. Conserved and variable structural features in the lipopolysaccharide of Pseudomonas aeruginosa. J. Endotoxin Res. **12**:324–36.

79. **Tang HB, DiMango E, Bryan R, Gambello M, Iglewski BH, Goldberg JB, Prince A**. 1996. Contribution of specific Pseudomonas aeruginosa virulence factors to pathogenesis of pneumonia in a neonatal mouse model of infection. Infect. Immun. **64**:37–43.

80. **Priebe GP, Dean CR, Zaidi T, Meluleni GJ, Coleman FT, Coutinho YS, Noto MJ, Urban TA, Pier GB, Goldberg JB**. 2004. The galU Gene of Pseudomonas aeruginosa is required for corneal infection and efficient systemic spread following pneumonia but not for infection confined to the lung. Infect. Immun. **72**:4224–32.

81. **Cabral DA, Loh BA, Speert DP**. 1987. Mucoid Pseudomonas aeruginosa resists nonopsonic phagocytosis by human neutrophils and macrophages. Pediatr. Res. **22**:429–31.

82. **Oliver AM, Weir DM**. 1985. The effect of Pseudomonas alginate on rat alveolar macrophage phagocytosis and bacterial opsonization. Clin. Exp. Immunol. **59**:190–6.

83. **Ryder C, Byrd M, Wozniak DJ**. 2007. Role of polysaccharides in Pseudomonas aeruginosa biofilm development. Curr. Opin. Microbiol. **10**:644–8.

84. **Pollack M**. The role of exotoxin A in pseudomonas disease and immunity. Rev. Infect. Dis. **5 Suppl 5**:S979–84.

85. **Jørgensen R, Wang Y, Visschedyk D, Merrill AR**. 2008. The nature and character of the transition state for the ADP-ribosyltransferase reaction. EMBO Rep. **9**:802–9.

86. **Wilson R, Sykes DA, Watson D, Rutman A, Taylor GW, Cole PJ**. 1988. Measurement of Pseudomonas aeruginosa phenazine pigments in sputum and assessment of their contribution to sputum sol toxicity for respiratory epithelium. Infect. Immun. **56**:2515–7.

87. **Usher LR, Lawson RA, Geary I, Taylor CJ, Bingle CD, Taylor GW, Whyte MKB**. 2002. Induction of neutrophil apoptosis by the Pseudomonas aeruginosa exotoxin pyocyanin: a potential mechanism of persistent infection. J. Immunol. **168**:1861–8.

88. **Heinrichs DE, Young L, Poole K**. 1991. Pyochelin-mediated iron transport in Pseudomonas aeruginosa: involvement of a high-molecular-mass outer membrane protein. Infect. Immun. **59**:3680–4.

89. **Ochsner UA, Johnson Z, Lamont IL, Cunliffe HE, Vasil ML**. 1996. Exotoxin A production in Pseudomonas aeruginosa requires the iron-regulated pvdS gene encoding an alternative sigma factor. Mol. Microbiol. **21**:1019–28.

90. **Kessler E, Safrin M, Abrams WR, Rosenbloom J, Ohman DE**. 1997. Inhibitors and specificity of Pseudomonas aeruginosa LasA. J. Biol. Chem. **272**:9884–9.

91. **Cowell BA, Twining SS, Hobden JA, Kwong MSF, Fleiszig SMJ**. 2003. Mutation of lasA and lasB reduces Pseudomonas aeruginosa invasion of epithelial cells. Microbiology **149**:2291–9.

92. **Meyers DJ, Palmer KC, Bale LA, Kernacki K, Preston M, Brown T, Berk RS**. 1992. In vivo and in vitro toxicity of phospholipase C from Pseudomonas aeruginosa. Toxicon **30**:161–9.

93. **Tsui LC**. 1995. The cystic fibrosis transmembrane conductance regulator gene. Am. J. Respir. Crit. Care Med. **151**:S47–53.

94. **O'Sullivan BP, Freedman SD**. 2009. Cystic fibrosis. Lancet **373**:1891–904.

95. **Hassett DJ, Korfhagen TR, Irvin RT, Schurr MJ, Sauer K, Lau GW, Sutton MD, Yu H, Hoiby N**. 2010. Pseudomonas aeruginosa biofilm infections in cystic fibrosis: insights into pathogenic processes and treatment strategies. Expert Opin. Ther. Targets **14**:117–30.

96. **Martinez JL, Fajardo A, Garmendia L, Hernandez A, Linares JF, Martínez-Solano L, Sánchez MB**. 2009. A global view of antibiotic resistance. FEMS Microbiol. Rev. **33**:44–65.

97. **Andersson DI, Levin BR**. 1999. The biological cost of antibiotic resistance. Curr. Opin. Microbiol. **2**:489–93.

98. **Lipsitch M, Levin BR**. 1997. The population dynamics of antimicrobial chemotherapy. Antimicrob. Agents Chemother. **41**:363–73.

99. **Bennett PM**. 2008. Plasmid encoded antibiotic resistance: acquisition and transfer of antibiotic resistance genes in bacteria. Br. J. Pharmacol. **153 Suppl** :S347–57.

100. **Walsh C**. 2000. Molecular mechanisms that confer antibacterial drug resistance. Nature **406**:775–81.

101. **Hartman BJ, Tomasz A**. 1984. Low-affinity penicillin-binding protein associated with beta-lactam resistance in Staphylococcus aureus. J. Bacteriol. **158**:513–6.

102. **Katayama Y, Ito T, Hiramatsu K**. 2000. A new class of genetic element, staphylococcus cassette chromosome mec, encodes methicillin resistance in Staphylococcus aureus. Antimicrob. Agents Chemother. **44**:1549–55.

103. **Ito T, Katayama Y, Asada K, Mori N, Tsutsumimoto K, Tiensasitorn C, Hiramatsu K**. 2001. Structural comparison of three types of staphylococcal cassette chromosome mec integrated in the chromosome in methicillin-resistant Staphylococcus aureus. Antimicrob. Agents Chemother. **45**:1323–36.

104. **International Working Group on the Classification of Staphylococcal Cassette Chromosome Elements (IWG-SCC)**. 2009. Classification of staphylococcal cassette chromosome mec (SCCmec): guidelines for reporting novel SCCmec elements. Antimicrob. Agents Chemother. **53**:4961–7.

105. **Lowy FD**. 1998. Staphylococcus aureus infections. N. Engl. J. Med. **339**:520–532.

106. **Dissemond J, Körber A, Lehnen M, Grabbe S**. 2005. [Methicillin-resistant Staphylococcus aureus (MRSA) in chronic wounds: therapeutic options and perspectives]. J. Dtsch. Dermatol. Ges. **3**:256–62.

107. **King MD, Humphrey BJ, Wang YF, Kourbatova E V, Ray SM, Blumberg HM**. 2006. Emergence of community-acquired methicillin-resistant Staphylococcus aureus USA 300 clone as the predominant cause of skin and soft-tissue infections. Ann. Intern. Med. **144**:309–17.

108. **Klevens RM, Morrison MA, Nadle J, Petit S, Gershman K, Ray S, Harrison LH, Lynfield R, Dumyati G, Townes JM, Craig AS, Zell ER, Fosheim GE, McDougal LK, Carey RB, Fridkin SK**. 2007. Invasive methicillin-resistant Staphylococcus aureus infections in the United States. JAMA **298**:1763–71.

109. **Tillotson GS, Draghi DC, Sahm DF, Tomfohrde KM, Del Fabro T, Critchley IA**. 2008. Susceptibility of Staphylococcus aureus isolated from skin and wound infections in the United States 2005-07: laboratory-based surveillance study. J. Antimicrob. Chemother. **62**:109–15.

110. **Smith TL, Pearson ML, Wilcox KR, Cruz C, Lancaster M V, Robinson-Dunn B, Tenover FC, Zervos MJ, Band JD, White E, Jarvis WR**. 1999. Emergence of vancomycin resistance in Staphylococcus aureus. Glycopeptide-Intermediate Staphylococcus aureus Working Group. N. Engl. J. Med. **340**:493–501.

111. **Chang S, Sievert DM, Hageman JC, Boulton ML, Tenover FC, Downes FP, Shah S, Rudrik JT, Pupp GR, Brown WJ, Cardo D, Fridkin SK**. 2003. Infection with vancomycin-resistant Staphylococcus aureus containing the vanA resistance gene. N. Engl. J. Med. **348**:1342–7.

112. **Tsiodras S, Gold HS, Sakoulas G, Eliopoulos GM, Wennersten C, Venkataraman L, Moellering RC, Ferraro MJ**. 2001. Linezolid resistance in a clinical isolate of Staphylococcus aureus. Lancet **358**:207–8.

113. **Marty FM, Yeh WW, Wennersten CB, Venkataraman L, Albano E, Alyea EP, Gold HS, Baden LR, Pillai SK**. 2006. Emergence of a clinical daptomycin-resistant Staphylococcus aureus isolate during treatment of methicillin-resistant Staphylococcus aureus bacteremia and osteomyelitis. J. Clin. Microbiol. **44**:595–7.

114. **Lister PD, Wolter DJ, Hanson ND**. 2009. Antibacterial-resistant Pseudomonas aeruginosa: clinical impact and complex regulation of chromosomally encoded resistance mechanisms. Clin. Microbiol. Rev. **22**:582–610.

115. **Strateva T, Yordanov D**. 2009. Pseudomonas aeruginosa - a phenomenon of bacterial resistance. J. Med. Microbiol. **58**:1133–48.

116. **Kos VN, Déraspe M, McLaughlin RE, Whiteaker JD, Roy PH, Alm RA, Corbeil J, Gardner H**. 2015. The resistome of Pseudomonas aeruginosa in relationship to phenotypic susceptibility. Antimicrob. Agents Chemother. **59**:427–36.

117. **Carmeli Y, Troillet N, Eliopoulos GM, Samore MH**. 1999. Emergence of antibiotic-resistant Pseudomonas aeruginosa: comparison of risks associated with different antipseudomonal agents. Antimicrob. Agents Chemother. **43**:1379–82.

118. **Oliver A, Cantón R, Campo P, Baquero F, Blázquez J**. 2000. High frequency of hypermutable Pseudomonas aeruginosa in cystic fibrosis lung infection. Science **288**:1251–4.

119. **Maciá MD, Borrell N, Pérez JL, Oliver A**. 2004. Detection and susceptibility testing of hypermutable Pseudomonas aeruginosa strains with the Etest and disk diffusion. Antimicrob. Agents Chemother. **48**:2665–72.

120. **Snyder AB, Worobo RW**. 2014. Chemical and genetic characterization of bacteriocins: antimicrobial peptides for food safety. J. Sci. Food Agric. **94**:28–44.

121. **Okuda K, Zendo T, Sugimoto S, Iwase T, Tajima A, Yamada S, Sonomoto K, Mizunoe Y**. 2013. Effects of bacteriocins on methicillin-resistant Staphylococcus aureus biofilm. Antimicrob. Agents Chemother. **57**:5572–9.

122. **Crandall AD, Montville TJ**. 1998. Nisin resistance in Listeria monocytogenes ATCC 700302 is a complex phenotype. Appl. Environ. Microbiol. **64**:231–7.

123. **Witzenrath M, Schmeck B, Doehn JM, Tschernig T, Zahlten J, Loeffler JM, Zemlin M, Müller H, Gutbier B, Schütte H, Hippenstiel S, Fischetti VA, Suttorp N, Rosseau S**. 2009. Systemic use of the endolysin Cpl-1 rescues mice with fatal pneumococcal pneumonia. Crit. Care Med. **37**:642–9.

124. **Fenton M, Casey PG, Hill C, Gahan CG, Ross RP, McAuliffe O, O'Mahony J, Maher F, Coffey A**. The truncated phage lysin CHAP(k) eliminates Staphylococcus aureus in the nares of mice. Bioeng. Bugs **1**:404–7.

125. **Delmar JA, Su C-C, Yu EW**. 2014. Bacterial multidrug efflux transporters. Annu. Rev. Biophys. **43**:93–117.

126. **Birck MR, Holler TP, Woodard RW**. 2000. Identification of a Slow Tight-Binding Inhibitor of 3-Deoxy- d - m anno -octulosonic Acid 8-Phosphate Synthase. J. Am. Chem. Soc. **122**:9334–9335.

127. **Twort FW**. 1915. An investigation on the nature of ultra-microscopic viruses. Lancet **186**:1241–1243.

128. **d´Hérelle F**. 1917. Sur un microbe invisible antagoniste des bacilles dysentériques. Crit. Rev. Acad. Sci. Paris 373.

129. **d'Hérelle F**. 1922. The bacteriophage: its role in immunity. Williams & Wilkins, Baltimore.

130. **Summers W**. 1999. Félix d´Hérelle and the origins of molecular biology. Yale University Press, New Haven, Conn.

131. **Bruynoghe R, J M**. 1921. Essais de thérapeutique au moyen du bacteriophage. C. R. Soc. Biol. 1120–1121.

132. **Rice TB**. 1930. Use of bacteriophage filtrates in treatment of suppurative conditions: report of 300 cases. Am J Med Sci 345–360.

133. **Schless RA**. 1932. Staphylococcus aureus meningitis. Am. J. Dis. Child. **44**:813.

134. **Alisky J, Iczkowski K, Rapoport A, Troitsky N**. 1998. Bacteriophages show promise as antimicrobial agents. J. Infect. **36**:5–15.

135. **Weber-Dabrowska B, Mulczyk M, Górski A**. 2000. Bacteriophage therapy of bacterial infections: an update of our institute's experience. Arch. Immunol. Ther. Exp. (Warsz). **48**:547–51.

136. **Chanishvili N, Tediashvili M, Chanishvili T**. 2002. Phages and experience for their application in the former Soviet Union. IUMS Congr.

137. **Karam JD**. 2005. Bacteriophages: the viruses for all seasons of molecular biology. Virol. J. **2**:19.

138. **HERSHEY AD, CHASE M**. 1952. Independent functions of viral protein and nucleic acid in growth of bacteriophage. J. Gen. Physiol. **36**:39–56.

139. **Brüssow H, Hendrix RW**. 2002. Phage genomics: small is beautiful. Cell **108**:13–6.

140. **Brüssow H, E K**. 2005. Phage ecology, p. 129 –164. *In* Kutter, E, A., S (eds.), Bacteriophages: Biology and Application. CRC Press, Boca Raton, Florida.

141. **Neve H, Kemper U, Geis A, Heller J**. 1994. Monitoring and characterization of lactococcal bacteriophage in a dairy plant. Kiel Milchwirtsch Forschungsber 167–178.

142. **Kennedy J, G B**. 1987. Bacteriophages in foods. John Wiley & Sons, Wiley, New York.

143. **Ackermann H-W**. 2009. Phage classification and characterization. Methods Mol. Biol. **501**:127–40.

144. **Ackermann H**. 2011. Bacteriophage taxonomy. Microbiol. Aust. 90–94.

145. **Ackermann HW**. 2006. Classification of Bacteriophages. Oxford University Press, New York.

146. **Rees PJ, Fry BA**. 1981. The morphology of staphylococcal bacteriophage K and DNA metabolism in infected Staphylococcus aureus. J. Gen. Virol. **53**:293–307.

147. **Pantůcek R, Rosypalová A, Doskar J, Kailerová J, Růzicková V, Borecká P, Snopková S, Horváth R, Götz F, Rosypal S**. 1998. The polyvalent staphylococcal phage phi 812: its host-range mutants and related phages. Virology **246**:241–52.

148. **Gupta R, Prasad Y**. 2011. Efficacy of polyvalent bacteriophage P-27/HP to control multidrug resistant Staphylococcus aureus associated with human infections. Curr. Microbiol. **62**:255–60.

149. **Knight J**. 2002. Superbugs reveal chink in armour. Nature **417**:477–477.

150. **García P, Rodríguez L**. 2010. Food biopreservation: promising strategies using bacteriocins, bacteriophages and endolysins. Trends Food Sci. … **21**:373–382.

151. **Hanlon GW**. 2007. Bacteriophages: an appraisal of their role in the treatment of bacterial infections. Int. J. Antimicrob. Agents **30**:118–28.

152. **Fischetti VA**. 2005. Bacteriophage lytic enzymes: novel anti-infectives. Trends Microbiol. **13**:491–6.

153. **Richards FF**. 1969. The Genetics of Bacteria and their Viruses. Yale J. Biol. Med. Yale Journal of Biology and Medicine.

154. **Boyd EF, Brüssow H**. 2002. Common themes among bacteriophage-encoded virulence factors and diversity among the bacteriophages involved. Trends Microbiol. **10**:521–9.

155. **Levin B, Bull J**. 2004. Population and evolutionary dynamics of phage therapy. Nat. Rev. Microbiol. **2**:166–173.

156. **Skurnik M, Pajunen M, Kiljunen S**. 2007. Biotechnological challenges of phage therapy. Biotechnol. Lett. **29**:995–1003.

157. **Bruttin A, Brüssow H**. 2005. Human volunteers receiving Escherichia coli phage T4 orally: a safety test of phage therapy. Antimicrob. Agents Chemother. **49**:2874–8.

158. **Matsuzaki S, Rashel M, Uchiyama J, Sakurai S, Ujihara T, Kuroda M, Ikeuchi M, Tani T, Fujieda M, Wakiguchi H, Imai S**. 2005. Bacteriophage therapy: a revitalized therapy against bacterial infectious diseases. J. Infect. Chemother. **11**:211–9.

159. **Abedon ST, Thomas-Abedon C**. 2010. Phage therapy pharmacology. Curr. Pharm. Biotechnol. **11**:28–47.

160. **Skurnik M, Strauch E**. 2006. Phage therapy: facts and fiction. Int. J. Med. Microbiol. **296**:5–14.

161. **Mann NH**. 2008. The potential of phages to prevent MRSA infections. Res. Microbiol. **159**:400–5.

162. **Kutter E, De Vos D, Gvasalia G, Alavidze Z, Gogokhia L, Kuhl S, Abedon ST**. 2010. Phage therapy in clinical practice: treatment of human infections. Curr. Pharm. Biotechnol. **11**:69–86.

163. **Ryan E, Gorman S**. 2011. Recent advances in bacteriophage therapy: how delivery routes, formulation, concentration and timing influence the success of phage therapy. J. Pharm. … **63**:1253–1264.

164. **Abedon ST**. 2011. Bacteriophages and Biofilms: Ecology, Phage Therapy, Plaques. Nova Science Publishers.

165. **Goodridge LD**. 2010. Designing phage therapeutics. Curr. Pharm. Biotechnol. **11**:15–27.

166. **Hyman P, Abedon ST**. 2010. Bacteriophage host range and bacterial resistance. Adv. Appl. Microbiol. **70**:217–48.

167. **Brüssow H, Canchaya C, Hardt W**. 2004. Phages and the evolution of bacterial pathogens: from genomic rearrangements to lysogenic conversion. Microbiol. Mol. **68**:560–602.

168. **Sander M, Schmieger H**. 2001. Method for host-independent detection of generalized transducing bacteriophages in natural habitats. Appl. Environ. Microbiol. **67**:1490–3.

169. **Clark J, March J**. 2006. Bacteriophages and biotechnology: vaccines, gene therapy and antibacterials. Trends Biotechnol. **24**:212–218.

170. **Harris SR, Feil EJ, Holden MTG, Quail MA, Nickerson EK, Chantratita N, Gardete S, Tavares A, Day N, Lindsay JA, Edgeworth JD, de Lencastre H, Parkhill J, Peacock SJ, Bentley SD**. 2010. Evolution of MRSA during hospital transmission and intercontinental spread. Science **327**:469–74.

171. **Nakai T, Park SC**. 2002. Bacteriophage therapy of infectious diseases in aquaculture. Res. Microbiol. **153**:13–18.

172. **Goodridge LD**. 2004. Bacteriophage biocontrol of plant pathogens: fact or fiction? Trends Biotechnol. **22**:384–5.

173. **Higgins JP, Higgins SE, Guenther KL, Huff W, Donoghue AM, Donoghue DJ, Hargis BM**. 2005. Use of a specific bacteriophage treatment to reduce Salmonella in poultry products. Poult. Sci. **84**:1141–5.

174. **Borysowski J, Weber-Dabrowska B, Górski A**. 2006. Bacteriophage endolysins as a novel class of antibacterial agents. Exp. Biol. Med. (Maywood). **231**:366–77.

175. **Zavascki AP, Carvalhaes CG, Picão RC, Gales AC**. 2010. Multidrug-resistant Pseudomonas aeruginosa and Acinetobacter baumannii: resistance mechanisms and implications for therapy. Expert Rev. Anti. Infect. Ther. **8**:71–93.

176. **Dabrowska K, Opolski A, Wietrzyk J, Switala-Jelen K, Boratynski J, Nasulewicz A, Lipinska L, Chybicka A, Kujawa M, Zabel M, Dolinska-Krajewska B, Piasecki E, Weber-Dabrowska B, Rybka J, Salwa J, Wojdat E, Nowaczyk M, Gorski A**. 2004. Antitumor activity of bacteriophages in murine experimental cancer models caused possibly by inhibition of beta3 integrin signaling pathway. Acta Virol. **48**:241–8.

177. **Dabrowska K, Skaradziński G, Jończyk P, Kurzepa A, Wietrzyk J, Owczarek B, Zaczek M, Switała-Jeleń K, Boratyński J, Poźniak G, Maciejewska M, Górski A**. 2009. The effect of bacteriophages T4 and HAP1 on in vitro melanoma migration. BMC Microbiol. **9**:13.

178. **Gorski A, Dabrowska K, Switala-Jeleń K, Nowaczyk M, Weber-Dabrowska B, Boratynski J, Wietrzyk J, Opolski A**. 2003. New insights into the possible role of bacteriophages in host defense and disease. Med. Immunol. **2**:2.

179. **Hall-Stoodley L, Costerton JW, Stoodley P**. 2004. Bacterial biofilms: from the natural environment to infectious diseases. Nat. Rev. Microbiol. **2**:95–108.

180. **Zobell CE**. 1943. The Effect of Solid Surfaces upon Bacterial Activity. J. Bacteriol. **46**:39–56.

181. **Stoodley P, Sauer K, Davies DG, Costerton JW**. 2002. Biofilms as complex differentiated communities. Annu. Rev. Microbiol. **56**:187–209.

182. **Tang D, Wang W**. 1998. Successful cure of an extensive burn injury complicated with mucor wound sepsis. Burns **24**:72–3.

183. **Sauer K, Cullen MC, Rickard AH, Zeef LAH, Davies DG, Gilbert P**. 2004. Characterization of nutrient-induced dispersion in Pseudomonas aeruginosa PAO1 biofilm. J. Bacteriol. **186**:7312–26.

184. **Chiang P, Burrows LL**. 2003. Biofilm Formation by Hyperpiliated Mutants of Pseudomonas aeruginosa. J. Bacteriol. **185**:2374–2378.

185. **Whitchurch CB, Tolker-Nielsen T, Ragas PC, Mattick JS**. 2002. Extracellular DNA required for bacterial biofilm formation. Science **295**:1487.

186. **Ma L, Conover M, Lu H, Parsek MR, Bayles K, Wozniak DJ**. 2009. Assembly and development of the Pseudomonas aeruginosa biofilm matrix. PLoS Pathog. **5**:e1000354.

187. **Lazăr V, Chifiriuc MC**. 2010. Architecture and physiology of microbial biofilms. Roum. Arch. Microbiol. Immunol. **69**:95–107.

188. **Dickschat JS**. 2010. Quorum sensing and bacterial biofilms. Nat. Prod. Rep. **27**:343–69.

189. **Otto M**. 2008. Staphylococcal biofilms. Curr. Top. Microbiol. Immunol. **322**:207–28.

190. **Stoodley P, Wilson S, Hall-Stoodley L, Boyle JD, Lappin-Scott HM, Costerton JW**. 2001. Growth and detachment of cell clusters from mature mixed-species biofilms. Appl. Environ. Microbiol. **67**:5608–13.

191. **Yarwood JM, Bartels DJ, Volper EM, Greenberg EP**. 2004. Quorum Sensing in Staphylococcus aureus Biofilms. J. Bacteriol. **186**:1838–1850.

192. **Periasamy S, Joo H-S, Duong AC, Bach T-HL, Tan VY, Chatterjee SS, Cheung GYC, Otto M**. 2012. How Staphylococcus aureus biofilms develop their characteristic structure. Proc. Natl. Acad. Sci. U. S. A. **109**:1281–6.

193. **Sakuragi Y, Kolter R**. 2007. Quorum-sensing regulation of the biofilm matrix genes (pel) of Pseudomonas aeruginosa. J. Bacteriol. **189**:5383–6.

194. **Davies DG, Parsek MR, Pearson JP, Iglewski BH, Costerton JW, Greenberg EP**. 1998. The involvement of cell-to-cell signals in the development of a bacterial biofilm. Science **280**:295–8.

195. **Allesen-Holm M, Barken KB, Yang L, Klausen M, Webb JS, Kjelleberg S, Molin S, Givskov M, Tolker-Nielsen T**. 2006. A characterization of DNA release in Pseudomonas aeruginosa cultures and biofilms. Mol. Microbiol. **59**:1114–28.

196. **De Kievit TR, Gillis R, Marx S, Brown C, Iglewski BH**. 2001. Quorum-sensing genes in Pseudomonas aeruginosa biofilms: their role and expression patterns. Appl. Environ. Microbiol. **67**:1865–73.

197. **Davey ME, Caiazza NC, O'Toole GA**. 2003. Rhamnolipid surfactant production affects biofilm architecture in Pseudomonas aeruginosa PAO1. J. Bacteriol. **185**:1027–36.

198. **Dusane DH, Zinjarde SS, Venugopalan VP, McLean RJC, Weber MM, Rahman PKSM**. 2010. Quorum sensing: implications on rhamnolipid biosurfactant production. Biotechnol. Genet. Eng. Rev. **27**:159–84.

199. **Boles BR, Thoendel M, Singh PK**. 2005. Rhamnolipids mediate detachment of Pseudomonas aeruginosa from biofilms. Mol. Microbiol. **57**:1210–23.

200. **Ghafoor A, Hay ID, Rehm BHA**. 2011. Role of exopolysaccharides in Pseudomonas aeruginosa biofilm formation and architecture. Appl. Environ. Microbiol. **77**:5238–46.

201. **Ma L, Wang J, Wang S, Anderson EM, Lam JS, Parsek MR, Wozniak DJ**. 2012. Synthesis of multiple Pseudomonas aeruginosa biofilm matrix exopolysaccharides is post-transcriptionally regulated. Environ. Microbiol. **14**:1995–2005.

202. **Sutherland IW**. 2001. Biofilm exopolysaccharides: a strong and sticky framework. Microbiology **147**:3–9.

203. **Costerton JW, Cheng KJ, Geesey GG, Ladd TI, Nickel JC, Dasgupta M, Marrie TJ**. 1987. Bacterial biofilms in nature and disease. Annu. Rev. Microbiol. **41**:435–64.

204. **Costerton JW, Stewart PS, Greenberg EP**. 1999. Bacterial biofilms: a common cause of persistent infections. Science **284**:1318–22.

205. **De Beer D, Stoodley P, Lewandowski Z**. 1997. Measurement of local diffusion coefficients in biofilms by microinjection and confocal microscopy. Biotechnol. Bioeng. **53**:151–8.

206. **Lam J, Chan R, Lam K, Costerton JW**. 1980. Production of mucoid microcolonies by Pseudomonas aeruginosa within infected lungs in cystic fibrosis. Infect. Immun. **28**:546–56.

207. **Høiby N, Bjarnsholt T, Givskov M, Molin S, Ciofu O**. 2010. Antibiotic resistance of bacterial biofilms. Int. J. Antimicrob. Agents **35**:322–332.

208. **Hoyle BD, Costerton JW**. 1991. Bacterial resistance to antibiotics: the role of biofilms. Prog. Drug Res. **37**:91–105.

209. **Spoering AL, Lewis K**. 2001. Biofilms and planktonic cells of Pseudomonas aeruginosa have similar resistance to killing by antimicrobials. J. Bacteriol. **183**:6746–51.

210. **Lewis K**. 2008. Multidrug tolerance of biofilms and persister cells. Curr. Top. Microbiol. Immunol. **322**:107–31.

211. **Moyed HS, Bertrand KP**. 1983. hipA, a newly recognized gene of Escherichia coli K-12 that affects frequency of persistence after inhibition of murein synthesis. J. Bacteriol. **155**:768–75.

212. **Espeland EM, Wetzel RG**. 2001. Complexation, Stabilization, and UV Photolysis of Extracellular and Surface-Bound Glucosidase and Alkaline Phosphatase: Implications for Biofilm Microbiota. Microb. Ecol. **42**:572–585.

213. **McNeill K, Hamilton I.** 2003. Acid tolerance response of biofilm cells of Streptococcus mutans. FEMS Microbiol. Lett. **221**:25–30.

214. **Teitzel GM, Parsek MR**. 2003. Heavy metal resistance of biofilm and planktonic Pseudomonas aeruginosa. Appl. Environ. Microbiol. **69**:2313–20.

215. **Le Magrex-Debar E, Lemoine J, Gellé MP, Jacquelin LF, Choisy C**. 2000. Evaluation of biohazards in dehydrated biofilms on foodstuff packaging. Int. J. Food Microbiol. **55**:239–43.

216. **Fu W, Forster T, Mayer O, Curtin JJ, Lehman SM, Donlan RM**. 2010. Bacteriophage cocktail for the prevention of biofilm formation by Pseudomonas aeruginosa on catheters in an in vitro model system. Antimicrob. Agents Chemother. **54**:397–404.

217. **Harper D, Parracho H, Walker J, Sharp R, Hughes G, Werthén M, Lehman S, Morales S**. 2014. Bacteriophages and Biofilms. Antibiotics **3**:270–284.

218. **Lu TK, Collins JJ**. 2007. Dispersing biofilms with engineered enzymatic bacteriophage. Proc. Natl. Acad. Sci. U. S. A. **104**:11197–202.

219. **Sutherland IW, Hughes KA, Skillman LC, Tait K**. 2004. The interaction of phage and biofilms. FEMS Microbiol. Lett. **232**:1–6.

220. **Kelly D, McAuliffe O, Ross RP, Coffey A**. 2012. Prevention of Staphylococcus aureus biofilm formation and reduction in established biofilm density using a combination of phage K and modified derivatives. Lett. Appl. Microbiol. **54**:286–91.

221. **O'Flaherty S, Ross RP, Meaney W, Fitzgerald GF, Elbreki MF, Coffey A**. 2005. Potential of the polyvalent anti-Staphylococcus bacteriophage K for control of antibiotic-resistant staphylococci from hospitals. Appl. Environ. Microbiol. **71**:1836–1842.

222. **Sillankorva S, Oliveira R, Vieira MJ, Sutherland I, Azeredo J**. 2004. Pseudomonas fluorescens infection by bacteriophage PhiS1: the influence of temperature, host growth phase and media. FEMS Microbiol. Lett. **241**:13–20.

223. **Verma V, Harjai K, Chhibber S**. 2009. Restricting ciprofloxacin-induced resistant variant formation in biofilm of Klebsiella pneumoniae B5055 by complementary bacteriophage treatment. J. Antimicrob. … **26**:313–23.

224. **Adams M**. 1959. Bacteriophages. Interscience Publishers Inc, New York.

225. **Pajunen M, Kiljunen S, Skurnik M**. 2000. Bacteriophage phiYeO3-12, specific for Yersinia enterocolitica serotype O:3, is related to coliphages T3 and T7. J. Bacteriol. **182**:5114–20.

226. **Boulanger P**. 2009. Purification of bacteriophages and SDS-PAGE analysis of phage structural proteins from ghost particles. Methods Mol. Biol. **502**:227–238.

227. **Pickard DJJ**. 2009. Preparation of bacteriophage lysates and pure DNA. Methods Mol. Biol. **502**:3–9.

228. **Maiden MC, Bygraves JA, Feil E, Morelli G, Russell JE, Urwin R, Zhang Q, Zhou J, Zurth K, Caugant DA, Feavers IM, Achtman M, Spratt BG**. 1998. Multilocus sequence typing: a portable approach to the identification of clones within populations of pathogenic microorganisms. Proc. Natl. Acad. Sci. U. S. A. **95**:3140–5.

229. **Enright MC, Day NP, Davies CE, Peacock SJ, Spratt BG**. 2000. Multilocus sequence typing for characterization of methicillin-resistant and methicillin-susceptible clones of Staphylococcus aureus. J. Clin. Microbiol. **38**:1008–15.

230. **Feil EJ, Enright MC**. 2004. Analyses of clonality and the evolution of bacterial pathogens. Curr. Opin. Microbiol. **7**:308–13.

231. **Kot W, Vogensen FK, Sørensen SJ, Hansen LH**. 2014. DPS - A rapid method for genome sequencing of DNA-containing bacteriophages directly from a single plaque. J. Virol. Methods **196**:152–6.

232. **Aziz RK, Bartels D, Best AA, DeJongh M, Disz T, Edwards RA, Formsma K, Gerdes S, Glass EM, Kubal M, Meyer F, Olsen GJ, Olson R, Osterman AL, Overbeek RA, McNeil LK, Paarmann D, Paczian T, Parrello B, Pusch GD, Reich C, Stevens R, Vassieva O, Vonstein V, Wilke A, Zagnitko O**. 2008. The RAST Server: rapid annotations using subsystems technology. BMC Genomics **9**:75.

233. **Standards NCCLS**. 2003. Approved standard: M7-A6. Methods for dilution antimicrobial susceptibility tests for bacteria that grow aerobically.

234. **Pfankuch, E., Kausche GA**. 1940. Isolierung und übermikroskopische Abbildung eines Bakteriophagen. Naturwissenschaften **28:46**.

235. **Gentile M, Gelderblom HR**. 2005. Rapid viral diagnosis: role of electron microscopy. New Microbiol. **28**:1–12.

236. **Nwaneshiudu A, Kuschal C, Sakamoto FH, Anderson RR, Schwarzenberger K, Young RC**. 2012. Introduction to confocal microscopy. J. Invest. Dermatol. **132**:e3.

237. LIVE/DEAD BacLight Bacterial Viability Kit, for microscopy quantitative assays.

238. **Cerca N, Oliveira R, Azeredo J**. 2007. Susceptibility of Staphylococcus epidermidis planktonic cells and biofilms to the lytic action of staphylococcus bacteriophage K. Lett. Appl. Microbiol. **45**:313–7.

239. **Sambrook J, Russell DW**. 2001. Molecular Cloning - Sambrook & Russel - Vol. 1, 2, 3. CSH Press.

240. **Pires D, Sillankorva S, Faustino A, Azeredo J**. 2011. Use of newly isolated phages for control of Pseudomonas aeruginosa PAO1 and ATCC 10145 biofilms. Res. Microbiol. **162**:798–806.

241. **McNerney R, Wilson S., Sidhu A., Harley V., Al Suwaidi Z, Nye P., Parish T, Stoker N.** 1998. Inactivation of mycobacteriophage D29 using ferrous ammonium sulphate as a tool for the detection of viable Mycobacterium smegmatis and M. tuberculosis. Res. Microbiol. **149**:487–495.

242. **Park DJ, Drobniewski FA, Meyer A, Wilson SM**. 2003. Use of a phage-based assay for phenotypic detection of mycobacteria directly from sputum. J. Clin. Microbiol. **41**:680–8.

243. **Abramson JH**. 2011. WINPEPI updated: computer programs for epidemiologists, and their teaching potential. Epidemiol. Perspect. Innov. **8**:1.

244. **Alves DR, Gaudion A, Bean JE, Perez Esteban P, Arnot TC, Harper DR, Kot W, Hansen LH, Enright MC, Jenkins ATA**. 2014. Combined use of bacteriophage K and a

novel bacteriophage to reduce Staphylococcus aureus biofilm formation. Appl. Environ. Microbiol. **80**:6694–703.

245. **D'Hérelle F**. 1938. Le Phénomène de la Guérison dans les Maladies Infectieuses. Masson et cie, Paris.

246. **O'Flaherty S, Ross RP, Flynn J, Meaney WJ, Fitzgerald GF, Coffey A**. 2005. Isolation and characterization of two anti-staphylococcal bacteriophages specific for pathogenic Staphylococcus aureus associated with bovine infections. Lett. Appl. Microbiol. **41**:482–6.

247. **Cerveny KE, DePaola A, Duckworth DH, Gulig PA**. 2002. Phage therapy of local and systemic disease caused by Vibrio vulnificus in iron-dextran-treated mice. Infect. Immun. **70**:6251–62.

248. 2009. Bacteriophages: Methods and Protocols, Volume 1: Isolation, Characterization and Interactions. Humana Press.

249. **Klockgether J, Munder A, Neugebauer J, Davenport CF, Stanke F, Larbig KD, Heeb S, Schöck U, Pohl TM, Wiehlmann L, Tümmler B**. 2010. Genome diversity of Pseudomonas aeruginosa PAO1 laboratory strains. J. Bacteriol. **192**:1113–21.

250. **Zankari E, Hasman H, Cosentino S, Vestergaard M, Rasmussen S, Lund O, Aarestrup FM, Larsen MV**. 2012. Identification of acquired antimicrobial resistance genes. J. Antimicrob. Chemother. **67**:2640–4.

251. **Joensen KG, Scheutz F, Lund O, Hasman H, Kaas RS, Nielsen EM, Aarestrup FM**. 2014. Real-time whole-genome sequencing for routine typing, surveillance, and outbreak detection of verotoxigenic Escherichia coli. J. Clin. Microbiol. **52**:1501–10.

252. **Streisinger G, Emrich J, Stahl MM**. 1967. Chromosome structure in phage t4, iii. Terminal redundancy and length determination. Proc. Natl. Acad. Sci. U. S. A. **57**:292–5.

253. **Kwan T, Liu J, DuBow M**. 2005. The complete genomes and proteomes of 27 Staphylococcus aureus bacteriophages. Proc. … **102**:5174–5179.

254. **Cui Z, Song Z, Wang Y, Zeng L, Shen W, Wang Z, Li Q, He P, Qin J, Guo X**. 2012. Complete genome sequence of wide-host-range Staphylococcus aureus phage JD007. J. Virol. **86**:13880–1.

255. **Gu J, Liu X, Lu R, Li Y, Song J, Lei L, Sun C, Feng X, Du C, Yu H, Yang Y, Han W**. 2012. Complete genome sequence of Staphylococcus aureus bacteriophage GH15. J. Virol. **86**:8914–5.

256. **Madden T**. 2003. The BLAST Sequence Analysis Tool, p. Chapter 16. *In* The NCBI Handbook.

257. **Deghorain M, Van Melderen L**. 2012. The Staphylococci Phages Family: An Overview. Viruses **4**:3316–3335.

258. **Łobocka M, Hejnowicz MS, Dąbrowski K, Gozdek A, Kosakowski J, Witkowska M, Ulatowska MI, Weber-Dąbrowska B, Kwiatek M, Parasion S, Gawor J, Kosowska H, Głowacka A**. 2012. Genomics of staphylococcal Twort-like phages--potential therapeutics of the post-antibiotic era. Adv. Virus Res. **83**:143–216.

259. **Sillankorva S, Neubauer P, Azeredo J**. 2008. Isolation and characterization of a T7-like lytic phage for Pseudomonas fluorescens. BMC Biotechnol. **8**:80.

260. **Ceyssens P-J, Miroshnikov K, Mattheus W, Krylov V, Robben J, Noben J-P, Vanderschraeghe S, Sykilinda N, Kropinski AM, Volckaert G, Mesyanzhinov V, Lavigne R**. 2009. Comparative analysis of the widespread and conserved PB1-like viruses infecting Pseudomonas aeruginosa. Environ. Microbiol. **11**:2874–83.

261. **Fukuda K, Ishida W, Uchiyama J, Rashel M, Kato S, Morita T, Muraoka A, Sumi T, Matsuzaki S, Daibata M, Fukushima A**. 2012. Pseudomonas aeruginosa keratitis in mice: effects of topical bacteriophage KPP12 administration. PLoS One **7**:e47742.

262. **Jarrell K, Kropinski AM**. 1977. Identification of the cell wall receptor for bacteriophage E79 in Pseudomonas aeruginosa strain PAO. J. Virol. **23**:461–6.

263. **Kelman Z, O'Donnell M**. 1995. Dna Polymerase III Holoenzyme: Structure and Function of a Chromosomal Replicating Machine. Annu. Rev. Biochem. **64**:171–200.

264. **Pires DP, Kropinski AM, Azeredo J, Sillankorva S**. 2014. Complete Genome Sequence of the Pseudomonas aeruginosa Bacteriophage phiIBB-PAA2. Genome Announc. **2**.

265. **Ceyssens P-J, Hertveldt K, Ackermann H-W, Noben J-P, Demeke M, Volckaert G, Lavigne R**. 2008. The intron-containing genome of the lytic Pseudomonas phage LUZ24 resembles the temperate phage PaP3. Virology **377**:233–8.

266. **Lavigne R, Burkal'tseva M V, Robben J, Sykilinda NN, Kurochkina LP, Grymonprez B, Jonckx B, Krylov VN, Mesyanzhinov V V, Volckaert G**. 2003. The genome of bacteriophage phiKMV, a T7-like virus infecting Pseudomonas aeruginosa. Virology **312**:49–59.

267. **Lammens E, Ceyssens P-J, Voet M, Hertveldt K, Lavigne R, Volckaert G**. 2009. Representational Difference Analysis (RDA) of bacteriophage genomes. J. Microbiol. Methods **77**:207–13.

268. **Drulis-Kawa Z, Mackiewicz P, Kęsik-Szeloch A, Maciaszczyk-Dziubinska E, Weber-Dąbrowska B, Dorotkiewicz-Jach A, Augustyniak D, Majkowska-Skrobek G, Bocer T, Empel J, Kropinski AM**. 2011. Isolation and characterisation of KP34--a novel φKMV-like bacteriophage for Klebsiella pneumoniae. Appl. Microbiol. Biotechnol. **90**:1333–45.

269. **Young R, Bläsi U**. 1995. Holins: form and function in bacteriophage lysis. FEMS Microbiol. Rev. **17**:191–205.

270. **Wang IN, Smith DL, Young R**. 2000. Holins: the protein clocks of bacteriophage infections. Annu. Rev. Microbiol. **54**:799–825.

271. **Stover CK, Pham XQ, Erwin AL, Mizoguchi SD, Warrener P, Hickey MJ, Brinkman FS, Hufnagle WO, Kowalik DJ, Lagrou M, Garber RL, Goltry L, Tolentino E, Westbrock-Wadman S, Yuan Y, Brody LL, Coulter SN, Folger KR, Kas A, Larbig K, Lim R, Smith K, Spencer D, Wong GK, Wu Z, Paulsen IT, Reizer J, Saier MH, Hancock RE, Lory S, Olson M V**. 2000. Complete genome sequence of Pseudomonas aeruginosa PAO1, an opportunistic pathogen. Nature **406**:959–64.

272. **Lavigne R, Burkal'tseva M V, Robben J, Sykilinda NN, Kurochkina LP, Grymonprez B, Jonckx B, Krylov VN, Mesyanzhinov V V, Volckaert G**. 2003. The genome of bacteriophage φKMV, a T7-like virus infecting Pseudomonas aeruginosa. Virology **312**:49–59.

273. **Paddison P, Abedon ST, Dressman HK, Gailbreath K, Tracy J, Mosser E, Neitzel J, Guttman B, Kutter E**. 1998. The roles of the bacteriophage T4 r genes in lysis inhibition and fine-structure genetics: a new perspective. Genetics **148**:1539–50.

274. **Ceyssens P-J, Brabban A, Rogge L, Lewis MS, Pickard D, Goulding D, Dougan G, Noben J-P, Kropinski A, Kutter E, Lavigne R**. 2010. Molecular and physiological analysis of three Pseudomonas aeruginosa phages belonging to the “N4-like viruses”. Virology **405**:26–30.

275. **Miller A, Wood D, Ebright RH, Rothman-Denes LB**. 1997. RNA polymerase beta’ subunit: a target of DNA binding-independent activation. Science **275**:1655–7.

276. **Abedon ST, Yin J**. 2009. Bacteriophage plaques: theory and analysis. Methods Mol. Biol. **501**:161–74.

277. **Wang Q, Smith C**. 2008. Molecular biology genes to proteins, 3rd edition by B. E. Tropp. Biochem. Mol. Biol. Educ. **36**:318–319.

278. **Goerke C, Pantucek R, Holtfreter S, Schulte B, Zink M, Grumann D, Bröker BM, Doskar J, Wolz C**. 2009. Diversity of prophages in dominant Staphylococcus aureus clonal lineages. J. Bacteriol. **191**:3462–8.

279. **Lindsay JA, Holden MTG**. 2006. Understanding the rise of the superbug: investigation of the evolution and genomic variation of Staphylococcus aureus. Funct. Integr. Genomics **6**:186–201.

280. **Nanda AM, Thormann K, Frunzke J**. 2015. Impact of spontaneous prophage induction on the fitness of bacterial populations and host-microbe interactions. J. Bacteriol. **197**:410–9.

281. **Yamaguchi T, Hayashi T, Takami H, Ohnishi M, Murata T, Nakayama K, Asakawa K, Ohara M, Komatsuzawa H, Sugai M**. 2001. Complete nucleotide sequence of a Staphylococcus aureus exfoliative toxin B plasmid and identification of a novel ADP-ribosyltransferase, EDIN-C. Infect. Immun. **69**:7760–71.

282. **Kaneko J, Kimura T, Narita S, Tomita T**. 1998. Complete nucleotide sequence and molecular characterization of the temperate staphylococcal bacteriophage φPVL carrying Panton–Valentine leukocidin genes. Gene **215**:57–67.

283. **Ohnishi M, Kurokawa K, Hayashi T**. 2001. Diversification of Escherichia coli genomes: are bacteriophages the major contributors? Trends Microbiol. **9**:481–5.

284. **El Haddad L, Ben Abdallah N, Plante P-L, Dumaresq J, Katsarava R, Labrie S, Corbeil J, St-Gelais D, Moineau S**. 2014. Improving the safety of Staphylococcus aureus polyvalent phages by their production on a Staphylococcus xylosus strain. PLoS One **9**:e102600.

285. **Allen HK, Looft T, Bayles DO, Humphrey S, Levine UY, Alt D, Stanton TB**. 2011. Antibiotics in feed induce prophages in swine fecal microbiomes. MBio **2**.

286. **Tormo MA, Ferrer MD, Maiques E, Ubeda C, Selva L, Lasa I, Calvete JJ, Novick RP, Penades JR**. 2008. Staphylococcus aureus Pathogenicity Island DNA Is Packaged in Particles Composed of Phage Proteins. J. Bacteriol. **190**:2434–2440.

287. **Spilman MS, Damle PK, Dearborn AD, Rodenburg CM, Chang JR, Wall EA, Christie GE, Dokland T**. 2012. Assembly of bacteriophage 80α capsids in a Staphylococcus aureus expression system. Virology **434**:242–50.

288. **Rountree PM**. 1949. The Serological Differentiation of Staphylococcal Bacteriophages. J. Gen. Microbiol. **3**:164–173.

289. **Xia G, Corrigan RM, Winstel V, Goerke C, Gründling A, Peschel A**. 2011. Wall teichoic Acid-dependent adsorption of staphylococcal siphovirus and myovirus. J. Bacteriol. **193**:4006–9.

290. **Hsieh S-E, Lo H-H, Chen S-T, Lee M-C, Tseng Y-H**. 2011. Wide host range and strong lytic activity of Staphylococcus aureus lytic phage Stau2. Appl. Environ. Microbiol. **77**:756–61.

291. **Kwiatek M, Parasion S, Mizak L, Gryko R, Bartoszcze M, Kocik J**. 2012. Characterization of a bacteriophage, isolated from a cow with mastitis, that is lytic against Staphylococcus aureus strains. Arch. Virol. **157**:225–34.

292. **Boles BR, Thoendel M, Singh PK**. 2004. Self-generated diversity produces “insurance effects” in biofilm communities. Proc. Natl. Acad. Sci. U. S. A. **101**:16630–5.

293. **Rakhuba D, Kolomiets E, Dey E, Novik G**. 2010. Bacteriophage receptors, mechanisms of phage adsorption and penetration into host cell. Pol. J. Microbiol **59**:145–155.

294. **Baptista C, Santos MA, São-José C**. 2008. Phage SPP1 reversible adsorption to Bacillus subtilis cell wall teichoic acids accelerates virus recognition of membrane receptor YueB. J. Bacteriol. **190**:4989–96.

295. **Hejkal TW, Wellings FM, Lewis AL, LaRock PA**. 1981. Distribution of viruses associated with particles in waste water. Appl. Environ. Microbiol. **41**:628–34.

296. **Narang HK, Codd AA**. 1981. Frequency of preclumped virus in routine fecal specimens from patients with acute nonbacterial gastroenteritis. J. Clin. Microbiol. **13**:982–8.

297. **Langlet J, Gaboriaud F, Gantzer C**. 2007. Effects of pH on plaque forming unit counts and aggregation of MS2 bacteriophage. J. Appl. Microbiol. **103**:1632–8.

298. **Zemb O, Manefield M, Thomas F, Jacquet S**. 2013. Phage adsorption to bacteria in the light of the electrostatics: a case study using E. coli, T2 and flow cytometry. J. Virol. Methods **189**:283–9.

299. **Esteban PP, Alves DR, Enright MC, Bean JE, Gaudion A, Jenkins ATA, Young AER, Arnot TC**. 2014. Enhancement of the antimicrobial properties of bacteriophage-K via stabilization using oil-in-water nano-emulsions. Biotechnol. Prog.

300. **Krylov V, Shaburova O, Krylov S, Pleteneva E**. 2013. A genetic approach to the development of new therapeutic phages to fight Pseudomonas aeruginosa in wound infections. Viruses **5**:15–53.

301. **Essoh C, Blouin Y, Loukou G, Cablanmian A, Lathro S, Kutter E, Thien HV, Vergnaud G, Pourcel C**. 2013. The susceptibility of Pseudomonas aeruginosa strains from cystic fibrosis patients to bacteriophages. PLoS One **8**:e60575.

302. **Cao Z, Zhang J, Niu YD, Cui N, Ma Y, Cao F, Jin L, Li Z, Xu Y**. 2015. Isolation and characterization of a “phiKMV-like” bacteriophage and its therapeutic effect on mink hemorrhagic pneumonia. PLoS One **10**:e0116571.

303. **Wittmann J, Dreiseikelmann B, Rohde M, Meier-Kolthoff JP, Bunk B, Rohde C**. 2014. First genome sequences of Achromobacter phages reveal new members of the N4 family. Virol. J. **11**:14.

304. **Kushkina AI, Tovkach FI, Comeau AM, Kostetskii IE, Lisovski I, Ostapchuk AM, Voychuk SI, Gorb TI, Romaniuk L V**. 2013. Complete Genome Sequence of Escherichia Phage Lw1, a New Member of the RB43 Group of Pseudo T-Even Bacteriophages. Genome Announc. **1**.

305. **Labrie S, Samson J, Moineau S**. 2010. Bacteriophage resistance mechanisms. Nat. Rev. Microbiol. **8**:317–327.

306. **Hatfull GF**. 2008. Bacteriophage genomics. Curr. Opin. Microbiol. **11**:447–53.

307. **Lima-Mendez G, Toussaint A, Leplae R**. 2011. A modular view of the bacteriophage genomic space: identification of host and lifestyle marker modules. Res. Microbiol. **162**:737–46.

308. **Coenye T, Nelis HJ**. 2010. In vitro and in vivo model systems to study microbial biofilm formation. J. Microbiol. Methods **83**:89–105.

309. **McCoy WF, Bryers JD, Robbins J, Costerton JW**. 1981. Observations of fouling biofilm formation. Can. J. Microbiol. **27**:910–7.

310. **Kharazmi A, Giwercman B, Hoiby N**. 1999. Robbins device in biofilm research. Methods Enzym. 207–215.

311. **Jass J, Costerton JW, Lappin-Scott HM**. 1995. Assessment of a chemostat-coupled modified Robbins device to study biofilms. J. Ind. Microbiol. **15**:283–289.

312. **Coenye T, De Prijck K, De Wever B, Nelis HJ**. 2008. Use of the modified Robbins device to study the in vitro biofilm removal efficacy of NitrAdine^{TM}, a novel disinfecting formula for the maintenance of oral medical devices. J. Appl. Microbiol. **105**:733–740.

313. **Leunisse C, van Weissenbruch R, Busscher HJ, van der Mei HC, Albers FW**. 1999. The artificial throat: a new method for standardization of in vitro experiments with tracheo-oesophageal voice prostheses. Acta Otolaryngol. **119**:604–8.

314. **Stepanović S, Vuković D, Dakić I, Savić B, Švabić-Vlahović M**. 2000. A modified microtiter-plate test for quantification of staphylococcal biofilm formation. J. Microbiol. Methods **40**:175–179.

315. **Monod J**. 1950. La technique de culture continue: theorie et applications. Ann. d'Institute Pasteur **79**:390 – 410.

316. **McGuckin MA, Lindén SK, Sutton P, Florin TH**. 2011. Mucin dynamics and enteric pathogens. Nat. Rev. Microbiol. **9**:265–78.

317. **Valle J, Toledo-Arana A, Berasain C, Ghigo J-M, Amorena B, Penadés JR, Lasa I**. 2003. SarA and not sigmaB is essential for biofilm development by Staphylococcus aureus. Mol. Microbiol. **48**:1075–87.

318. **French GL**. 2006. Bactericidal agents in the treatment of MRSA infections--the potential role of daptomycin. J. Antimicrob. Chemother. **58**:1107–17.

319. **Sato K, Inoue Y, Fujii T, Aoyama H, Mitsuhashi S**. 1986. Antibacterial activity of ofloxacin and its mode of action. Infection **14 Suppl 4**:S226–30.

320. **Tanji Y, Shimada T, Yoichi M**. 2004. Toward rational control of Escherichia coli O157: H7 by a phage cocktail. Appl. Microbiol. … **64**:270–4.

321. **Gu J, Liu X, Li Y, Han W, Lei L, Yang Y, Zhao H, Gao Y, Song J, Lu R, Sun C, Feng X**. 2012. A method for generation phage cocktail with great therapeutic potential. PLoS One **7**:e31698.

322. **Matic I, Radman M, Taddei F, Picard B, Doit C, Bingen E, Denamur E, Elion J**. 1997. Highly variable mutation rates in commensal and pathogenic Escherichia coli. Science **277**:1833–4.

323. **Kirby AE**. 2012. Synergistic action of gentamicin and bacteriophage in a continuous culture population of Staphylococcus aureus. PLoS One **7**:e51017.

324. **Kim M, Ryu S**. 2011. Characterization of a T5-like coliphage, SPC35, and differential development of resistance to SPC35 in Salmonella enterica serovar typhimurium and Escherichia coli. Appl. Environ. Microbiol. **77**:2042–50.

325. **Henry M, Biswas B, Vincent L, Mokashi V, Schuch R, Bishop-Lilly KA, Sozhamannan S**. 2012. Development of a high throughput assay for indirectly measuring phage growth using the OmniLog(TM) system. Bacteriophage **2**:159–167.

326. **Luria SE, Delbrück M**. 1943. Mutations of Bacteria from Virus Sensitivity to Virus Resistance. Genetics **28**:491–511.

327. **Bohannan BJM, Lenski RE**. 2000. Linking genetic change to community evolution: insights from studies of bacteria and bacteriophage. Ecol. Lett. **3**:362–377.

328. **Walters MC, Roe F, Bugnicourt A, Franklin MJ, Stewart PS**. 2003. Contributions of antibiotic penetration, oxygen limitation, and low metabolic activity to tolerance of Pseudomonas aeruginosa biofilms to ciprofloxacin and tobramycin. Antimicrob. Agents Chemother. **47**:317–23.

329. **Singh R, Ray P, Das A, Sharma M**. 2010. Penetration of antibiotics through Staphylococcus aureus and Staphylococcus epidermidis biofilms. J. Antimicrob. Chemother. **65**:1955–8.

330. **Fegan M, Francis P, Hayward AC, Davis GH, Fuerst JA**. 1990. Phenotypic conversion of Pseudomonas aeruginosa in cystic fibrosis. J. Clin. Microbiol. **28**:1143–6.

331. **LeChevallier MW, Cawthon CD, Lee RG**. 1988. Inactivation of biofilm bacteria. Appl. Environ. Microbiol. **54**:2492–9.

332. **Terry JM, Piña SE, Mattingly SJ**. 1991. Environmental conditions which influence mucoid conversion Pseudomonas aeruginosa PAO1. Infect. Immun. **59**:471–7.

333. **Mceldowney S, Fletcher M**. 1986. Effect of Growth Conditions and Surface Characteristics of Aquatic Bacteria on Their Attachment to Solid Surfaces. Microbiology **132**:513–523.

334. **Landry RM, An D, Hupp JT, Singh PK, Parsek MR**. 2006. Mucin-Pseudomonas aeruginosa interactions promote biofilm formation and antibiotic resistance. Mol. Microbiol. **59**:142–51.

335. **Lai SK, Wang Y-Y, Hanes J**. 2009. Mucus-penetrating nanoparticles for drug and gene delivery to mucosal tissues. Adv. Drug Deliv. Rev. **61**:158–71.

336. **Ramphal R, Arora SK**. 2001. Recognition of mucin components by Pseudomonas aeruginosa. Glycoconj. J. **18**:709–13.

337. **Chen P, Abercrombie JJ, Jeffrey NR, Leung KP**. 2012. An improved medium for growing Staphylococcus aureus biofilm. J. Microbiol. Methods **90**:115–8.

338. **Hoskisson PA, Hobbs G**. 2005. Continuous culture--making a comeback? Microbiology **151**:3153–9.

339. **Capparelli R, Parlato M, Borriello G, Salvatore P, Iannelli D**. 2007. Experimental phage therapy against Staphylococcus aureus in mice. Antimicrob. Agents Chemother. **51**:2765–73.

340. **Carvalho CM, Gannon BW, Halfhide DE, Santos SB, Hayes CM, Roe JM, Azeredo J**. 2010. The in vivo efficacy of two administration routes of a phage cocktail to reduce numbers of Campylobacter coli and Campylobacter jejuni in chickens. BMC Microbiol. **10**:232.

341. **Henry M, Lavigne R, Debarbieux L**. 2013. Predicting in vivo efficacy of therapeutic bacteriophages used to treat pulmonary infections. Antimicrob. Agents Chemother. **57**:5961–8.

342. **Lemaitre B, Hoffmann J**. 2007. The host defense of Drosophila melanogaster. Annu. Rev. Immunol. **25**:697–743.

343. **Bergin D, Reeves EP, Renwick J, Wientjes FB, Kavanagh K**. 2005. Superoxide production in Galleria mellonella hemocytes: identification of proteins homologous to the NADPH oxidase complex of human neutrophils. Infect. Immun. **73**:4161–70.

344. **Zdybicka-Barabas A, Mak P, Jakubowicz T, Cytryńska M**. 2014. Lysozyme and defense peptides as suppressors of phenoloxidase activity in Galleria mellonella. Arch. Insect Biochem. Physiol. **87**:1–12.

345. **Wojda I, Jakubowicz T**. 2007. Humoral immune response upon mild heat-shock conditions in Galleria mellonella larvae. J. Insect Physiol. **53**:1134–44.

346. **Bidla G, Hauling T, Dushay MS, Theopold U**. 2009. Activation of insect phenoloxidase after injury: endogenous versus foreign elicitors. J. Innate Immun. **1**:301–8.

347. **Nappi AJ, Christensen BM**. 2005. Melanogenesis and associated cytotoxic reactions: applications to insect innate immunity. Insect Biochem. Mol. Biol. **35**:443–59.

348. **Jander G, Rahme LG, Ausubel FM**. 2000. Positive correlation between virulence of Pseudomonas aeruginosa mutants in mice and insects. J. Bacteriol. **182**:3843–5.

349. **Ramarao N, Nielsen-Leroux C, Lereclus D**. 2012. The insect Galleria mellonella as a powerful infection model to investigate bacterial pathogenesis. J. Vis. Exp. e4392.

350. **Desbois AP, Coote PJ**. 2011. Wax moth larva (Galleria mellonella): an in vivo model for assessing the efficacy of antistaphylococcal agents. J. Antimicrob. Chemother. **66**:1785–90.

351. **Fedhila S, Daou N, Lereclus D, Nielsen-LeRoux C**. 2006. Identification of Bacillus cereus internalin and other candidate virulence genes specifically induced during oral infection in insects. Mol. Microbiol. **62**:339–55.

352. **Fuchs BB, O'Brien E, Khoury JB El, Mylonakis E**. 2010. Methods for using Galleria mellonella as a model host to study fungal pathogenesis. Virulence **1**:475–82.

353. **Devienne KF, Raddi MSG**. 2002. Screening for antimicrobial activity of natural products using a microplate photometer. Brazilian J. Microbiol. **33**:166–168.

354. **Gibreel TM, Upton M**. 2013. Synthetic epidermicin NI01 can protect Galleria mellonella larvae from infection with Staphylococcus aureus. J. Antimicrob. Chemother. **68**:2269–73.

355. **Seed KD, Dennis JJ**. 2009. Experimental bacteriophage therapy increases survival of Galleria mellonella larvae infected with clinically relevant strains of the Burkholderia cepacia complex. Antimicrob. Agents Chemother. **53**:2205–8.

356. **Abbasifar R, Kropinski AM, Sabour PM, Chambers JR, MacKinnon J, Malig T, Griffiths MW**. 2014. Efficiency of bacteriophage therapy against Cronobacter sakazakii in Galleria mellonella (greater wax moth) larvae. Arch. Virol. **159**:2253–61.

357. **Peleg AY, Monga D, Pillai S, Mylonakis E, Moellering RC, Eliopoulos GM**. 2009. Reduced susceptibility to vancomycin influences pathogenicity in Staphylococcus aureus infection. J. Infect. Dis. **199**:532–6.

358. **Kehl-Fie TE, Zhang Y, Moore JL, Farrand AJ, Hood MI, Rathi S, Chazin WJ, Caprioli RM, Skaar EP**. 2013. MntABC and MntH contribute to systemic Staphylococcus aureus infection by competing with calprotectin for nutrient manganese. Infect. Immun. **81**:3395–405.

359. **Jin L, Li J, Nation RL, Nicolazzo JA**. 2012. Effect of systemic infection induced by Pseudomonas aeruginosa on the brain uptake of colistin in mice. Antimicrob. Agents Chemother. **56**:5240–6.

360. **Marra AR, Bar K, Bearman GML, Wenzel RP, Edmond MB**. 2006. Systemic inflammatory response syndrome in adult patients with nosocomial bloodstream infection due to Pseudomonas aeruginosa. J. Infect. **53**:30–5.

361. **Peleg AY, Jara S, Monga D, Eliopoulos GM, Moellering RC, Mylonakis E**. 2009. Galleria mellonella as a model system to study Acinetobacter baumannii pathogenesis and therapeutics. Antimicrob. Agents Chemother. **53**:2605–9.

362. **Giannouli M, Palatucci AT, Rubino V, Ruggiero G, Romano M, Triassi M, Ricci V, Zarrilli R**. 2014. Use of larvae of the wax moth Galleria mellonella as an in vivo model to study the virulence of Helicobacter pylori. BMC Microbiol. **14**:228.

363. **Lu TK, Koeris MS**. 2011. The next generation of bacteriophage therapy. Curr. Opin. Microbiol. **14**:524–31.

364. **DeChatelet LR, Mullikin D, Shirley PS, McCall CE**. 1974. Phagocytosis of live versus heat-killed bacteria by human polymorphonuclear leukocytes. Infect. Immun. **10**:25–9.

365. **Angus AA, Lee AA, Augustin DK, Lee EJ, Evans DJ, Fleiszig SMJ**. 2008. Pseudomonas aeruginosa induces membrane blebs in epithelial cells, which are utilized as a niche for intracellular replication and motility. Infect. Immun. **76**:1992–2001.

Publications

International Journal of Antimicrobial Agents 46 (2015) 196–200

Contents lists available at ScienceDirect

International Journal of Antimicrobial Agents

journal homepage: http://www.elsevier.com/locate/ijantimicag

Assessing phage therapy against *Pseudomonas aeruginosa* using a *Galleria mellonella* infection model

M.L. Beeton[a,*,1], D.R. Alves[b,1], M.C. Enright[c], A.T.A. Jenkins[b]

[a] Department of Biomedical Sciences, Cardiff Metropolitan University, Western Avenue, Cardiff CF5 2YB, UK
[b] Department of Chemistry, University of Bath, Claverton Down, Bath BA2 7AY, UK
[c] School of Healthcare Sciences, Manchester Metropolitan University, John Dalton Building, Chester Street, Manchester M1 5GD, UK

ARTICLE INFO

Article history:
Received 6 February 2015
Accepted 15 April 2015

Keywords:
Pseudomonas aeruginosa
Phage therapy
Galleria mellonella
Infection model

ABSTRACT

The *Galleria mellonella* infection model was used to assess the *in vivo* efficacy of phage therapy against laboratory and clinical strains of *Pseudomonas aeruginosa*. In a first series of experiments, *Galleria* were infected with the laboratory strain *P. aeruginosa* PAO1 and were treated with varying multiplicity of infection (MOI) of phages either 2 h post-infection (treatment) or 2 h pre-infection (prevention) via injection into the haemolymph. To address the kinetics of infection, larvae were bled over a period of 24 h for quantification of bacteria and phages. Survival rates at 24 h when infected with 10 cells/larvae were greater in the prevention versus treatment model (47% vs. 40%, MOI = 10; 47% vs. 20%, MOI = 1; and 33% vs. 7%, MOI = 0.1). This pattern held true when 100 cells/larvae were used (87% vs. 20%, MOI = 10; 53% vs. 13%, MOI = 1; 67% vs. 7%, MOI = 0.1). By 24 h post-infection, phages kept bacterial cell numbers in the haemolymph 1000-fold lower than in the non-treated group. In a second series of experiments using clinical strains to further validate the prevention model, phages protected *Galleria* when infected with both a bacteraemia (0% vs. 85%) and a cystic fibrosis (80% vs. 100%) isolate. Therefore, this study validates the use of *G. mellonella* as a simple, robust and cost-effective model for initial *in vivo* examination of *P. aeruginosa*-targeted phage therapy, which may be applied to other pathogens with similarly low infective doses.

1. Introduction

Multidrug-resistant bacterial pathogens pose an ever-increasing threat to human health. This problem is in part due to a lack of novel antibiotics approved for use over the last few decades, resulting in an urgent need to identify new avenues for treating bacterial infections, especially those caused by Gram-negative pathogens [1]. *Pseudomonas aeruginosa* is an opportunistic pathogen that is a leading cause of infection among burn victims and patients with cystic fibrosis (CF). It is also responsible for a large number of healthcare-associated infections. To make matters worse, *P. aeruginosa* is associated with hypermutability and, due to high antibiotic selective pressure, has given rise to the emergence of multidrug-resistant strains in the population; thus, concerns about available effective treatments are growing [2,3]. In the UK, resistance to two or more antibiotics among *P. aeruginosa* isolated from the lungs of CF patients has risen to 40% [4]. This is a worrying statistic as colonisation of the CF lung with *P. aeruginosa* is a predictor of poor prognosis and is associated with a two- to three-fold increased risk of death over an 8-year period [5]. For this reason, novel anti-infectives are needed.

Facing such a scenario, interest in phage therapy in Western society has experienced a resurgence after research into this area fell out of favour following the discovery of antibiotics. Bacteriophages (or phages) are viral particles able to infect bacterial cells with high specificity, taking over cellular function to replicate their genomes. Upon maturation, the bacterial cell wall is lysed to release viral progeny.

Phage therapy can be broadly subdivided into four main categories [6]: (i) conventional phage therapy using mainly lytic phages to lyse target bacterial species; (ii) modified phage therapy using genetically altered phages with favourable properties, such as non-lytic replication to avoid the possibility of endotoxic shock when bacterial cells are lysed; (iii) treatment with enzymes derived from phages, such as administration of endolysins to selectively

* Corresponding author. Tel.: +44 29 2020 5557.
E-mail address: mbeeton@cardiffmet.ac.uk (M.L. Beeton).
[1] The two authors contributed equally to this article.

http://dx.doi.org/10.1016/j.ijantimicag.2015.04.005
0924-8579/

degrade the bacterial peptidoglycan cell wall; and (iv) the concept of combination therapy with phages and antibiotics, where phages exhibit properties to degrade polysaccharide components of biofilms therefore allowing antibiotics to penetrate and elicit an action [7].

Although *in vitro* systems allow for a reductionist approach to examining phage interactions with target bacteria, they do not take into account a more complex *in vivo* system. Mammalian models are an excellent means of testing phage therapy but require ethical approval, significant infrastructure and funds. The *Galleria mellonella* model fills the void between these two systems, providing a cheap, reliable and ethics-free system for testing novel antimicrobials [8]. Here we describe the first use of the *G. mellonella* model to evaluate the efficacy of phage therapy both for treatment and prophylaxis of *P. aeruginosa* infection.

2. Materials and methods

2.1. Bacterial strains and preparation of inoculum

Phage therapy was assessed using *P. aeruginosa* PAO1 and two low-passage clinical isolates (PA45291 and BC09007) isolated from bacteraemia and CF samples, respectively. Bacteria were grown to mid-log phase in Luria–Bertani (LB) broth (Sigma-Aldrich, Dorset, UK) and were washed once in phosphate-buffered saline (PBS). Cells were re-suspended in PBS to a final concentration of 1×10^8 CFU/mL and were diluted accordingly in PBS to the required inoculum size for each experiment.

2.2. Phage cocktail preparation and titration

All six distinct phages were propagated on *P. aeruginosa* PAO1 strain and were combined to establish a cocktail suspension. The genomic sequence of the six phages can be found in the National Center for Biotechnology Information (NCBI) GenBank database under accession nos. KR054028–KR054033, with a full description of the phages detailed elsewhere (submitted). Briefly, 100 μL of phage lysate and 100 μL of host growing culture were mixed and left for 5 min at room temperature. Following incubation, 3 mL of LB soft agar (Sigma-Aldrich) containing 0.65% bacteriological agar (Sigma-Aldrich)was added and poured onto agar plates. Following overnight incubation at 37 °C, plates displaying confluent lysis were selected and 3 mL of SM buffer [5 M NaCl, 1 M $MgSO_4$, 1 M Tris–HCl (pH 7.5), 0.01% w/v gelatine] and 2% (v/v) chloroform (Sigma-Aldrich)were added before incubation at 37 °C for 4 h. High-titre phage solution was removed from the plates, centrifuged ($8000 \times g$, 10 min) to remove cell debris and then filter-sterilised (pore size, 0.22 μm). A polyethylene glycol (PEG) (Sigma-Aldrich) purification step was further added to remove any possible bacterial debris from the suspensions. Briefly, 10% (w/v) PEG (*MW* 8000) was added to the lysate and left overnight at 4 °C. The next day, the solution was centrifuged (4000 rpm, 30 min) to obtain a PEG–phage pellet. The pellet was re-suspended gently in 1 mL of SM buffer and was vortexed thoroughly. The final solutions were stored at 4 °C. All of the necessary dilutions were performed in SM buffer. For titration of the bacteriophage content in the haemolymph, a similar methodology to the propagation was followed. Several dilutions were mixed with host bacterial cells and 3 mL of soft agar was added and poured onto agar plates. Following overnight incubation, plaques were counted to determine the phage titre.

2.3. Galleria mellonella phage therapy assay

Larvae of *G. mellonella* were obtained from Livefood UK Ltd. (Rooks Bridge, UK). Larvae were stored at 4 °C and were used within 1 week. A modified methodology developed by Peleg et al. was used to infect each *G. mellonella* [8]. Briefly, *G. mellonella* were surface-sterilised with a FASTAID pre-injection swab (Sigma-Aldrich) containing 70% ethanol (Sigma-Aldrich). Using a pair of tweezers, each *G. mellonella* was restrained and, using a 26 G Terumo syringe (VWR International, Lutterworth, UK), 10 μL of inoculum containing either 100 or 10 cells of *P. aeruginosa* was delivered into the larval haemolymph behind the last proleg. For the treatment model, phage suspension was delivered behind the last proleg on the opposite side to the bacterial injection site 2 h post-infection, and for the prevention experiment phage suspension was given 2 h pre-infection. All experiments used 15 larvae per treatment. A positive control group (larvae infected and treated with PBS solution) and two negative control groups (one group injected with PBS only, assessing the impact of any negative effect from the injection process; and one group injected with phage suspension only, assessing toxicity of the phage cocktail) were also included. Larvae were placed into Petri dishes and were incubated at 37 °C. *G. mellonella* were examined hourly after 15 h post-infection and were recorded as dead when they did not move in response to touch.

2.4. Bleeding larval haemolymph

The prevention model was used to follow the kinetics of bacteria and phage interactions within the larval haemolymph over time. The phage cocktail, or PBS, was administered 2 h prior to infection and the phage titre was initially quantified within the haemolymph at the time of infection (time zero). *G. mellonella* were infected with 100 cells of *P. aeruginosa* PAO1 and at 8 h and 24 h three *G. mellonella* were sacrificed and bled following incision made with forceps to quantify phage and *P. aeruginosa* both in phage- and PBS-treated *G. mellonella*. Titrations of haemolymph were made in SM buffer for phage counts. Quantification of PAO1 was done by preparing serial dilutions of haemolymph in 10 mM ferrous ammonium sulfate (FAS) (Sigma-Aldrich) for inactivation of extracellular phage. Bacteria were enumerated by total viable count of FAS dilutions onto LB agar. Inactivation of phages by FAS was confirmed prior to experimental procedure (data not shown). To rule out the possibility of PAO1 evolving phage resistance during *in vivo* infection, re-isolated PAO1 were subjected to plaque assay to confirm susceptibility.

2.5. Statistical analysis

Kaplan–Meier survival curves and log-rank (Mantel–Cox) statistical test were performed using GraphPad Prism (GraphPad Software Inc., La Jolla, CA).

3. Results

3.1. Treatment of infection

In this study, two models of phage and infection interactions were examined. The first was a treatment whereby *G. mellonella* was infected with either 10 or 100 cells of *P. aeruginosa* PAO1 and left to allow an infection to establish for 2 h. Varying multiplicity of infection (MOI) of phage were then administered and mortality was observed over 48 h. No mortality was recorded in the PBS controls. However, *G. mellonella* treated with PBS died quicker when infected with 100 cells compared with 10 cells. Administration of phage, displaying lytic activity against PAO1 *in vitro*, prolonged the survival of *G. mellonella* in a dose-dependent manner, but 0% survival was eventually seen in all groups by 30 h (Fig. 1A and B). At 24 h there was 100% mortality in the infected and untreated *G. mellonella*, but 40% survival for those infected with 10 cells and treated with a MOI of 10 compared with 20% survival in those infected with

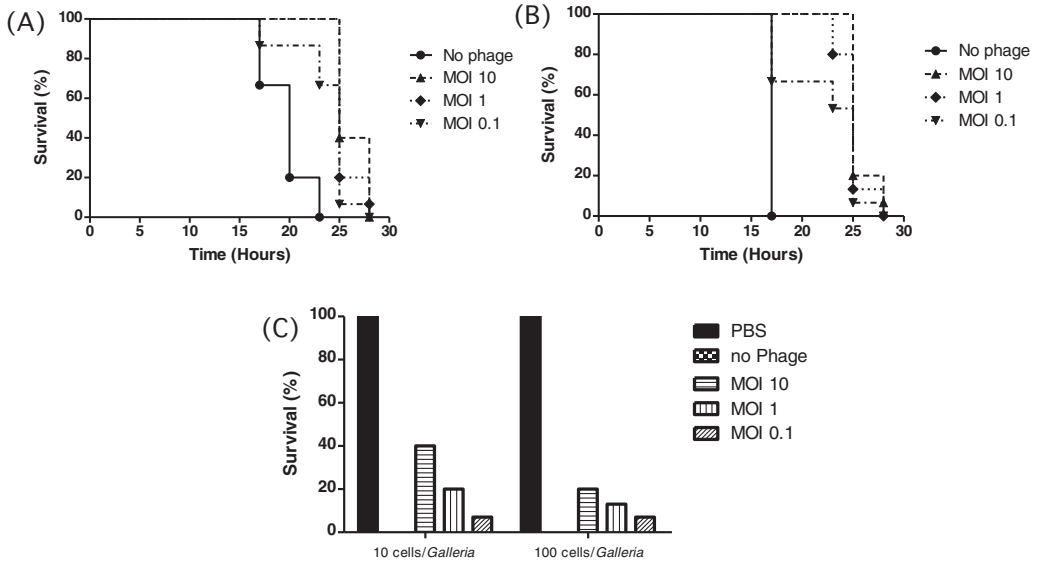

Fig. 1. Kaplan–Meier survival curves of *Galleria mellonella* infected with (A) 100 cells or (B) 10 cells of *Pseudomonas aeruginosa* PAO1 and treated with phage at varying multiplicity of infection (MOI) 2 h post-infection. (C) Percentage of *G. mellonella* survival at 24 h. PBS, phosphate-buffered saline.

100 cells at the same MOI (Fig. 1A and B). A statistically significant difference was seen between the survival curves as determined by log-rank (Mantel–Cox) test ($P < 0.0001$).

3.2. Prevention of infection

The second model examined the effect of prevention of infection whereby *G. mellonella* was given a prophylactic dose of phage 2 h prior to infection with *P. aeruginosa* PAO1. Similarly to the treatment experiment, *G. mellonella* infected with 100 cells died quicker than those infected with 10 cells when given PBS 2 h before infection (Fig. 2A and B). At 24 h, survival ranged from 80% in *G. mellonella* infected with 100 cells and given a MOI of 100 to 35% in those given a MOI of 0.1 (Fig. 2A). Survival ranged from 90% to 60% in *G. mellonella* infected with 10 cells and given MOIs of 100 and 1, respectively (Fig. 2B). A statistically significant difference was seen between the survival curves as determined by log-rank (Mantel–Cox) test ($P < 0.0001$).

3.3. Kinetics of Pseudomonas aeruginosa infection and effect of phage treatment

To understand the kinetics of a *P. aeruginosa* infection within *G. mellonella*, larvae were infected with 100 cells using the prevention model of infection. Bacteria and phage were quantified at set time points by bleeding the haemolymph. Recovered volumes of haemolymph ranged from 20 μL to 40 μL, but numbers were standardised upon analysis. No endogenous *P. aeruginosa* or phage with lytic activity against *P. aeruginosa* PAO1 were detected in the uninfected controls. For *G. mellonella* that were given *P. aeruginosa* PAO1 only, the number of cells isolated from the haemolymph increased over the duration of the experiment. By 24 h, all *G. mellonella* were

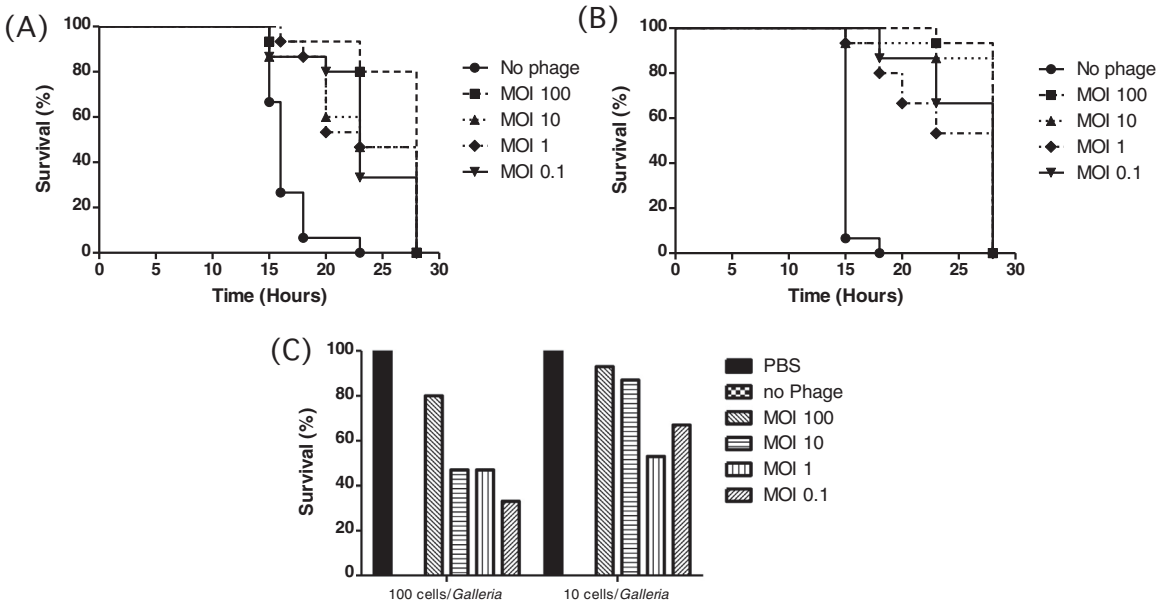

Fig. 2. Kaplan–Meier survival curves of *Galleria mellonella* infected with (A) 100 cells or (B) 10 cells of *Pseudomonas aeruginosa* PAO1 and pre-treated with phage at varying multiplicity of infection (MOI) 2 h pre-infection. (C) Percentage of *G. mellonella* survival at 24 h. PBS, phosphate-buffered saline.

dead and number of *P. aeruginosa* were in the order of 10^8 CFU/mL. The second group of *G. mellonella* was given a prophylactic dose of phage 2 h prior to infection and then phage and bacteria were quantified over the course of the infection. The number of *P. aeruginosa* PAO1 was comparable with that of the non-treated *G. mellonella* after 8 h of infection, but were three orders of magnitude less at 24 h compared with the non-treated *G. mellonella*. These *G. mellonella* were alive at 24 h. The number of phages increased over the duration of the infection, reaching a peak titre at 24 h of 10^8 PFU/mL.

3.4. *Low-passage clinical isolates of* Pseudomonas aeruginosa

To validate the model of phage therapy with *P. aeruginosa*, we sought to test the model with low-passage clinical strains isolated from patients with bacteraemia or CF (Fig. 4A and B). With the PA45291 bacteraemia strain, all infected *G. mellonella* were dead by 24 h, whereas there was 60% survival at 28 h in the group treated with phage at a MOI of 10. When *G. mellonella* were infected with the BC09007 CF strain there was little mortality at 24 h (90%) when given PBS as treatment, but there was 100% survival in the phage-treated group. By 40 h, all *G. mellonella* were then dead.

4. Discussion

To avoid a scenario whereby society is plunged back into a pre-antibiotic era, there is an urgent need to identify novel antibacterial agents. Phage therapy offers a novel non-antibiotic approach to help in this battle. Phage therapy offers a different mode of action compared with antibiotics and therefore antibiotic-resistant organisms can still be susceptible to phages. In addition, phages are highly selective and will therefore not wipe out the host microbiota, unlike antibiotics, as well as being deemed safe in trials [9–11].

The *G. mellonella* infection model provides a system that can bridge the gap between *in vitro* studies and more advanced mammalian studies, giving initial proof-of-principle data. Mammalian models are crucial for testing the efficacy of phages prior to human trials, but drawbacks include the need for sufficient infrastructure, substantial costs as well as the need for ethical approval. *G. mellonella* larvae have been used to examine numerous host–pathogen interactions ranging from studies of pathogenicity to antimicrobial activity, with a small number of these examining the potential for phage therapy [12–14].

The *P. aeruginosa* PAO1 strain proved to be highly virulent, with only 10 cells per *G. mellonella* required to result in mortality at 24 h. This is a very low infective dose in this model, with organisms such as *Staphylococcus aureus* requiring 10^5–10^6 cells/*G. mellonella* for mortality, *Acinetobacter baumannii* requiring $>10^4$ and *Helicobacter pylori* requiring 10^6–10^7 cells for establishment of infection [15–17]. This low infectious dose is of particular interest as it reduces the chances of endotoxic shock due to rapid lysis of high numbers of Gram-negative bacterial cells.

Two models of therapy were examined. The first was a treatment methodology whereby an acute 2-h infection was allowed to establish prior to administration of phage. At all MOIs of phage there was prolonged survival of *G. mellonella* regardless of whether 10 or 100 bacterial cells were used as the inoculum. Although there was increased survival compared with the control, there was a difference in survival depending on the number of cells in the inoculum. Presumably the 10-fold higher inoculum of 100 cells versus 10 cells meant that the infection had become more established within the 2-h time frame therefore reducing the efficacy of the phage to prolong survival.

The second model examined the ability to prevent infection using prophylactic administration of phage 2 h prior to infection. When compared with the treatment model, prophylactic

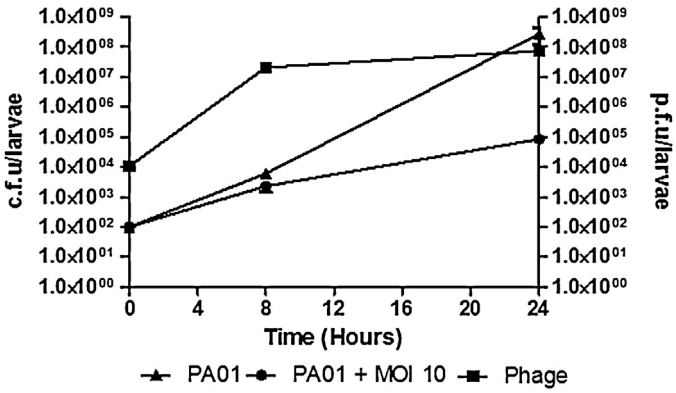

Fig. 3. *In vivo* kinetics of *Pseudomonas aeruginosa* PAO1 infection within *Galleria mellonella* with and without phage treatment. MOI, multiplicity of infection.

administration of phage resulted in greater survival after 24 h at all comparable MOI values. Presumably this increased efficacy was the result of phage being able to distribute throughout the haemolymph over the 2-h period prior to infection, whereas in the treatment model the bacteria will have had opportunity to establish and begin to express toxins. Interesting was the observation of greater survival among *G. mellonella* that received the higher inoculum of 100 cells compared with 10 cells. This may have been due to the higher number of bacterial cells, resulting in an increased chance of bacteria and phage interaction resulting in a more rapid amplification of the phage.

In both models, phage-treated *G. mellonella* eventually succumbed to the infection, resulting in mortality by 30 h post-infection. For this reason, we explored the kinetics of both the *P. aeruginosa* infection as well as the effect of phage on bacterial numbers *in vivo*. The most striking observation was the comparison between numbers of *P. aeruginosa* in the phage-treated and untreated *G. mellonella*. At 24 h the phage had kept the number of *P. aeruginosa* to 1000-fold less than the non-treated *G. mellonella*, but even in the presence of high titres of phage there had still been active growth, and therefore infection, from *P. aeruginosa* over the duration of the experiment. We had previously hypothesised that the reason for eventual mortality was the lack of available phage for clearance. From Fig. 3 it is clear that this is not the case owing to the high titre of phage within the haemolymph, although the MOI had shifted from 100 to <1 by 24 h. This hypothesis was also ruled out by an experiment where *G. mellonella* was given a second dose of phage 4 h after an initial dosing, but there was no difference when compared with the single dose control (data not shown). One possibility for the continual survival of PAO1 in the presence of a high titre of phage was the evolution of phage resistance within the *G. mellonella*. This was ruled out after observation of no bacterial growth when co-cultivating *P. aeruginosa* single colonies, recovered at 24 h after phage treatment, and a suspension of phage cocktail (data not shown). The final explanation for the survival could be the intracellular localisation of *P. aeruginosa*. In these experiments only bacterial numbers within extracted haemolymph were examined. *Pseudomonas aeruginosa* is known to have the ability to invade epithelial cells, which would protect from attack by the phage [18]. This highlights one of the limitations of phage therapy on pathogens that are able to exist and replicate in an intracellular environment. Perhaps combination therapy with antibiotics that can enter host cells, such as a fluoroquinolone or tetracycline, would have aided in clearance, but this was beyond the scope of this study. This potential intracellular survival strategy would also explain why the prevention model showed improved survival compared with the treatment model, whereby the *P. aeruginosa* will have establish within cells before the *G. mellonella* received a dose of the phage.

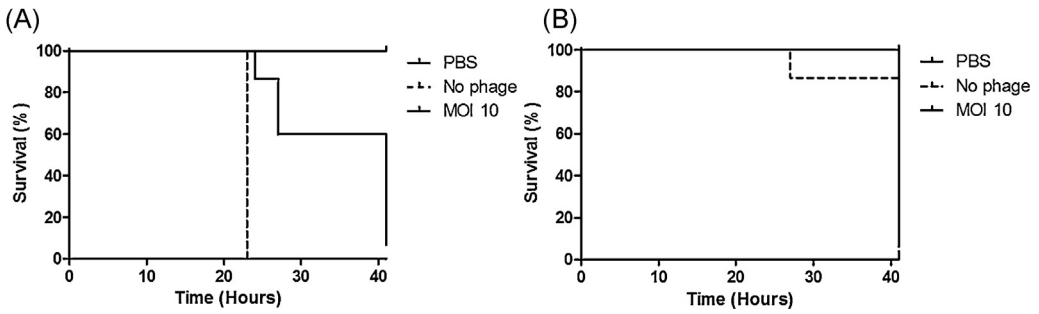

Fig. 4. Kaplan–Meier survival curves of *Galleria mellonella* infected with 10 cells of (A) *Pseudomonas aeruginosa* PA45291 (bacteraemia isolate) or (B) *P. aeruginosa* BC09007 (cystic fibrosis isolate) and pre-treated with phage at a multiplicity of infection (MOI) of 10 at 2 h pre-infection. PBS, phosphate-buffered saline.

Although we hypothesise that the lack of *P. aeruginosa* clearance was due to intracellular localisation, there must have been a degree of extracellular replication of cells within the haemolymph to allow for the observed propagation of the phage over time.

Finally, we looked to demonstrate the effectiveness of the phage model on clinical isolates of *P. aeruginosa*. To do this, the prevention model was repeated with clinical isolates from a bacteraemia and a CF infection. Here the acute isolate resulted in rapid mortality of the *G. mellonella* within 24 h, with 85% survival when given phage at a MOI of 10. Interestingly, the CF isolate was less virulent at 24 h compared with the bacteraemia and PAO1 strains, but 100% mortality was then seen by 40 h. In conclusion, we present data for the use of *G. mellonella* as a simple, robust and cost-effective model for initial examination of *P. aeruginosa*-targeted phage therapy.

Funding

This study was supported by the Engineering and Physical Sciences Research Council (EPSRC) (Grant number EP/I027602/1) Healthcare Partnership.

Competing interests

None declared.

Ethical approval

Not required.

References

[1] Boucher HW, Talbot GH, Bradley JS, Edwards JE, Gilbert D, Rice LB, et al. Bad bugs, no drugs: no ESKAPE! An update from the Infectious Diseases Society of America. Clin Infect Dis 2009;48:1–12.
[2] Barbier F, Wolff M. Multi-drug resistant *Pseudomonas aeruginosa*: towards a therapeutic dead end? [in French]. Med Sci (Paris) 2010;26:960–8.
[3] Oliver A, Mena A. Bacterial hypermutation in cystic fibrosis, not only for antibiotic resistance. Clin Microbiol Infect 2010;16:798–808.
[4] Pitt TL, Sparrow M, Warner M, Stefanidou M. Survey of resistance of *Pseudomonas aeruginosa* from UK patients with cystic fibrosis to six commonly prescribed antimicrobial agents. Thorax 2003;58:794–6.
[5] Emerson J, Rosenfeld M, McNamara S, Ramsey B, Gibson RL. *Pseudomonas aeruginosa* and other predictors of mortality and morbidity in young children with cystic fibrosis. Pediatr Pulmonol 2002;34:91–100.
[6] Viertel TM, Ritter K, Horz HP. Viruses versus bacteria—novel approaches to phage therapy as a tool against multidrug-resistant pathogens. J Antimicrob Chemother 2014;69:2326–36.
[7] Bedi M, Verma V, Chhibber S. Amoxicillin and specific bacteriophage can be used together for eradication of biofilm of *Klebsiella pneumoniae* B5055. World J Microbiol Biotechnol 2009;25:1145–51.
[8] Peleg AY, Monga D, Pillai S, Mylonakis E, Moellering Jr RC, Eliopoulos GM. Reduced susceptibility to vancomycin influences pathogenicity in *Staphylococcus aureus* infection. J Infect Dis 2009;199:532–6.
[9] Bruttin A, Brussow H. Human volunteers receiving *Escherichia coli* phage T4 orally: a safety test of phage therapy. Antimicrob Agents Chemother 2005;49:2874–8.
[10] Dethlefsen L, Huse S, Sogin ML, Relman DA. The pervasive effects of an antibiotic on the human gut microbiota, as revealed by deep 16S rRNA sequencing. PLoS Biol 2008;6:e280.
[11] Paul VD, Sundarrajan S, Rajagopalan SS, Hariharan S, Kempashanaiah N, Padmanabhan S, et al. Lysis-deficient phages as novel therapeutic agents for controlling bacterial infection. BMC Microbiol 2011;11:195.
[12] Abbasifar R, Kropinski AM, Sabour PM, Chambers JR, MacKinnon J, Malig T, et al. Efficiency of bacteriophage therapy against *Cronobacter sakazakii* in *Galleria mellonella* (greater wax moth) larvae. Arch Virol 2014;159:2253–61.
[13] Kamal F, Dennis JJ. *Burkholderia cepacia* complex phage–antibiotic synergy (PAS): antibiotics stimulate lytic phage activity. Appl Environ Microbiol 2015;81:1132–8.
[14] Seed KD, Dennis JJ. Experimental bacteriophage therapy increases survival of *Galleria mellonella* larvae infected with clinically relevant strains of the *Burkholderia cepacia* complex. Antimicrob Agents Chemother 2009;53:2205–8.
[15] Giannouli M, Palatucci AT, Rubino V, Ruggiero G, Romano M, Triassi M, et al. Use of larvae of the wax moth *Galleria mellonella* as an in vivo model to study the virulence of *Helicobacter pylori*. BMC Microbiol 2014;14:228.
[16] Gibreel TM, Upton M. Synthetic epidermicin NI01 can protect *Galleria mellonella* larvae from infection with *Staphylococcus aureus*. J Antimicrob Chemother 2013;68:2269–73.
[17] Peleg AY, Jara S, Monga D, Eliopoulos GM, Moellering Jr RC, Mylonakis E. *E. Galleria mellonella* as a model system to study *Acinetobacter baumannii* pathogenesis and therapeutics. Antimicrob Agents Chemother 2009;53:2605–9.
[18] Angus AA, Lee AA, Augustin DK, Lee EJ, Evans DJ, Fleiszig SM. *Pseudomonas aeruginosa* induces membrane blebs in epithelial cells, which are utilized as a niche for intracellular replication and motility. Infect Immun 2008;76:1992–2001.